The mechanism of *grk* mRNA anchoring during *Drosophila* oogenesis

Jan Soetaert

PhD thesis
The University of Edinburgh
June 2009

Abstract

Messenger RNA localization is a widespread mechanism of posttranscriptional regulation of gene expression in multicellular organisms ranging from yeast to mammals. In *Drosophila* oocytes, *gurken* (*grk*) mRNA is transported by Dynein to produce a local secreted signal to the overlying follicle cells. This signal is responsible for setting up the primary axes in the oocyte. *grk* mRNA is transcribed in nurse cells and transported into the oocyte where it localizes at two distinct stages of oogenesis, thus targeting the translation of Grk/TGFalpha protein, first to the posterior and later to the dorso-anterior (DA) corner where it is translated. Gurken protein signals to the overlying follicle cells to establish the dorsal fate of the oocyte. *grk* transcripts are transported by Dynein in EM-dense particles on microtubules. These particles are not associated with vesicles nor membrane-bound and contain many copies of *grk* mRNA, Dynein and hnRNP Squid. At the DA corner transport particles assemble into large EM-dense cytoplasmic anchoring complexes called Sponge Bodies. In this thesis I present evidence that at their dorso-anterior destination, *grk* transcripts are statically anchored by Dynein, independently of functional Egalitarian and Bicaudal D, which are required for Dynein transport. I show by the disrupting the protein's function after it has fulfilled its role in transport that hnRNP Squid is involved in the formation and maintenance of these Sponge Bodies. I provide evidence by EM and fluorescent microscopy that Sponge Bodies share many of components of translational regulation pathways found in Processing Bodies. I show by small RNA interference experiments and by genetic analysis that the structural role of Dynein heavy chain is a unique feature of the Sponge Bodies and that such a function does not occur in Processing Bodies in *Drosophila*. I show that the localization and anchoring of RNA in Sponge Bodies is not a unique feature of *grk* mRNA but that *I* factor RNA is also localized to Sponge bodies. The work presented tries to elucidate the function of Sponge Bodies in translational control of *grk* mRNA and illustrates by EM the dynamic nature of the Sponge Body structure during oogenesis. My results suggest that Sponge Bodies are RNA granules that are similar to Processing Bodies in a way that they are involved in translational regulation but unlike Processing Bodies depend on Dynein for their structural integrity. I propose that Sponge Bodies are RNA dependent granules that form by the recruitment of proteins involved in the anchoring and translational regulation.

Declaration

I hereby declare that this thesis is my own work and that the experiments described in the following pages were performed by myself, unless otherwise stated. The experiments were performed in the Welcome Trust Centre for Cell Biology, University of Edinburgh, in the Department of Biochemistry in Oxford and the Cell Microscopy Centre in Utrecht, the Netherlands.

Jan Soetaert

June 2009

Acknowledgments

First of all I would like to thank you, the reader of this document. It means the effort was not in vain.
I would like to thank my supervisors Ilan Davis and David Finnegan for making this thesis possible with their enthusiasm, encouragement and patience. This research was made possible by financial support of the Darwin Trust and the Wellcome Trust. Special thanks to David for lending me a desk to write on. For scientific advice I am owed special gratitude to Carine Meignin and Catherine Rabouille. Thanks to Richard Parton there are nice colorful pictures in this thesis. I have to thank Catherine Rabouille, Bram Herpers and Despina Xanthakis for teaching me the art of EM and for their hospitality at the Cell Microscopy Centre in Utrecht.

I want to thank the whole Davis and Finnegan lab for making this PhD a joyful and social experience.

Writing a thesis is not without risk of loosing mental health. Thanks to Alessia for all the love and understanding in difficult times. Alba might not realize it yet, but she made me put it all in context and kept me going. I also have to thank everyone who was there for a chat when I lost my ‘joie de vivre’.

Please keep on reading.

Table of Contents

Table of Figures

Abbreviations

3'UTR	3' untranslated region
5'UTR	5' untranslated region
AAA	ATPases Associated with diverse cellular activities
Ago	Argonaute
Bcd	Bicoid
Bic-D	Bicaudal D
BRE	Bruno response element
ConA	Concanavalin A
CPEB	Cytoplasmatic polyA end binding
DA	Dorso-anterior
DAPI	4,6-diamidino-2-phenylindole
Dhc	Dynein heavy chain
DIC	Diffraction interference contrast
Dic	Dynein intermediate chain
DLC2A	Dynein light chain 2A
Dlc	Dynein light chain
DV	Dorso-ventral
DNA	Deoxyribonucleic acid
EDTA	Ethylenediaminetetraacetic acid
EGFR	Epidermal growth factor receptor
Egl	Egalitarian
EJC	Exon-exon junction complex
EM	Electron microscopy
Exu	Exuperantia
FISH	Fluorescence *in situ* hybridization
GFP	Green fluorescent protein
GLS	*gurken* localization signal
Grk	Gurken
Hb	Hunch back
hnRNP	heterogeneous nuclear ribonucleoprotein
HRP	Horse radish peroxidase
IHEM	*In situ* hybridization electron microscopy
ILS	*I* factor localization signal
Kb	Kilo base
KDa	Kilo Dalton
Khc	Kinesin heavy chain
Klc	Kinesin light chain
Me31B	Maternal expression on 31B
µl	Microlitre
MBP	Myelin basic protein
mm	Millimeter
mM	Millimolar
µm	Micrometer
mRNA	Messenger RNA

MT	Mictrotubule
MTOC	Microtubule organizing centre
NGS	Normal goat serum
Nls	nuclear localization signal
Orb	oo18 RNA-binding protein
PB	Processing Body
PBS	Phosphate buffered saline
PBT	PBS/0.1%tween
PBTrx	PBS/0.3%Triton X 100
PCR	Polymerase chain reaction
PFA	Paraformaldehyde
RBD	RNA binding domain
RNA	Ribonucleic acid
RNAi	RNA interference
RNAsin	RNAse inhibitor
RNP	Ribonucleoprotein
RRM	RNA recognition motif
SB	Sponge Body
SG	Stress Granule
Sqd	Squid
TIA-1	Tumor inducing antigen 1
TP	Transport Particle
Tris	Tris(hydroxymethyl)-amino-methane
Triton-X 100	octylphenoxypolyethoxyethanol
Tween 20	Polyoxyethylene sorbitan monolaurate
YFP	Yellow fluorescent protein

1

Introduction

The genome of a living organism contains all the information needed for a cell to survive, grow and replicate. The correct functioning of the cell involves a very fine regulation of 'reading' this genome. The timing of switching certain genes on or off is crucial to fulfill all the necessary life functions. The cell has a repertoire of regulation and control mechanisms to assure that the amount of a certain gene product at a specific time and region in the cell is correct. The importance of mRNA localization in this gene regulation has become more and more obvious in the last decade. In this thesis I use mRNA localization in the oocytes of *Drosophila melanogaster*, more specific *gurken* mRNA, as a model to study this process.

1.1. mRNA localization and cell polarization

Multicellular eukaryote organisms are highly polarized and consist of many different tissues and cell types. Even at the cellular level polarization occurs. This can be very obvious for some cell types such as neuronal cells that consist of a cell body with radiating axons. The first polarized cell in the life cycle of an organism is the gamete. How these asymmetries are achieved has been one of the central questions in Developmental Biology. A widely used organism to study polarization events during gametogenesis is *Drosophila melanogaster* because of its long history in biological study and the well-established genetic tools. *Drosophila* has a short life cycle, its oocytes are easy to dissect and image and during oogenesis multiple polarization events take place.

1.1.1. *Drosophila* oogenesis

In the ovaries, *Drosophila melanogaster* produces egg chambers that will become eggs that are fertilized before the female lays them. Egg chambers are a cluster of 16 germline cells enveloped in a monolayer of somatic epidermal follicle cells that are responsible for the secretion of the eggshell (Wu et al., 2008). The egg chambers progress through oogenesis in ovarioles, a string of egg chambers organized in order by successive age (Figure 1A). Their development can be divided in 14 stages, seven previtellogenic (stage 1-7) and seven vitellogenic stages (stage 8-14) (King, 1970). An egg chamber starts its life as a stem cell in a structure called the germarium (Figure 1B) that undergoes an asymmetric division into a daughter stem cell and a cystoblast. The cystoblast then undergoes four incomplete mitotic divisions resulting in a cluster of 16 cells connected by cytoplasmic bridges called the ring canals (Spradling, 1993) (Figure 1C). Because of the incomplete divisions, 2 of the 16 cells will have 4 ring canals and accumulate more transcripts and proteins. Only one of these cells will become the oocyte. The other cell with 4 ring canals reverts to the fate of one of the other 15 cells thus becoming a nurse cell. Nurse cells are polytene cells that produce transcripts and proteins that are transported into the growing oocyte through ring canals. By stage 2 the cluster of germline cells has been surrounded by follicle cells and the oocyte has been specified. At this point, the egg chamber has left the germarium and is connected to the other stages by stalk cells derived from the follicle cells (Xi et al., 2003). The oocyte is transcriptionally inactive (King and Burnett, 1959) and shares its cytoplasm with the nurse cells through the ring canals.

The nurse cells start to replicate their DNA and begin to produce cellular components that are transported into the oocyte (Dej and Spradling, 1999). At stage 1, a microtubule organizing center (MTOC) has formed in the oocyte with microtubules (MT) extending through the ring canals and into the nurse cells (Theurkauf et al., 1992). Transport along the MT is a very important mechanism in the oocyte and depolymerizing the MT network leads to egg chambers that fail to form an oocyte in early stages due to transport anomalies of oocyte determinants (Koch and Spitzer, 1983) or fail to localize important transcripts for axis formation (reviewed by Lasko (Lasko, 1999)) later in oogenesis. From mid-oogenesis on several mRNAs localize to trigger a cascade of events that break up the symmetry of the oocyte and set up the axis for the future fly. The most studied examples are *oskar* (*osk*) mRNA that localizes to the posterior and will be translated into a protein important for the formation of the future germline and the abdomen, *gurken* (*grk*) mRNA from which the protein will trigger a signaling cascade that will set up the dorso-ventral axis and *bicoid* (*bcd*) mRNA that will provide the oocyte with determinants for the anterior structures (Figure 2) (reviewed in Huynh and St Johnston, 2004; Johnstone and Lasko, 2001). The following will explain the importance of mRNA localization and describe the mechanisms that work to achieve the asymmetric localization of these transcripts.

Figure 1 Early oogenesis

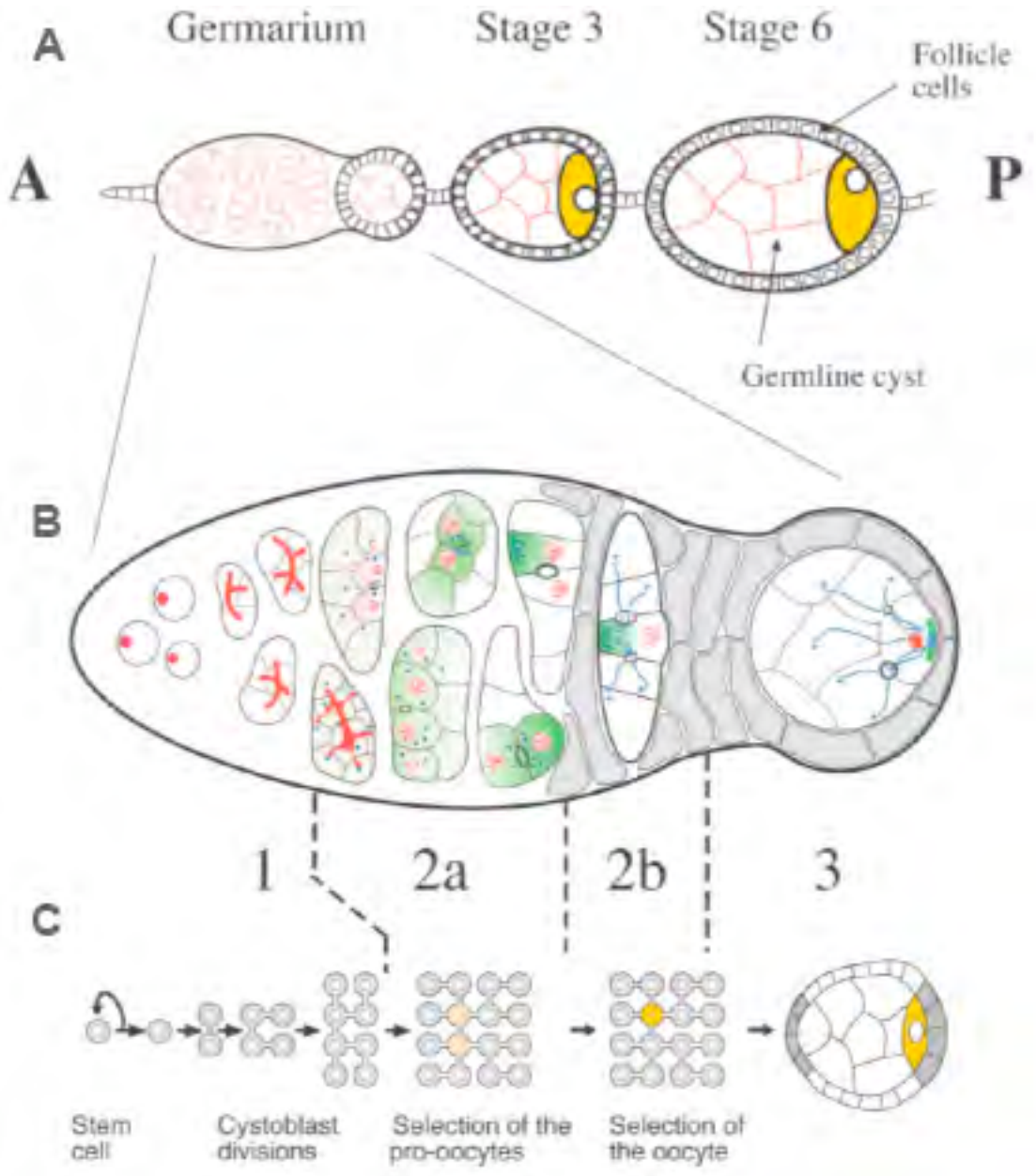

Figure 1 Early oogenesis. (A) A schematic drawing of an ovariole showing the germarium linked to a string of progressing stages of egg chambers. Conventionally the anterior (A) is shown on the left the posterior (P) on the right. (B) The outtake shows the germarium divided into different regions and (C) how this relates to the cystoblast divisions. Adapted from (Huynh and St Johnston, 2004).

Figure 2 Localized transcripts define the major axis in oogenesis

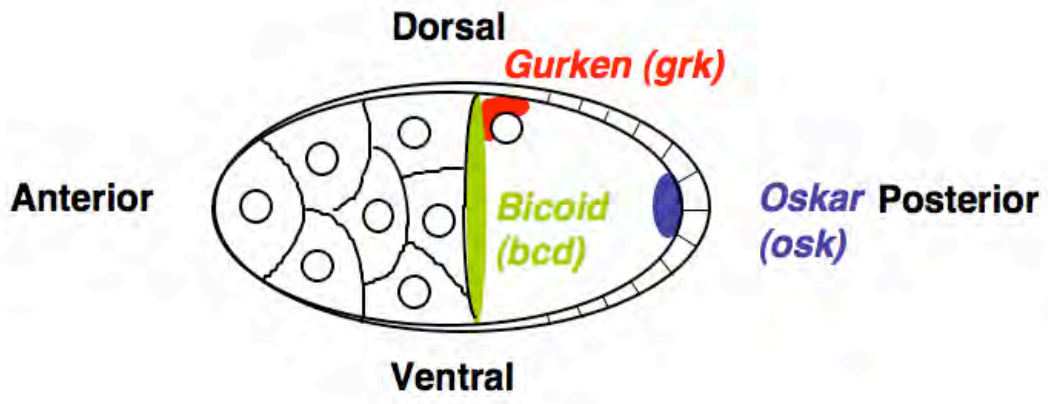

Figure 2. Localized mRNAs produce local morphogens that contribute to the formation of the major body axis in the future embryo. Oskar signaling will set up the posterior structures and germline, Gurken signaling is responsible for setting up the antero-posterior axis first and later for setting up the dorso-ventral axis and Bicoid for the anterior structures.

1.2. Biological importance of RNA localization

Polarization of a cell involves asymmetric distribution of proteins, often mediated through localized transcripts. RNA localization is a widespread phenomenon from yeast (Paquin and Chartrand, 2008) to mammals (Martin and Ephrussi, 2009). As many as 71% of all examined *Drosophila* transcripts show a subcellular localization during embryonic development (Lecuyer et al., 2007). There are 2 main reasons for localizing transcripts rather than the protein they encode. The first reason is to prevent the negative physiological effects of the protein when it is mislocalized. For example, *Drosophila* egg chambers that ectopically express Gurken (Grk) protein, will form dorsal structures in the wrong place because the wrong follicle cells receive a dorsalising signal (Kelley, 1993) and mislocalization of *oskar (osk)* and *nanos (nos)* mRNA in the oocyte will lead to the formation of a second abdomen and thorax where the head should be (Ephrussi et al., 1991; Gavis and Lehmann, 1992). The second reason is that some proteins bind to a ligand that is expressed ubiquitously and therefore it is important that at least one component is spatially restricted. Myelin Basic Protein (MPB) from the myelin compartments of the oligodendrocyte axon for instance interacts with membranes and causes them to compact. To transport MBP from the cell body to the myelin sheath of the oligodendrocyte axons would cause it to stick to every membrane it came across (Carson et al., 1997). Therefore it is the *mbp* mRNA that is localized. This is also the case for Tau and MAP2 in neurons. These two proteins bind microtubules (MT) (Aronov et al., 2001) that are very abundant in the cell and therefore have to localize their transcripts to dendrites or axons respectively. RNA localization defects during development can result in severe embryonic phenotypes as mentioned above in *Drosophila* and are also linked to human pathologies. The best-known example is fragile X mental retardation syndrome (FXS), caused by mutations in the *fragile X mental retardation 1 (FMR1)* gene (reviewed in (Dahm and Macchi, 2007)). FMR protein is an RNA binding protein and mutations lead to localization defects in multiple RNA cargos during neuronal development (Dahm and Macchi, 2007). Two other human diseases linked to RNA localization defects are spinal muscular atrophy (SMA) and spinocerebellar ataxia (SCA) both inherited neurodegenerative diseases (Dahm and Macchi, 2007).

1.2.1. mRNA localization in the oocyte defines the axis of the future embryo

In the oocyte, several mRNAs concentrate in certain regions in order to set up the primary body axis. The localization is needed to restrict the morphogen spatially in order to confine the signalling where it will induce cell fate. The first axis that is drawn in the oocyte itself is the antero-posterior axis. This first polarization event in the egg chamber occurs by signals from the stalk cells that connect the posterior of the eggchamber with the anterior of the older one. These signals cause the eggchamber to round up and make the oocyte and the posterior follicle cells to produce E-cadherin, Armadillo and α-Catenin, adhesion molecules that anchor the oocyte in a posterior position (Gonzalez-Reyes and St Johnston, 1998). Once this primary polarization is established, *grk* mRNA localizes to the posterior of the oocyte producing a local concentration of Grk, a member of the Transforming Growth Factor-α (TGF-α) family (Fig 3C). Grk binds to the epidermal growth factor (EGF) receptor Torpedo of the overlying follicle cells. This leads to a signal transduction cascade activating the mitogen activated protein kinase (MAPK) (Gonzalez-Reyes et al., 1995) causing the posterior follicle cells to secrete an unknown signal that causes a MT network reorganization (Theurkauf, 1992). Although the signal itself has not been found yet, recent studies with germline clones have shown that a functional tumor inducing Salvador/Warts/Hippo pathway is required in the polar follicle cells to induce this unknown signal (Meignin et al., 2007). This reorganization is necessary to relocate the nucleus that resides at the posterior up to this stage to the dorsoanterior corner (DA) and for the correct localisation of *bicoid* (*bcd*) and *oskar (osk)* mRNA to their final sites in the oocyte. By defining the posterior follicle cells, *grk* mRNA localization has defined the antero-posterior axis. Then *grk* mRNA localizes to the DA corner forming a cap around one side of the nucleus (Gonzalez-Reyes et al., 1995; Roth et al., 1995) (Fig 3C). Previous work in our laboratory has shown that this process takes place in two Dynein dependent steps. In the first step, Dynein transports *grk* mRNA to the anterior of the oocyte and in the second to the DA corner (MacDougall et al., 2003). Gurken protein produced locally at the cap binds to EGF receptors of the overlying follicle cells. The resulting signal transduction defines their dorsal fate (Gonzalez-Reyes et al., 1995; Neuman-Silberberg and Schüpbach, 1993) setting up a dorso-ventral axis.

Proteins of the dorsal group genes such as Pipe, Nudel and Windbeutel are deposited in the vitelline membrane by the ventral follicle cells triggering a ventralising signal cascade via a uniformly distributed Toll receptor, determining the ventral side of the dorso-ventral axis (Schupbach and Wieschaus, 1991; Stein et al., 1991). In *grk* mutants, Pipe excretion is not restricted to the ventral side of the oocyte resulting in aberrant dorso-ventral patterning (Sen et al., 1998). The intersection of Grk with Decapentaplegic protein, expressed in the posterior follicle cells, defines the formation and positioning of the dorsal appendages (Peri and Roth, 2000). Another function of Grk is to guide dorsal migration of the border cells to form the micropyle where the male gametes will enter at fertilization. The border cells are a cluster of cells that delaminate from the follicle epithelium at the anterior of the oocyte and migrate between the nurse cells towards the DA follicle cells (reviewed in (Montell, 2003)). This happens in two separate steps, from the anterior pole towards the oocyte and from there upwards to the DA (Montell et al., 1992). EGFr activation in the border cells directs their migration towards the source of Grk signaling (Duchek and Rorth, 2001).

The reorganization of the MT network as a result of Grk signaling allows the posterior localization of *oskar (osk)* mRNA (Fig 3B). The accumulation of Oskar protein is necessary for the formation of the future posterior structures and the formation of the germ cells (Williamson and Lehmann, 1996). *osk* mRNA is transcribed in the nurse cells and transported along the MT to the oocyte. This transport is dependent on Bic-D and Egalitarian, two linker proteins of the Dynein motor that mediates transport towards the minus-ends of the MTs (Bullock and Ish-Horowicz, 2001; Clark et al., 2007). In the oocyte *osk* mRNA is transported by Kinesin I towards the plus-ends of the MT (Brendza et al., 2000; Erdelyi et al., 1995). It can be detected in the oocyte as early as in the germarium (Kim-Ha et al., 1991) but localizes actively from stage 7 onwards to the anterior pole (Ephrussi et al., 1991). *osk* mRNA is then transported towards the posterior pole where it is localized for the rest of oogenesis. Mutations of *cappuccino* and *spire* cause premature cytoplasmic streaming, a Kinesin Heavy Chain dependent flowing of the ooplasm (Palacios and Johnston, 2002) and prevent *osk* mRNA from localizing (Emmons et al., 1995; Theurkauf, 1994). Careful time lapse imaging in living oocytes revealed a small bias in transport of *osk* containing particles towards the posterior pole (Zimyanin et al., 2008). When premature cytoplasmic

streaming is induced by actin depolymerisation, MTs align with their plus-ends in the direction of the streaming (Manseau et al., 1996). Using this assay, it was revealed that the majority of the *osk* containing particles move towards the plus-end of the microtubules (Zimyanin et al., 2008). They confirmed in *Kinesin Heavy chain* and *Dynein heavy chain* mutant oocytes that it is only the Kinesin motor that transports *osk* RNA containing particles in both posterior and anterior direction, suggesting that the bias in the posterior localization is a direct effect of a small bias in MT network with the plus-ends towards the posterior pole (Zimyanin et al., 2008). As opposed to most other localizing mRNAs during oogenesis, splicing at the first exon-exon junction of *osk* mRNA is required for its correct localization (Hachet and Ephrussi, 2004; Palacios, 2002). Important proteins in this process are Mago Nashi and Y14 (Hachet and Ephrussi, 2001; Mohr et al., 2001; Newmark and Boswell, 1994; Palacios, 2002). Time lapse movies in exon-exon junction complex (EJC) mutants as well as TropomyosinII mutants reveal a reversed bias in the movement of the *osk* mRNA containing particles towards the anterior pole suggesting a role in switching from a Dynein mediated transport in the nurse cells to a Kinesin mediated transport in the oocyte (Zimyanin et al., 2008). At the posterior pole, *osk* mRNA translation is derepressed by proteins such as Staufen, Vasa and Tudor (Johnstone and Lasko, 2004; Kim-Ha et al., 1995; Markussen et al., 1995; Thomson and Lasko, 2004).

bicoid (bcd) mRNA localization at the anterior and *nanos* (*nos*) mRNA to the posterior result in opposing gradients of Bcd and Nos protein in the embryo that are involved in antero-posterior patterning (Berleth et al., 1988a; Lieberfarb et al., 1996). *bcd* mRNA is transcribed in the nurse cells and is transported through the ring canals into the oocyte where it accumulates at the anterior at stage 8 to 10 (Berleth et al., 1988a). *bcd* mRNA is found in the oocyte at stage 5 to 6 and localizes in an anterior ring from stage 8 onwards (Berleth et al., 1988b; St Johnston et al., 1989) (Figure 3A). At stages 9-10, *bcd* mRNA accumulates in an anterior ring and in peripheral regions around the nurse cell nuclei (St Johnston et al., 1989). Interestingly, when fluorescently labeled *bcd* RNA is injected in the oocyte, it localizes to the cortex nearest to the site of injection but when injected in the nurse cells it localizes as the endogenous transcript. Correct localization of *bcd* at this stages requires an intact MT network as well as a functional minus-end directed motor Dynein (Duncan and Warrior, 2002; Januschke et al., 2002; Pokrywka and Stephenson, 1991). When

injected *bcd* mRNA is aspirated out of the nurse cells and is reinjected in another egg chamber, it localizes as the endogenous *bcd* mRNA regardless of the site of injection (Cha et al., 2001). This suggests the transcript needs to recruit trans acting factors in the nurse cell cytoplasm for correct localization. Cha et al. revealed that *bcd* mRNA needs to form a complex with Exuperantia (Exu) in the nurse cells to be targeted to the MTs at the anterior cortex during mid-oogenesis (Cha et al., 2001). After stage 10, when nurse cell dumping occurs, *bcd* RNA localization partially recovers in *exu* mutants (Riechmann and Ephrussi, 2004). Dumping is a process in which the nurse cell initiate apoptosis and extrude their contents into the oocyte by actin-dependent contractions. Live cell imaging revealed that the majority of *bcd* at the anterior accumulates after the initiation of dumping (Weil et al., 2006). After dumping at stage 10b until stage 13, *bcd* mRNA does not anchor at its final destination but remains in a steady state at the anterior cortex by continual active transport. The maintenance of *bcd* mRNA at the anterior cortex in these late stages of oogenesis requires an active Dynein motor for transport and an intact MT network (Weil et al., 2006). Also actin is required to anchor the MT to the anterior cortex (Weil et al., 2006). At stage 14 when the oocyte is mature and can be stored for weeks until fertilization in the female, *bcd* RNA is statically anchored at the anterior cortex independent on the MT network or an active Dynein motor but requires the actin network to maintain anchored (Weil et al., 2008). Upon egg activation, the actin network reorganizes from a tightly packed to a diffuse network and *bcd* is released from the cortex (Weil et al., 2008). The resulting gradient of *bcd* mRNA is then translated and produces a gradient of Bcd protein that will determine the anterior cell fates (Berleth et al., 1988b; Driever and Nüsslein-Volhard, 1988).

From the examples above it is clear that the localization of an RNA is not an isolated event. A defect in localization of one RNA will lead to patterning defects that can impair the localization of other RNAs downstream of this event. This thesis will concentrate in particular on *grk* mRNA localization as a model to study mRNA localization and anchoring.

Figure 3 Localized mRNAs during oogenesis

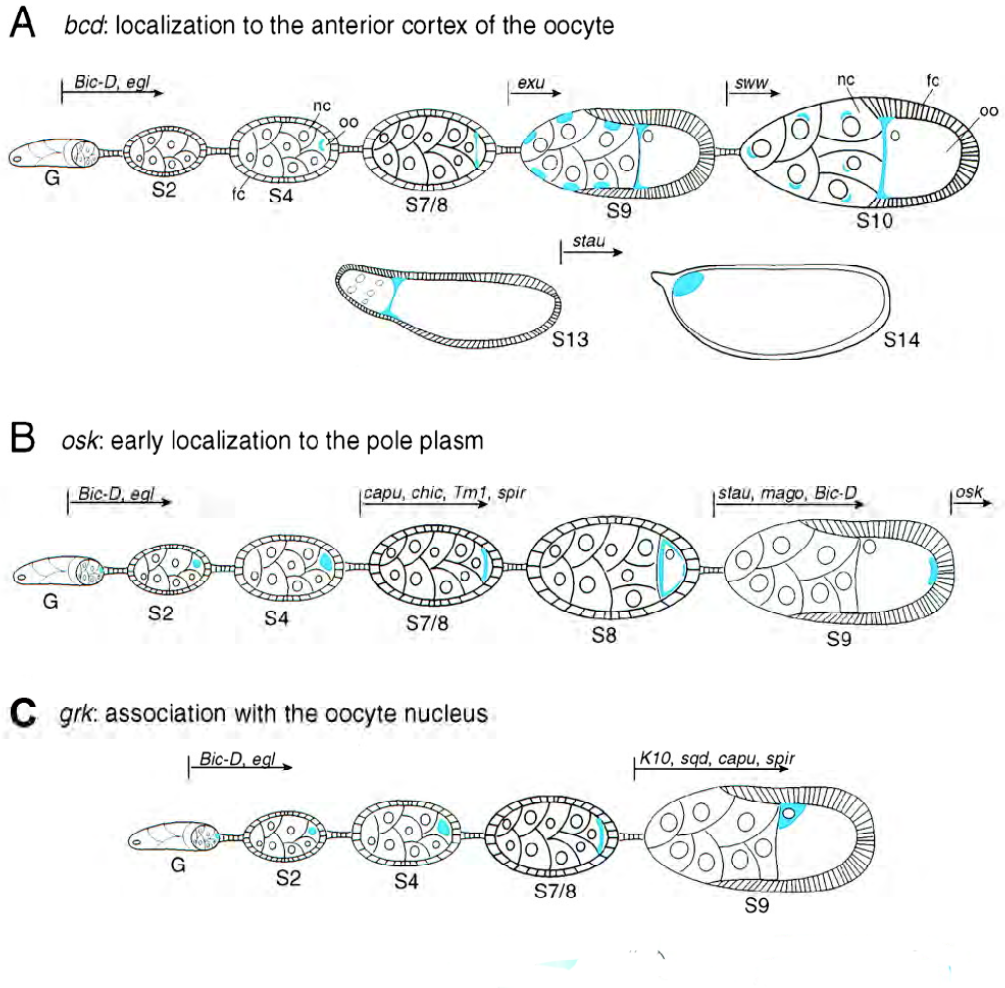

Figure 3 Localized mRNAs during oogenesis

Schematic representation of the 3 major localized mRNAs during oogenesis. The period for which the functions of particular genes are required for localization are represented by the arrows. The stages of oogenesis are represented by the numbers under the egg chambers. Nurse cells (nc), follicle cells (fc), oocyte (oo). Figure modified from (Lasko, 1999)

1.3. Mechanisms of mRNA localization

Asymmetric mRNA localization can be achieved by a variety of distinct mechanisms. RNA can be locally synthesized by an asymmetrically localized nucleus, there might be local protection from degradation at a specific site, the transcripts can diffuse passively and anchor or the transport is actively mediated by molecular motors along the cytoskeleton (St Johnston, 2005). The last mechanism is the most studied so far and depends on the actin or MT network to transport the RNA to the final destination in the cell. Well studied examples and that have become models for the study in mRNA localization are *β-actin* mRNA in the leading edges chicken fibroblast cells (Lavoie et al., 2004), *ASH1* mRNA in localization to the forming bud in *S. cerevisiae* (Paquin and Chartrand, 2008), *vg1* and *an* mRNA to the vegetal and animal pole in *X. leavis (King et al., 2005)*. Some of these will be discussed in more detail later. RNA localization consists of one or more transport steps that lead to an accumulation of transcripts at their final destination. Transcripts can remain in a continuously transported state at their final destination or can be statically anchored.

1.3.1. Active transport along the cytoskeleton

As stated before, active transport of mRNAs takes place in most if not all organisms. Active transport is dependent on the cytoskeleton and cellular motors to move cargoes in the cell.

1.3.1.1. Actin mediated transport

Transport along the actin microfilaments is dependent on the Myosin motor complex. Myosin moves on the microfilaments in an ATP dependent way transporting RNA-protein complexes (Lopez de Heredia and Jansen, 2004). In *Saccharomyces cerevisiae,* as many as 23 mRNAs have been shown to localize to the bud in a Myosin/actin dependent way (Shepard et al., 2003). A very well studied example of these is *ASH1 mRNA.* The Myosin motor transports *ASH1* mRNA to the bud tip where Ash1p represses the expression of HO in the daughter cell, preventing its ability to switch mating type (Amon, 1996). *ASH1* mRNA transport is mediated through the She1/She2/She3 complex. She2p, an RNA binding protein binds to *ASH1* mRNA in the nucleus of the mother cell and binds to She1p via the linker protein She3. She1p is the yeast Myosin-V that transports *ASH1* mRNA to the bud tip (Bertrand et al., 1998; Bohl et al., 2000; Long et al., 2000). Myosin-V does not accumulate at the bud tip in

she2 mutants showing that the cargo is modulating the motors activity and retention at the tip (Kruse et al., 2002). Recently it was shown that ASH1 mRNA particles and ER tubules migrate together to the bud tip (Schmid et al., 2006). This comigration is dependent on cotransport mediated by Myo4p and She3p and association of the RNP with the ER mediated by the RNA binding She2p (Schmid et al., 2006). This mechanism is probably quite common as in *Xenopus laevis* Vg1 binding protein Vera, that binds several localizing RNAs, also associates with the ER (Deshler et al., 1997). Also Staufen, involved in mRNA localization in several cell types cofractionates and colocalizes with rough ER in *X. laevis* (Allison et al., 2004). In *Drosophila* cotransport of RNA and vesicles has only been implicated for *osk* mRNA (Cohen, 2005). Another example is the transport of *β-actin* mRNA in fibroblasts and in neuronal cells by Myosin II (Latham et al., 2001).

In *Drosophila* there are some polarity defects linked to actin regulation. Mutations in *cappuccino, spire* and *chickadee* show premature cytoplasmic streaming and prevent the accumulation of *osk* mRNA at the posterior (Manseau et al., 1996; Manseau and Schüpbach, 1989). This mislocalization in these mutants is caused by the effect of actin depolymerisation on the MT organization. In *Drosophila*, actin is of less importance for mRNA transport and transcripts are localized on the MT network by their associated motors Dynein and Kinesin (Tekotte and Davis, 2002). Actin is however often involved in the anchoring of the RNA (Martin and Ephrussi, 2009).

1.3.1.2. The actin associated motor Myosin V

Myosin V, as discussed above, has been linked to cargo transport along actin microfilaments. The motor composes of two heavy chains and one light chain. The heavy chain has a motor domain in its amino terminal end with binding sites for actin and for ATP. The long neck has binding sites for Calmodulin and a coiled coil region provides a dimerisation site. The Calmodulin binding ability has been suggested to be a calcium dependent regulating mechanism. The carboxyl terminal region is responsible for cargo binding (Reck-Peterson et al., 2000) (Figure 4). Myosin V has a single ATP-binding site per head (Vale, 2003) and functions as an enzyme that hydrolyzes a single ATP molecule per step during motion (Rief et al., 2000).

Figure 4 Mysosin V motor

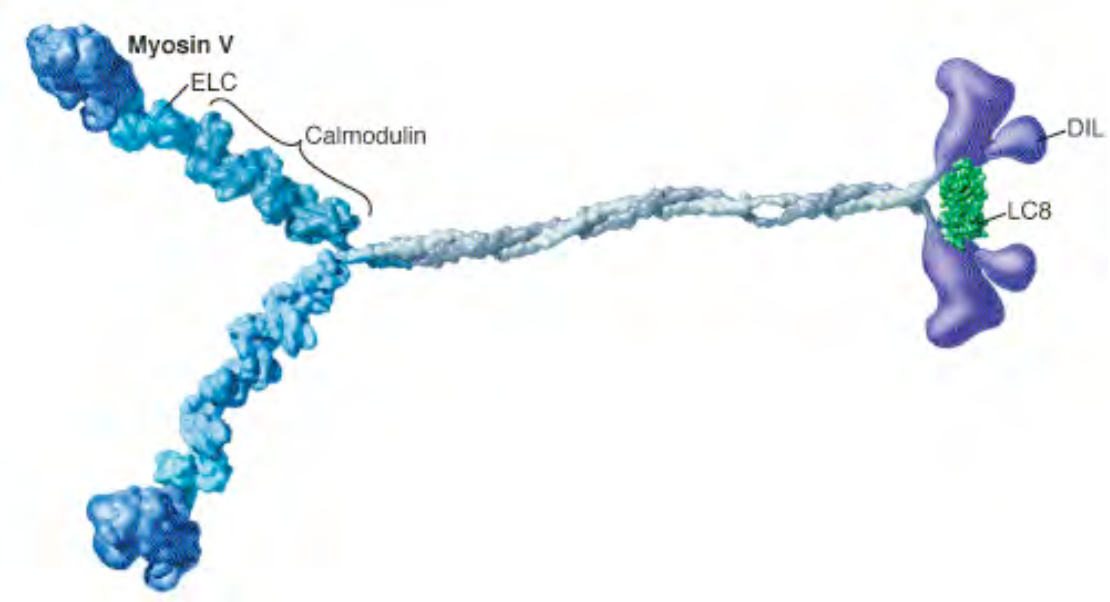

Figure 4 Representation of the Myosin V motor

Surface model based upon atomic resolution structures. The motor catalytic domains are displayed in blue, mechanical amplifiers in light blue, and tail domains implicated in cargo attachment are shown in purple. Essential light chain (ELC), Dilute Domain (DIL), Light Chain 8 (LC8), Calmodulin binding site (Calmodulin) (Vale, 2003).

1.3.1.3. Microtubule mediated transport

In *Drosophila melanogaster*, MT dependent transport is responsible for the localization of many mRNAs among whitch the three major localizing mRNA determinants at mid-oogenesis. *grk* mRNA localizes to the dorso-anterior (DA) corner, *bcd* to the anterior and *osk* to the posterior to set up the oocyte polarity (Berleth et al., 1988b; Ephrussi et al., 1991; Kim-Ha et al., 1991; Neuman-Silberberg and Schüpbach, 1993; Nusslein-Volhard et al., 1987). Microtubules have the largest diameter of all cytoskeleton filaments and transport molecules and organelles over a wide range of distances. The MTs are composed of 13 protofilaments, each composed of heterodimers that contain two subunits: α- and β-tubulin (Darnell et al., 1990). In general, MTs nucleate from a microtubule organization centre (MTOC). Most MTOCs contain γ-tubulin as opposed to the α- and β-tubulin in the heterodimers that form the MT filaments (Moritz and Agard, 2001). In early previtellogenic oocytes, an

MTOC localizes to the posterior cortex of the oocyte. MT nucleate from this MTOC with their minus-ends focused in the oocyte, directing the localization of important oocyte determinants towards the oocyte (Grieder et al., 2000; Theurkauf, 1992; Theurkauf et al., 1993). The best-known examples of oocyte determinants are Bic-D and Egalitarian (de Cuevas et al., 1997). As the oocyte is transcriptionally silent, mRNA and proteins have to be transported from the polyploid nurse cells to the oocyte (King and Burnett, 1959; Spradling, 1993). This transport is dependent on MTs (Pokrywka and Stephenson, 1995) and include *grk* mRNA (Neuman-Silberberg and Schüpbach, 1993). An unidentified signal from the posterior follicle cells as a result of Grk/EGFr signaling triggers a MT reorganization that is required for the localization of *grk*, *bcd* and *osk* mRNA in mid-oogenesis. As a consequence, mutations in proteins that act in Grk signaling will cause defects in the MT network organization and will often be reflected in polarity defects. These mutations are called the spindle class genes and include alleles of *vasa, aubergin, encore, maelstrom, okra* and the spindle genes themselves (Steinhauer and Kalderon, 2006). Protein kinase A (PKA) was one of the first factors identified as being required for germline MT rearrangement (Lane and Kalderon, 1994) and is required for proper disassembly of the MTOC at the posterior at stage 6 (Lane and Kalderon, 1994; Steinhauer and Kalderon, 2005). The PKA mutant phenotype is very similar to a *grk* mutant phenotype with the distinction that the oocyte nucleus migrates normally and that the posterior follicle cells are specified correctly (Steinhauer and Kalderon, 2005). The function of PKA in MT reorganization in oogenesis has been shown to be specific to the germline (Lane and Kalderon, 1994) and independent from cAMP regulation on the signal transduction pathway (Steinhauer and Kalderon, 2005). Transport along MT is mediated by members of the Kinesin and Dynein motor families. Kinesin is mostly plus-end directed while Dynein is minus-end directed (Steinhauer and Kalderon, 2006).

1.3.1.4. The microtubule associated motor Kinesin

Kinesin dependent transport has been intensively studied in neurons. Dendritic localization of mRNAs is mediated by Kinesin to the plus-end of the MT. The key examples are *myelin basic protein (MPB)* mRNA, *ß-actin* mRNA

calcium/calmodulin-dependent kinase-2α (camKII2α) mRNA and *microtubule associated protein 2 (MAP2)* mRNA localization. Kinesin I is a two-headed homodimer with a single ATP-binding site within each head. Like Myosin V, Kinesin I has a single ATP-binding site per head (Vale and Milligan, 2000). Kinesin I is a robust and efficient transporter *in vitro.* A single motor can attach to a cargo and take many successive steps before detaching from the microtubule (Visscher et al., 1999) or many motors may act together for transport with higher force and distance (Vershinin et al., 2007). *In vivo*, lipid droplets engage with multiple motors but that does not influence traveled distance (Shubeita et al., 2008). In the *Drosophila* oocyte, Kinesin I transports *osk* mRNA to the posterior pole of the oocyte (Brendza et al., 2002; Januschke et al., 2002) and is responsible for cytoplasmic streaming (Palacios and Johnston, 2002). It has also been suggested that Kinesin I forms a complex with Dynein in order to cycle the motor proteins between the opposite MT poles (Januschke et al., 2002).

Figure 5 Representation of the Kinesin I motor

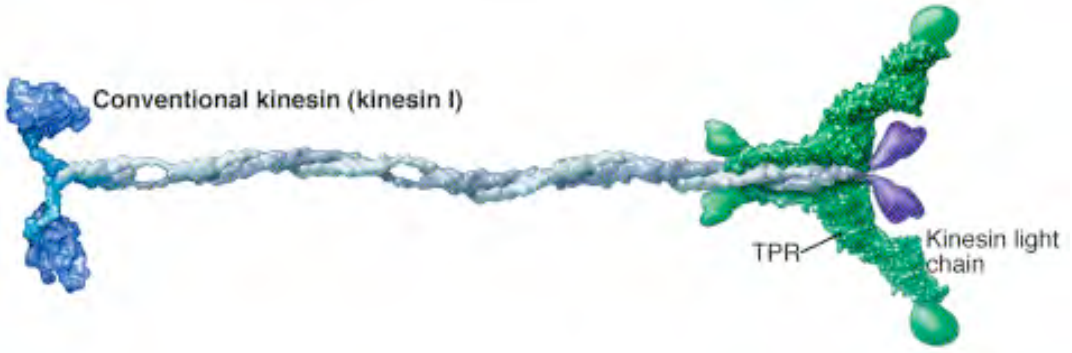

Figure 5 Representation of the Kinesin I motor

Surface model based upon atomic resolution structures. The motor catalytic domains are displayed in blue, mechanical amplifiers or neck linker in light blue, and tail domains implicated in cargo attachment are shown in purple. (Vale, 2003).

1.3.1.5. The microtubule associated motor Dynein

The Dynein motor, like other motors, “walks” on the MT network by repeated cycles of coordinated association and dissociation with their cytoskeleton tracks. This

involves a series of conformational changes of the motor head domain mediated by ATP hydrolysis (reviewed in (Hirokawa, 1993; Vale, 2003; Vale and Milligan, 2000)). Cytoplasmic Dynein is a huge multi-component motor complex (1000-2000kDa) where a homodimer of 2 heavy chains act as the fundamental motor component (Mizuno et al., 2004). Dynein heavy chain (Dhc) is composed of a globular head structure, a stalk and a stem (Figure 6). The stalk is responsible for MT binding, the stem links the motor to the other motor components such as Dynein intermediate chain, Dynein intermediate light chain and different homologues of Dynein light chain (Sakato and King, 2004). These Dlc components seem to vary from tissue to tissue (Susalka and Pfister, 2000). Dynein belongs to the ATPase associated with diverse cellular activities (AAA) family of proteins (King, 2000; Neuwald et al., 1999). Each of the two heads consists of seven globular domains, of which six are AAA domains. They are arranged in a ring around a central cavity. AAA1-4 can bind ATP, whereas AAA5 and AAA6 do not. AAA1 has been shown to be the main site of ATP hydrolysis (Mallik and Gross, 2004) (Figure 6).

The activity of the motor can be regulated by three different mechanisms: regulation of the motor domain itself, regulation by controlling the amount of Dynein motors that are functioning together and by means of accessory proteins (Mallik and Gross, 2004). It has been hypothesized that the high complexity of the Dynein motor compared to the much simpler structures of Kinesin and Myosin motors is needed for the much higher degree of regulation (Mallik and Gross, 2004). The stalling force of Dynein is much lower (Gross et al., 2000; Mallik et al., 2004) than that for Kinesin (Visscher et al., 1999) and Myosin (Mehta et al., 1999; Rief et al., 2000) but can be regulated better. For example, the stalling force of Dynein increases by a factor 3 when the ATP concentration is increased ten fold *in vitro* compared to only 20% for Kinesin (Mallik et al., 2004). *In vitro* studies show that the step size of unloaded single Dynein motor is a mixture of 24 and 32nm steps but when the motor has to move a load it can shift down gears to a step size of 8nm and a force up to 1.1pN (Mallik et al., 2004). In *Drosophila*, the Dynein mediated transport of lipid droplets has a stalling force that is regulated in steps of 1.1 pN, which is the stall force for one motor molecule (Mallik et al., 2004). This points clearly in the direction of transport by multiple motors *in vivo*. Lissencephaly-1 (Lis-1) is a regulator protein that has been linked to neuronal migration, nuclear positioning in the *Drosophila* oocyte and

regulates the ATPase activity of Dhc *in vitro* by binding directly to the AAA1 subunit (Mesngon et al., 2006; Swan et al., 1999). Dynein requires the Dynactin complex for *in vivo* function (Burkhardt et al., 1997). Dynactin, a complex consisting of multiple subunits (Fig 6B), regulates Dynein motor activity. The subunit $P150^{glued}$ induces long-range movement of Dynein along MTs (Schroer, 2004). It is believed that the bulk of the other Dynactin subunits are involved in interaction with different cellular structures such as cargos (Schroer, 2004). The Dynein motor has been reported to display bidirectional movement with an overall directionality towards the minus-ends of the MT (Levy et al., 2006; Mallik et al., 2005; Ross et al., 2006; Vendra et al., 2007). It has been proposed that bidirectional movement of motors and their cargo allows the cell to regulate the cargo destination or to overcome obstacles in the cell (Ross et al., 2006). The plus-end directed movements of Dynein are independent on Kinesin and are suppressed by Dynactin (Vendra et al., 2007). Bicaudal D (Bic-D) and Egalitarian (Egl) are also acting in the motor activity. Egl binds to the C terminus of Bic-D that binds to Dynamitin, another subunit of Dynactin (Hoogenraad et al., 2001; Hoogenraad et al., 2003). Mutants for *egl* and *dynein light chain (dlc)* do not maintain oocyte cell fate, showing the importance of Dynein mediated transport in early oocyte specification (Carpenter, 1994; Huynh and St Johnston, 2000; Navarro et al., 2004). Bic-D and Egl are required for apical localization of the wingless and pair rule transcripts in the embryo (Bullock and Ish-Horowicz, 2001; Delanoue and Davis, 2005; Navarro et al., 2004; Wilkie and Davis, 2001). Studies on lipid droplet movement have shown that Bic-D is involved in their bidirectional movement in embryos (Larsen et al., 2008). Recently, Dynein has been implicated in anchoring of *wingless* mRNA in the blastoderm embryo independent of its function as a motor (Delanoue and Davis, 2005). Recently, immuno-electron microscopy (IEM) studies by our lab and collaborators revealed that *grk* mRNA is transported in transport particles containing multiple RNA and Dynein molecules, suggesting multiple motors are involved in their transport (Delanoue et al., 2007). It was upon the start of this project unknown whether Dynein is involved in maintaining *grk* mRNA at the DA corner nor if this is as a static anchor or by continuous transport. In this thesis I try to unveil some of the mysteries of the function of the Dynein and regulating proteins Bic-D and Egl in tethering *grk* mRNA at the DA corner.

Figure 6 Structure of the Dynein motor complex

A

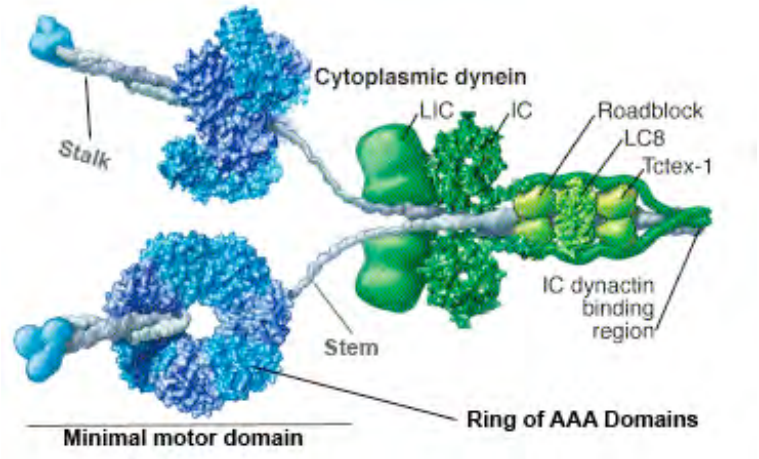

B

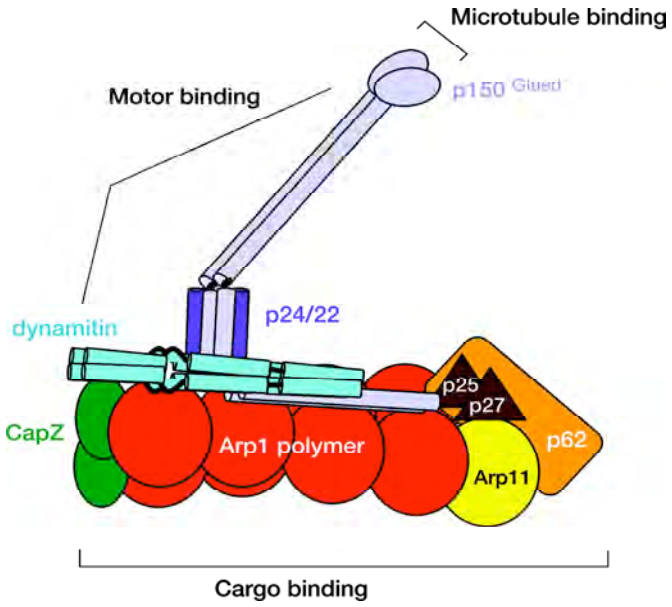

Figure 6 Representation of the Dynein motor and Dynactin complex

(A) Surface model based upon atomic resolution structures. The motor catalytic domains are displayed in blue, mechanical amplifiers in light blue, and tail domains implicated in cargo attachment are shown in purple. Dynein is shown in mixed purple, blue shading to illustrate the distinct domains that comprise the motor head, four of which are likely to be functional ATP binding AAA+ domains. The stalks extending from the ring bind to microtubules at their globular tips. (Vale, 2003)

(B) Schematic representation of Dynactin and its known subunits. The overall structure was derived from quick-freeze, deep-etch, rotary shadow electron microscopy (Schroer, 2004).

1.3.2. RNA anchoring

Anchoring of mRNA, or rather its retention at its final destination is not well understood. Some RNAs are continuously transported to their final destination and others are statically anchored. In the case of *bcd* mRNA it even switches from one mechanism to the other during oogenesis (Weil et al., 2006; Weil et al., 2008). Actin and actin binding proteins play an important role in the retention of RNAs that are transported along the actin network (Lopez de Heredia and Jansen, 2004). Anchoring of *bcd* mRNA in late oogenesis, transported along the MT by Dynein, requires actin (Weil et al., 2006; Weil et al., 2008). Actin is also required for retention for *osk* in *Drosophila* and *vg1* in Xenopus (Lopez de Heredia and Jansen, 2004; St Johnston, 2005). Dhc, Bic-D and Egl accumulate apically with *wingless* and *pair rule* mRNA in the embryo when these transcripts are injected. This accumulation of motor components suggests that Dynein motor complex has a role in anchoring. Injection of anti-Dhc antibodies leads to the disruption of mRNA anchoring independent of the motors activity as inactivation of Egl did not result in a loss of anchoring (Delanoue and Davis, 2005). It has been proposed that Dynein switches from a molecular motor to a static anchor upon delivery of its cargo (Delanoue and Davis, 2005). It is not known how the motor can accomplish this switch nor how it functions as an anchor. Exciting work in our lab at the beginning of my project showed that *grk* mRNA is statically anchored at the DA corner of the oocyte (Delanoue et al., 2007) and the anchoring structures themselves were studied by electron microscopy (EM). EM revealed that *grk* mRNA is anchored at the DA corner in large structures that have a sponge like appearance and are interdigitated with endoplasmatic reticulum. Upon further examination it was confirmed that these structures were Sponge Bodies (SBs) (Delanoue et al., 2007). The anchoring of *grk* mRNA in SBs is independent of the MT network and does not require actin. Until the start of this thesis it was not known what the anchor in this process was and what the nature of SBs was.

1.3.3. *Cis*-acting factor: RNA localization signals or zip codes

Active mRNA localization is mediated by *cis*-acting factors in the mRNA sequence. These *cis*-acting factors or zip codes are recognized by transacting factors through recognition of their primary sequence and/or the secondary structure (Jansen, 2001), although ongoing studies are showing more and more the importance of the tertiary structure (Gilligan and Sampath, 2008; Lukavsky et al., 2003). Zip codes are often

situated in the 3'UTR of the transcripts and their localization of the transcripts is mediated by binding proteins (Jansen, 2001). *ß-actin* mRNA is one of the examples of RNA that contain a zip code in the 3'UTR (Kislauskis et al., 1994, Zhang, 2001 #3388). Zip code binding protein 1 (ZBP1) binds to the zipcode in the nucleus and recruits Myosin II upon export from the nucleus in rat neuroblastoma and mouse glioma cell lines. It is then transported to the newly forming protrusions. At the final destination ZBP1 is phosphorylated by Src, allowing the translation of *ß-actin* mRNA (Huttelmaier et al., 2005). Many localization elements have been identified in *Drosophila* and other model organisms (for review see Van De Bor et al. 2004) and biocomputational algorithms have been developed to predict secondary localization elements (Hamilton et al., 2009; Rivas and Eddy, 2000; Rivas et al., 2001). The zip codes are often predicted to form stem loop structures as found for *bcd, grk, I* factor and several other mRNAs localized in the *Drosophila* oocyte and embryo (Van De Bor et al., 2005; MacDonald, 1990; Macdonald and Struhl, 1988; Seeger and Kaufman, 1990). In the case of *grk* mRNA, the zip code for DA localization at stage 9 of oogenesis has been narrowed down to a 64nt long sequence in the 5' end of the coding region of the gene. This Gurken localization signal (GLS) has a predicted stem loop structure (Van De Bor et al., 2005). Sequences in the 5' UTR of the transcript seem to be required for localization in late oogenesis (Saunders and Cohen, 1999). Although some evidence shows that also the 3' UTR is also involved in localization, this is most likely an effect of the reporter construct on the secondary structure of the *gurken localization element* (GLE) (Thio et al., 2000; Van De Bor et al., 2005). The *bicoid* localization element (BLE) is another well-studied example of such a stem loop structures. The first 625 nucleotides of the 3'UTR were found to be required for *bicoid* mRNA localization to the anterior of the oocyte (Macdonald and Struhl, 1988). Localization of the transcript takes place in sequential steps for which three different stem loops are required. A 50 nucleotide long sequence in stem loop V called the BLE1 is responsible for transport of the mRNA into the oocyte and initial accumulation at the anterior (Macdonald et al., 1993). Stem loop V and VI regulate the accumulation at the anterior and stem loop III is required for the anchoring at the anterior of the oocyte (Macdonald and Kerr, 1998).

Figure 7 *gurken* transcript and localization signal

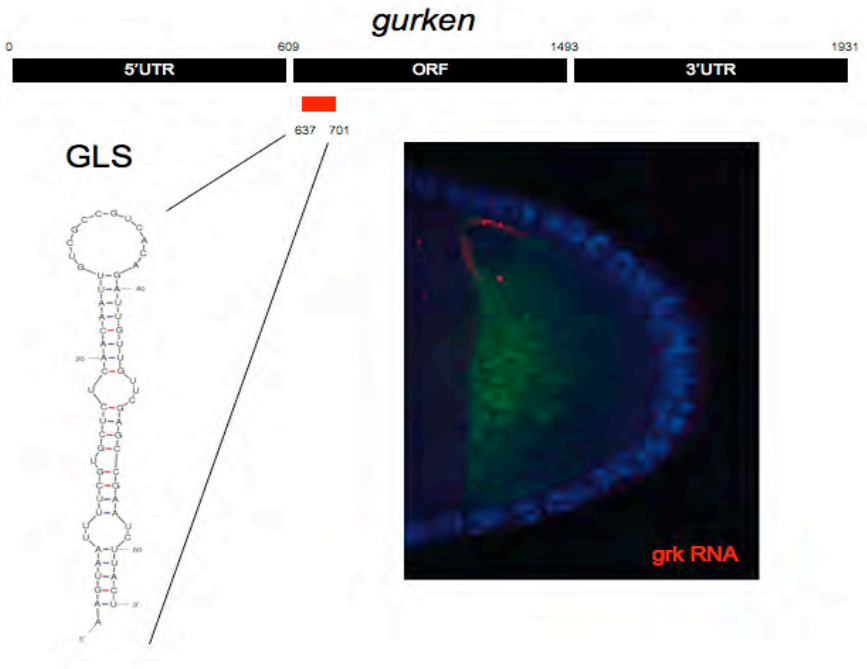

Figure 7 *grk* transcript and localization signal GLS

Schematic representation of the *grk* transcript. Redrawn from (Van De Bor et al., 2005). The magnification shows an M-fold prediction for the GLS for a temperature of 298K (Zuker, 2003). The M-fold software is available at http://mfold.bioinfo.rpi.edu/. The picture shows a stage 9 oocyte into which fluorescently labelled *grk* RNA was injected and allowed to localize to the DA corner.

1.3.4. *Trans*-acting factors in mRNA localization

The localization of mRNAs is mediated by transacting factors binding to cis-acting elements in the mRNA. The best-characterized protein in mRNA localization is Staufen (Micklem et al., 2000). It has 5 double stranded RNA binding domains (dsRBD) that are highly conserved throughout the animal kingdom (Micklem et al., 2000). These domains are able to bind double stranded RNA and stem-loop structures (Ramos et al., 2000). In *Drosophila*, Staufen is required for the posterior localization of *osk* mRNA (Ephrussi et al., 1991; Kim-Ha et al., 1991), it has been shown to anchor *bcd* mRNA at the anterior (St Johnston et al., 1989) and *osk* mRNA in the posterior of the oocyte (Rongo et al., 1995; St Johnston et al., 1991) and is needed for the basal, actin dependent localization of *prospero* mRNA in neuroblast division during embryogenesis (Li et al., 1997, Shen, 1998 #2702). The function of Staufen in oogenesis is to target the mRNA to the MT network (Ferrandon et al., 1994) and to anchor it at its destination (Micklem et al., 2000). In *osk* mutants lacking the Bruno response element (BRE) in the 3' UTR, Bruno mediated translational repression is alleviated. The resulting bicaudal phenotype in these mutants is less severe in *staufen* mutants, implying a role for Staufen in translational regulation of *osk* mRNA (Kim-Ha et al., 1995). Deletion experiments have shown that dsRBD5 is responsible for translational activation of *osk* (Micklem et al., 2000). Staufen is the first transacting factor that has been shown to mediate both actin and MT mediated localization. Staufen does not seem to have a function in *grk* mRNA localization.

Exuperantia (exu) has been shown to be the transacting factor for localization that has to be recruited by *bcd* mRNA in the nurse cells (Berleth et al., 1988b; Cha et al., 2001; St Johnston et al., 1989)}. Swallow is also required for *bcd* mRNA localization. It has been shown to bind to the Dynein light chain of the Dynein motor complex and suggested to be the adapter to enable the motor complex to transport *bcd* mRNA (Schnorrer et al., 2000).

The recruitment of transacting factors often starts in the nucleus with members of the heterogeneous nuclear ribonucleoprotein (hnRNP) family. hnRNPs are involved in packaging of the RNA and some of them are involved in shuttling the RNA from the nucleus to the cytoplasm (Shyu and Wilkinson, 2000). Many examples are reviewed

in (Johnstone and Lasko, 2001) such as hnRNP A2 in *X. leavis*, involved in *myelin basic protein* mRNA localization and VgRBP60 that binds *vgl* mRNA. In *Drosophila*, an important member of this family, Squid (Sqd), is involved in the localization of *grk* and *osk* mRNA (Norvell et al., 2005; Norvell et al., 1999). Sqd interacts with another hnRNP, Hrb27C/Hrp48 that binds directly *grk* mRNA and binds to Sqd and Ovarian Tumor (Otu) and is required for correct localization of *grk* mRNA (Goodrich et al., 2004). In this thesis I will look into the roles of Sqd in the anchoring of *grk* mRNA and I will discuss this protein in more details in chapter 4. Mutant flies for *K10*, believed to be acting upstream of Sqd, also have an anterior localization of *grk* mRNA and the resulting dorsalised phenotype (Neuman-Silberberg and Schüpbach, 1993; Wieschaus et al., 1978).

1.3.4.1. Translational regulation and axis formation

mRNA localization and translational regulation have to be tightly coupled during oogenesis as ectopic expression leads to polarity defects. This process involves keeping the transcript in translational repressed state until it is localized. At its final site of localization, derepression takes place to allow translation initiation. There are two classes of mutations that affect correct Grk protein expression. In the first class the translational repression during transport is prematurely alleviated and Grk is ectopically translated as seen in *sqd* and *K10* mutants (Kelley, 1993; Norvell et al., 1999; Serano et al., 1995)}. In the second the translation initiation of *grk* mRNA is impaired as seen in *encore* and *vasa* mutants (Hawkins et al., 1997; Styhler et al., 1998; Tomancak et al., 1998).

The 3'UTR of the *grk* transcript is required for translational repression (Saunders and Cohen, 1999). The presence of Bruno response elements in the 3'UTR suggests that Bruno is involved in the translational repression of *grk* mRNA (Kim-Ha et al., 1995). In Bruno overexpression experiments, localized Grk protein levels are reduced even though Grk seems more abundant in the rest of the oocyte (Filardo and Ephrussi, 2003). In addition, Bruno also colocalizes with *grk* mRNA at the DA corner during stage 10 (Webster et al., 1997). Bruno might act through initiation of translation through the eukaryotic initiation factor 4E (eIF4E) as transgenes expressing a constitutively activated version of eIF4E suppress the *bruno* mutant phenotype (Yan and Macdonald, 2004). Bruno has been shown to bind Cup, an eIF4E binding protein,

which is required for the repression *osk* mRNA translation (Nakamura et al., 2004), again pointing in the direction of a role for Bruno in *grk* mRNA translational repression. The fact that Bruno and Sqd interact *in vitro*, suggests that Sqd might link *grk* mRNA to Bruno when the transcript is exported out of the nucleus to prevent premature translation (Norvell et al., 1999). Recent studies in mosaic eggchambers for wild type and sqd^{1X77} revealed that *grk* mRNA originating from nurse cells that do not express Sqd, could localize correctly by recruiting Sqd produced by the wild type nurse cells but that the mRNA in these eggchambers would be prematurely translated along the anterior circumference of the oocyte (Caceres and Nilson 2009). The observation that *grk* transcripts are abnormally regulated in *sqd* germline mosaics, even though these mosaics have the same chromosome complement as *sqd* heterozygotes where *grk* mRNA localization and translation is like in wild type flies, shows that the roles of Sqd in translational repression and localization can be uncoupled. Sqd must function in the nurse cells to regulate the translation of *grk* mRNA in the oocyte cytoplasm (Caceres and Nilson, 2009). Recent pull down experiments confirmed that Sqd forms a complex with Cup, PaBP55B, Imp and HRP48 (Clouse et al., 2008). Clouse *et al.* propose a model in which the translational repression of *grk* mRNA during transport is mediated trough the interaction of Bruno, Cup and eIF4E (Figure 8). Bruno binds to the BREs the 3'UTR of *grk* mRNA and Cup interacts with Bruno in a complex with Sqd, HRP48, Imp and Otu. Cup binds eIF4E competing with eIF4G in binding eIF4E. This interaction of eIF4E and eIF4G is necessary for translation initiation. Once *grk* mRNA is localized at the DA corner, binding of PABP55B to eIf4G increases its binding affinity for eIF4E, facilitating translation initiation. They showed also that PABP55B binds to Encore (Enc) in an RNA independent way (Clouse et al., 2008). Encore is required for activation of *grk* mRNA translation in mid-oogenesis (Hawkins et al., 1997) and heterozygosity for *pAbp55B* is able to enhance the ventralized phenotype in an *enc* mutant background (Clouse et al., 2008). These results show that PABP55B and Encore must act together in activating translation of *grk* mRNA at the DA corner (Clouse et al., 2008). As Encore is the only protein in this process that is not involved in *osk* translational regulation (Van Buskirk et al., 2000), it might be responsible, to a certain extend, for the specificity of *grk* translational control in respect to other mRNAs. Encore is a large protein that colocalizes with *grk* mRNA at the DA corner. This has led to the

hypothesis that it might act as a scaffold protein that helps to mediate the transition from translational repression to activation of *grk* mRNA (Clouse et al., 2008).

Another translational regulation pathway of *grk* mRNA involves Vasa, a DEAD box helicase that is responsible for translational activation of *grk* mRNA via interaction with eIF5B (Johnstone and Lasko, 2004). In *vasa* mutants, *grk* mRNA is slightly mislocalized but more strikingly, the Grk protein levels are drastically reduced (Styhler et al., 1998; Tinker et al., 1998; Tomancak et al., 1998, Van Buskirk, 2000 #3079). Vasa is post-translationally modified in response to a meiotic checkpoint when double stranded break repair is delayed. This results in a downregulation of *grk* translation and polarity defects (Ghabrial and Schupbach, 1999). For the same reason, mutations in the piRNA pathway lead to polarity defects. piRNAs are short interfering RNA with a length of 24 to 30 nt (Bernstein et al., 2001) that have been suggested to work in the silencing of retrotransposons (Aravin et al., 2001; Brennecke et al., 2008; Chen et al., 2007; Kalmykova et al., 2004; Pane et al., 2007; Sarot et al., 2004; Vagin et al., 2006). When the piRNA pathway is compromised, retrotransposon and stellate locus silencing is relieved, the resulting transposition leads to double strand breaks and a checkpoint activation. Chk2 disrupts axis specification by disrupting MT organization and by Vasa phosphorylation (Klattenhoff et al., 2007). Finally, when Grk protein is produced at the DA corner, it signals to the overlaying follicle cells. Cable (Cbl) mediated endocytosis mops up any ectopic signaling of Grk to follicle cells away form the DA corner, restricting Grk signaling to a tight region at the DA corner (Chang et al., 2008).

It is very important for the cell to keep mRNA translationally silent during transport and anchoring until the protein is required for signaling. Interestingly, sometimes the proteins involved in translational repression have also a role in transport itself like Sqd that is required for the second step of *grk* mRNA transport as well as for the silencing of *grk* mRNA during transport (Caceres and Nilson, 2009; Kelley, 1993; MacDougall et al., 2003; Norvell et al., 2005; Norvell et al., 1999). There might be more proteins that have this double function or have a role in anchoring. As these transacting factors interact directly with the RNA, they might be involved in structuring the anchoring complexes.

Figure 8 Model for *grk* mRNA translational regulation

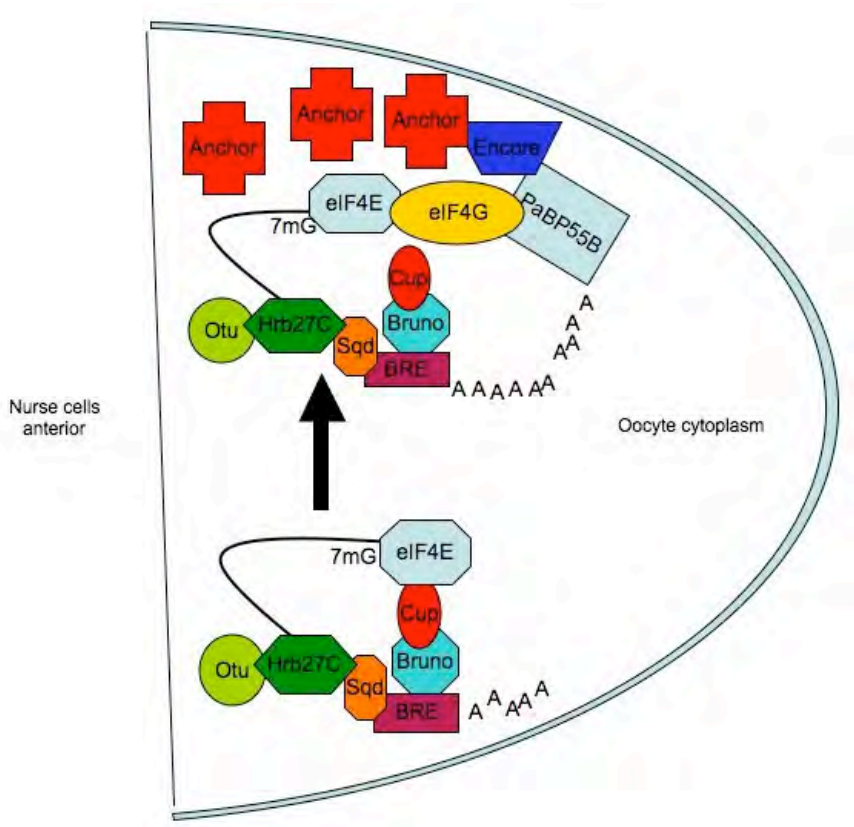

Figure 8 Model for the translational repression of *grk* mRNA during transport

Translational repression of *grk* mRNA before complete localization at the DA corner is mediated by Sqd, Hrp48, Otu and Cup. Once fully localized, PABP55B mediates translational activation of *grk*. Encore could be responsible for the transition from translational repression to activation through association with a cytoplasmic anchor. Redrawn from (Clouse et al., 2008).

1.4. RNA Granules

Nascent RNA is decorated by cap binding proteins, splicing factors and nuclear export factors that allow them to be exported from the nucleus. Once in the cytoplasm, RNA recruits a variety of proteins depending on their fate in the cell. Localizing RNAs will assemble a transport particle containing motor proteins and transacting factors. At their final destination, RNA and regulating proteins appear as a granule that can be seen as a small factory containing the machinery for posttranscriptional regulation. RNA granules are classified depending on function, cell type and composition. Recent discoveries revealed that they are not static entities but that they can change size, composition and even interact with one another (Anderson and Kedersha, 2008). *grk* mRNA is transported in transport particles and anchored in SBs (Delanoue et al., 2007) both RNA containing granules. Why *grk* is anchored in RNA granules and whether its translation is regulated when anchored is not known. In the following I describe the most relevant cytoplasmic RNA granules.

1.4.1. Germ cell granules

Germ cell granules are the oldest example of granules and were first described by Metschnikoff (1865) in the larvae of a fly, *Miastor metraloas* (Metschnikoff, 1865). The dark staining granules observed were later described in other species as polar granules in *Drosophila melanogaster*, germinal granules in *Xenopus laevis* and P granules in *Caenorhabditis elegans* and are required for germ cell specification. The germ cell granules all contain maternal transcripts, RNA helicases, decapping enzymes and translation initiation factors (Anderson and Kedersha, 2006, 2008; Navarro and Blackwell, 2005; Stebbins-Boaz et al., 2004) giving them the ability to initiate translation and control translational and mRNA decay.

1.4.2. Neuronal granules

Neuronal granules contain translationally silent mRNAs that are transported to dendritic synapses where they need to be rapidly available for translation upon exogenous stimuli (Krichevsky and Kosik, 2001). Beside mRNA they contain small and large ribosomal subunits, translation initiation factors and RNA binding proteins that regulate mRNA function. Even though the neuronal granules contain these components, mRNAs in neuronal granules are translationally silent until they reach

the synapse and are transported to the dendrites via Kinesins (Hirokawa and Takemura, 2005; Kanai et al., 2004). *CamKIIα, β-actin, MAP2* and *BC1* mRNA are the most intensively studied examples of transcripts that are transported in the neuronal granules (Smith, 2004).

1.4.3. Stress granules

Several external factors such as heat, ischemia, oxidative stress or viral infection makes the cell go into an emergency translational arrest resulting in a disassembly of the polysomes (Anderson and Kedersha, 2002). In response to stress, the cell activates a process of molecular triage of the mRNAs that are leaving the disassembling polysomes (Anderson and Kedersha, 2002, 2006). This triage determines whether the RNA will be degraded or will reenter translation when stress is alleviated. The stress granules (SG) are a mere morphological consequence of the sudden recruitment of proteins involved in this triage process (Anderson and Kedersha, 2002). SGs have long been thought to be a static dumping place for the mRNA upon stress but recent studies show that they are very dynamic structures that interact with sponge bodies (see below) actively sorting the mRNA (Anderson and Kedersha, 2008). The assembly of SGs happens in distinct phases in which different classes of proteins are recruited. Typically it starts with a stalled initiation caused by stress or eIF4A inactivation (Anderson and Kedersha, 2008). Several eIF2α kinases sense stress and are responsible for eIF2α phosphorylation (Harding et al., 2000a; Harding et al., 2000b; Kawai et al., 2004; Srivastava et al., 1998; Wek et al., 1995). This leads to a reduced level of eIF2-GTP-$tRNA_i^{Met}$ that is required for cap-dependent initiation of translation (Anderson and Kedersha, 2002). As a consequence, internal ribosome entry site (IRES) containing mRNAs are translated in stressed cells, as their initiation is cap-independent (Robert et al., 2006). eIF2α phosphorylation leads to stalled initiation complexes and the formation of non canonical 48S mRNP complexes and a ribosome run-off (Kedersha et al., 1999). Drugs such as cycloheximide that inhibit translation elongation will prevent SG assembly, drugs like puromycin that cause premature termination cause SG assembly (Kedersha et al., 2000). The second stage of SG formation is called the nucleation in which 48S complexes recruit SG nucleation proteins. These proteins are involved in mRNA stabilization and translational silencing. Some examples are G3BP, TTP, FMRP, CPEB Ago2,

Pumilio, RCK, Smaug and TIA-1 (Anderson and Kedersha, 2008). Once the nucleation is initiated, SGs recruit the rest of the proteins that are typical for their composition such as eIF3m eIF4F, PABP-1 and small ribosomal subunits (Anderson and Kedersha, 2008). In the third phase or secondary aggregation and crosslinking, PABP-1 that is bound to the polyA tail of the transcripts is aggregating the smaller SG nuclei and progressively forms microscopically visible SGs(Kedersha et al., 2000). In the 4th phase or tertiary recruitment, non-RNA binding proteins are recruited and mRNA sorting is starting to occur. This recruitment is also called the piggyback recruitment phase (Yang et al., 2006; Yu et al., 2007). Finally mRNA undergoes Triage in the 5th phase. Several RNA binding proteins can escort specific mRNAs between SGs and PBs (Anderson and Kedersha, 2008). SGs disassemble in a rapid dispersion of the proteins rather than a fragmentation (Kedersha et al., 2000; Kedersha et al., 2005).

1.4.4. Processing bodies

Processing bodies or P bodies are distinct cytoplasmic entities that differ from SGs mainly in that they do not require eIF2α phosphorylation for their formation (Kedersha et al., 2005). Typically the PBs are the site of RNA silencing and decay. They contain the machinery for general mRNA decay such as deadenylase CCR4, decapping enzymes and enhancer complexes DCP1/2, Human enhancer of decapping large subunit Hedls, hEdc3 and RCK or p54 (Bashkirov et al., 1997; Eystathioy et al., 2002; Ingelfinger et al., 2002). 5' to 3' degradation occurs thanks to the presence of XRN1 (Cougot et al., 2004). Proteins such as SMG5, SMG7 and UPF1 represent the nonsense mediated decay surveillance pathway. Lsm1-7 form a heptamer that regulate nonsense mediated decay proteins and RNP assembly (Ingelfinger et al., 2002; Unterholzner and Izaurralde, 2004). Mammalian cells typically contain components of the RNA induced silencing complex, a property they do not share with budding yeast (Liu et al., 2005a; Liu et al., 2005b; Sen and Blau, 2005). The Argonaut proteins and miRNA are the key components in this process as well as GW182, an RNA binding protein that binds Ago and takes part in the miRNA dependent silencing pathway are found in P bodies (Liu et al., 2005b; Sen and Blau, 2005). Although a lot of these components do not exist in yeast, knocking them down does impair PB function. The presence of eukaryotic initiation factor eIF4E and the RNA helicase p54/RCK which silences translation, suggests the role of PBs in translational

regulation (Cougot et al., 2004; Kedersha et al., 2005). PBs also contain a variety of RNA binding proteins that have been linked to mRNA translation and decay. Examples of these are TTP, BRF1, CEPB, 4-ET and Smaug (Anderson and Kedersha, 2006). RNA mediated silencing and decay in P bodies were intensively studied in *Saccharomyces cerevisiae* that do not contain SG. Many of the yeast PB components overlap with mammalian SG components and they share many properties. Both RNPs increase in size and number in response to stress (Teixeira et al., 2005) and both contain mRNA that are in equilibrium with the polysomes (Brengues et al., 2005). Polysome disassembly by overexpression of *Dhh1* and *Pat1* causes PB assembly in yeast cells (Coller and Parker, 2005) in a similar way as Puromycin treated cells form SGs in mammalian cells (Kedersha et al., 2000).

Interestingly, *Schizosaccaromyces pombe* assembles SG like structures under heat-induced stress (Dunand-Sauthier et al., 2002) that contain eIF3, eIF4A and RNA. It is tempting to suggest an evolutionary link between PBs and SGs.

PBs and SGs share a lot of components but are distinct structures. They interact with each other in response to stress. Real-time fluorescence imaging shows volatile PBs docking to the more stable SGs(Kedersha et al., 2005). Anderson *et al.* propose a model in which SGs act as mediators between polysomes and PBs. In their model SGs are acting as active triage modules for the mRNA to be sorted in mRNA that has to be degraded and others that have to remain translationally silent (Anderson and Kedersha, 2008).

1.5. Sponge bodies

Sponge bodies are a structure in *Drosophila* egg chambers. They were first described by Wilsch-Brauninger *et al*. as a subcellular structure involved in the assembly and transport of *cis*- and *trans*-acting elements involved in mRNA localization. They discovered this structure by EM searching for the function Exuperantia in the localization of *bicoid* mRNA in the oocyte. They found that Exu was highly enriched in a sponge like structure that consisted of ER like cisternae embedded in an amorphous electron dense mass of proteins. Sponge bodies are not surrounded by a membrane and are often associated with mitochondria. It was found that they contain mRNA in general and that Exu is found in them but is not a structural element as SBs still occur in mutant

oocytes and their morphology is unchanged. Colchicine treatment showed that MTs are not a structural component of SB. EM study revealed that SBs surround Vasa containing Nuage particles. Nuage Particles are EM dense RNPs in the germline of which the function is still obscure and that are conserved throughout the animal kingdom. Some authors believe them to be the precursors of the Polar Granules because they share key components such as Vasa, Tudor and Aubergine (Findley et al., 2003). The fact that SBs are associated with mitochondria and Vasa containing structures suggests that they are the orthologue of the mitochondrial cloud in the *Xenopus* oocyte, believed to give rise to the germinal granules. Interestingly, in *Drosophila* it is the Vasa containing nuage that is believed to be the precursor of polar granule (Wilsch-Brauninger et al., 1997). We recently have shown by IEM that *grk* mRNA is anchored in SBs (Delanoue et al., 2007). It is not known why *grk* mRNA is anchored in these structures as opposed to continuous transport like *bcd*. Grk protein signals in early oogenesis to the posterior follicle cells and later to the follicle cells at the DA (Gonzalez-Reyes et al., 1995; Neuman-Silberberg and Schüpbach, 1993). It is not known if *grk* is also anchored in SBs at the early stages or if *grk* is translated in SBs. SBs have only been described in *Drosophila* oocytes. SBs have been named after their appearance on EM micrographs rather than their function. The exact nature of SBs is not known. It has not been investigated if they are similar to any of the more common granules but are sometimes referred to as PBs (Lin et al., 2008). It is important for the understanding of the function of SBs as well as our understanding of anchoring that the nature of SBs is better characterized. For example: what are the factors involved in anchoring? Is the main difference between *grk* RNA and *bcd* RNA that *grk* has a second transport step towards the DA corner or is it the capacity to anchor that makes it accumulate to the DA corner? This thesis tries to address whether SBs are indeed the PBs of the oocytes and how the translation of *grk* mRNA is relates to these SBs.

Figure 9 Sponge body visualized with different EM techniques

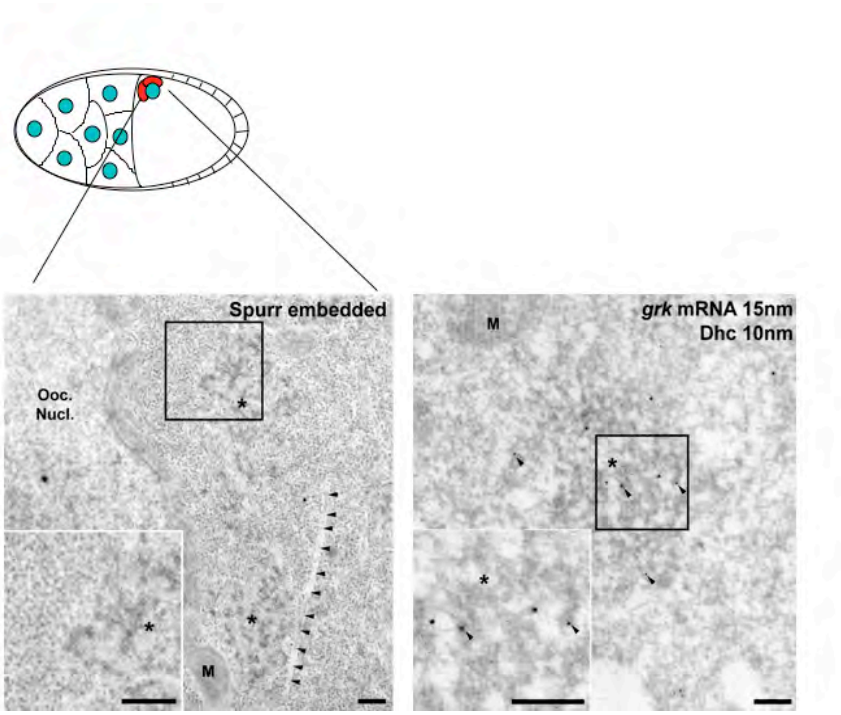

Figure 9 Sponge body visualized with different EM techniques

The appearance of SBs in EM micrographs taken from Spurr (resin) embedded oocytes and cryosections of oocytes combined with immunolabeling. The contrast in the Spurr embedded oocytes is much higher but does not allow for antibody labeling. (*) SB, (arrowhead) MT in the Spurr embedded oocyte, Dhc labeling in the cryosection, (M) Mitochondria, (Ooc. Nucl.) Oocyte nucleus. Scale bar 200nm. Pictures taken from (Delanoue et al., 2007).

1.5. Aims

In this thesis I investigate the roles of the Dynein motor in the anchoring of *grk* RNA at the DA corner in stage 9 oocytes. I approach this by looking at anchoring in mutants for the Dynein cofactors Egalitarian and Bicaudal D (Chapter 3). I also develop of a new assay to study the roles of transacting factor hnRNP Squid in anchoring of *grk* RNA (Chapter 4). In Chapter 5 I study of the nature of Sponge Bodies and their relation to Processing Bodies. Furthermore I look at the role of Sponge Bodies in *grk* RNA translation and try to develop a tool to study the timing of *grk* RNA translation (Chapter 6). Finally I study *I* factor RNA anchoring at the dorso-anterior corner and determine whether *I* factor RNA anchors in Sponge Bodies and whether these are the same as for *grk* RNA (Chapter 7).

2

Materials and Methods

2.1. Molecular work

2.1.1. Solutions and reagents

All recipes for solutions can be found in Molecular Cloning, A Laboratory Manual (Sambrook et al., 1989), unless stated otherwise. Chemicals used for buffers and solutions were bought from Sigma, BDH and Fisher unless stated otherwise.

Restriction enzymes were obtained from Roche or New England Biolabs. T7, T3 and SP6 polymerases, phosphatases and ligases were bought from Roche or Promega. DNAse and RNAse inhibitor were obtained from Promega. RNAse A was bought from Sigma. All enzymes were used according to the manufacturers instructions.

Phosphate buffer saline (PBS), Luria Betani medium (LB), LB-agar plates with Ampicilin or Kanamycin were prepared by the Swann building media kitchen (Edinburgh) and or by the Rodney Porter media kitchen (Oxford), according to the following recipes. PBS contained 8g NaCl, 0.2g KCl, 1.44g Na_2HPO_4 0.24 g KH_2PO_4 per liter H_2O and the pH was adjusted to 7.4 with concentrated HCl. LB buffer contained 10g Difco Bacto Tryptone 10g Difco Bacto Yeast Extract, 5g NaCl per liter. LB agar plates contained 16g Difco Bacto Tryptone, 10g Difco Bacto Yeast Extract, 5g NaCl and 15g agar per liter.

2.1.1.1. Antibodies

Antibody	Animal	Application	Dilution	Source	Reference
anti-Sqd A 2G9	Mouse	WB, injection	1/1000 and 20mg/ml	T. Schupbach	
anti-Sqd A 1B11	Mouse	injection	20mg/ml	T. Schupbach	
anti-GFP G6539	Mouse	Injection	25mg/ml	Sigma Aldrich	(Delanoue et. al, 2007)
anti-Grk 1D12 concentrate	Mouse	IF, IEM	1/100, 1/20	Developmental Studies Hybridoma Bank	(Queenan et al.,1999)
ECL Mouse IgG HRP-linked	Sheep	WB	1/5000	GE Healthcare Life Sciences	
ECL Rabbit IgG HRP-linked	Donkey	WB	1/5000	GE Healthcare Life Sciences	
Alexa Fluor 488 goat anti-Rabbit IgG	Goat	IF	1/500	Molecular Probes	
Alexa Fluor 546 goat anti-Rabbit IgG	Goat	IF	1/500	Molecular Probes	
Alexa Fluor 488 goat anti-Mouse IgG	Goat	IF	1/500	Molecular Probes	
Alexa Fluor 568 goat anti-Mouse IgG	Goat	IF	1/500	Molecular Probes	
Alexa Fluor goat 488 anti-Rat IgG	Goat	IF	1/500	Molecular Probes	
Alexa Fluor goat 568 anti-Rat IgG	Goat	IF	1/500	Molecular Probes	
Anti-Dynein	Rabbit	IF, WB, IEM	1/1000, 1/1000, 1/300	Eurogentec	
anti-Me31B monoclonal	Mouse	IEM	1/1000	Nakamura	
anti-Me31B	Rabbit	IEM	1/100	Nakamura	(Nakamura et al., 2001)
anti-Mouse	Rabbit	IEM	1/250	Dako	
anti-rat	Rabbit	IEM	1/300	Dako	
anti-biotin	Rabbit	IEM	1/10000	Rockland	
anti-Dig-Alkaline-Phosphatase	Sheep	IEM	1/500	Roche	

Anti-Dig-POD Fab fragments	Sheep	ISH	1/500	Roche
anti-GW182	Rat	IF	1/250	E. Izzauralde
anit-Tral	Rat	IF	1/250	E. Izzauralde
anti-GFP A6455 polyclonal	Rabbit	IEM	1/200	Molecular Probes
PolyA gold conjugates		IEM	Batch specific	Cell Microscopy Centre, Utrecht

2.1.2. Growth of bacterial cultures

Plasmid DNA was amplified in XL1 Blue heat-shock competent cells. These XL1 Blue cells were made using the $CaCl_2$ protocol described in Sambrook et al. (Sambrook et al., 1989). A 100µl aliquot of cells was thawed on ice and transformation of up to 100ng of DNA was done by a heat-shock at 42°C for 1 minute after they had spend 30 minutes on ice. After a short recovery of 2 minutes on ice, 750µl of LB medium was added and cells were incubated shaking at 37° for 1 to 2 hours. Cells were plated on LB agar plates complemented with the appropriate antibiotic for plasmid selection. Ampicilin was used at 50µg/ml, Kanamycin at 50µg/ml and Chloramphenicol at 170µg/ml. After incubation for 24h at 37°C separate colonies were picked and inoculated in LB medium with antibiotic for overnight culture. Mixing 0.5ml of a 60% sterile glycerol solution with 0.5ml culture in log phase provided a glycerol stock. The mixture was frozen in liquid nitrogen and stored at -80°C. Once a glycerol stock was made, cultures for plasmid amplification could be inoculated straight from the frozen stock.

2.1.3. Plasmid and DNA purification

All plasmid DNA and PCR products were cleaned up with Quiagen kits following the manufacturers instructions.

2.1.4. RNA *in vitro* transcription for injections

Fluorescently labeled sense RNA for injection was made by incorporating Alexa Fluor 488-5-UTP or Alexa Fluor 546-5-UTP in the RNA. Alexa Fluor labeled UTPs were bought from Molecular Probes and Digoxigenin (DIG) and Biotin labeled RNA was made using Roche labeling kits containing DIG or Biotin conjugated to UTP. The conditions used in these reactions are as follows. Fluorescently labeled sense RNA was transcribed in 50µl reaction volume consisting of 5µl transcription buffer, 1-3ug of linearised plasmid, 2 units of polymerase T7, T3, or SP6 depending on the plasmid used, 0.4mM ATP, 0.4mM CTP, 0.36mM UTP, and 0.04mM Alexa UTP, 0.12 mM GTP and 0.3 mM 7mG(‘5)ppp(5’)G CAP analogue, 40 units of RNAse inhibitor and 30mM DTT. DIG and Biotin labeled RNA was made in the same volume with a

different concentration of UTPs being 1mM ATP, 1mM CTP, 1mM GTP, 0.65 mM UTP, 0.35 mM biotinylated UTP and 2.4mM 7mG(‘5)ppp(5’) CAP analogue.
The DNA was transcribed for 2 hours at 37°C and 1µl of this reaction was run on a 1% agarose gel to check for degradation and quantity of the transcript after which the DNA template was digested for 5 minutes with 2 units of DNAse I (Promega). Unincorporated nucleotides were then removed on a Roche G50 spin column following the manufacturers instructions. The RNA was precipitated with 1/5 volume Ammonium Acetate and 2.5 volumes 100% Ethanol. The RNA was left to precipitate over night at -20°C or 30 minutes at -80°C. The RNA was spun down for 30 minutes and the pellet washed in 70% Ethanol. RNA was reconstituted in 6-15µl dH_2O depending on the amount detected on the agarose gel.

2.1.5. RNA *in vitro* transcription for *in situ* hybridization

DIG and Biotinylated labeled antisense probes were made with a Roche DIG or Biotin labeling mix. The reaction was performed in 20µl and composed of 1 µg linearised template, 1mM ATP, 1mM CTP, 1mM GTP, 0.65mM UTP, 0.35 mM biotinylated UTP, 40mM Tris-HCl, pH 8.0, 6mM $MgCl_2$, 10mM dithiotreitol (DTT) and 2mM spermidin. Transcription was allowed for 2 hours at 37°C after which the quantity and quality was checked on a 1% agarose gel. Cleanup and was done in the same way as for RNA for injections. The probe was reconstituted in 49µl H_2O and 1µl RNAse inhibitor (Promega).

2.1.6. RNA transcription for RNAi knockdown experiments

Primers were designed with a T7 promoter site overhang (see addendum). The DNA was amplified from a Plasmid of the DCG collection by PCR. The PCR product was transcribed with a T7 Megascript high yield transcription kit from AMBION. The transcription reaction was incubated at 37°C for 4 hours. After transcription, the reaction was purified by Phenol Chloroform (1:1) extraction, followed by a Chloroform extraction. The aqueous phase was recovered and the RNA was precipitated with 1 volume of Isopropanol. The mixture was chilled for 30 minutes at -20°C and centrifuged at 14000g at 4°C for 15 minutes. The pellet was left to dry on the air and resuspended in dH_2O. To anneal the sense and antisense strand, the RNA was boiled on a heat block for 15 minutes and left to cool down to room temperature

in the same heat block after switching it off. Double stranded RNA was stored at -20°C. The concentration was estimated by using a spectrophotometer in a quartz cuvette at an absorption wavelength of 260nm.

2.1.7. Western Blotting on ovary extract

Ovary extracts were made by crushing 10 pairs of ovaries in 200µl of 1x extraction buffer (EB) with a plastic pestle. EB was made of 20mM Tris pH 8.00, 100mM NaCl 2mM DTT and protease inhibitor in H_2O. To prevent protein degradation, the extract was kept on ice at all times. The sample was spun down for 5 minutes at 14000g to separate the extract in three liquid phases: yolk, proteins and cell debris**.** The middle phase with the proteins was isolated with a pipette and after another 5 minutes spin at 14000g the concentration of the protein extract was estimated by means of a Bradford test. The calibration curve was made with bovine serum albumin as a standard. The extract was denatured for 3 minutes at 95°C and spun again. The extract was run on a SDS polyacryamide gel made following the recipe in Molecular cloning, a laboratory handbook (Sambrook et al., 1989) and run in Tris-Glycine buffer (15.1g Tris buffer, 94g Glycine, 50ml of 10% SDS). Typically the resolving gel was pH8.8 and the stacking gel had a pH of 6.8. Alternatively precast NuPAGE Bis Tris gradient 4-12% gels from Invitrogen were used and run in MOPS (10x, Invitrogen) buffer. The proteins were transferred onto optitran reinforced nitrocellulose membrane (Schleicher and Schuell) overnight at 4°C with an ice pack at 30V 90mA. The membrane was blocked in 5% milk in TTBS (Tween Tris Buffer Saline) for 1 hour. TTBS was made up as a 10x solution. The 1x solution consisted of 5mM Tris and 15mM NaCl and 0.5% Tween20 (v/v). After this the primary antibody was incubated in 2% milk in TTBS for 45 minutes followed by a wash in 2% milk in TTBS. Secondary antibody was conjugated to horseradish peroxidase 1:5000. After washing in TTBS, an enhanced chemiluminescent detection (ECL) kit (Amersham) was used to visualize the protein bands on light sensitive film (Kodak). Negatives were developed by hand in developer for 1 to 2 minutes and fixed in fixative in the dark room.

2.1.8. Western blotting on S2 cells

$1x10^6$ Cells were lysed in lysis buffer (50 mM Tris-HCl, 150 mM NaCl, 1% Nonidet P-40, pH 7.8) at 37°C for 15 minutes. This extract was run on a 5% SDS PAGE resolving gel pH8.8 with a stacking gel with pH 6.8. The gel was run in Tris-Glycin buffer to resolve the 530 kDa Dynein heavy chain. The proteins were transferred on a optitran reinforced nitrocellulose membrane overnight at 30V, 90mA at 4°C. Antibody staining and visualization of the proteins was done in the same way as for ovary extracts.

2.1.9. PCR

Standard conditions for a 50µl reaction were used, as follows. 50ng template DNA, 5µl of 10XPCR buffer containing 15mM $MgCl_2$, 500Mm KCL and 100mM Tris-HCl (Roche), 0.2mM Utlrapure dNTPs (Roche), 1mM Primer each (MWG) and 2.5 Units Taq Polymerase (Roche).

2.1.10. Concentrating antibodies

Antibodies were concentrated with a vivaspin 500 polyethersulfone membrane (Sartorius) with a 30kDa cut off at 12000g until the volume was sufficiently reduced.

2.2. *Drosophila* Protocols

2.2.1. *Drosophila* fly stocks

All fly strains were initially kept on standard yeasted cornmeal-agar medium at 21°C. 1litre was made up of 10.7g Agar, 78.6g Glucose, 44.3g Brewers yeast, 71.4g Maize meal, 5.7g Fermipan Yeast, 2.7g Nipagin in 20ml of Ethanol and 3.2 ml Propionic acid. The medium is boiled and cooled to 40°C before pouring into bottles or vials to set). Due to a move of the lab, the last 16 months an altered recipe was used (1l consisted of 4.68g agar, 46.8g maize meal, 8.31g soy meal, 14.8g yeast, 46.8g malt, 46.15ml molasses, 5.06ml Propionic acid, 0.324ml Orthophosphoric acid and 30ml of a 10% Nipagen in Ethanol solution).

For injections of living egg chambers, flies were kept at 25°C at low density and well fed conditions. Flies were kept for 2-3 days on medium and instant yeast (Fermipan)

after eclosion before dissection to enrich the ovaries with healthy stage 9 eggchambers.

2.2.2. Fly strains

The wild type strain used was *OregonR* and was originally obtained from Bloomington stock centre and has been used in the lab for many years.

The *sqd*^{1} allele is described in Kelley (1993) (Kelley, 1993) and the *sqd*^{1}*/TM3, Sb* flies were a gift of given to us by Trudi Schupbach. Homozygote flies for the *squid1* allele were carefully selected as *sqd*^{1} has a bristle phenotype of its own.

The *squidGFP* flies were created in a protein trap mutagenesis screen (*squid::GFP line 44-1*) and were given to us by Alain Debec (Norvell et al., 2005).
me31BGFP is a line obtained from Nakamura and is an insertion on the X chromosome (Nakamura et al., 2001).

w^{+}*; grk*^{2b6}*/Cyo and w*$^{+}$*; grk*^{2E12}*/Cyo* were obtained from T. Schupbach. The heteroallelic combination in the F1 offspring of the cross between these flies was used for *grk* null experiments as described in Neuman-Silberberg et al. (Neuman-Silberberg and Schüpbach, 1993).

dhc64C$^{6-6}$*/TM6B, Tb, Hu and dhc*$^{6-12}$*/ TM3, Ser* originate from T. Hays' lab. They were used to generate heteroallelic flies to study Dynein function in P-bodies.

The *Bic-D* mid-oogenesis mutant (*Bic-D*^{mom}) flies were generated by the following cross described in (Swan and Suter, 1996): *w; Df(2L)TW119/CyO; P[w+hsBic-D]-94/+×w;Bic- D*^{r8}*/CyO.* From late third instar larvae on, the offspring *was* given two 37°C heat shocks of 30 minutes per day, lasting for 3 to 4 days to rescue the *Bic-D* null mutation. The *Bic-D*^{r8}*/Df(2L)TW119; P[w+hsBic-D]-94/+ (Bic-D*^{mom}*)* flies were then dissected and injected to study Bic-D function in transport and anchoring. These flies were a gift from Beate Suter.

egl^{wu50}*/Cyo* was described in (Schupbach and Wieschaus, 1991) and *egl*^{3e}*/Cyo* was generated by Ephrussi and Pelegri (Pelegri and Lehmann, 1994) both strains were a

gift from Mary Bownes. The heteroallelic combination of these flies was used to study the role of Egalitarian in transport and anchoring.

G413/Cyo; *G147/TM3* were used for the negative control for RNAseA injection in chapter 5 and were a gift from the Rorth lab. They contained to GFP insertions that originate from a gene trap screen (Morin et al., 2001). The flies contained 2 GFP insertions *G413* and *G147* which correspond to BasiginGFP and JupiterGFP respectively.

2.2.3. Microinjection of oocytes

Ovaries were dissected on a 24x50mm coverslip #1 (VWR) in thoroughly oxygenated halocarbon oil series 95 (KMZ Chemicals Ltd). Dissection of the egg chambers consists of pulling at the germarium and slide the detached ovariole in the oil over the glass surface aligning them for injection. In this way oocytes could be kept alive up to 2 hours. The physical friction is removing all cell debris and tissue surrounding the ovariole making imaging easier. Lined up oocytes were injected with an Eppendorf Femtotip needle by use of a piezo-controlled micromanipulator (Burleigh). The pressure line was based upon Tritch components with a Zeiss needle holder. The pressure to inject came from a Nitrogen gas cylinder and was usually between 3 and 5 Bar.

2.2.4. Dissection of Macrophages

Concanavalin A (ConA) coated coverslips 24x24 mm coverslip #1 were glued to a custom made steel sample holder with silicon grease. The sample holder was made out of a 2mm thick stainless steel measuring 75 x 25 mm with a 20mm hole drilled in the middle. The coverslips were then covered with 200µl of Schneiders medium complemented with 10% heat inactivated (1 hour at 68°C) bovine calf serum (Gibco). Third instar larvae were thoroughly washed in PBS. Macrophages were obtained by rupturing the cuticle of the washed larvae into the Schneiders medium. A piece of semi permeable membrane was put on top of the medium to prevent evaporation. The sample was then incubated in a humidity chamber made of a petridish with wet filter paper. The macrophages were allowed to spread on the Concanavalin A for minimum 30 minutes before further fixing.

2.2.5. Schneider Cell culture

Schneider cells used were of the S2 strain and were inoculated at a density of $1.2x10^6$ to $4x10^6$ cells/ml in Schneiders insect medium (Sigma) complemented with 10% heat inactivated (1 hour at 68°C) fetal calf serum (Gibco). The S2 cell line originated from a primary culture of late stage (20-24 hours old) *Drosophila melanogaster* embryos (Schneider, 1972). Cells were grown at 25°C in Falcon tissue culture flasks and checked daily for cell growth and density. Cell cultures were reinoculated in fresh medium when cells were detaching from the coated surface and started to grow in suspension. This passaging was done by knocking the flask on the table to detach the cells and after mixing them by pipetting up and down several times, they were counted in an improved Neubeuer cell counter. The cells were reinoculated in fresh medium at a density that was never below $1X10^6$ cells/ml.

2.2.6. Adhering Schneider cells to conA coverslips

S2 cells were counted in an improved Neubeuer cell counter. ConA coated coverslips were covered with a cell suspension of 2 to 6 x 10^5 cells. Cells were allowed to adhere for 1 hour before fixing and immunostaining.

2.2.7. RNAi knockdown experiments in Schneider cells

To avoid concentrating the cells by spinning them down, the supernatants of adherent cells was carefully reduced to roughly 2 ml before detaching and counting them. This drastically improves survival of the cells. Cells were counted and a $1x10^6$ cells/ml suspension was made in serum free Schneiders medium. 15μg of double stranded RNA was then added in 1 ml of cell suspension. After 1 hour of starvation at room temperature, 2ml of medium complimented with fetal calf serum was added and cells were incubated at 25°C. Samples were taken at day 4 and 5 after transfection.

2.2.8. *In situ* hybridization of *Drosophila* oocytes

In situ hybridizations were performed as previously described by Tautz and Pfeifle (Tautz and Pfeifle, 1989) and Wilkie *et al.* (Wilkie et al., 1999). Dissected oocytes were fixed for 20 minutes by adding a 4% PFA in PBS solution. Oocytes were

carefully detached from the coverslip and transferred to a glass dissection cup for washing. The oocytes were rinsed for minimum 3 times 10 minutes in PBT (PBS, 0.1%Tween 20 (v/v)) or until most of the Halocarbon oil was removed. The samples were stored in 100% Methanol for at least 2 hours at -20°C. They were rehydrated through a series of Methanol/PBT dilutions with decreasing Methanol concentrations for at least five minutes each. The oocytes were then postfixed for 15 minutes in 3.7% Formaldehyde/PBT and washed 5x5 minutes in PBT to remove all traces of fixative. Ovaries were then washed in hybridization buffer/PBT (1:1) for 10 minutes and transferred into hybridization buffer for another 10 minutes. Hybridization buffer consisted of 50% deionised formamide, 5x SSC, 50µg/ml heparin, 0.1% Tween 20 (v/v) (in nuclease free H_2O and pH adjusted to 6.5 with concentrated HCl). Prehybridization was carried out in hybridization buffer with added *E. coli* tRNA (100µg/ml) at 70°C for at least 2h. Hybridization was carried out overnight at 63°C with DIG labeled probe in hybridization buffer complemented with tRNA. The oocytes were then washed two times in hybridization solution for 30 minutes at 63°C, one in PBT/hybridization solution for 30 minutes at 63°C and four in PBT at RT for 30 minutes each. DIG labeled probes were detected by incubation with anti-DIG antibody conjugated to horseradish peroxidase (HRP)(sheep antiDIG-POD Fab fragment, Roche) for 2 hours at room temperature (1:1000 in PBT). Egg chambers were washed 2x30 minutes and the HRP coupled antibody was visualized by incubation with tyramide cyanine-3 (cy3) in amplification buffer (1:50) (TSA Direct, NEN Life sciences, UK or Molecular Probes). The reaction was allowed to proceed for 5 minutes before washing with PBT (3x10min). Egg chambers were then stained with DAPI and mounted with Vectashield.

2.2.9. Immunofluorescence of *Drosophila* oocytes

Drosophila oocytes were dissected and fixed as described above. After rinsing the halocarbon of, three washes were performed in PBS/Tritonx100 0.3% (PBTrx) for five minutes each to permeabilize the membranes. The oocytes were blocked in 10% NGS in PBTrx for two hours. Incubation with the primary antibody was carried out overnight at 4°C on a shaker. After three 20 minute washes, oocytes were incubated with a secondary antibody coupled to an Alexa fluorochrome (Molecular probes). Incubation with the secondary antibody was carried out at room temperature for two

hours. After washing 3 times in PBS and a DAPI staining in PBS, ovaries were mounted in Vectashield medium.

2.2.10. Immunofluorescence on macrophages and S2 cells

Concanavalin A coated coverslips with adherent cells were transferred to a 6-well plate. Fixative was freshly made as a 90% Methanol, 4%PFA and 5mM NaHCO3 pH9 solution and cooled on dry ice for at least 30 minutes. The cells were fixed by adding 3ml of the fixative on the cells with a prechilled 5ml Gilson tip. The 6-well plate was then transferred onto dry ice in a closed Styrofoam box for 15 minutes. The cells were then allowed to warm up to room temperature for 15 minutes before rinsing twice with PBS. Cells were blocked in a 10% BSA/PBT solution for 1 hour. Immunostaining was done by incubating the coverslips cells down on top of a 200µl drop of antibody solution on parafilm. The primary antibody was incubated for 1 to 4 hours. After this the cells were rinsed in PBS in a 6-well plate the secondary antibody was incubated for 2 hours. The coverslips were washed in 3 times PBS for 10 minutes and DAPI was added in the last wash. The coverslips were rinsed in distilled water Before mounting in Vectashield.

2.3. Light Microscopy

All imaging was done on a Deltavision widefield microscope (Applied Precision Inc.) based on an original design by Sedat and Agard. The setup is composed of an Olympus IX70 inverted microscope combined with a cooled CCD camera (Roper Coolsnap HQ, 12 bit camera). 100X magnifications were taken with an objective with a numerical aperture of 1.35. Immersion oil with refractive index 1.515 for fixed samples and 1.534 for Halocarbon oil mounted samples was used to minimize spherical aberration. The filter sets used were Sedat Quad set (Chroma) and a custom EGFP or YFP set (Olympus). The imaging software controlling the microscope hardware was Softworx. Out of focus light was reassigned to its original source using iterative deconvolution algorithms (Davis, 2000).

2.3.1. Concanavalin A (ConA) coated coverslips

24mmX24mm coverslips were cleaned by washing them twice in dH_2O for 10 minutes. Hereafter they were soaked in 0.5M HCl for 1 hour. After 3 washes of 10 minutes with ddH_2O, the coverslips were soaked in 100% Ethanol for 30 minutes. The

coverslips were than dipped in a 0.5mg/ml ConA (Patricell ltd.) solution in dH_2O. Dipping was initially done individually until a coating rack (EMS) was bought. The excess ConA solution was drained with Wattman filterpaper and the coverslips were left to dry in a laminar flow cabinet. The shelf life of the coverslips was considered to be 3 months at room temperature.

2.4. Electron Microscopy (EM)

2.4.1. Sample preparation for Cryosectioning

Oocytes were dissected as described for microinjection. After injection and incubation cells were fixed by adding a drop of 2% Paraformaldehyde (PFA) (EM grade), 0.2% Glutaraldehyde (GA) in a 0.1M Phosphate buffer pH7.4. The Phosphate buffer was made as a 0.2M stock solution at a pH 7.4 by mixing a 4.15% (w/v) Na2HPO4 and 0.62% (w/v) NaH_2PO4 solution. Fixing was done for over 3 hours up to overnight. Ovarioles were carefully recovered from the coverslip and washed until all halocarbon oil was removed in a 1% PFA in 0.1M Phosphate buffer. Oocytes were kept in this 1% PFA solution until imbedding into gelatin for cutting. In case of *in situ* hybridization, oocytes were fixed in a 4% PFA solution in Phosphate buffer.

2.4.2. Gelatin embedding

Oocytes were stained with a drop of toluidine blue solution and embedded in 10% food grade gelatin. Toluidine blue is a basic dye and used as a quick stain for light microscopic "orientation sections" used by electron microscopists. The gelatin was made up by dissolving 10g pork skin gelatin powder (Sigma) in 75ml 0.1M phosphate buffer. After stirring for 10 minutes at room temperature the solution was heated to 68°C for 4-6 hrs. When the gelatin had dissolved the solution was cooled down to 37°C and 200µl of a 10% azide solution was added. This was then complemented to 100ml. The homogenous 10% gelatin solution was poured into 5ml vials and stored at 4°C until use.

For embedding the oocytes were transferred to a droplet of gelatin on a microscope slide coated with parafilm. To keep the gelatin in liquid phase, this had to be done on a stretching table at 37 to 40°C. After transfer into the gelatin, the slide was removed from the stretching table. After 10 seconds at room temperature, a piece of parafilm was placed on top of the gelatin droplet to create a flat surface. The slide was then

transferred on ice and small cubes of approximately 1mm^3 containing the oocyte were cut out of the gelatin. The blocks were then desiccated overnight in 2.3M Sucrose solution at 4°C while constantly stirring on a wheel. The Sucrose acts as a cryoprotectant preventing the formation of ice crystals in the sample. The desiccated gelatin blocks were mounted on an aluminum pin (rivet) in the cold room and transferred into liquid nitrogen. Samples were stored in specially designed sample containers at -196°C. The design of these containers can be obtained from the CMC Utrecht.

2.4.3. Cryosectioning for EM

A block face was trimmed at -101°C with a glass knife. Glass knives were made out of Pittsburgh glass rods on a Leica knife maker using the balanced break method (Tokuyasu and Okamura, 1959). Utlrathin cryosections (60nm) were cut on a Leica ultra microcryotome at -121°C using a Drukker (Element 6) Ultra cryo dry diamond knife 45° with a clearing angle of 6°. Sections were picked up with a freshly made 1:1 mixture of 2.3M sucrose in PB and 2% Methylcellulose solution. These solutions were cold (4°C) to avoid precipitates when mixing. The loop used for pickup was made out of stainless steel wire (0.3mm diameter) and had a diameter of 2.5mm). Sections were then transferred to a grid. Sections for antibody staining were collected on copper grids 50 mesh with a carbon coated Formvar grid. For ISH nickel grids 50 mesh were used as copper reacts with the hybridization buffer forming precipitates.

2.4.4. Immuno-electron microscopy (IEM)

For Single and double labeling of cryosections, the protocol described by Slot et al (Slot et al., 1991) was followed. Grids were incubated with the sections down on droplets of buffers. The labeling sequence was as follows: the embedding material was removed by floating the grids on 2% gelatin in PBS for 27 minutes at 37°C. Free Aldehyde groups were quenched by minimum 5 washes in a 0.15% Glycine in PBS solution followed by a blocking step of 3 minutes in a 1% BSA in PBS solution. Then the primary antibody was incubated for 30 minutes to an hour in a 1% BSA/PBS solution. The excess antibody was washed away with minimum 5 washes of 2 minutes in 0.1%BSA in PBS. Mouse and rat antibodies were detected by a bridging IgG raised in rabbit (Rockland) to increase the binding capacity for protein A coupled colloidal

gold (CMC). Minimum 5 washes of 2 minutes in 0.1%BSA/PBS were done to rinse uncoupled antibodies. Then protein A gold was diluted in 1%BSA/PBS as instructed for that batch and grids were incubated for 20 minutes. Rabbit antibodies were immediately labeled with proteinA gold complexes. Excess gold was washed of with at least 10 washes of 2 minutes in PBS. The colloidal gold was than stabilized on 1% GA in PBS for 5 minutes. For double labeling the sections were rinsed 5 times on PBS and the process was repeated from the Glycine step onwards. For single labeling, the sections were washed 10 times for 1 minute on ddH_2O. Negative staining was accomplished by incubation of the cryosections in a 2% Uranyl Oxalate Ph 7 for 5 minutes followed by Uranyl Acetate in methyl cellulose at pH 4 on ice for 15 minutes.

2.4.5. Electron microscopy images

All pictures were made on a Jeol 1200 EX, Jeol 1010 or a Philips Technai at a 60kV for resin embedded and 80kV for cryo sections. Photographic film (Kodak) was developed and scanned with an Epson Perfection 4990.

3

The role of *trans*-acting factors Egalitarian and Bicaudal D in the anchoring of *grk* RNA

3.1. Introduction

Renald Delanoue from our lab and Bram Herpers were investigating how *grk* mRNA is transported and anchored by IEM when I started this PhD. They excitedly found that *grk* mRNA is transported in EM dense particles that are associated with the MT and Dynein (Delanoue et al., 2007). They named these particles transport particles (TP). In contrast to *ASH1* mRNA and *vg1* mRNA, these TPs are not associated with ER (Allison et al., 2004; Deshler et al., 1997; Schmid et al., 2006). Delanoue et al. also found that they are not surrounded by a membrane themselves (Delanoue et al., 2007). They showed that TPs contain SqdGFP, Dynein heavy chain (dhc) and Egalitarian (Egl) (Delanoue et al., 2007). At its final destination they found that *grk* mRNA is statically anchored (Delanoue et al., 2007) in large EM dense structures previously described as Sponge Bodies (Delanoue et al., 2007; Wilsch-Brauninger et al., 1997). Previously it had been shown in the blastoderm embryo that the anchoring of *pair rule* transcripts is dependent on MT and Dynein (Delanoue and Davis, 2005). Blocking ATPase activity in the cell by Vanadate injections showed that the activity of the Dynein motor was not required for this static anchoring in embryos and the cofactors Bicaudal D (Bic-D) and Egalitarian (Egl) that are required for transport (Bullock and Ish-Horowicz, 2001) were not required for the anchoring either (Delanoue and Davis, 2005). Disruption of the actin network did not result in a disruption of anchoring of *pair rule* transcripts in blastoderm embryos. In the case of *grk* mRNA, it was not known if the anchoring is static and whether it is dependent on the Dynein motor and its cofactors Bic-D and Egl. Renald Delanoue showed by injecting disrupting antibodies that Dhc, apart from its role in transport along the MT, is required for the anchoring of *grk* mRNA. Disruption of Dhc led to fast disintegration of the SB structure and a loss of anchoring when studied by IEM. This disintegration was rapid and was seen as a diffusion of SqdGFP and the injected *grk* mRNA (Delanoue et al., 2007). Morphological studies of SBs in oocytes of dhc^{6-6}/dhc^{6-12} flies, a heteroallelic combination of hypomorph alleles that affect the transport function of the Dynein motor but allow egg chambers to progress through oogenesis (Clark et al., 2007; Delanoue et al., 2007; MacDougall et al., 2003; Mische et al., 2007), revealed that SBs are almost absent in stage 9 oocytes (Delanoue et al., 2007). It was however unclear whether the anchoring of *grk* mRNA needed an intact active motor to function as an anchor.

3.2. Aims of this chapter

In this chapter I address the function of Bic-D and Egl in the anchoring of *grk* mRNA by injecting *in vitro* labeled *grk* RNA into a genetic null background. Anchoring of *grk* mRNA was then studied morphologically by IEM.

3.3. Results

3.3.1. Egalitarian is not required for *grk* mRNA anchoring at the DA corner

Renald Delanoue showed that Dhc is required for anchoring of *grk* RNA by injecting *in vitro* labeled RNA into a stage 9 wild type oocyte and disrupting the function of Dhc. He did this by injecting antibodies against Dhc after the RNA had localized. Antibody injection resulted in a rapid dispersion of the RNA from the DA corner and a loss of SBs in the oocytes both observable by fluorescence and EM. To show a role for Egl in *grk* mRNA anchoring he injected antibodies against this protein into stage 9 oocytes that were injected with *in vitro* labeled *grk* RNA. Disrupting the function of Egl when *grk* RNA is fully anchored did not have any effect on anchoring. When he preinjected wild type stage 9 oocytes with antibodies against Egl, *grk* RNA did not localize, illustrating the role of Egl in active transport but not in static anchoring (Delanoue et al., 2007). One could argue that the antibodies are targeting a domain of Egl that is only involved in transport but not in anchoring. Especially as Egl and Bic-D accumulate at the anchoring site in SBs (Delanoue et al., 2007). To confirm that Egl has no role in anchoring, I injected a mixture of biotinylated and A546 labeled *grk* RNA (5:1) into transheterozygous oocytes for egl^{WU50}/egl^{3e}. egl^{WU50} has been characterized to be a protein null (Schupbach and Wieschaus, 1991) and egl^{3e} was isolated by Ephrussi and Pelegri as a dominant suppressor of Bic-D and shown be mutated in the C terminal domain that interacts with Dynein light chain (Navarro et al., 2004). The transheterozygous combination results in ovaries from which the majority of the egg chambers have the typical *egl* phenotype of egg chambers that have failed to determine the oocyte fate. Although a very few oocytes do develop and injecting the RNA mixture in stage 9 oocytes in the middle of the oocyte never resulted in a visible localization of the RNA to the DA corner by fluorescence microscopy as can be observed in wild type oocytes (data not shown). Examination by IEM by Bram Herpers of these oocytes shows that this injected RNA does not localize to SBs in the middle of the oocyte 40 minutes after injection (Figure 10). This

experiment shows that even if these egg chambers developed an oocyte, transport by the Dynein motor is impaired. However, when I injected these oocytes close to the oocyte nucleus, the RNA localized to the DA corner. We presume this is passive diffusion rather than active transport, as we show in the previous injection experiment that there is no transport in these oocytes. When Bram Herpers examined the *egl* null oocytes I injected with labeled *grk* RNA mixture close to the DA corner by IEM he confirmed that the *grk* RNA was anchored in SBs just like in wild type oocytes showing that Egl is required for transport but not for the anchoring nor the structure of the SBs (Figure 11A-A').

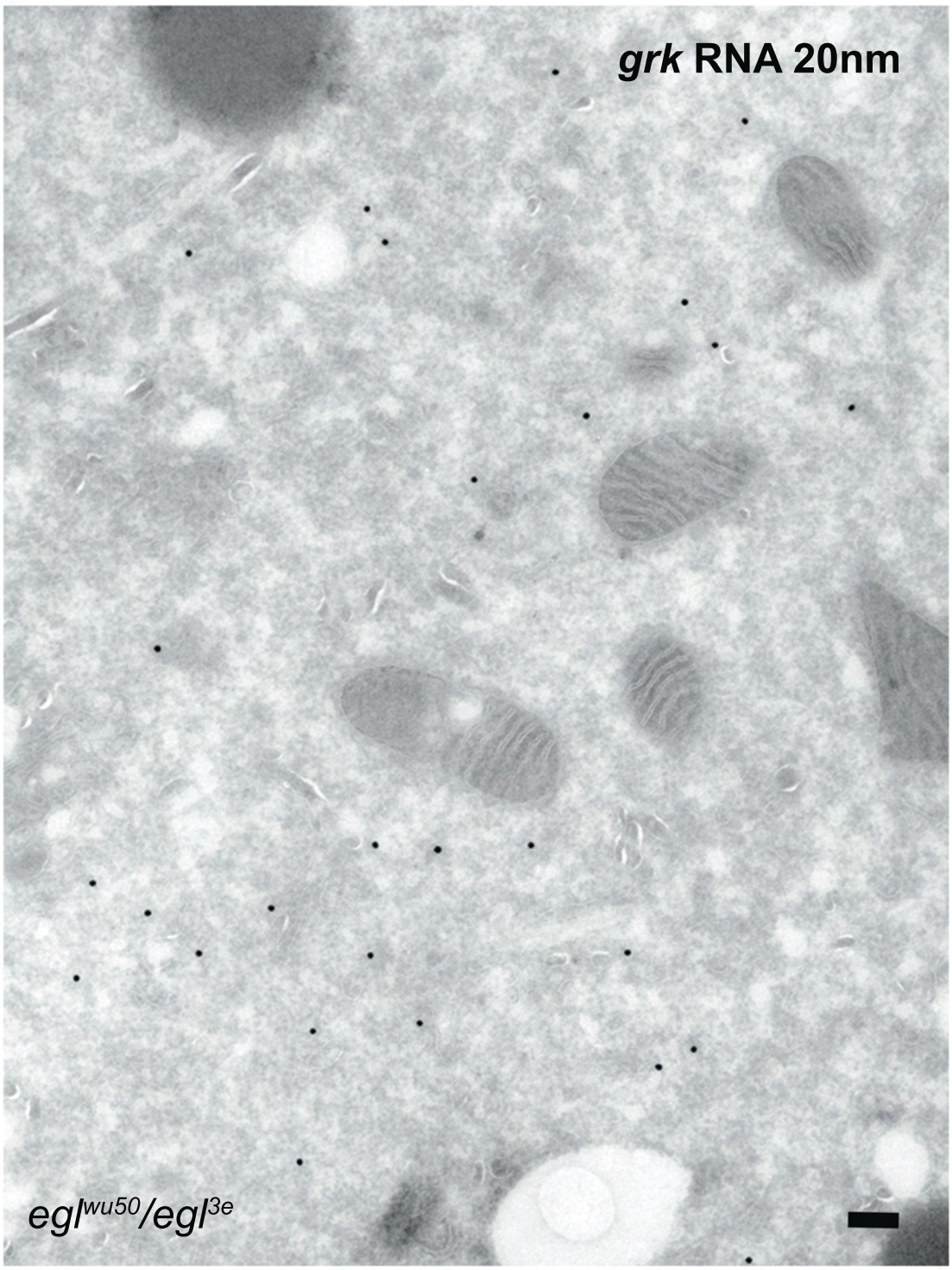

Figure 10 Egalitarian is required for transport of *gurken* mRNA in stage 9 oocytes

Biotinylated grk RNA injected in *egl*^{wu50}/*egl*^{3e} oocytes 40 min after injection.
Micrograph taken at the middle of the oocyte. *grk* RNA labeled with 20nm gold did not localize to the DA corner and did not localize to SB. Biotin labeled with 20nm gold, scale bar 200nm.

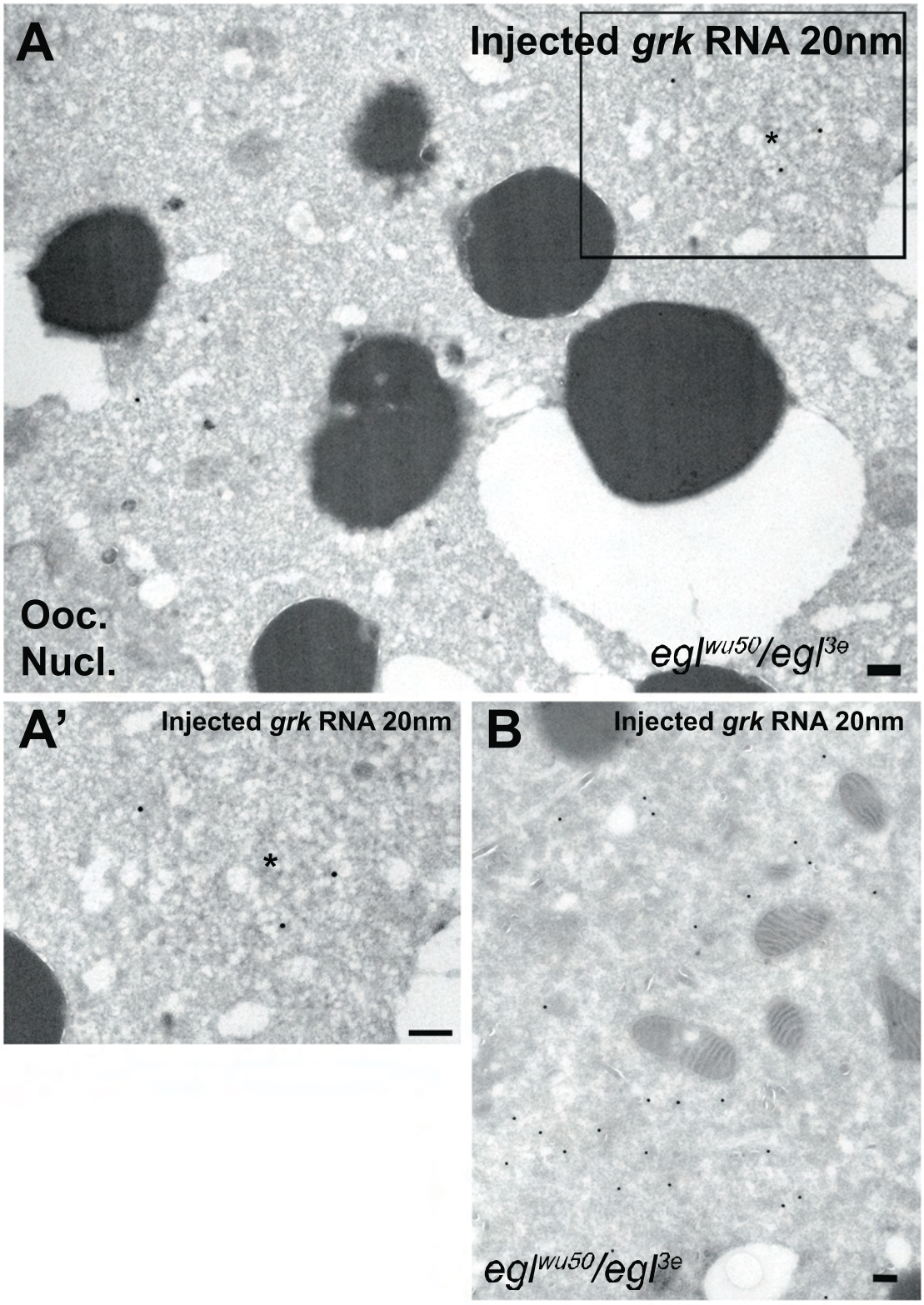

Figure 11 Egalitarian is not required for the anchoring of *gurken* mRNA in stage 9 oocytes

Biotinylated *grk* RNA injected in egl^{wu50}/egl^{3e} oocytes 1 hour after injection. (A A') *grk* mRNA injected close to the nucleus localizes to SBs (*). (A') Enlarged boxed region in A shows grk RNA labeling in a sponge body. (B) same as figure 10, *grk* RNA injected at the middle of the oocyte where *grk* mRNA does not associate with SB. This shows that in an *egl* null background, *grk* RNA is not transported nor anchored in SB in the middle of the oocyte but is anchored in SB at the DA corner in SB independently of Egl. Biotin labeled with 20nm gold, (*) Sponge Body, (Ooc Nucl.) Oocyte Nucleus, scale bar 200nm.

3.3.2. Bicaudal-D is not required for *grk* RNA anchoring at the DA corner

As the Sponge Bodies at the DA corner are also enriched in Bic-D, this protein might also have a function in anchoring (Delanoue et al., 2007). Inhibition of Bic-D function by antibody injection has not been described before. Bic-D is required for multiple patterning processes during oogenesis. At the very beginning of oogenesis it is required for oocyte differentiation resulting in oocytes with 16 nurse cells in mutant flies (Mohler and Wieschaus, 1986; Ran et al., 1994). *Bic-D* mutant flies also fail to form the crucial MTOC in the oocyte required for the localization of the mRNAs involved in oocyte patterning (Ran et al., 1994; Suter and Steward, 1991; Theurkauf et al., 1993). Apart from a role in oogenesis, Bic-D has also been reported to be required for zygotic viability (Ran et al., 1994). This makes it impossible to study its role in anchoring by conventional null mutant analysis. To overcome these problems I generated Bic-D mid-oogenesis mutant (Bic-D^{mom}) flies as described by Swan et al. (Swan and Suter, 1996). These flies contain a *Bic-D* construct under the hsp70 promoter in a *Bic-D* null background allowing expression of the protein during early oogenesis. I heat shocked third instar larvae from the cross w;Df(2L)TW119/CyO; P[w+hsBic-D]-94/+ × w;Bic-D^{r8}/CyO for 30 minutes at 37°C during 4 consecutive days. This allowed to overcome the zygotic lethality in *Bic-D^{r8}/Df(2L)TW119; P[w+hsBic-D]-94/+* (Bic-D^{mom}) and allowed development of an oocyte with MTOC. As the oocyte progresses through oogenesis, Bic-D disappears by protein turnover and has been reported to lack Bic-D protein five and a half days after heat shock (Swan and Suter, 1996). Stage 9 oocytes of these flies were injected with a mixture of biotinylated and Alexa 546 labeled *grk* RNA (5:1) close to the DA corner as the RNA does not localize actively when injected in the middle of the oocyte (data not shown). By injecting close to the oocyte nucleus we hoped to make the RNA anchor independently from the motor activity of Dynein. The oocytes were fixed and were sent to Bram Herpers to be processed for IEM. He labeled sections for Bic-D to confirm they were indeed null for the protein (data not shown) and labeled the sections for biotin to visualize the injected RNA. He confirmed that the RNA was localized to SBs at the DA corner (Figure 12A) and that the RNA colocalizes in SBs with the SB marker Me31B (Figure 12B). This experiment shows that Bic-D is not required for the anchoring of injected *grk* RNA at the DA corner or for SB integrity.

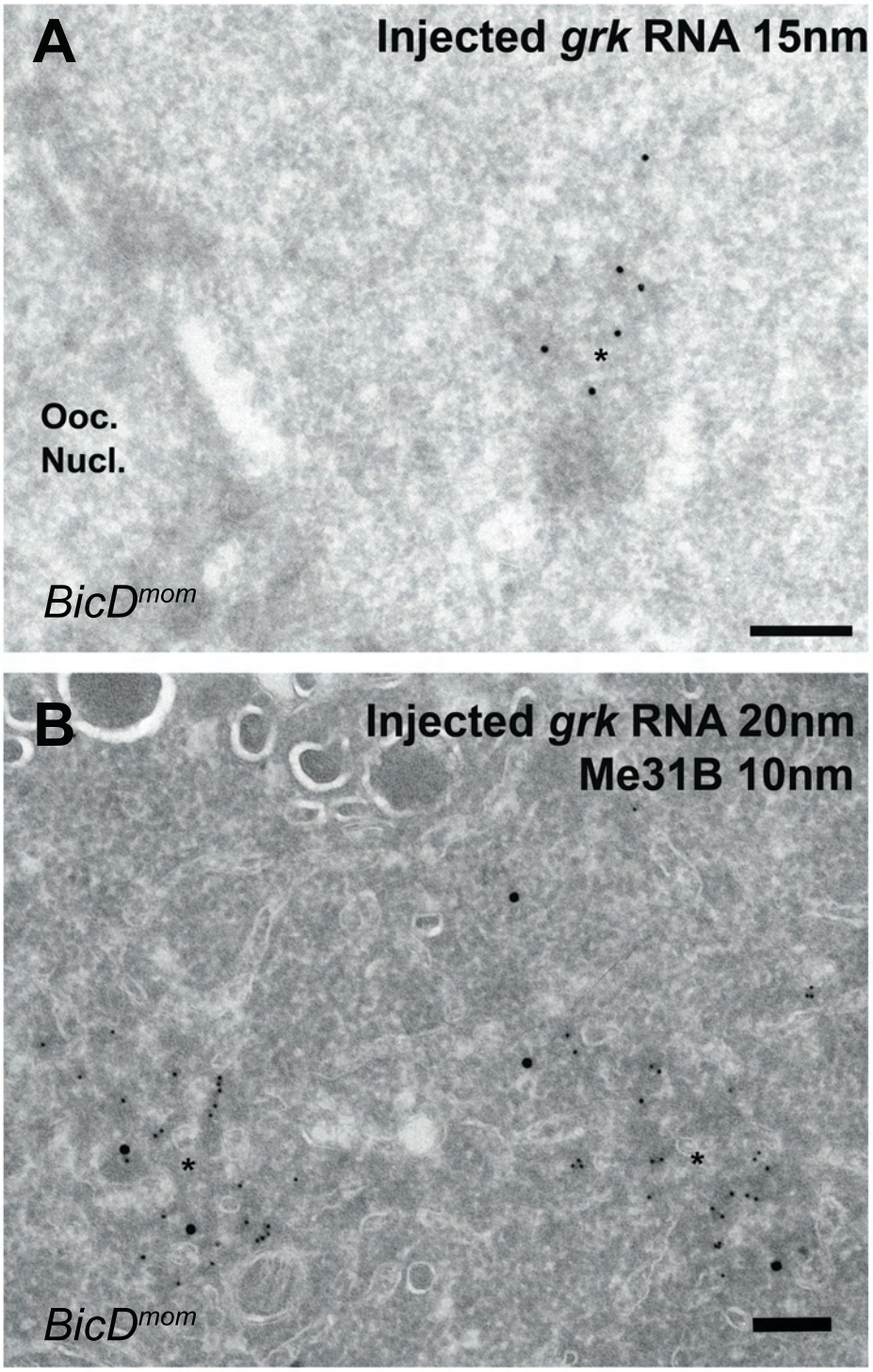

Figure 12 Bic-D is not required for the anchoring of *gurken* RNA in stage 9 oocytes

Biotinylated *grk* RNA injected in $BicD^{mom}$ oocytes 40 min after injection. (A) *grk* mRNA injected close to the nucleus localizes to SB (*). (B) Same experiment as in (A) but SBs are labeled for Me31B as a marker. Morphology in (A) and colabeling of biotin and SB marker Me31B in (B) show a localization of grk RNA to SB independent of Bic-D. Biotin labeled with 20nm gold, Me31B with 10nm gold, (Ooc. Nucl.) Oocyte Nucleus, scale bar 200nm.

3.4. Discussion

The antibody injection assay to disrupt Egl suggests that the activity of the motor is not required for anchoring. However, it could be argued that the antibody could not target the protein as well during anchoring as during transport or that the antibody targets a domain solely involved in transport. This would not exclude a role for Egl in anchoring per se. The fact that injected *grk* RNA in an *egl* null background could still be found in the anchoring structures when injected closely enough to the nucleus so that transport of the transcript is not required shows that Egl does not have a role in anchoring. Although one could argue that the egg chamber injected has developed an oocyte means that this specific oocyte still expresses some functional Egl protein. However, the injection assay in the middle of these oocytes shows that the function in transport of Egl is abolished in these eggchambers. We can conclude from this that a functional Dynein motor complex with Egl is required for transport of *grk* RNA but that Egl and thus a functional motor is not required for anchoring and integrity of the SB. The injection assay in Bic-D^{mom} egg chambers provided us with a tool to circumvent zygotic lethality and to have functional Bic-D protein in early oocyte development but have a protein null for later oocyte stages. From our injections we learned that Bic-D is also not required for anchoring. Taken together the roles of Bic-D and Egl in the functionality of the Dynein motor complex we conclude that Dynein functions as a static anchor for *grk* mRNA in SBs at the DA corner of the oocyte. As SBs are mostly absent in stage 9 oocytes of *Dhc* mutant oocytes (Delanoue et al., 2007), Dhc might function in the anchoring of many other RNAs. As Dynein is required for nuclear positioning and retention in many organisms (Morris, 2003) it looks like its role in anchoring is not restricted to RNA. Other motors have been implied in tethering functions. Myosin V for example has been shown to switch from an active motor to an anchor under load (Altman et al., 2004) which was proposed to be involved in stabilizing the actin network and linking proteins to the actin structures (Miller, 2004). Kinesin like proteins also interact with static cell components, coupling the MT to the mating protrusion or Shmoo tip in budding yeast (Maddox et al., 2003). Together with our data, this suggests that the switch from a dynamic motor to a static anchor is more common for the Kinesin, Myosin and Dynein motor.

4

Roles of hnRNP Squid in the anchoring of *grk* RNA

4.1. Introduction

Several transacting factors have been identified that are involved in the localization of *grk* mRNA in *Drosophila* (Goodrich et al., 2004; Van Buskirk and Schupbach, 2002). The most intensively studied of these is Squid. *Squid* (*sqd*), also known as Hrp40, encodes an RNA binding protein and is a member of the heterogeneous nuclear ribonucleoproteins (hnRNP). These are involved in a wide range of cellular processes such as transcription, splicing, nuclear transport, localization, translation and protein stability (Dreyfuss et al., 2002). Sqd is a member of the shuttling class of hnRNPs and its homologues include human hnRNPA1, Npl3 and Hrp1 in *S. cerevisiae*, as well as *C. tentans* Hrp36 (Norvell et al., 1999). Sqd contains two RNA binding domains and like most other hnRNPs binds a wide range of transcripts. In general, functional specificity is thought to be generated by combinations of different hnRNPs rather than single hnRNPs performing individual and unique functions. The protein contains an M9-like nuclear shuttling motif (Dreyfuss et al., 2002; Swanson and Dreyfuss, 1999), which suggest it has a role in nuclear export and transport of the RNA. Sqd has a series of complex functions in different tissues. In the germline Sqd is required for localization of *grk, osk* and *I* factor mRNA (Kelley, 1993; Norvell et al., 2005; Steinhauer and Kalderon, 2005; Van De Bor et al., 2005). A *sqd* null mutant that lacks Sqd protein is not viable due to its many basic cellular functions but an allele called *squid*^{1} (*sqd*^{1}), a P element insertion in the 5'UTR of the gene, provides a mutant that lacks expression in the germline (Norvell et al., 1999). Interestingly, in a *sqd*^{1} mutant, *grk* mRNA fails to complete the second step in a two-step localization process (MacDougall et al., 2003) leading to a localization along the entire anterior cortex of the oocyte (Norvell et al., 1999). This mislocalization results in an ectopic expression of Grk accompanied by the typical phenotype of dorsalised eggs.

Squid comes in three major isoforms: SqdA, SqdB and SqdS (Figure 13). Rescue experiments in a germline null revealed different roles for the three isoforms in dorso-ventral (DV) axis formation during oogenesis (Norvell et al., 1999). By creating transgenic flies expressing only one isoform it was found that SqdS and SqdB are localized in the nurse cell nuclei and SqdS also in the oocyte nucleus, whereas SqdA has a cytoplasmic expression pattern. SqdS could partially rescue the localization of *grk* mRNA and Grk protein, whereas in flies only expressing SqdA, over 90% of the late stage oocyte have *grk* mRNA mislocalized to the anterior. Interestingly, the

amount of WT eggs is roughly the same as in transgenic flies carrying only the SqdS isoform. Norvell et al. conclude from these results that SqdA has role in the translation *grk* RNA. A combination of SqdA and SqdS was able to completely restore WT phenotype, suggesting a complementary role in *grk* mRNA localization and translation for these two isoforms. Introducing SqdB in a sqd^{1} background does not rescue *grk* mRNA localization (Norvell et al., 1999). Recent studies in germline mosaic egg chambers for *sqd* revealed that the role for Sqd in translational repression and localization of *grk* mRNA can be functionally separated. They showed that the SqdA isoform needs to be recruited in the nurse cells in order to repress ectopic translation in the oocyte but that *grk* mRNA transcribed from *sqd* null nurse cells can recruit Sqd protein originating from the wild type nurse cells present in the oocyte to ensure correct localization (Caceres and Nilson, 2009). Endogenous *grk* mRNA colocalizes with Sqd in specialized structures that were identified as sponge bodies (Delanoue et al., 2007). As in the embryo this anchoring is dependent on Dynein but not on Bic-D and Egl. When *in vitro* labeled *grk* RNA is injected in oocytes of flies expressing a SqdGFP fusion protein, an accumulation of SqdGFP can be observed at the DA corner upon RNA localization (Delanoue et al., 2007). Previous work in our lab revealed that injected *grk* RNA localizes to the DA corner in two distinct phases. This localization was shown to be dependent on an intact MT network and a functional Dynein motor (MacDougall et al., 2003). In a *sqd* null background however, *grk* mRNA only completes the first step of the two-step localization process (Kelley, 1993; MacDougall et al., 2003). FRAP experiments on *sqd* null oocytes injected with fluorescently labeled *grk* RNA show that the RNA localized at the anterior in these mutants is in continuous transport. In comparison, FRAP experiments on fluorescently labeled *grk* RNA at the DA corner shows a static anchoring. The accumulation of SqdGFP at the anchoring site of *grk* RNA and the continuous transport at the anterior in the mutant oocytes might mean that Sqd is not only needed for localization but also has a function in anchoring of the transcript. Normally, one would study the function of a protein *in vivo* by comparing the phenotypes of a mutant to a wild type. As in sqd^{1} mutant oocytes the RNA does not localize to the site of anchoring it is very difficult to study this anchoring with traditional genetics. This problem could be overcome by the use of temperature sensitive alleles or other conditional alleles but those are not available and the creation takes a lot of time and effort.

Figure 13 Different isoforms of Squid

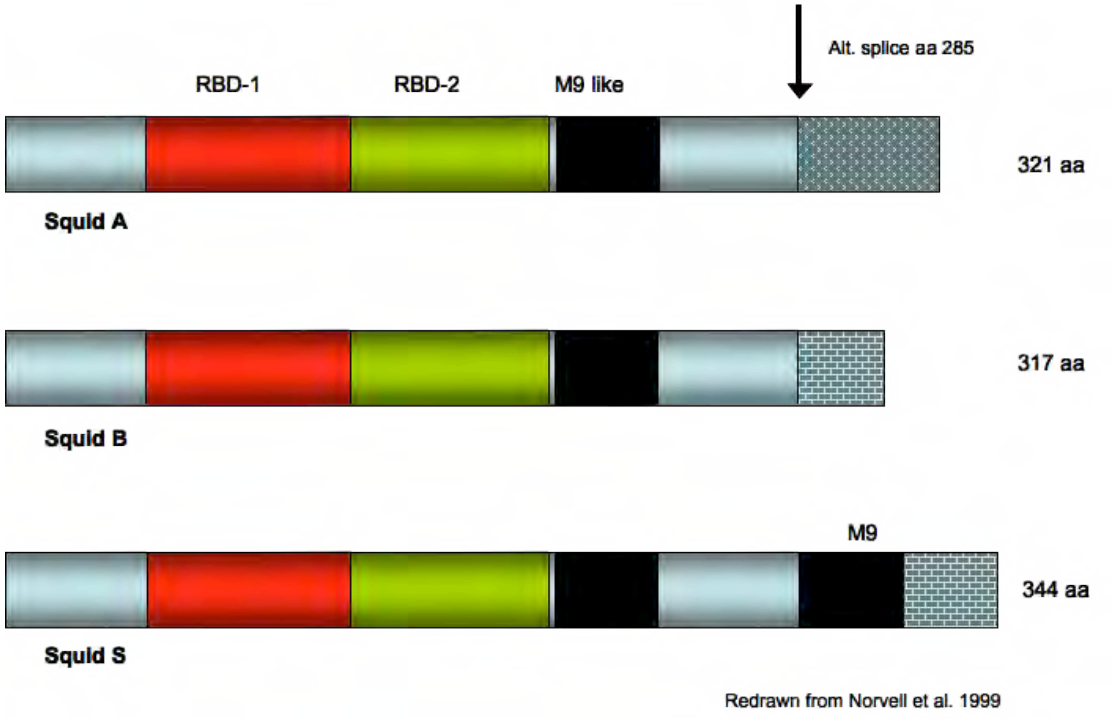

Figure 13 Different splicing isoforms of Squid.

The three isoforms contain 2 RBD domains and an M9 like nuclear shuttling domain. Squid S has an additional M9 domain. SqdA and SqdS can rescue the *sqd* null mutant phenotype whereas SqdB does not seem to have a role in oocyte polarity (Norvell et al., 1999).

4.2. Aims of this chapter

In this chapter I will describe how I developed a novel way to study the functions of Sqd after it has completed the second step of localization. Using this newly developed assay I will address the possible roles for Sqd in anchoring of *grk* mRNA. I will study the effect of disrupting Sqd function on the anchoring of injected as well as on endogenous *grk* mRNA by live cell fluorescence microscopy. I also study the effect on the anchoring structures at ultra structural level by immuno electron microscopy (IEM) on ultra thin cryo sections.

4.3. Results

4.3.1. Establishing a new assay to study Squid function

Functionally inhibitory antibodies have been used successfully in several cases, as an alternative to conditional alleles. For example, antibodies against Dynein Heavy Chain (Sharp et al., 2000; Vaisberg et al., 1993; Wilkie and Davis, 2001) and Egalitarian (Bullock and Ish-Horowicz, 2001; Delanoue and Davis, 2005) have successfully been used in inhibition experiments. I tried to disrupt the function of Squid by injecting monoclonal antibodies (T. Schüpbach) into wild type oocytes. The antibodies were injected into stage 9 oocytes at a concentration of 20mg/ml 15 minutes before the injection of fluorescently labeled *grk* RNA. If Sqd function were successfully inhibited, the injected *grk* RNA would not complete the second step of localization and would accumulate at the anterior of the oocyte. Unfortunately, the injected transcript localized into a tight cap around the nucleus as one would see in a wild type situation (Figure 14A-A', B-B'). The localization was not significantly different from oocytes that were not injected with anti-Sqd antibodies (Fisher exact test, N=10, p=1 for figure 14A and N=6, p=1 for figure14B). Even when the antibodies were 10 times concentrated no or very minor effect on *grk* RNA localization could be observed except that the oocytes seem to die much faster. We decided this was due to the toxicity of the amount of proteins injected. The affinity of anti-SqdA 2G9 for Sqd was tested on ovary extract by western blot analysis (Figure 15). The antibodies bind to Sqd but they do not inhibit the function of the protein.

To overcome this problem I tried to inhibit Sqd by targeting the GFP moiety of a SqdGFP fusion protein. The SqdGFP flies used for this experiment originated from a

protein trap mutagenesis screen (Norvell et al., 2005) devised by Morin et al. (Morin et al., 2001). In this line, a protein trap transposon element containing a piece of DNA coding for GFP was inserted in the first intron of the gene. All three isoforms carry the GFP molecule as alternative splicing is only affecting the second intron (Kelley, 1993). The fusion protein is expressed under the endogenous promoter reflecting the expression pattern of the wild type protein. Western blots on ovary extract revealed that only SqdGFP fusion protein is expressed and that endogenous Sqd is absent (Figure 15).

To test whether I could disrupt SquidGFP function by targeting the GFP fraction of the fusion protein, I tested whether antibody injection could prevent the second step of *grk* RNA localization. Therefore, a monoclonal Anti-GFP (Sigma) antibody was injected in stage 9 oocytes 15 minutes prior to *grk* RNA labeled with Alexa 546-UTP (Figure 16A-A"). 10 minutes after *grk* RNA injection, the labeled transcripts were localized to the anterior of the oocyte in the form of an anterior disc (Figure 16B-B"). The injected RNA failed to complete the second step of localization, as you would expect in a wild type oocyte (MacDougall et al., 2003). Even after 80 minutes, when *grk* RNA is normally fully localized, the RNA is still at the anterior (Figure 16C-C"). This is exactly what would happen in a *sqd* null background as Sqd is required for transport from the anterior to the DA corner (Norvell et al., 1999). Indeed, when injected in oocytes of homozygous sqd^{1} flies, Alexa546-UTP labeled *grk* RNA localizes to the anterior of the oocyte in a way indistinguishable from the antibody injected ones above (Figure 16D). As a positive control I injected the same RNA in wild type oocytes from OrR flies that were preinjected with the anti-GFP antibodies 15 minutes beforehand. *grk* RNA clearly localizes to the DA corner in a tight cap around the nucleus (Figure 16E) showing that the effect on *grk* localization in SqdGFP flies was due to the interaction with GFP. The observed anterior localization of *grk* mRNA in the SqdGFP oocytes preinjected with anti-GFP was significantly different from wild type oocytes preinjected with anti-GFP where grk mRNA localizes to the DA corner (Fisher exact test. N=15 of which 2 localized normally, $p<0.0001$). We do not know how this inhibition works biochemically. Presumably, the antibody crosslinks the GFP making the active domains of Sqd unavailable.

The effects we observe could in principle be due to the antibody crosslinking GFP and causing some kind of non-specific disruption of cell viability or function that is unrelated to Sqd function and *grk* mRNA localization. To test whether such non-specific effects are caused by binding to GFP by the anti-GFP antibody, the anti-GFP antibody was tested in oocytes of transgenic flies expressing GFP. I used *pUbNLSGFP*, which expresses GFP fused to a nuclear localization signal under the control of the polyUbiquitin promotor that is expressed in all tissues (Davis et al., 1995). I also used *pUbGFP33*, which also expresses GFP under the control of the polyUbiquitin promotor, but in this case the GFP is cytoplasmic, as it is not fused to a nuclear localization signal (Davis et al., 1995). I preinjected the oocytes of these strains with anti-GFP antibodies at a total protein concentration of 25mg/ml of which 5.8mg/ml were IgG. The RNA localized to the DA corner in a tight cap around the nucleus (data not shown). These results show that the anti-GFP injection specifically inhibits Sqd function as opposed to a toxic effect by crosslinking GFP. This experiment allowed us to inhibit Sqd *ad libendum* and thus provided us with a useful tool to study the role of Sqd in processes that take place after the first step of localization.

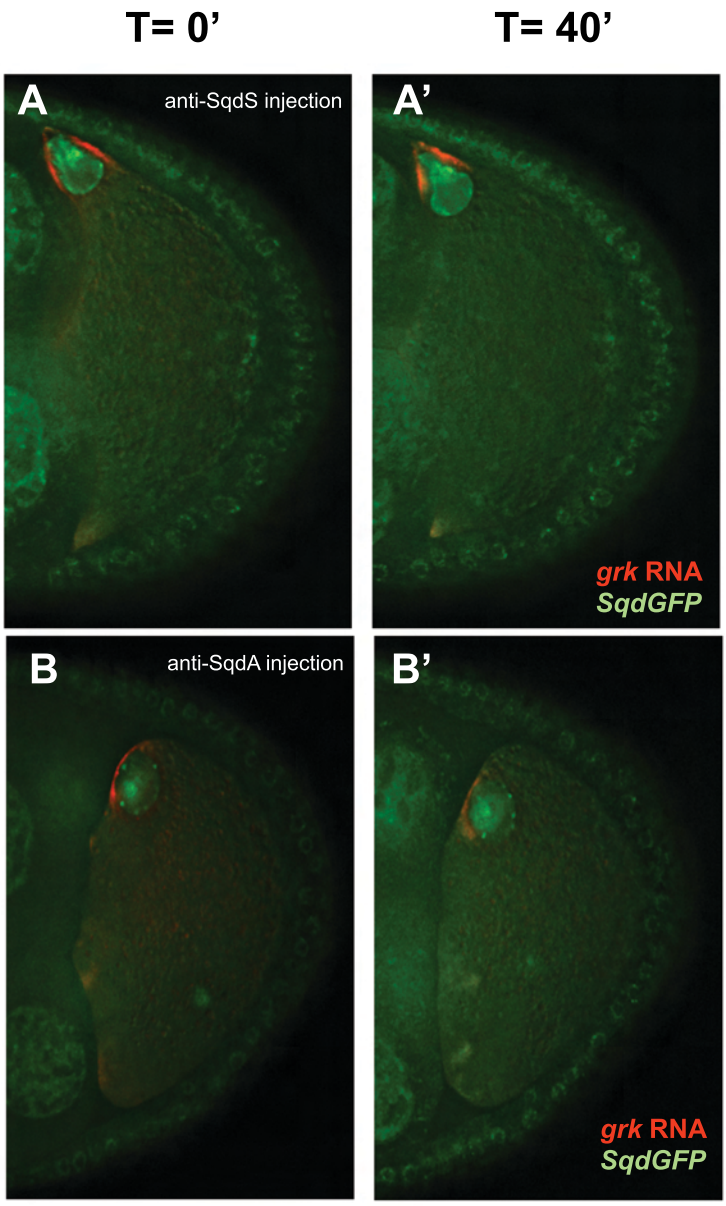

Figure 14a Injection of anti-Squid antibody does not affect anchoring of *grk* RNA

(A) *SqdGFP* (green) oocytes 15 min after injection with Alexafluor 546 labeled *grk* RNA (red). The RNA is anchored at the DA corner. anti-SqdS is injected at this timepoint (T=0).
(A') Injection of monoclonal anti-SqdS 1B11 at T=0 does not affect anchoring of grk RNA (red) 40 min after antibody injection (T=40). SqdGFP (green)
(B) *SqdGFP* (green) oocytes 15 min after injection with Alexafluor 546 labeled *grk* RNA (red). The RNA is anchored at the DA corner. anti-SqdA is injected at this timepoint (T=0).
(B') Injection of monoclonal anti-SqdA 2G9 at T=0 does not affect anchoring of grk RNA (red) 40 min after antibody injection (T=40).

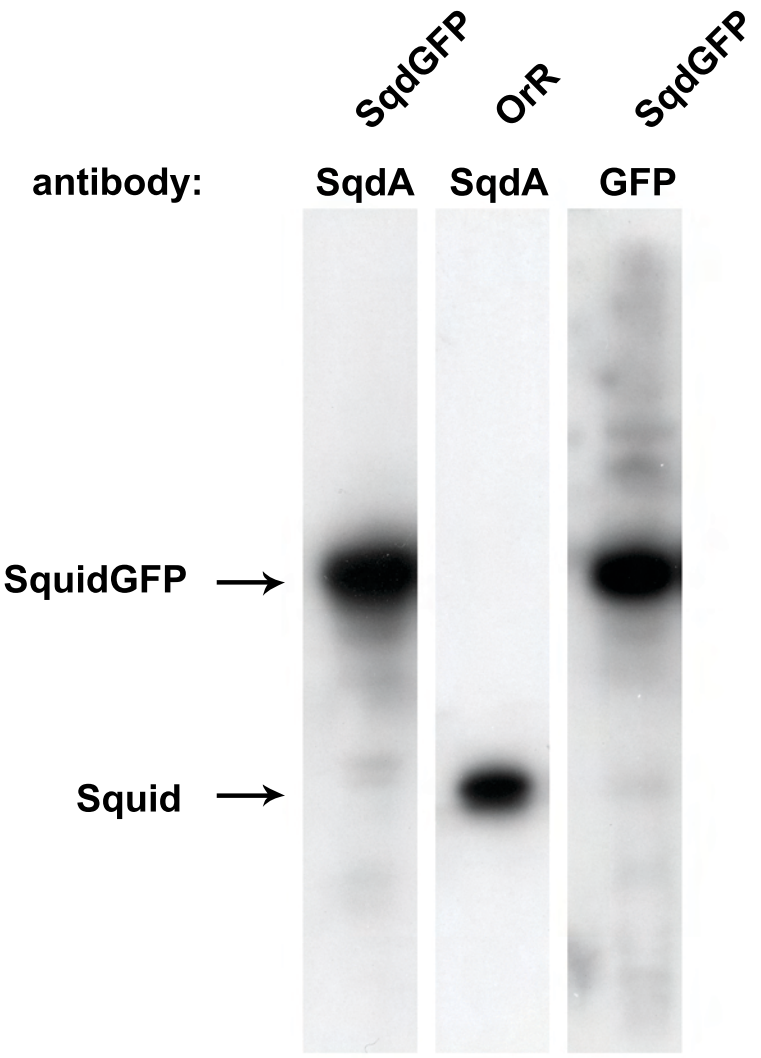

Figure 15 Squid expression in *SquidGFP* and wild type flies

Western blot analysis on *SqdGFP* versus OrR wild type ovaries. The blot shows that only SqdGFP is expressed in the *SqdGFP* ovaries and that wild type protein is absent. Wild type ovaries only express Squid.

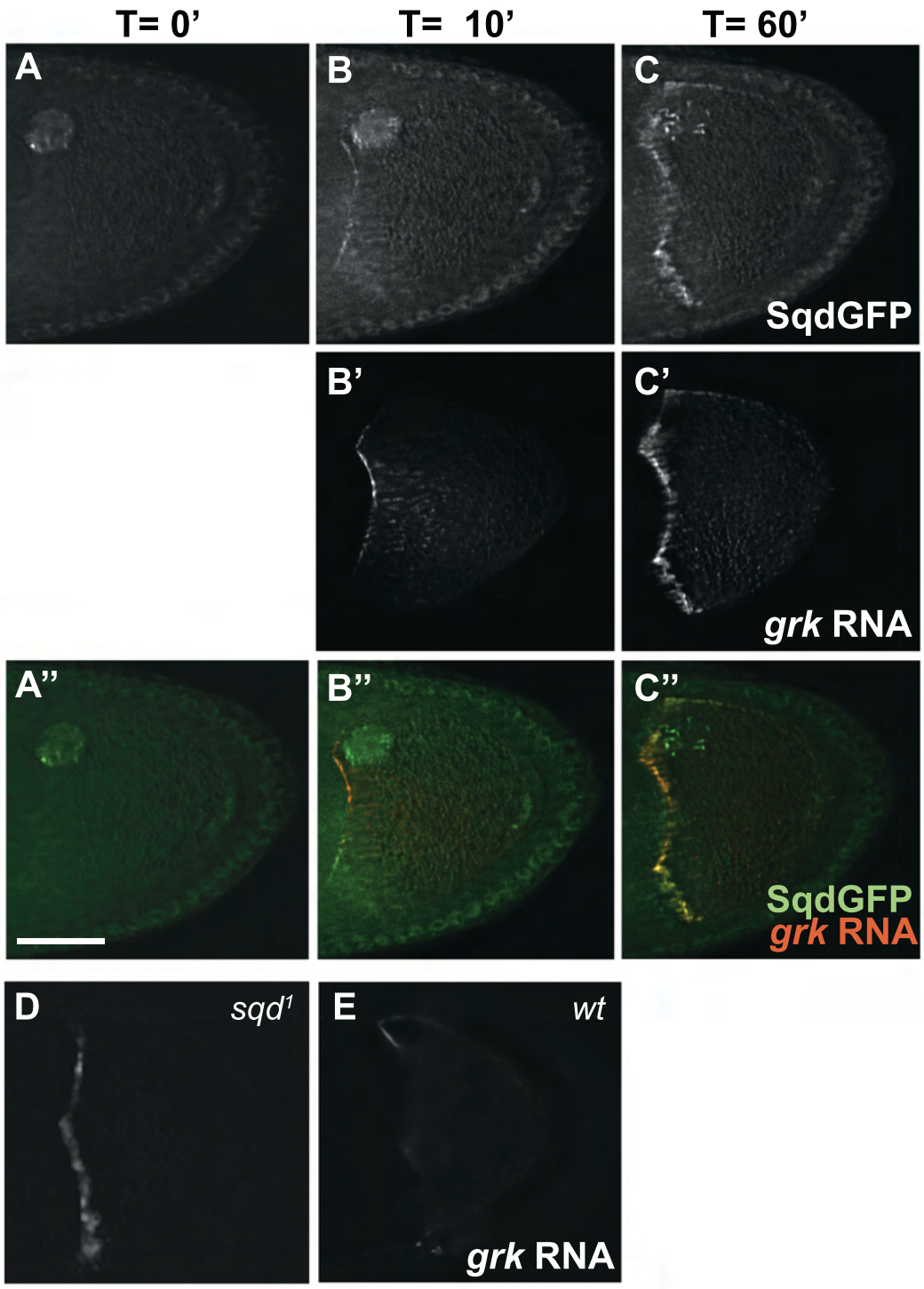

Figure 16 Anti-GFP injection inhibits Squid function

Preinjecting anti-GFP in a SqdGFP oocyte causes a localization defect of injected *grk* RNA that resembles a *sqd* null phenotype.

(A-A") *SqdGFP* stage 9 oocyte 15 min after injection with anti-GFP before injection of Alexafluor 546 labeled *grk* RNA

(B-B") *SqdGFP* oocyte 10 min after Alexafluor 546 labeled *grk* RNA. The RNA has reached the anterior of the oocyte

(C-C") *SqdGFP* oocyte 60 min after Alexafluor 546 labeled *grk* RNA. The RNA is still at the anterior and fails to reach the DA corner like in a sqd null background (D).

(D) *Sqd*[1] oocyte 50 min after Alexafluor 546 labeled *grk* RNA injection. In this *sqd* null background, the RNA remains at the anterior while in a wild type (E) the RNA localizes to a tight cap around the nucleus.

(E) OrR oocyte preinjected with anti-GFP, 50 min after Alexafluor 546 labeled *grk* RNA injection. There is no effect on *grk* RNA localization. Scale bar 30 µm

4.3.2. Squid is required for exogenous *grk* RNA anchoring

Being able to inhibit Sqd function at any stage during localization provided us with a powerful tool to study what the role is of the accumulation of Sqd protein at the DA corner upon *grk* anchoring. As stated above, this was not possible before because we lack conditional alleles for *sqd.*

To test for the role of Sqd in anchoring *grk* mRNA after its transport to the dorso-anterior corner is complete, I injected the anti-GFP antibodies on fully localized and anchored *grk* RNA. For this experiment fluorescently labeled *grk* RNA (Alexa546-UTP) was injected in stage 9 SqdGFP oocytes and allowed to localize to the DA corner. After 45 minutes when the RNA was fully localized (Figure 17A), an anti-GFP antibody was injected in the middle of the oocyte at a protein concentration of 25mg/ml of which 5.8mg/ml were IgG. Time-lapse movies were taken to follow the subsequent fate of anchored *grk* RNA (Figure 17). The effect of disrupting the function of SqdGFP was seen as a loss of anchoring. Particles containing *grk* RNA moved away from the DA corner (Figure 17B-B") and were completely detached from the DA corner after 30 minutes and found at the anterior (Figure 17C-C"), as seen in a sqd^{1} background injected with labeled *grk* RNA (Figure 16D), but not in wild type. In wild type oocytes preinjected with labeled *grk* RNA localized at the DA corner, injection of anti-GFP does not show any effect on anchoring. In fact, the RNA continues to localize even after the injection of the anti-GFP antibody (Figure 17D-D") (N=11). The observed effect in the anti-GFP injections is significantly different to the control injections (Fisher exact test, N=15 of which 1 did not have any effect on anchoring, $p<0.0001$). The Sponge bodies did not disperse as in inhibition experiments for Dhc (Delanoue et al., 2007) but fell apart into smaller particles. As a control I injected the anti-GFP antibody in transgenic *pUbEGFP33* and *pUbNLSGFP* flies after *grk* RNA was allowed to localize. There was no effect on the anchoring of *grk* RNA even 60 min after anti-GFP injection (Fisher exact test N=9, p=1 for NlsGFP and N=19, p=1 for EGFP33 oocytes) (Figure 17a A-A'and B-B').

To study the effect of inhibition of Sqd at the ultra structural level, I injected anti-GFP antibody into SqdGFP expressing oocytes as above but with the difference that they were preinjected with a mixture of biotinylated and Alexa 546 labeled *grk* mRNA

(5:1), allowed to localize to the DA corner. The oocytes were fixed for IEM and sent off to Bram Herpers from C. Rabouilles laboratory for cryosectioning and immunostaining. IEM revealed that inhibiting Sqd function disrupts the Sponge Bodies and *grk* RNA is found in particles that are indistinguishable from the transport particles that are found in a *sqd* null mutant injected with biotinylated *grk* RNA (Figure 18A and D). In comparison, I also preinjected *SqdGFP* oocytes with anti-GFP 15 minutes before injection of labeled *grk* RNA mix. The RNA was allowed to localize and fixed for EM. Bram Herpers processed these samples and labeled the sections for biotin and Dhc. The RNA was found at the anterior in transport particles (TPs) that are undistinguishable from TPs in sqd^{1} mutant oocytes and *SqdGFP* oocytes injected after *grk* RNA was allowed to localize (Figure 18C). These results show both at ultra structural and fluorescent level that Sqd is required for anchoring of injected *grk* RNA. In support of these data, Renald Delanoue from our lab performed FRAP experiments on wild type oocytes injected with fluorescently labeled *grk* RNA. He showed that when you bleach localizing injected fluorescently labeled *grk* RNA at the anterior, the fluorescent signal quickly recovers (Delanoue et al., 2007). This demonstrates that *grk* mRNA is in continuous transport in the first step of localization. When he bleaches an area of fully localized *grk* RNA at the DA corner, the fluorescence does not recover, showing that the RNA is statically anchored at the DA corner. He performed the same FRAP experiment in a sqd^{1} mutant and showed that *grk* RNA localized at the anterior is in at state of continuous active transport (Delanoue et al., 2007). These data show that in a sqd^{1} mutant *grk* RNA does not only fail to be transported to the DA corner but also does not anchor at the anterior. Instead, the RNA stays in transport at the anterior, confirming that the phenotype in sqd^{1} mutants is not only a localization defect but also an anchoring defect.

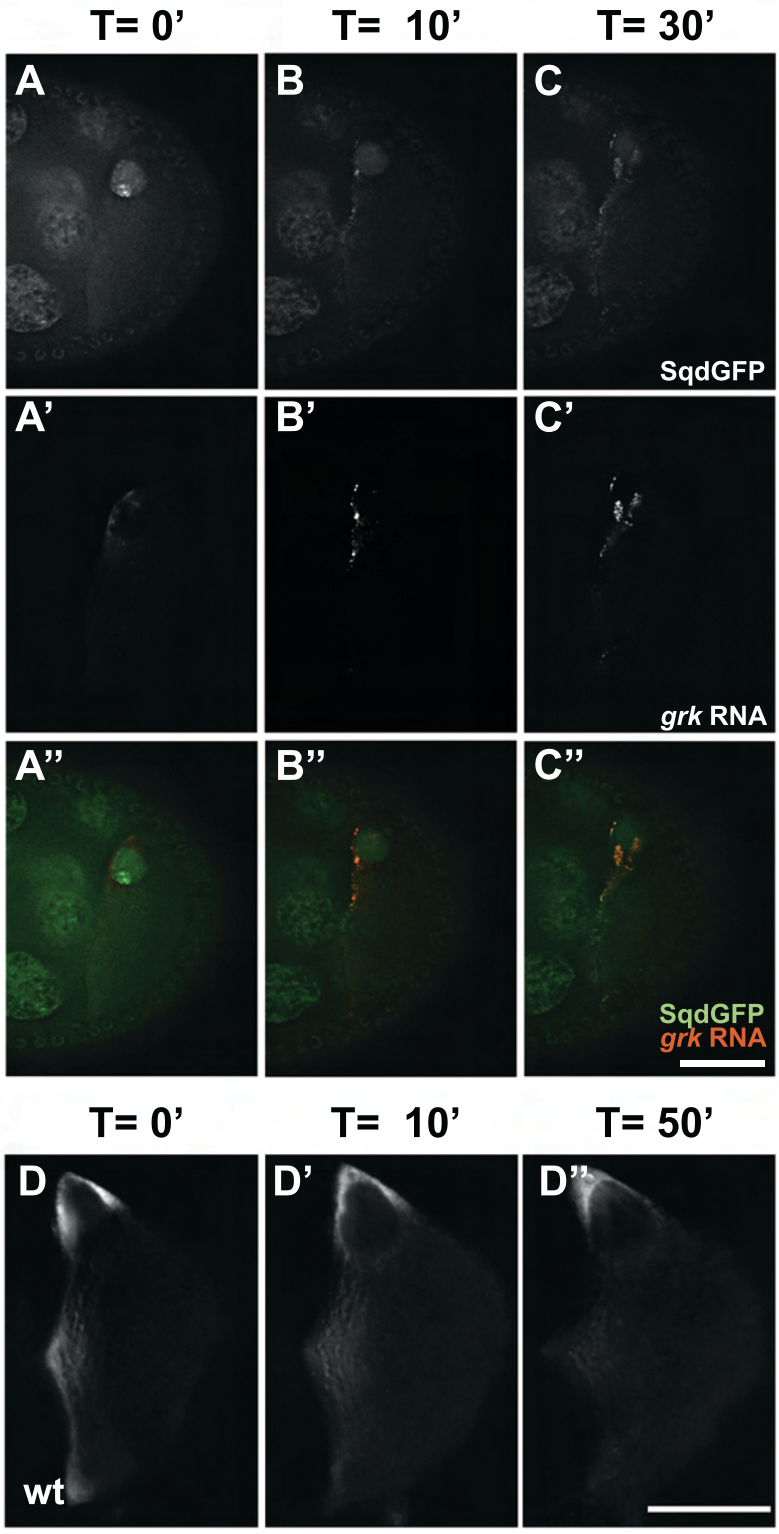

Figure 17 Squid is required for *gurken* RNA anchoring

(A-A") *SqdGFP* oocytes injected with Alexafluor 546 labeled *grk* RNA localized to the DA corner before antibody injection.
(B-B") *SqdGFP* oocytes 10 min after anti-GFP injection. *grk* RNA is detaching from the DA corner
(C-C") *SqdGFP* oocytes 30 min after anti-GFP injection. *grk* RNA has detached completely from the DA corner
(D-D") OrR oocytes injected with anti-GFP after Alexafluor 546 labeled *grk* RNA was injected and allowed to localize at time points 0, 10 and 50 min after antibody injection. There is no effect on the anchoring and the RNA continues to localize. Scale bar 30 µm

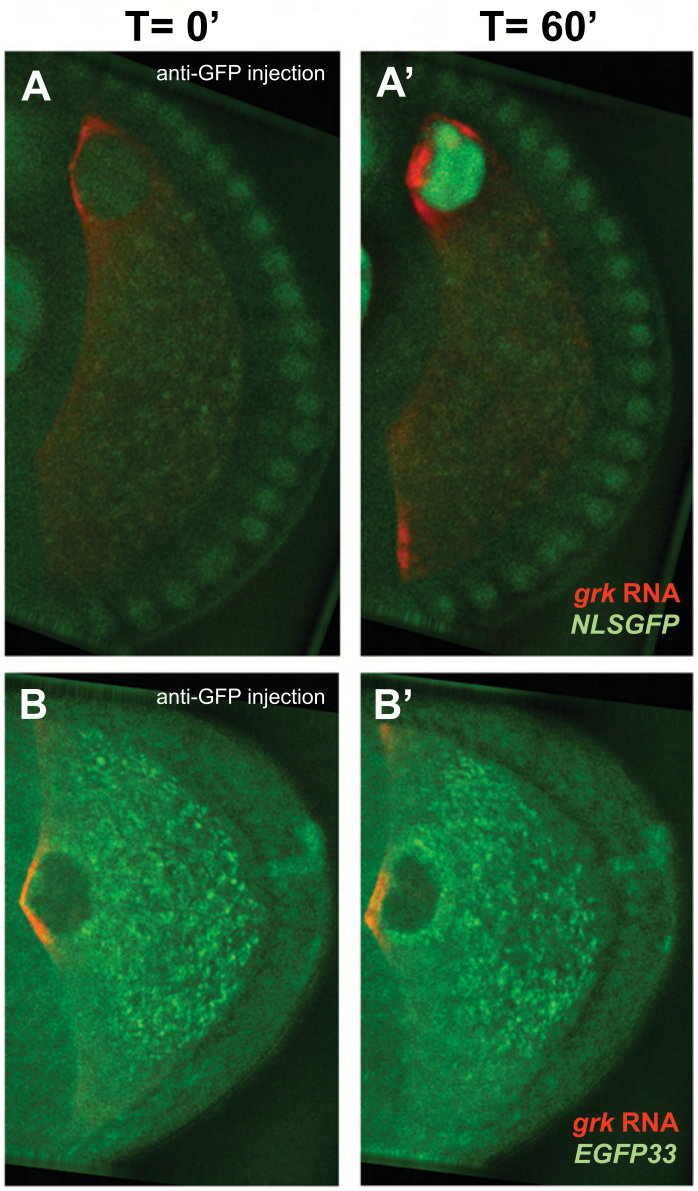

Figure 17b Anti-GFP negative control injections

(A) *NLSGFP* (grren) oocytes injected with Alexafluor 546 labeled *grk* RNA (red) localized to the DA corner. At this timepoint anti-GFP is injected (T=0)
(A') Injection of monoclonal anti-GFP does not affect anchoring 60 min (T=60) after antibody injection. *grk* RNA is still anchored at the DA corner.
(B) *EGFP33 (green)* oocytes injected with Alexafluor 546 labeled *grk* RNA (red) localized to the DA corner. At this timepoint anti-GFP is injected (T=0)
(B') Injection of monoclonal anti-GFP does not affect anchoring 60 min (T=60) after antibody injection.

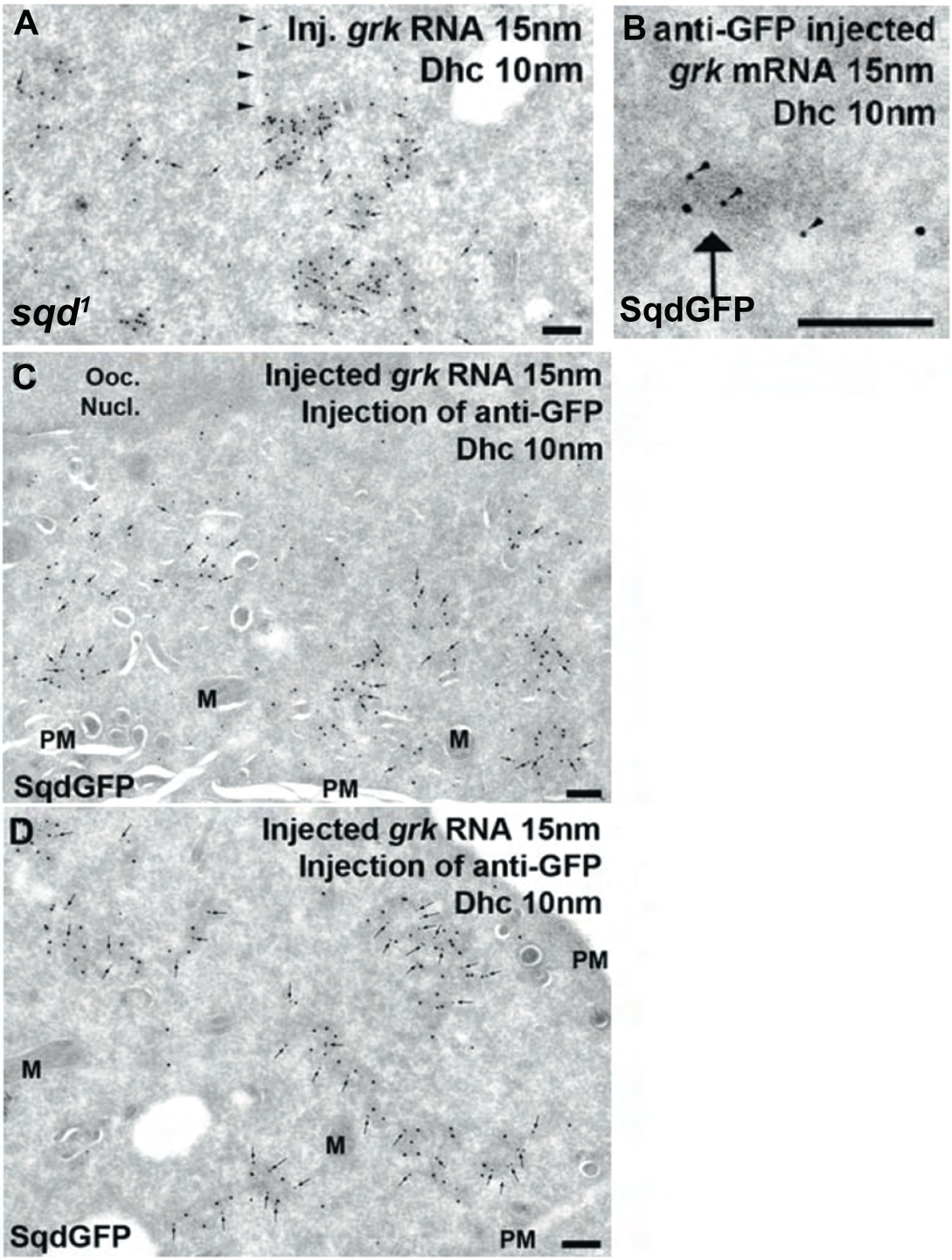

Figure 18 Squid is required for *gurken* RNA anchoring

(A) *sqd*[1] oocytes injected with biotinylated *grk* RNA localized to the anterior labeled for biotin with 15nm gold and Dhc with 10nm gold (arrows). The RNA is found in TP at the anterior (EM dense areas) and colocalizes with Dhc. MT (Arrowheads).

(B) *SqdGFP* oocytes 45 min after anti-GFP injection. *In situ* on grk mRNA labeled with 15nm gold, Dhc with 10nm gold (arrowheads). Endogenous *grk* mRNA is found in TP (Arrow) at the anterior colocalizing with Dhc

(C) *SqdGFP* oocytes preinjected with anti-GFP. Biotinylated *grk* RNA localizes in TP (arrow) at the anterior of the oocyte and colocalize with Dhc. Biotin labeled with 15nm gold, Dhc with 10nm gold (arrows)

(D) *SqdGFP* oocytes injected with anti GFP after biotinylated *grk* RNA was injected and allowed to localize. the RNA localizes in TP at the anterior and colocalizes with Dhc. Biotin labeled with 15nm gold, Dhc with 10nm. Scale bars 200 nm. (M) Mitochondria, (PM) Plasma membrane. Work in collaboration with Bram Herpers. Injections done by me, EM and figures by Bram Herpers (Delanoue et al., 2007)

4.3.3. Squid is required for the anchoring of endogenous *grk* mRNA

Disruption of anchoring of exogenous transcripts by inhibiting Sqd function could be argued to be artificial as overloading the oocyte with RNA might render anchoring structures unstable. Therefore we wanted to test what the effect of inhibiting Sqd would be on anchoring of endogenous *grk* mRNA. Therefore stage 9 oocytes of *SqdGFP* flies were injected with anti-GFP antibodies and incubated for 15 minutes before fixing in a 4% PFA solution. The endogenous *grk* transcript was visualized by FISH (Figure 19A-A") (N=8). In injected oocytes, *grk* mRNA could be found at the anterior of the oocyte in a similar distribution to *grk* mRNA in a sqd^{1} germline null mutant (Figure 16D). In uninjected oocytes, *grk* mRNA was still localized in a tight cap around the nucleus (Figure B-B") (N=7). As a negative control, the same experiment was performed in OrR wild type oocytes where no GFP is present (Figure 19C-C" (N=24) and D-D" (N=11)). To ensure exactly the same reaction conditions between the injected and the uninjected OrR oocytes, a Dextran FITC 70kDa was coinjected with the antibody and the FISH was performed on the injected and uninjected samples placed in the same tube. The anti-GFP had no effect on the anchoring of *grk* mRNA in wild type oocytes.

We also looked at the effect of SqdGFP inhibition on endogenous *grk* mRNA at EM level. SqdGFP stage 9 oocytes were injected with anti-GFP and fixed for *in situ hybridization* Electron Microscopy (IHEM). Bram Herpers did the processing and imaging of these samples. No *grk* mRNA was found in SBs. Instead, all *grk* mRNA was found in TPs at the anterior, morphologically undistinguishable from TPs found in a sqd^{1} mutant (Figure18B).

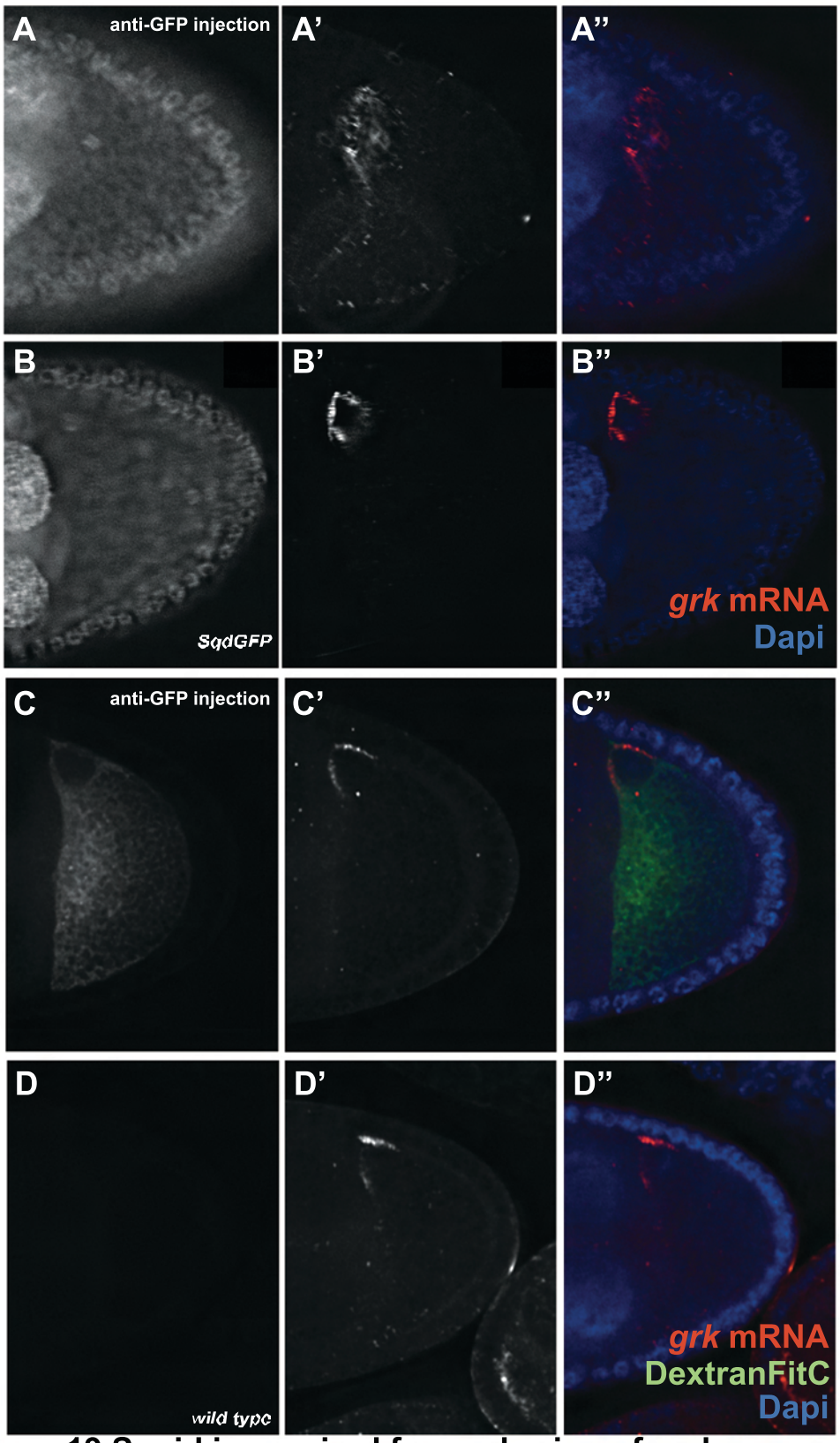

Figure 19 Squid is required for anchoring of endogenous *gurken* mRNA

(A-A'') Injection of anti-GFP in *SqdGFP* background 30 min before fixing. *grk* mRNA is found at the anterior (A')
(B-B'') Endogenous *grk* mRNA in a noninjected *SqdGFP* egg chamber.
(C-C'') Endogenous *grk* mRNA in OrR WT egg chamber injected with anti-GFP 30 min before fixing. DextranFitC is coinjected as a marker for injection.
(D-D'') Endogenous grk mRNA in a noninjected OrR WT egg chamber.

4.4. Discussion

The role of hnRNPs in nuclear export and cellular transport is better understood in mammals. The best-known example is *myelin basic protein* (MBP) mRNA. hnRNP A2 and A3 bind to a 21 nucleotide long zip code in the RNA called the hnRNP A2 response element or A2RE. It is generally accepted now that mRNA trafficking is regulated by interaction of *cis*- and *trans*-acting factors. hnRNPs play an important role as *trans*-acting factors. The importance of alternative splicing and posttranslational modifications of these transacting factors in RNA trafficking has been proposed. hnRNP A2 for instance occurs in at least four different isoforms each of which can be post transcriptionally modified by N-terminal acetylation, phosphorylation and methylation as reviewed by (Smith, 2004). To my knowledge, a possible role of hnRNPs in the anchoring of mRNA has never been reported. Our work on Squid provides the first evidence of an hnRNP with a direct role in anchoring of mRNA after it is transported to its final intracellular destination. Inhibition of Sqd by targeting the GFP inserted in the first intron has revealed a completely novel function for this hnRNP during oogenesis. Apart from its known requirement to complete the second step of localization and translational regulation (Caceres and Nilson, 2009; Clouse et al., 2008; Goodrich et al., 2004; MacDougall et al., 2003; Norvell et al., 1999), we showed that inhibiting the function of Sqd leads to a disintegration of the anchoring structures, the sponge bodies, into transport particles that are in continuous transport at the anterior of the oocyte. This is distinctly different from experiments inhibiting Dhc function where the anchoring structure disperses when inhibited (Delanoue et al., 2007). Injecting the inhibitory antibodies before the injection of *grk* mRNA leads to the formation of transport particles at the anterior that fail to anchor at the DA corner. Combining the results obtained by FISH and EM we can define 3 different consecutive stages in the localization of *grk* mRNA in the oocyte. The first is a localization of *grk* mRNA in TPs to the anterior. RNA containing transport particles are transported towards the minus-ends of the MT in a Dynein dependent manner (Delanoue et al., 2007; MacDougall et al., 2003) that does not require Sqd (Norvell et al., 1999). The second is the transport of the Sqd containing particles to the DA corner, previously shown to be dependent on Sqd. In a *sqd* null background, the TPs remain at the anterior where they are not anchored but in a continuous flux (Delanoue et al., 2007). One could argue in the light of the new

data presented here that this data could be explained by Sqd only having an anchoring function for *grk* mRNA without invoking a transport function. This alternative hypothesis for Sqd function would explain why TPs do not anchor at the DA corner, by suggesting that they diffuse away from the nucleus to accumulate at the anterior by continuous active transport that remains unaffected when Sqd function in anchoring is disrupted. Diffusion however, is much slower than directed transport and would in this case result in an accumulation of TPs in continuous transport at the DA corner. My data suggest a role for Sqd in the third step of localization where the TPs are incorporated and anchored in the sponge bodies. We showed here that Sqd has a structural role in these anchoring bodies. Disrupting Sqd after anchoring reverts the Sponge bodies to TPs that are presumably in continuous transport. We propose that Sqd is responsible for anchoring the TPs at the DA corner into the sponge bodies. The exact molecular mechanism by which this occurs remains unknown and might only be tractable when we understand more of the molecular details of the Dynein complex, all its many components and how they function in conjunction with transacting factors in mRNA localization. An important observation made is the fact that Sqd is present in the TPs at all stages of localization (Delanoue et al., 2007). The transition from TP to anchored RNP is thus not dependent on recruitment of Sqd and might be explained by a docking protein present in the SBs or Sqd might undergo a post translational modification and co-factors involved in the anchoring might be recruited. A question we did not address is the role of the different isoforms of Sqd. Further analysis of *grk* RNA injected into transgenic flies that only express a specific isoform of Sqd or a combination of those could reveal whether the different alleles act consecutively in transport and anchoring or that it is a joint effort. Another interesting question is whether Sqd is involved in the transport and anchoring of *grk* mRNA at earlier stages. In early stages of oogenesis, *grk* mRNA is found at the posterior of the oocyte where Grk protein signals to the polar cells. It is unknown whether the RNA migrates with the nucleus or if newly synthesized transcripts that are transported to the DA corner. As we have shown in our lab that Sqd is a general component of SBs (Delanoue et al., 2007) it is also likely to have a role in anchoring in early oogenisis. How anchoring at the posterior would link to Sqd independent transport to the anterior at stage 9 is an interesting question that could be addressed in further studies. *sqd* mutants also show a antero-posterior defects due to ectopic Osk translation (Norvell et al., 2005; Steinhauer and Kalderon, 2005). Whether this is due to a MT organization defect or a

direct defect in translational regulation is not agreed upon. Sqd could also have a role in *osk* mRNA anchoring, which could be tested in with the antibody injection I developed. Although *sqd* mutations do not have a role in the polarity of somatic follicle cells (Steinhauer and Kalderon, 2005), this has not been shown in other tissue.

We conclude that *grk* mRNA is transported in TPs in two distinct phases to the DA corner where it is anchored in sponge bodies. The second localization step is dependent on Sqd as well as the anchoring. To understand why *grk* mRNA is anchored in SBs we need to understand better what these SBS are and how the translational regulation of *grk* mRNA relates to this anchoring. These are questions I will address in the following chapters.

5

Are Sponge Bodies the Processing Bodies of the oocyte?

5.1. Introduction

Recent work by EM in the lab showed that *grk* mRNA is anchored at the DA corner in electron dense structures, interdigitated with ER and in close association with mitochondria. These were characteristics of the structures described by the Nusslein-Volhard lab (Delanoue et al., 2007; Wilsch-Brauninger et al., 1997). They named these structures Sponge Bodies (SBs). The SBs were proposed to contain *bicoid* mRNA (Wilsch-Brauninger et al., 1997), suggesting that they could be a class of RNA granules. Correct dorso-ventral patterning is dependent on correct localization of *grk* mRNA at the DA corner and a tightly regulated translational activation and regulation of the transcript. From the dorsalised phenotype in sqd^{l} mutants where *grk* mRNA is translated while being in transport, it is clear that the anchoring in SBs is very important in this translational regulation of *grk* RNA. Although the exact nature of SBs is unknown, experimental data from our lab and Nusslein-Volhards lab strongly suggest that SBs are a storage or processing unit for mRNA, regulating the translation. In Drosophila, PBs have been described in S2 cells as RNA containing particles consisting of proteins involved in translational repression, RNA degradation, RNA mediated gene silencing and RNA surveillance (Eulalio et al., 2007b). At the start of this project, PBs had not been intensively studied in the *Drosophila* female germline, and even now, data are scarce. The data that are available do not discriminate between SBs and PBs, treating them as one and the same entity (Lin et al., 2008; Liu and Gall, 2007). In collaboration with Bram Herpers I tried to establish whether SBs have similar functions as PBs. SB like structures are found throughout the egg chamber and Bram Herpers confirmed that the structures are enriched in Exu (unpublished work). The fact that the polysome-destabilizing drug Puromycin had no effect on the sponge bodies or its contents, confirmed that SBs were not stress granules (Bram Herpers, unpublished work). PBs have been shown to be depleted of ribosomes (Anderson and Kedersha, 2006) and when Bram Herpers labelled cryosections for P protein, a commonly used ribosome marker, the SBs were completely devoid of labelling whereas the surrounding cytoplasm showed dense gold labelling. P proteins are alanine rich phosphoproteins that are recognised by auto antibodies in patients suffering from systemic lupus erythematosus (Ghirardello et al., 2000). This data suggest that SBs and PBs are similar structures. Bram Herpers determined that all the SBs are enriched in Me31B and SqdGFP and that they are as good a marker for SBs as Exu (Bram Herpers, unpublished work) (Wilsch-Brauninger

et al., 1997). We continued to use these two proteins as a marker for the SBs in the oocyte in following experiments.

5.2. Aims of this chapter

In this chapter I investigate whether SBs are the PBs of the female germline in *Drosophila melanogaster*. I assess this by testing whether SBs are RNA containing complexes that depend on RNA for their existence and whether I can localize proteins involved in the different PB processes by IEM. Furthermore, I study whether Dhc has a structural role in *Drosophila* PBs in S2 cells.

5.3. Results

5.3.1. Sponge bodies depend on mRNA for their structure

PBs depend on RNA for their formation (Teixeira et al., 2005). A crucial experiment was to show that SBs contain RNA. Therefore I tried to establish the presence of polyadenylated transcripts by IHEM with a biotinylated poly T probe, 5'BIO-$T_{(40)x}$3'BIO3S (MWG). FISH on whole mount oocytes colabeled for Me31B were technically successful but it was impossible to draw conclusions as to a colocalization of RNA and SBs due to the high background labeling of Me31B. To get higher resolution data, I performed an *in situ* hybridization with this probe on ultra thin cryo-sections of wild type stage 9 oocytes. These experiments were not successful. Different annealing temperatures (38, 40, 42°C) were tested to localize the PolyA tail of endogenous transcripts. There was no difference in gold labeling on the tissue and the gelatin embedding material. As a negative control, sections of wild type oocytes were pretreated for 15 minutes with RNAse A 0.1mg/ml (Sigma). There was a substantial background labeling in this negative control that could not be distinguished from the non-treated sections (data not shown).

It proved difficult to show the presence of RNA in SBs by poly T *in situ* hybridization. Therefore, I tried to address this issue by looking at the effect of degrading the endogenous mRNA on the SB structure. To establish whether SB structure is dependent on RNA I digested the endogenous transcripts by injecting 0.1mg/ml RNAse A (sigma) in injection buffer into stage 9 Me31BGFP oocytes. A time-lapse movie was made to follow the GFP marked SBs and TPs. Before injection, the SBs can be seen as enriched foci of Me31BGFP at the DA and DV corner and the cortex of the oocyte (Figure 20A). Also fast moving TPs could be seen in the nurse

cells. Upon injection, SB structure is lost almost instantaneously and TPs disappear gradually within 10 minutes, showing that in the absence of RNA, the SBs and TPs disperse (Figure 20A') (N=10). As a negative control, stage 9 oocytes of flies expressing BasiginGFP and JupiterGFP were injected with RNAse A 0.1mg/ml. Basigin interacts with the actin network and localizes at plasma membranes whereas Jupiter binds to MT. There was no observable effect on the actin network nor the MT organization (Figure20B-B') (N=11). These results clearly show that SBs are dependent on RNA for their existence, a feature they share with PBs (Teixeira et al., 2005).

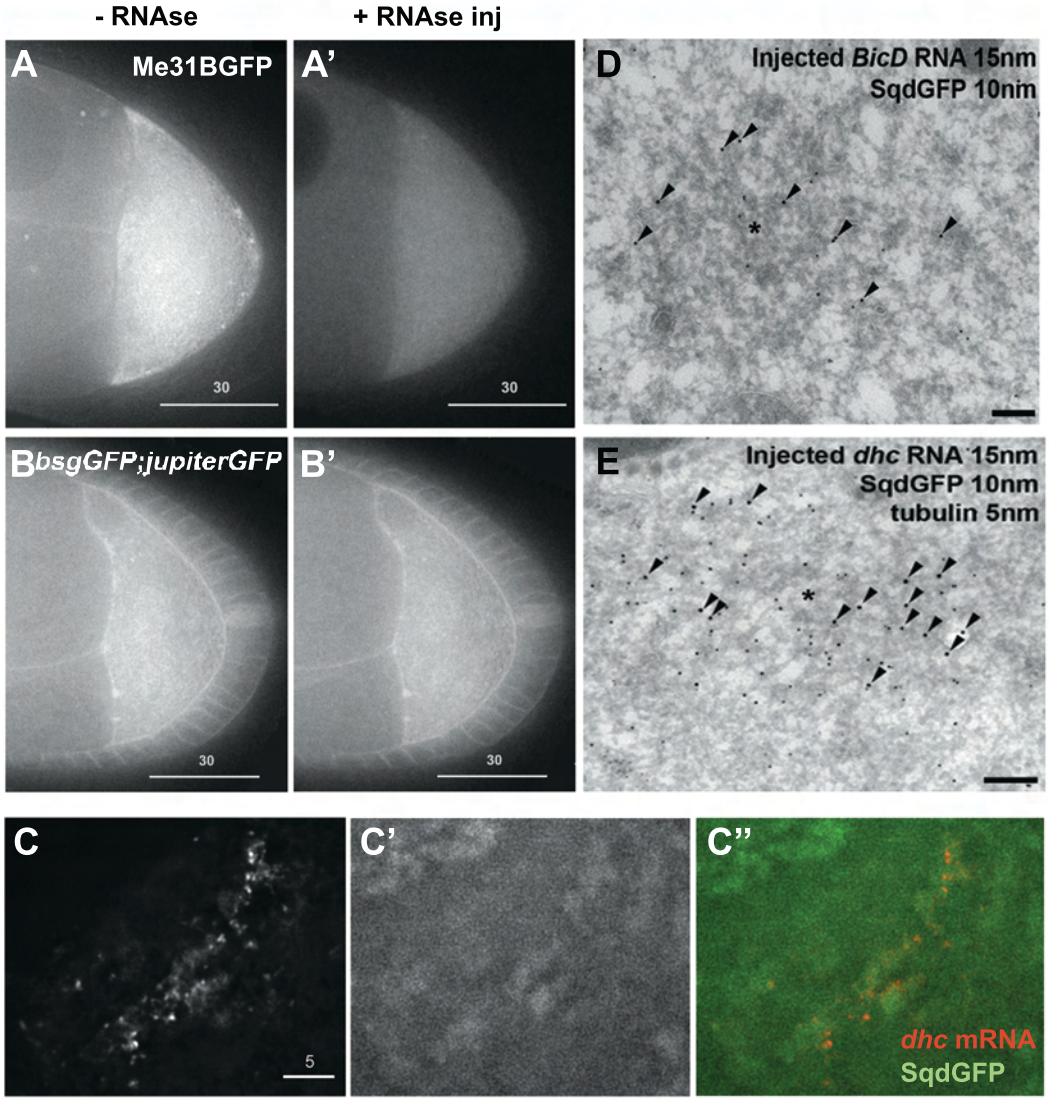

Figure 20 Sponge Body structure depends on RNA

(A-A') *Me31BGFP* oocytes before (A) injection and after (A') injection of RNAse A 0,1mg/ml. The SB structure visible in (A) disappeared in (A'). The reduction in Fluorescence in (A') is due to photobleaching.
(B-B') *bsgGFP;jupiterGFP* oocytes before (B) and after (B') injection of RNAse A 0,1mg/ml. Scale bar 30µm
There is no effect on the actin (*bsgCFP*) and MT (*jupiterCFP*) structure by digesting the RNA. Scale bar 30µm
(C C'') Injected *dhc* RNA (C) in *SqdGFP* (C') oocytes 45 minutes after injection. Scale bar 5µm
(D) *SqdGFP* oocytes injected with biotinylated *Bic-D* RNA localized for 45 min. Scale bar 200nm
(E) *SqdGFP* oocytes injected with biotinylated *dhc* RNA localized for 45 min. Scale bar 200nm
SB (*), Biotin 15nm (Arrowheads), SqdGFP 10 nm, MT 5nm gold labeling

5.3.2. Injected RNA localizes to sponge bodies

As shown above, SBs need RNA to maintain their structure as do PBs. I could not establish whether all endogenous mRNA resides in SBs but we have shown before that *grk* mRNA localizes to a specific subset of SBs at the DA corner of stage 9 oocytes and that injected *grk* RNA localizes to this subset of SBs. If SBs are the PBs of the oocyte, one would expect injected RNA to localize to these structures in order to be degraded or to regulate their translation. To test this, Bram Herpers and myself investigated if injected non-localizing RNAs would localize to SB. We injected biotinylated *dhc* RNA into stage 9 SqdGFP oocytes. The RNA was allowed to localize for 45 minutes and fixed for further examination by EM. A subset of the fixed oocytes was incubated with Streptavidin coupled to Alexa546 (molecular probes). The *dhc* RNA did not localize to the DA corner but formed concentrated foci at the site of injection that are enriched in SqdGFP (Figure 20C-C'') (N=14). Bram Herpers has shown before that Sqd is a good marker for the sponge bodies, from which we conclude that injected *dhc* RNA localizes to SB. We also injected biotinylated *Bic-D* RNA into stage 9 oocytes of *SqdGFP* flies. Labeling of ultrathin sections of *dhc* and *Bic-D* injections reveal a SB structure with colocalization of *Bic-D* or *dhc* RNA with SqdGFP (Figure 20D-E). It seems from these results that any RNA would be tethered to the SB. Intriguingly, earlier experiments done by Bram Herpers and Renald Delanoue show that injected *grk* RNA that lacks the *grk* localization signal (GLS) does not localize to SqdGFP enriched foci by EM (Delanoue et al., 2007). We also injected labeled *hunchback* RNA. *hb* is one of the GAP genes that are involved in embryonic patterning and is therefore not expressed in the germline (Tautz and Pfeifle, 1989; White and Lehmann, 1986). The colocalization of *hb* RNA and SqdGFP is not conclusive by fluorescent microscopy. We were not able to confirm with certainty that *hb* localizes to SBs by EM. These experiments show that SBs have the capacity to incorporate non-localizing RNA suggesting a role in RNA storage or degradation.

5.3.3. Components of the translational regulation machinery are found in sponge bodies

Processing Bodies are cytoplasmic structures depleted from ribosomes and contain RNA (Anderson and Kedersha, 2006). They contain series of proteins involved in

various translational regulating pathways. For example the homologue of Me31B (yeast Dhh1 and mammalian p54/rck), CPEB, decapping enzymes (Dcp1 and Dcp2), and Tra1 homologues (a protein from the Scd6 family) (Weston and Sommerville, 2006). PBs are thought to be structures for RNA storage after which they are either degraded, repressed or eventually allowed to re-enter translation (Brengues et al., 2005).

To link SBs to PBs we had to find common factors involved in these processes. The most convincing way to show the presence of a protein in a SB is by IEM. Common PB markers are the Me31B orthologues (Weston and Sommerville, 2006). One of the first SB markers we established was Me31B. I performed a labeling for Me31B of sections from stage 9 wild type oocytes (Figure 21A-A'). There is a clear concentration of gold labeling in the sponge like structures. This is true for all the SBs found in the oocyte and nurse cells. Me31B is a DEAD-box protein that forms cytoplasmic RNP complexes with localizing RNAs and Exuperantia in the *Drosophila* oocyte. During early oogenesis, loss of Me31B causes premature translation of localizing RNAs within nurse cells, without affecting their transport to the oocyte (Nakamura et al., 2001). Our previous work on Sqd shows that SBs are enriched in SqdGFP and that Sqd is required for SB structure. Bram Herpers confirmed that all the SBs found throughout the oocyte contain SqdGFP. As explained above hnRNP Sqd is involved in translational repression. Bram Herpers also showed that a range of other PB markers or translational regulators can be found in the SBs. He was able to label SBs of stage 9 oocytes for Bruno. Bruno has been shown to bind directly to mRNAs that contain Bruno Response Elements (BREs). Bruno is involved in translational repression of BRE containing RNAs mediated by eIF4E and Cup. Intriguingly, all SBs in the oocyte contain Bruno, suggesting translational repression by Bruno is a wide spread phenomenon during oogenesis. He also localized Orb, an orthologue of Cytoplasmic Polyadenylation Element Binding (CPEB) protein, a known translational repressor in its unphosphorylated state (Piccioni et al., 2005), to SB. Furthermore, he found that decapping enzyme Dcp1 and its enhancer Dcp2 were also enriched in SBs suggesting a role for SBs in mRNA degradation.

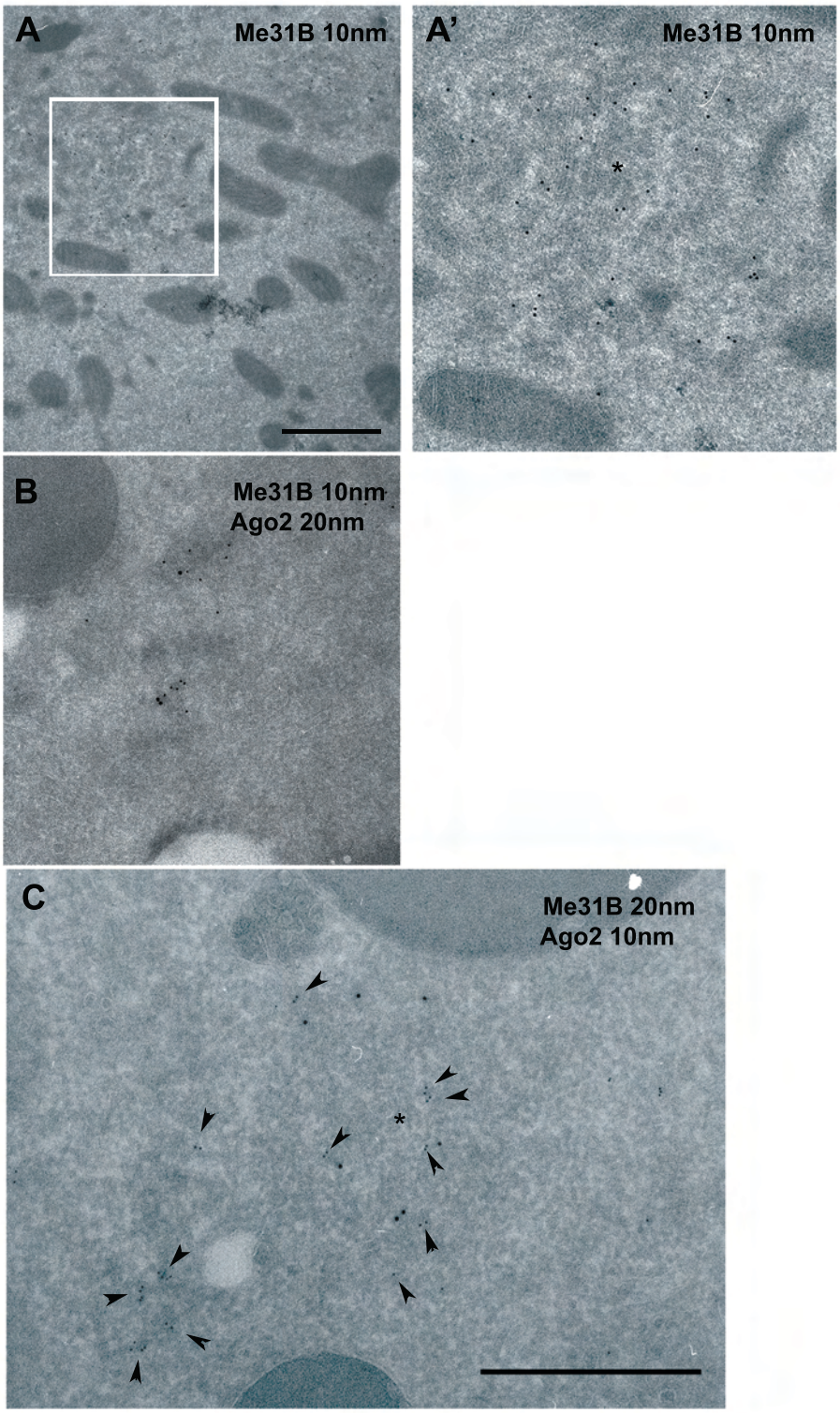

Figure 21 Sponge Bodies contain Processing Body markers

(A-A') Wild type oocyte labeled for Me31B with 10nm gold. Low magnification shows large SB with concentrated Me31B labeling and sponge like structure. (A') Enlargement of white box in A shows concentrated labeling for Me31B in SBs. Scale bar 500nm

(B) Wild type oocyte colabeled for Ago2 (20nm) and Me31B (10nm). Ago2 and Me31B colocalize in SBs.

(C) Wild type oocyte colabeled for Ago2 (10nm) (arrows) and Me31B (15nm). Both proteins colocalize in SBs. (*) Sponge Body, scale bar 1μm

5.3.4. Components of the RNA mediated gene silencing pathway are found in sponge bodies

PBs were originally described in yeast as RNPs involved in RNA degradation (Brengues et al., 2005; Teixeira et al., 2005). Later it was found that mammalian PBs also show miRNA mediated silencing activity (Chu and Rana, 2006; Pillai et al., 2005; Sen and Blau, 2005). In *Drosophila* S2 cells, it was shown that PBs form as a consequence of RNA mediated silencing (Eulalio et al., 2007b). Argonaute2 (Ago2) has been identified as part of the RNA-induced silencing complex (RISC). Ago2 is required for the unwinding of the siRNA duplex and loading of the siRNA onto the RISC complex in the *Drosophila* embryo (Okamura et al., 2004). The presence of short RNA mediated gene silencing is one of the characteristics of *Drosophila* PBs but upon the start of this project there was no direct evidence for microRNA dependent gene silencing in the germline. I performed a double labeling on sections of wild type stage 9 oocytes for Ago2 and Me31B showing a colocalization of the two proteins (Figure 21B-C). This confirmed that members of this pathway are present in SBs in the germline. To support this data, I injected biotinylated *grk* RNA into oocytes of an Ago2YFP expressing line. These flies were identified in a UK wide gene and protein annotation effort of a protein trap screen devised by the St. Johnston lab and in which our lab is taking part (Ryder et al., 2009). When *grk* RNA is injected and localized after injection, Ago2YFP is recruited to the DA corner (Figure 22A-A') (N=6). When I inject *grk* RNA into the nurse cell, Ago2 forms large foci (Figure 22A-B') (N=2). The reason I did not use fluorescently labeled RNA is that there was considerate bleed through from Alexa 546 and Alexa488 labeled RNA in the YFP channel. This experiment shows that Ago2 can be recruited to SBs together with *grk* RNA. However, a recent publication showed with a GFP reporter construct containing 4 miR-312 target sites in tandem that there is miRNA mediated silencing in the oocytes but that Ago1 protein does not colocalize with Bruno nor YFPDcp1, both SB markers. They showed that the SB marker Me31BGFP occurs in large foci and that neither the punctate Ago1GFP nor Ago2GFP show a similar distribution in stage 9 oocytes (Reich et al., 2009). They did not perform a colocalization experiment for Ago2 and SB markers, so it is possible they overlooked this localization of Ago2 to SBs. Also, it might be that because the RNA we inject is a heterogeneous mixture of

different lengths of *grk* RNA, capped and uncapped, and might contain dsRNA fragments, that some of it recruits the degradation machinery.

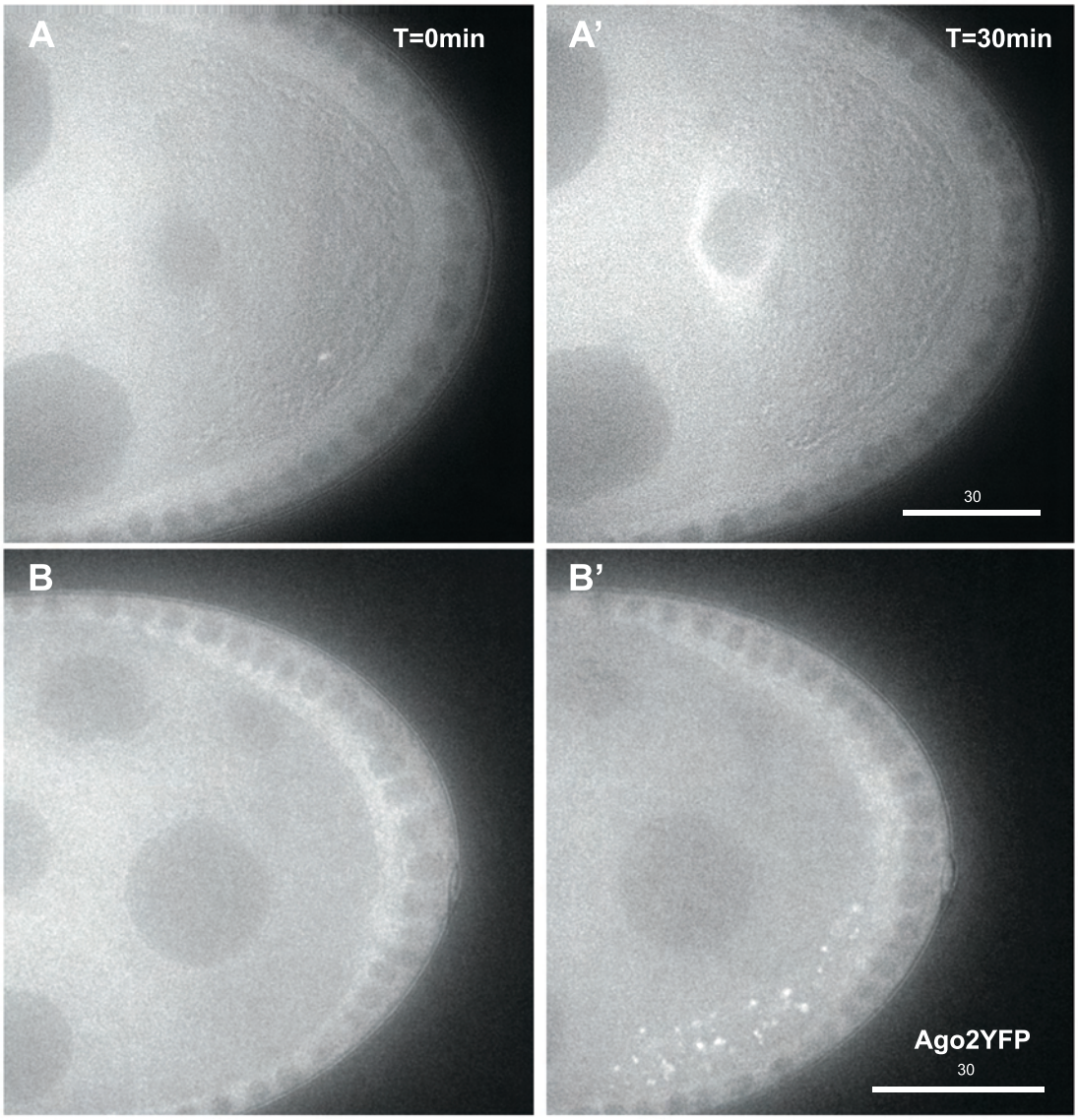

Figure 22 Ago2YFP is recruited by injected *gurken* RNA

(A-A') Ago2YFP is recruited to the DA corner with localizing *grk* RNA.
(A) shows the oocyte before injection of grk RNA. (A') Ago2YFP accumulates at the DA corner with *grk* RNA. Scale bar 30μm
(B-B') Ago2YFP is recruited to SB like structures upon RNA injection in the nurse cell. (B) Egg chamber before injection and (B') 30 min after injection. Scale bar 30μm

5.3.5. Structural roles for Dhc in Processing Bodies

The experiments above strongly suggest that SBs in the female germline are the equivalent structures to the PBs. The *Drosophila* orthologue of PBs were previously described in S2 cells (Eulalio et al., 2007a; Eulalio et al., 2007b). We have shown that Dhc has not only a role in anchoring of the RNA but is also required to maintain SB structure *in vivo* (Delanoue et al., 2007). A structural role for Dynein has not been established in the somatic PBs yet. I wanted to test whether Dhc has also an essential role for PB integrity. To investigate a structural role for Dhc in the *Drosophila* PBs an RNAi knockdown experiment was set up in S2 cells. 15μg of *dhc*, *dic* or *ampicilin* dsRNA was added on day 1. Samples were taken for western blotting on day 2 after transfection when maximal protein depletion is expected and an immunostaining was done on a sub-sample. On day 3 only an immunostaining was done because of quantity issues. Knocking down Dhc did not affect the viability of the S2 cells compared with the mock treated cells. For the western blotting, cell density was estimated as the average of 3 counts in a Neubauer improved cell counter. An equivalent of $1x10^6$ cells were lysed in 200 μl lysis buffer and 6.5 and 13 μl of this lysis product were loaded on a 5% TRIS-Glycin gel. Protein was transferred overnight on a nitrocellulose membrane and labeled with anti-Dhc antibodies for 2 hours. The protein was visualized with ECL labeling kit. Exposed Kodak films were developed by hand. The western blot shows that Dhc is below detection limit in the cells treated with *dhc* dsRNA but can be detected in the lanes with lysate of cells treated with *dic* dsRNA and mock treated cells (Figure 23). This shows that the RNAi knockdown was successful. To study the effect of knocking down Dhc on PBs, I performed an antibody labeling for GW182 and Trailer Hitch (Tral) at day 2 and day 3 after transfection. GW182 and Tral were the original markers used for PBs in S2 cells (Eulalio et al., 2007b). The cells were allowed to adhere to Concanavalin A coated coverslips for 30 min. They were fixed in cold Methanol supplemented with 4% PFA. In all the different treatments, all the cells labeled positive for GW182 or Tral and no difference in PB size or quantity could be observed between the samples supplemented with dsRNA and mock treated cells on day 2 after transfection (Figure 24A-D, observed cells >100 per treatment). The same was seen for day 3 (data not shown). As I did not perform a colabeling with Dhc and GW182 or Tral, I do not

know if all the cells are sufficiently depleted of Dhc but the uniformity of PBs labeling and the successful knockdown suggest that most of the cells are negative for Dhc. The S2 cell line originates from a primary culture derived from late stage (20-24 hours post hatching) *Drosophila melanogaster* embryos (Schneider, 1972). Many features of the S2 cell line suggest that they originate from a macrophage-like lineage. To verify the data obtained by the knockdown experiments, I looked at macrophages dissected out of third instar larvae of $dhc^{6\text{-}6}/dhc^{6\text{-}12}$ mutant flies. An allelic combination of $dhc^{6\text{-}6}$ and $dhc^{6\text{-}12}$ has been described to delay RNA transport and to lack SBs (Clark et al., 2007; Delanoue et al., 2007; MacDougall et al., 2003; Mische et al., 2007). The macrophages were allowed to adhere to ConA coated coverslips for 30 min before fixing them in cold Methanol with 4% PFA solution. After fixing, PBs were labeled for with GW182 (Figure 25A-B) or Tral antibodies (Figure 25C-D). There was no difference in PB size or quantity in WT (N=87 for GW182 labeling and N=19 for Tral labeling) and mutant macrophages (N=32 for GW182 labeling and N=48 for Tral labeling). Taken together these data strongly suggest that Dhc does not have a structural role in the *Drosophila* PBs originally described in S2 cells as opposed to SBs in the female germline.

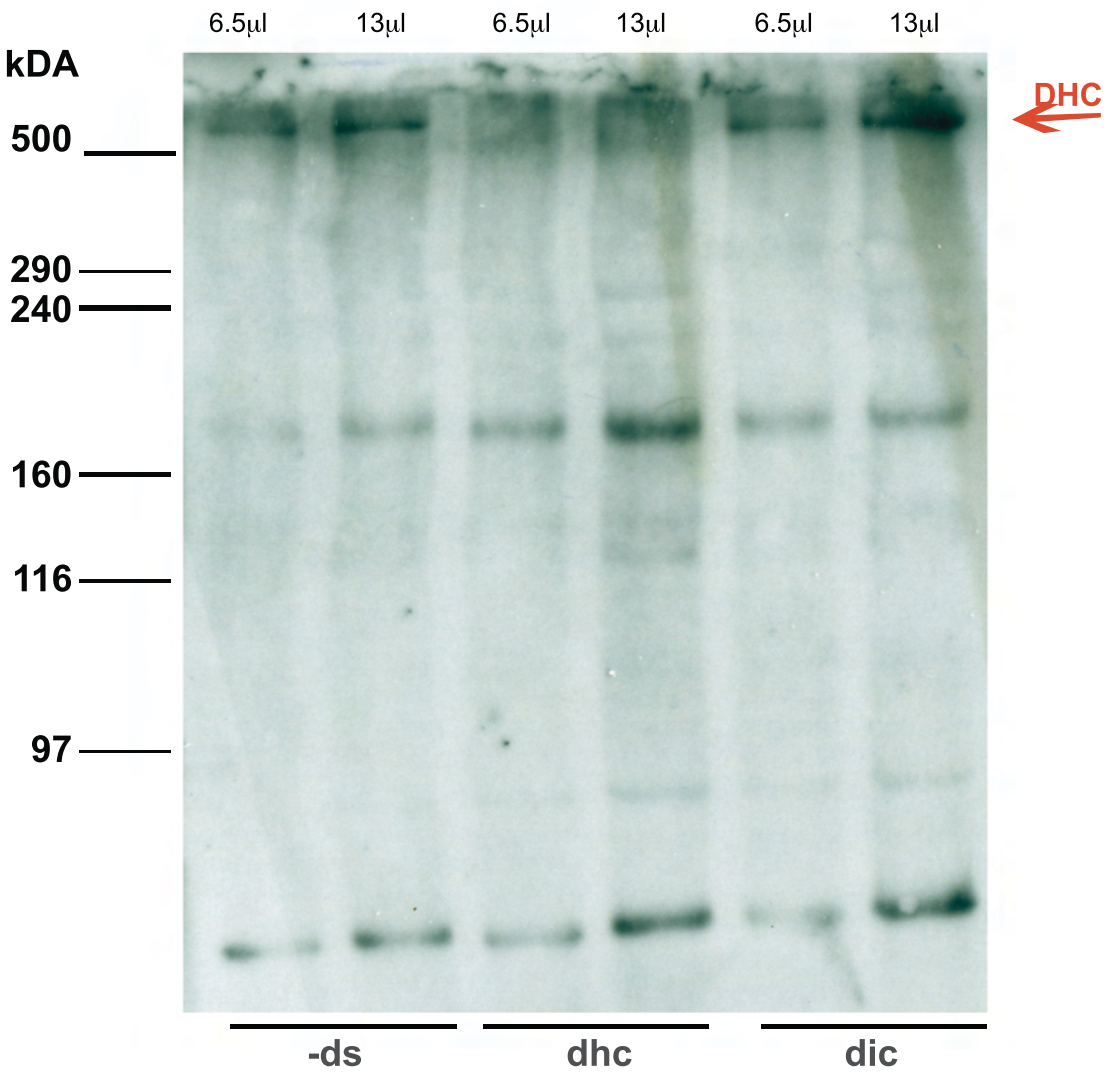

Figure 23 RNAi knockdown experiment in S2 cells

Western blot on whole cell lysate labeled for Dhc. The lanes represent 6.5 and 13 µl of a lysate of 1 million cells in 200µl buffer. The cells treated with *dhc* dsRNA clearly show a reduction of Dhc protein below detection limit compared to the negative control and the cells treated with *dic* dsRNA.
Nonspecific staining serves as a loading control

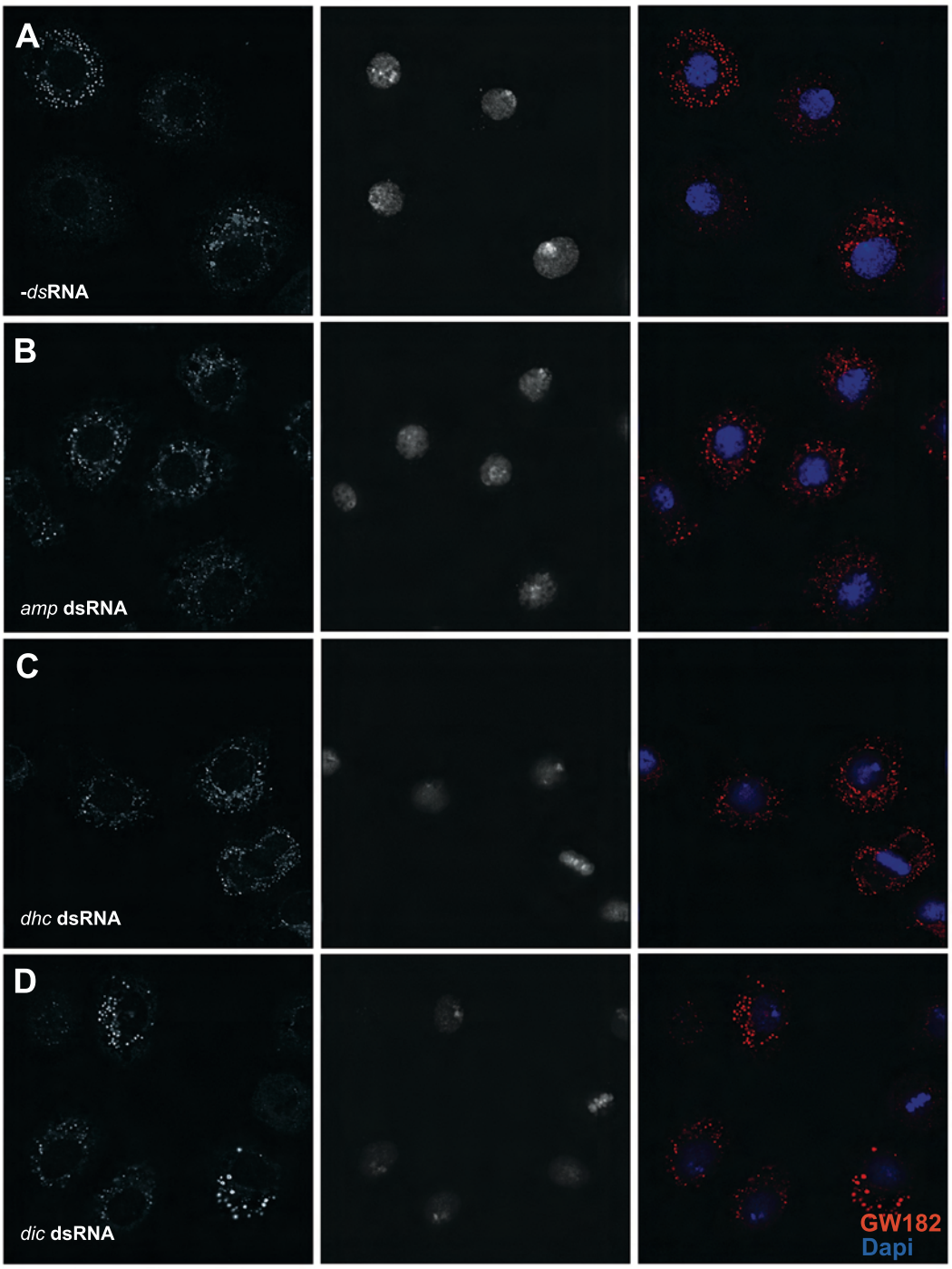

Figure 24 Function of Dynein heavy chain in *Drosophila* Processing Bodies

(A-D) S2 cells depleted for Dhc (C), Dic (D) compared to cells treated with *ampicilin* dsRNA (B) and mock treated cells (A). Cells are labeled with GW182 antibodies as a PB marker and DapI

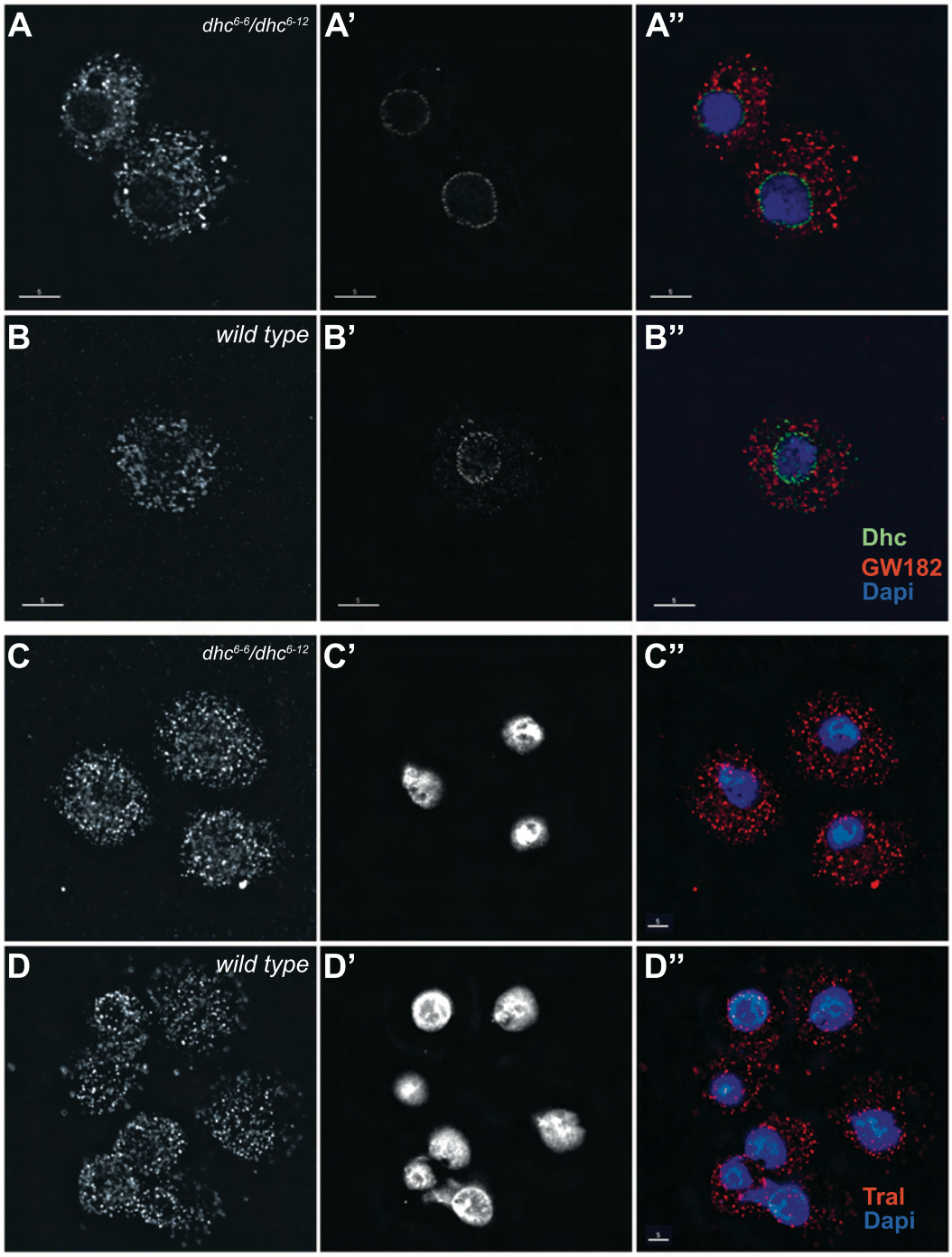

Figure 25 Dynein heavy chain is not required for PB integrity

(A-A'') Macrophages from *dhc*$^{6-6}$/*dhc*$^{6-12}$ flies labeled for GW182 (A) and Dhc (A')
(B-B'') Macrophages from wild type flies labeled for GW182 (B) and Dhc (B')
(C-C'') Macrophages from *dhc*$^{6-6}$/*dhc*$^{6-12}$ flies labeled for Tral (C) and Dapi (C')
(D-D'') Macrophages from wild type flies labeled for Tral (D) and Dapi (D')
Scale bar 5 μm

5.3.6. Ultrastructural analysis of S2 cells

The *Drosophila* PBs were first characterized in S2 cells by immunofluorescence. SBs have a very distinct sponge like structure in the oocyte. If SBs are related to PBs it would be interesting to see if they have a similar structure. *Drosophila* PBs have not yet been studied by EM to my knowledge although it has been reported that the human orthologue of PBs, the GW bodies, do not contain membranes or cisternae by IEM as SBs do (Yang et al., 2004). To locate the PBs in S2 cells, I cut ultrathin cryo sections of these cells and labeled them for known PB markers. The markers I chose were Me31B because the antibody has a very high affinity for the protein in SBs by IHEM and GW182 because it was the original marker for PBs in S2 cells. The Me31B antibody incubation did not give any labeling. As Me31B is not zygotically expressed (Nakamura et al., 2001) and as S2 cells are derived from embryos this is not unusual. The antibody against GW182 resulted in high background labeling due to a specific binding of the bridging antibody to the tissue. To overcome this I used a goat anti rat gold conjugate (BBI). This experiment did not result in a detectable signal. Examination of the sections for structural clues did not reveal any SB like structures (Figure 26A-A').

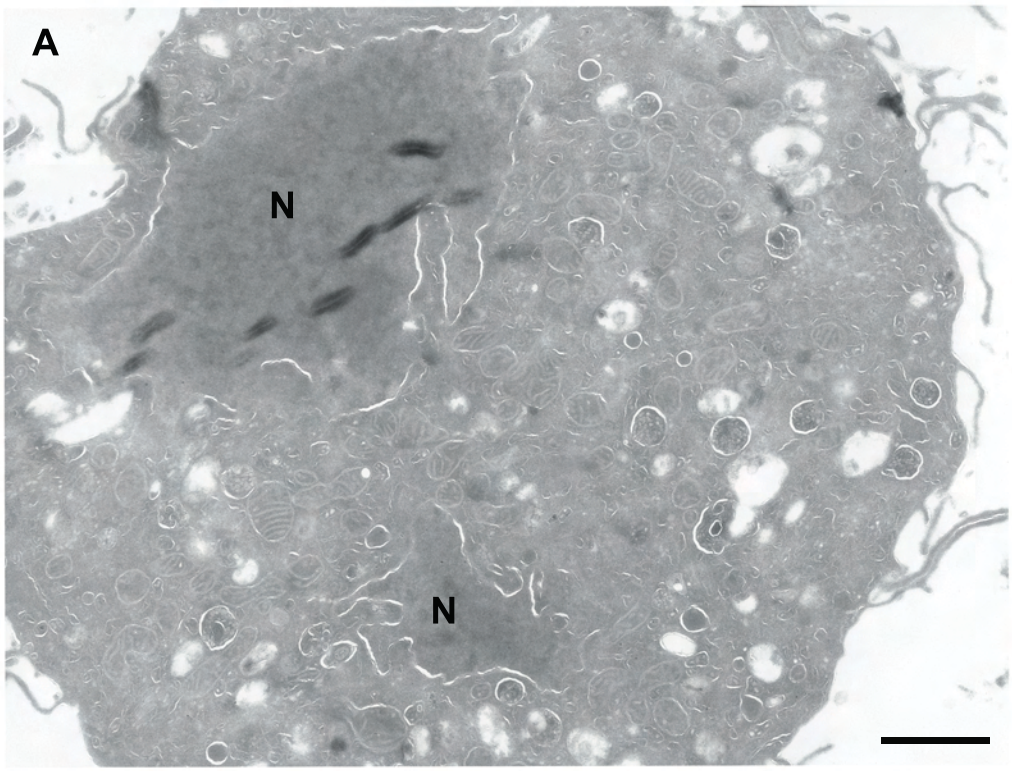

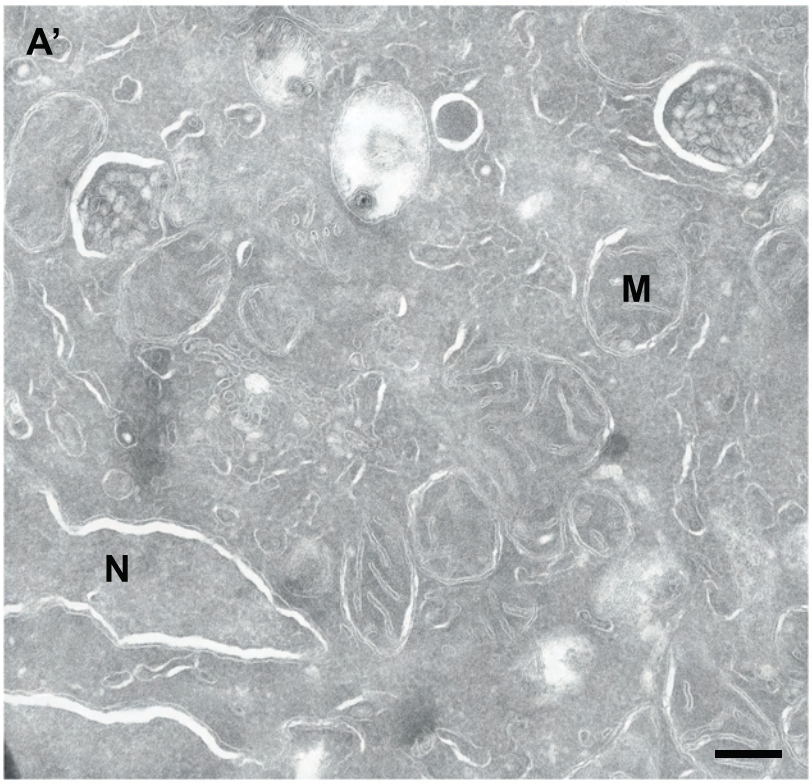

Figure 26 S2 cell at ultrastructural level

(A-A') Cryosection of an S2 cell. No obvious SB like structures can be detected. Nucleus (N), Mitochondria (M) Scale bar (A) 1μm, (A') 200nm

5.4. Discussion

The experiments above show that the SBs are RNPs that share components of most of the major processes that take place in PBs. The fact that SBs are dependent on RNA for their existence shows that they are most likely a concentration of proteins involved in translational regulation of the transcripts they decorate. Interestingly, SBs do rely on Dhc for their structure, a feature that is not shared with PBs. It seems that in the oocyte, at least in the case of *grk* mRNA, TPs containing the Dynein motor complex incorporate in the SBs where Dynein changes from a motor into a static anchor. In the PBs, Dynein does not have such a role. Whether Dhc has a role in transport of mRNA in the macrophages remains an unanswered question. Recently, a role for Dynein has been revealed for the formation and integrity of Stress Granules (SGs) in primary neurons (Tsai et al., 2009). These findings might suggest that SBs are closely related to neuronal SGs. However, my results together with the work done by Bram Herpers show that SBs are functionally related to the *Drosophila* PBs but that they differ in the fact that Dhc is a structural component. The data on *grk* mRNA transport to SBs suggest that there is a general mechanism by which SBs are formed by TPs that are transported by the Dynein motor after which the Dhc converts into a static anchor. The functions that PBs fulfill in the cell suggest that the composition of the "body" might change to fine tune its function. It might change upon the RNA it contains, the place in the cell it is found in and what the fate of its RNAs are. An attractive hypothesis is that a basic processing RNP is assembled to economize the cells resources and that the fine tuning of the regulation is obtained by recruiting certain proteins dependent on the task at hand. This might explain why in the oocyte, the SBs at the DA corner do not differ in composition for the tested proteins from SBs in the rest of the egg chamber.

6

The role of Sponge Bodies in the translational regulation of *grk* mRNA

6.1. Introduction

Grk protein is synthesized on the Endoplasmatic Reticulum (ER) as a transmembrane protein precursor after which it is transported to the Golgi apparatus where it is cleaved by a protease called Brother of Rhomboid (Ghiglione et al., 2002; Guichet et al., 2002; Urban et al., 2002) into a functional TGF-α protein. A stage 9 oocyte contains roughly 1000 transitional ER-Golgi (tER-Golgi) units uniformly distributed throughout the ooplasm (Herpers and Rabouille, 2004). Grk is processed at a specific subset of Golgi at the DA corner from where is transported towards the overlying follicle cells. It is the localization of *grk* mRNA that dictates which tER-Golgi units are used for Grk transport in stage 9 oocytes (Herpers and Rabouille, 2004). *grk* mRNA is anchored in a subset of SBs at the DA corner. We showed that these SBs are PB like structures containing proteins of the translational regulating pathways. Why *grk* mRNA is anchored in SBs and whether anchoring is needed for its tethering to the right subset of Golgi is not clear. In order to begin to understand why *grk* mRNA is anchored in SB, we need to know more about when it is anchored there in relation to the translation. One possibility is that *grk* transcripts are translated after being anchored in SBs. This leads to two possible scenarios: first that *grk* mRNA is stored in SBs in translationally silenced state and is exported from the SBs to the ER when the protein is required or secondly that *grk* is translated inside the SBs at the DA corner. The other possibility is that *grk* mRNA is translated upon arrival at the DA corner before it gets anchored and that the SBs are just a processing unit that mops up the excess RNA for storage or degradation.

6.2. Aims of this chapter

In this chapter I address the functional reason for the anchoring of *grk* mRNA in SB. In order to get an insight in the role of the SBs in *grk* translational regulation, it is necessary to find out whether *grk* is translated before or after it is anchored. I investigate *Grk* protein localization in stage 6 egg chambers by EM because this is the earliest stage where *grk* mRNA localization and localized production of Grk protein is required for axis formation in oocyte. I also tried to follow *grk* translation *in vivo*. I approached this by injecting *in vitro* transcribed *grk* RNA into a *grk* null background and follow *de novo* translation of Grk protein. Finally, I look at SB morphology in stages 6-9 of oogenesis by EM.

6.3. Results

6.3.1. Grk protein is found on the tER-Golgi in early stages

Bram Herpers has studied the sorting mechanisms of Grk protein in the tER and Golgi in stage 9 oocytes to great extent (Herpers and Rabouille, 2004). He also confirmed that Grk protein does not reside in SBs but on the tER-Golgi at that stage. He labeled cryosections for the P protein, a ribosome marker, and found that the SBs are completely devoid of functional ribosomes (unpublished data). It is therefore unlikely that *grk* is translated in the SB. Thus, *grk* mRNA has to be translated before it gets anchored in the SBs or the transcripts have to be exported from the SBs after anchoring for translation. Grk protein and transcript appear as early as stage 2A of the germarium but a localized *grk* mRNA and protein synthesis are seen for the first time at stage 6 (Neuman-Silberberg and Schüpbach, 1993; Neuman-Silberberg and Schüpbach, 1996). When Grk signaling is delayed until after stage 6, the oocyte nucleus does not migrate (Peri and Roth, 2000). It is not clear what portion of *grk* transcript and protein is migrating with the nucleus to the DA corner. Therefore it is necessary to study *grk* translation before nucleus migration to catch the first localized translation event. It would be interesting to see whether the endogenous transcript is also anchored in SBs in early stages and whether the anchoring in SBs takes place before or after the appearance of Grk protein in the posterior region. *grk* translation has not been studied by EM in earlier stages before. Studying *grk* expression by EM at stage 6 poses several problems. The transcript and protein are very low in abundance and as yolk particles only appear at stage 7, it is impossible to determine where the oocyte is compared to the nurse cells in a stage 6 during sectioning. I solved the latter by taking sections of the whole late stage 6 egg chambers. By EM I could locate the oocyte by its slightly different morphology. I then labeled sections roughly every 20μm into the egg chamber for Grk protein. In this way I could locate a region in the oocyte that contained Grk protein. Although extremely low in abundance (typically 5 to 10 gold particles per section) all labeling for Grk occurred on the Golgi or on the *trans*-Golgi Network (TGN), never in SBs (Figure 27A-B). The fact that none of the labeling is found in SBs indicates that *grk* mRNA is not translated in SBs. Finding Grk on the Golgi just like in stage 9 oocytes (Herpers and Rabouille, 2004) suggests that the translation is regulated in a similar way. I considered to perform an *in situ* hybridization on these sections to visualize the endogenous *grk* mRNA but as

the labeling efficiency is very low even in stage 9, where the transcript is much more abundant, I decided against this experiment.

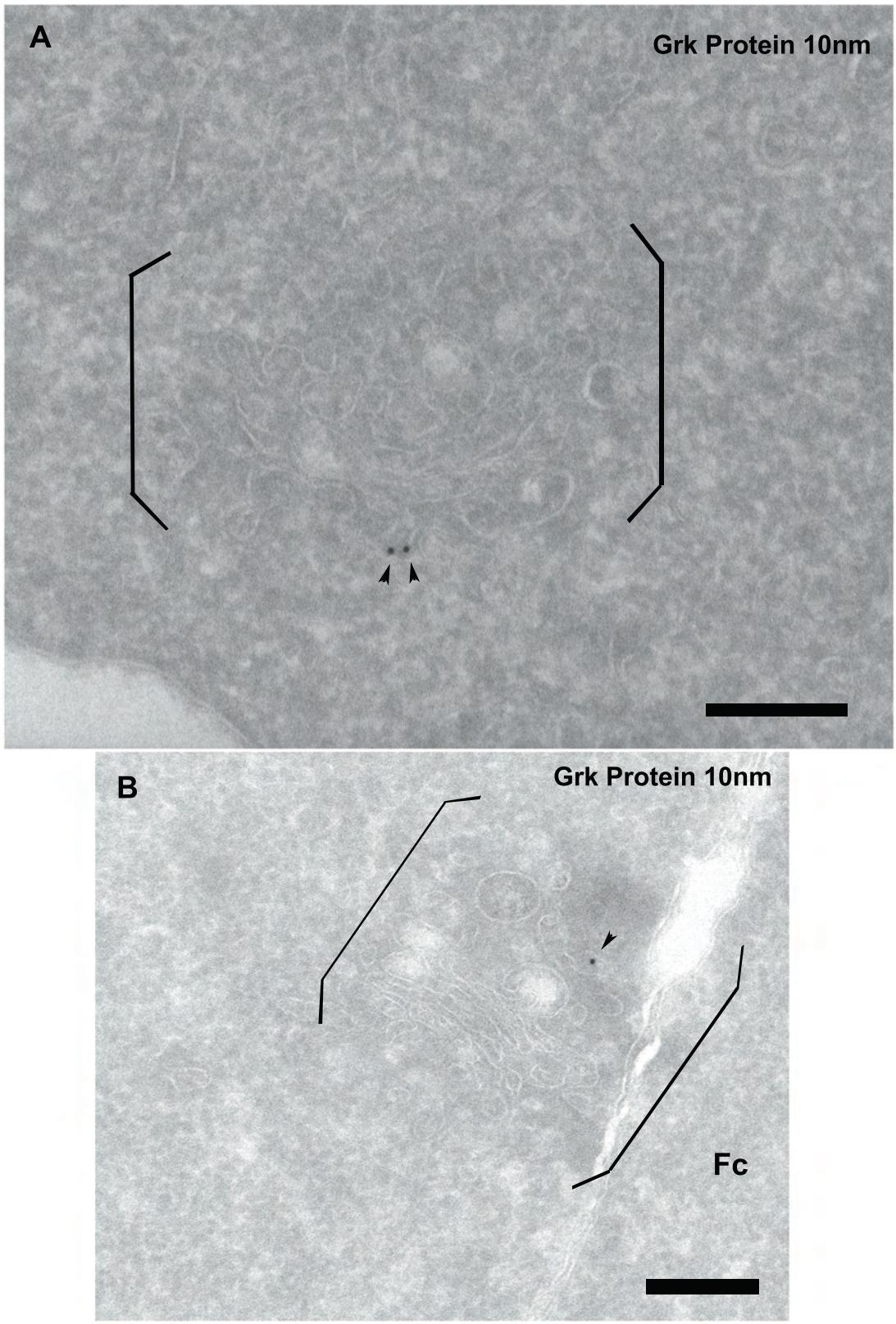

Figure 27 Gurken protein in a stage 6 egg chamber is found on Golgi

(A-B) Grk protein (10nm, arrow head) on the Golgi (brackets) in a stage 6 oocyte.
Pictures taken at the anterior side of the oocyte.
Follicle cell (Fc), Scale bar 200nm

6.3.2. Translation of endogenous *grk* transcripts

In order to determine whether Grk is translated before the transcripts are anchored in SBs or whether the RNA is exported from the SBs to be translated after anchoring I tried to translate Grk in a *grk* null background. This would allow me to verify whether Grk protein appears before or after the anchoring of the transcript in the SB. In this experiment I injected *in vitro* transcribed, non-labeled *grk* RNA in grk^{2b6}/grk^{E12} transheterozygote oocytes. This allelic combination has been described as a protein null (Neuman-Silberberg and Schüpbach, 1993). To be able to monitor localization, the non-labeled RNA was mixed with Alexa 546 labeled *grk* RNA (1/5). After the RNA was left to localize for 60 minutes the oocytes were fixed in 4% PFA in PBS and labeled for Grk protein. Grk protein can clearly be detected where the bulk of the RNA was found (Figure 28). It seems that Grk protein is not exactly where the RNA is but due to the amount of RNA, it is difficult to draw a conclusion. This experiment showed that *in vivo* translation of injected exogenous *grk* RNA is possible, enabling me to study the mechanisms of *grk* translation. The translation of injected transcripts would allow me to set up a pulse chase experiment in order to determine whether the transcripts are anchored before or after translation. By injecting *grk* RNA and fixing the injected oocytes at different time points I would be able to monitor by EM whether the RNA was translated before or after it was anchored in SB. While performing these pulse chase experiments, Caceres and Nilson published that *grk* mRNA has to recruit SqdA in the nurse cells in order to repress translation of *grk* mRNA during transport (Caceres and Nilson, 2009). This experiment confirms their results in a sense that injecting *grk* mRNA in the oocyte results in premature translation because it did not recruit SqdA in the nurse cells but unfortunately it rendered my assay inadequate to test the hypothesis. An alternative approach would be to inject the *grk* RNA into the nurse cells and let it localize to the oocyte. It should be tested whether there is still translation in the oocyte in this case.

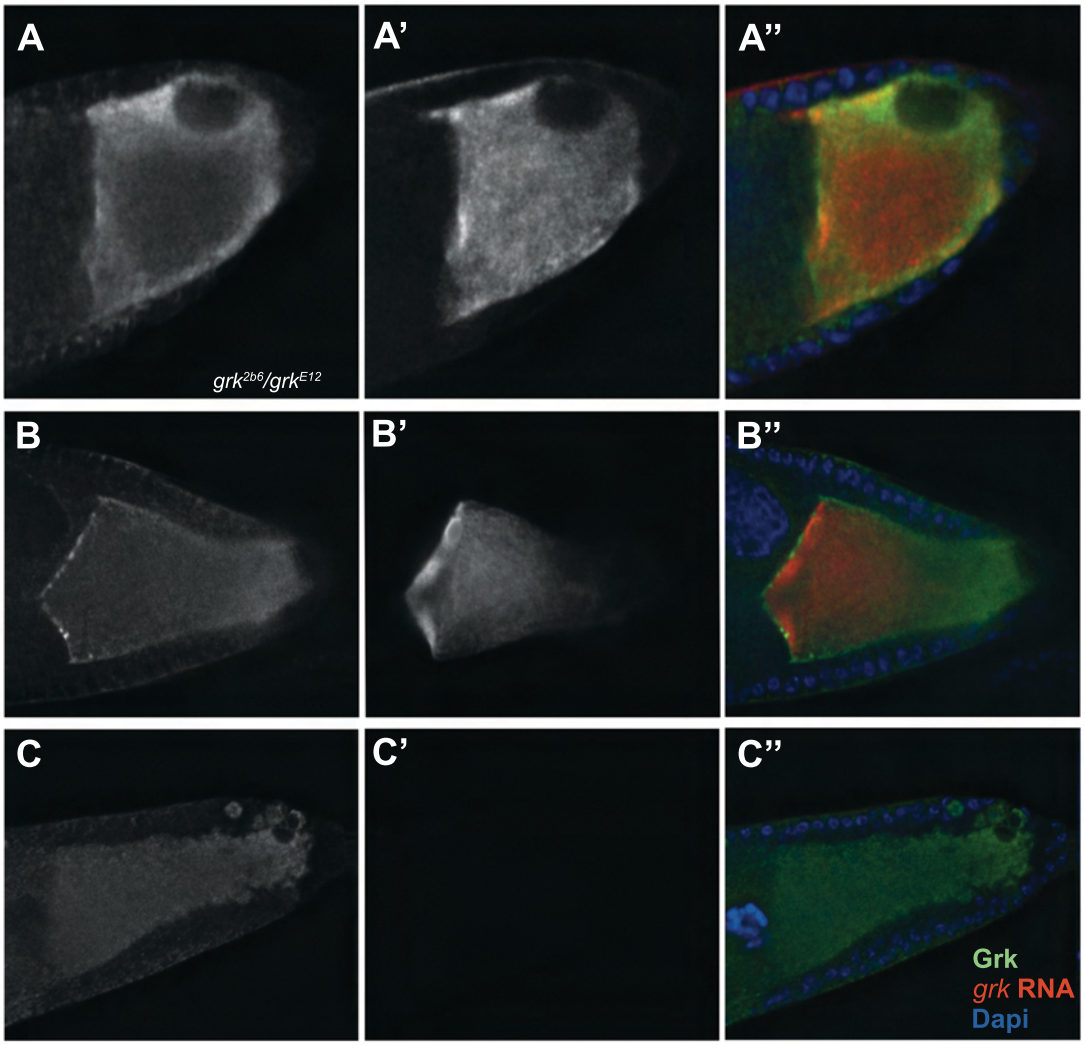

Figure 28 *gurken* mRNA translation in a *gurken* null background

(A-A'') Grk protein (A) in a grk^{2b6}/grk^{E12} oocyte, 1 hour after *grk* RNA (A') injection. In this example *grk* RNA localized to the anterior and partly to the posterior
(B-B'') Grk protein (B) in a grk^{2b6}/grk^{E12} oocyte,1hour after grk RNA (B') injection. In this example grk RNA localized to the anterior.
(C-C'') Grk protein expression in a non-injected grk^{2b6}/grk^{E12} oocyte

6.3.3. Sponge Bodies during earlier stages of oogenesis

We have shown that *grk* mRNA is anchored in SBs in stage 9 oocytes but we do not have information about anchoring at earlier stages. As injecting is very difficult at this stage, I wanted to confirm that there are also SBs in stage 6 by EM. Live cell imaging of Me31BGFP expressing oocytes reveal foci of Me31BGFP (Figure 29A) at stage 6 as well as in later stages. Also SqdGFP can be seen in this stage by fluorescence (data not shown), both indicating there are SBs at this early stage. I looked at Spurr (resin) imbedded oocytes from the collection of C. Rabouilles lab. The oocyte contains a very dense network of SBs. The majority of the cytoplasm is taken up by SB material (Figure 30). As described by Wilsch-Brauninger, I could also find SBs in the nurse cells, typically surrounding Nuage particles (Figure 31) (Wilsch-Brauninger et al., 1997). The abundance of SBs however was much lower than in the oocyte and its structure seemed to differ from that in the oocyte. This might reflect that the nurse cells are producing the bulk of the proteins for the oocyte, not needing to store the transcripts. It is possible that oocytes need to store a lot of transcripts in SBs for translation later in oogenesis. EM micrographs of Spurr embedded stage 9 oocytes (Figure 32A-B) revealed that the SBs in the oocyte (Figure 32B) and nurse cells (Figure 32A) contain less EM transparent material than the ones at stage 6. This manifests itself on the micrographs as white regions in the SBs. This indicates that the composition of the SBs changes during oogenesis. The abundance of SBs in a stage 6 oocyte is also much higher compared to a stage 9 egg chamber. I was also able to take pictures at a late stage 7 to early stage 8 oocyte (Figure 33). The overall structure of the SBs was the same as in a stage 6. The presence of SBs at stage 6 makes it tempting to speculate that *grk* mRNA is also anchored in SBs at this early stages.

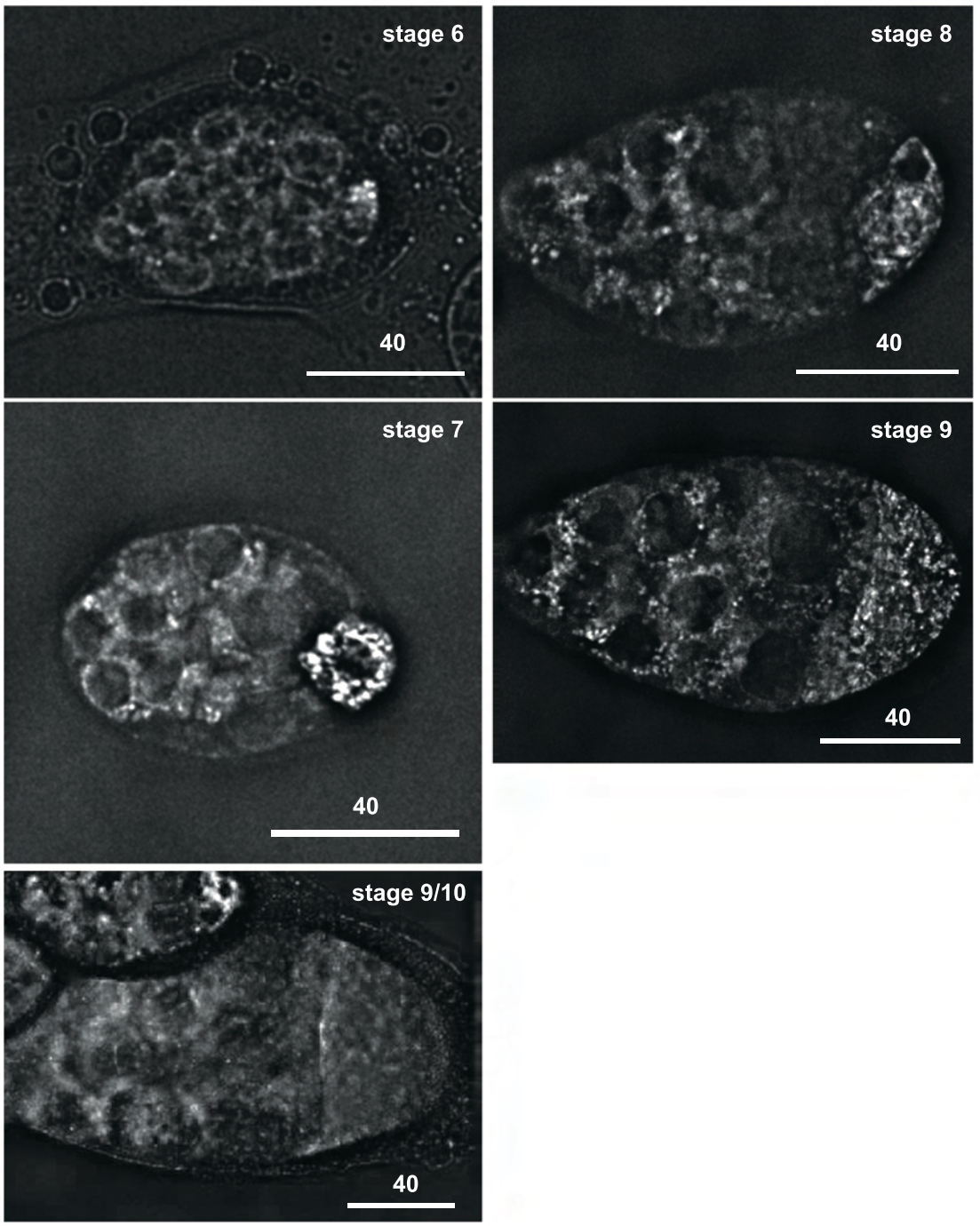

Figure 29 Me31BGFP expression during oogenesis

Me31BGFP expression in eggchambers during stages 6 to late 9/early 10A. Scale bar 40μm

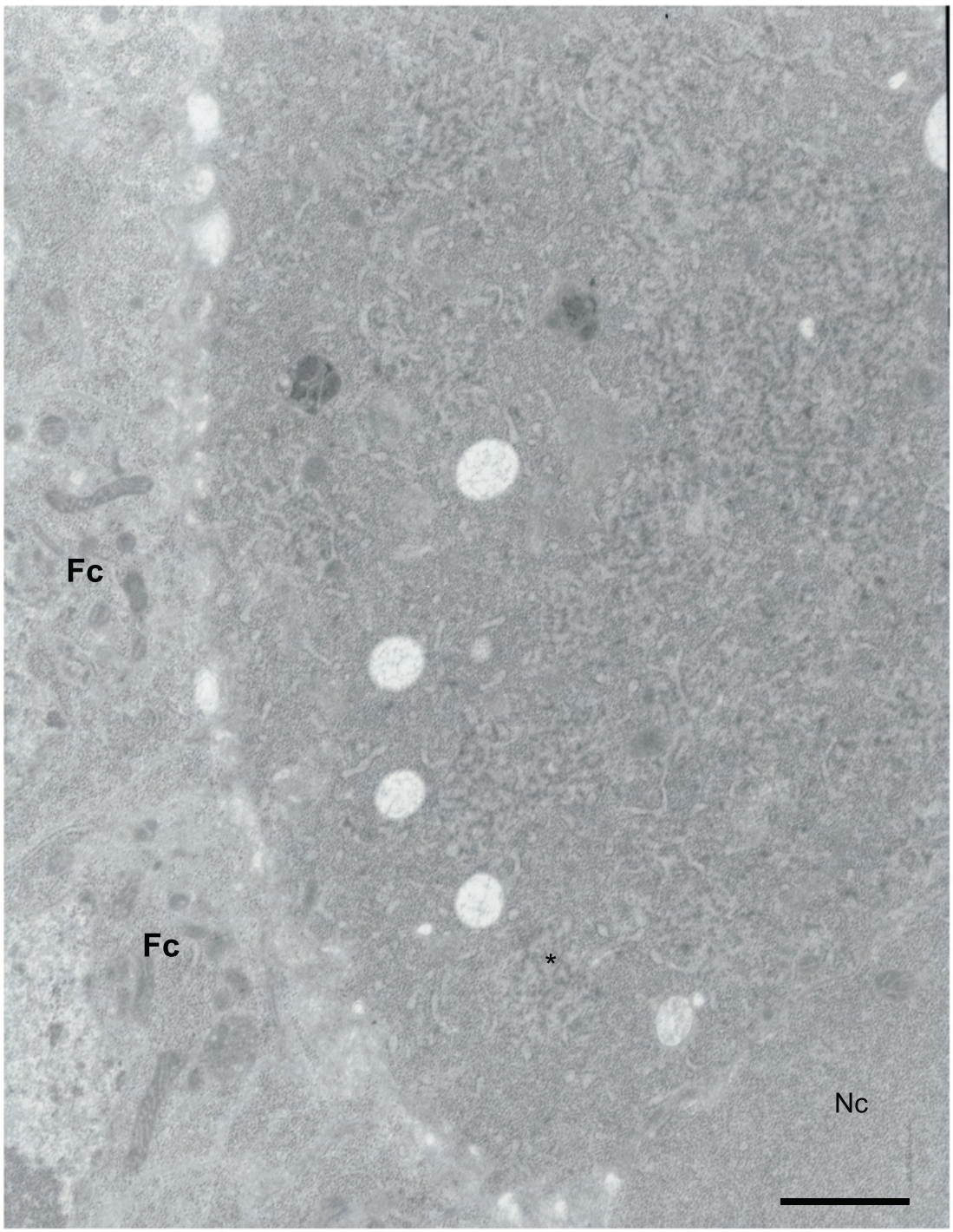

Figure 30 Sponge Body structure at a stage 6 oocyte

Sponge bodies in a stage 6 oocyte. One SB is marked with a (*), Follicle cell (FC), Nurse cell (Nc) Scale bar 1μm

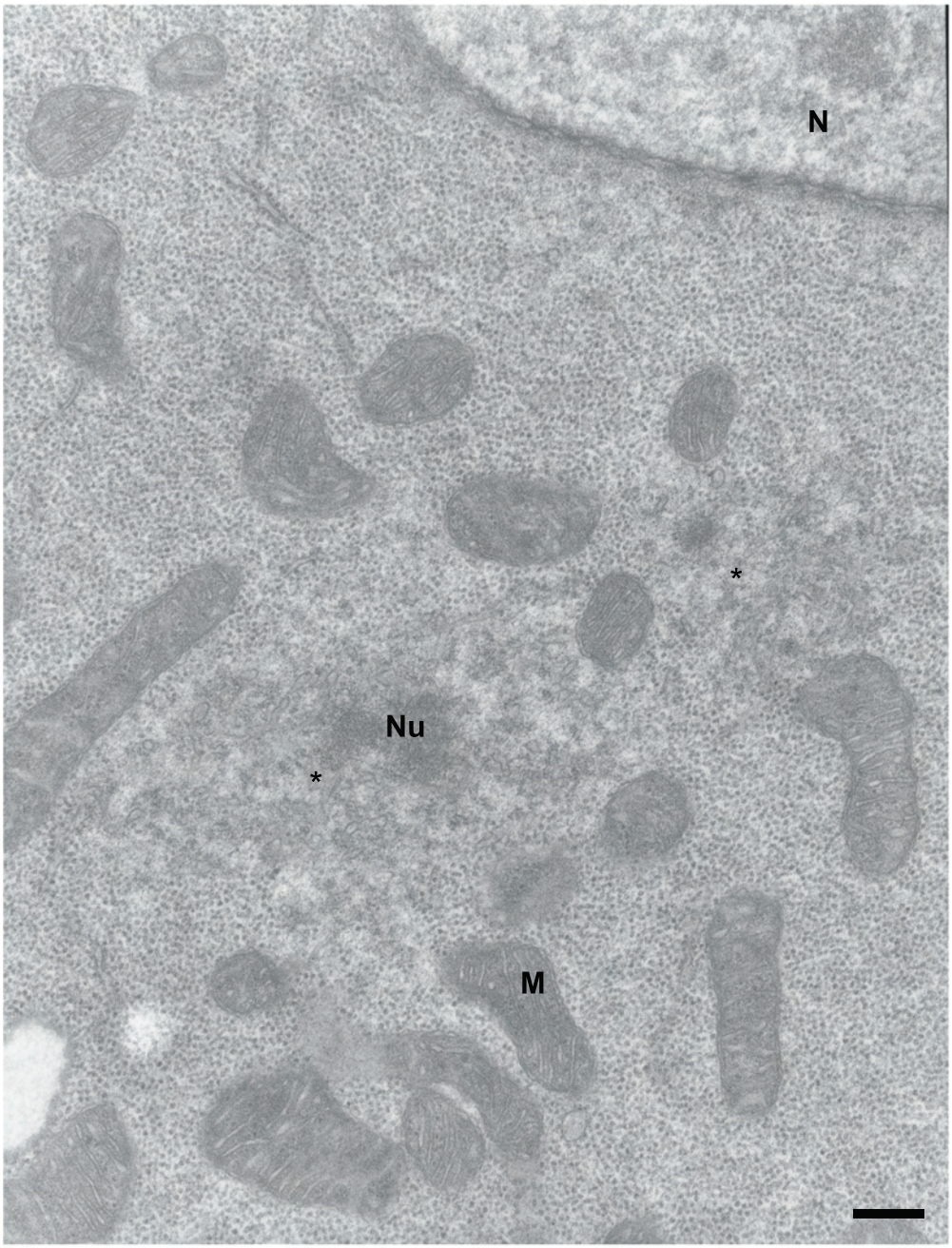

Figure 31 Nurse cell Sponge Body structure at a stage 6 egg chamber

Sponge bodies in a stage 6 egg chamber nurse cell. SB (*), Mitochondria (M), Nucleus (N), Nuage (Nu). Scale bar 1μm

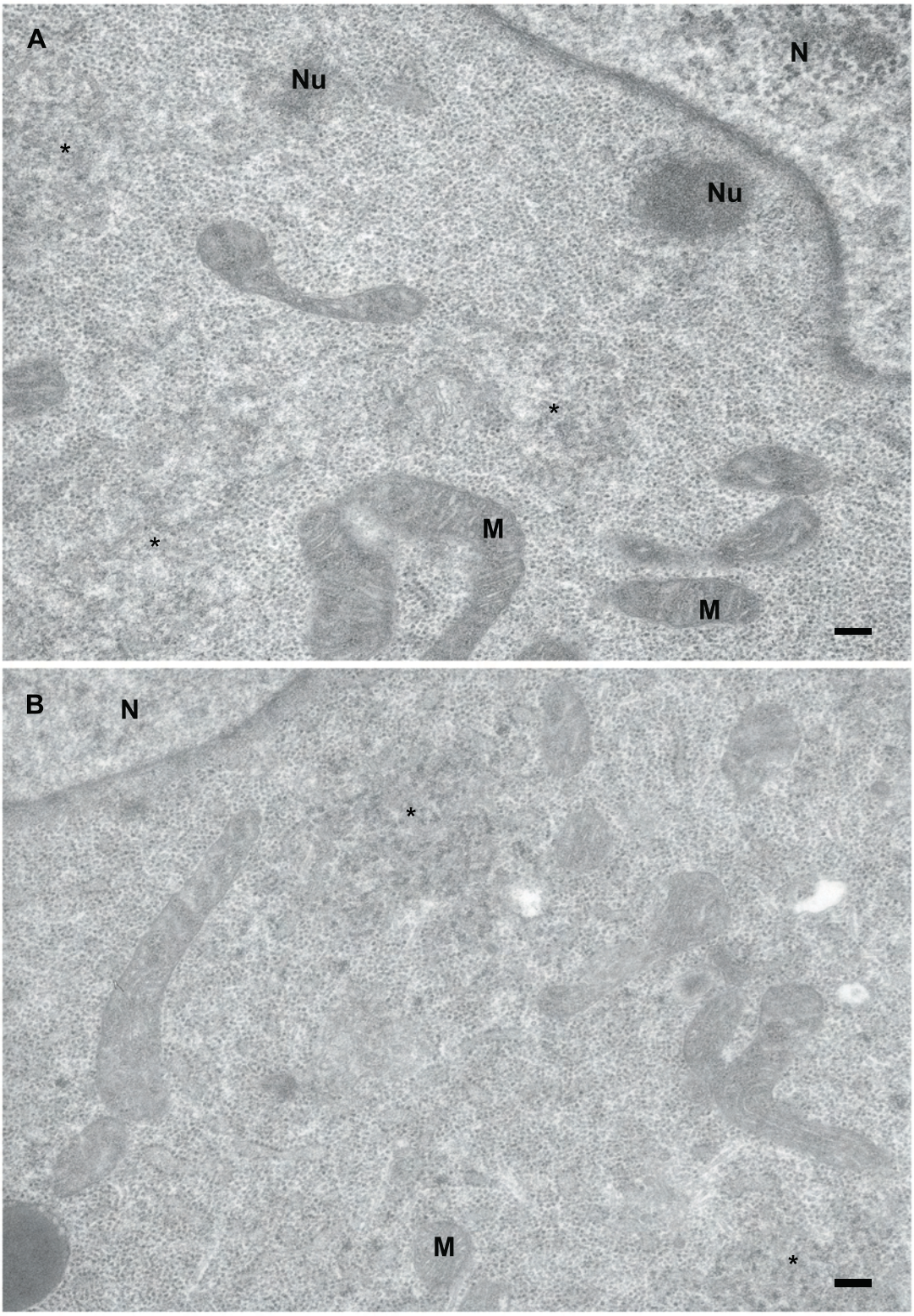

Figure 32 Sponge Body structure at a stage 9 egg chamber

(A) Sponge Bodies in a stage 9 egg chamber nurse cell.
(B) Sponge Bodies in a stage 9 egg chamber oocyte.
SB (*), Mitochondria (M), Nucleus (N), Nuage (Nu). Scale bar 1μm

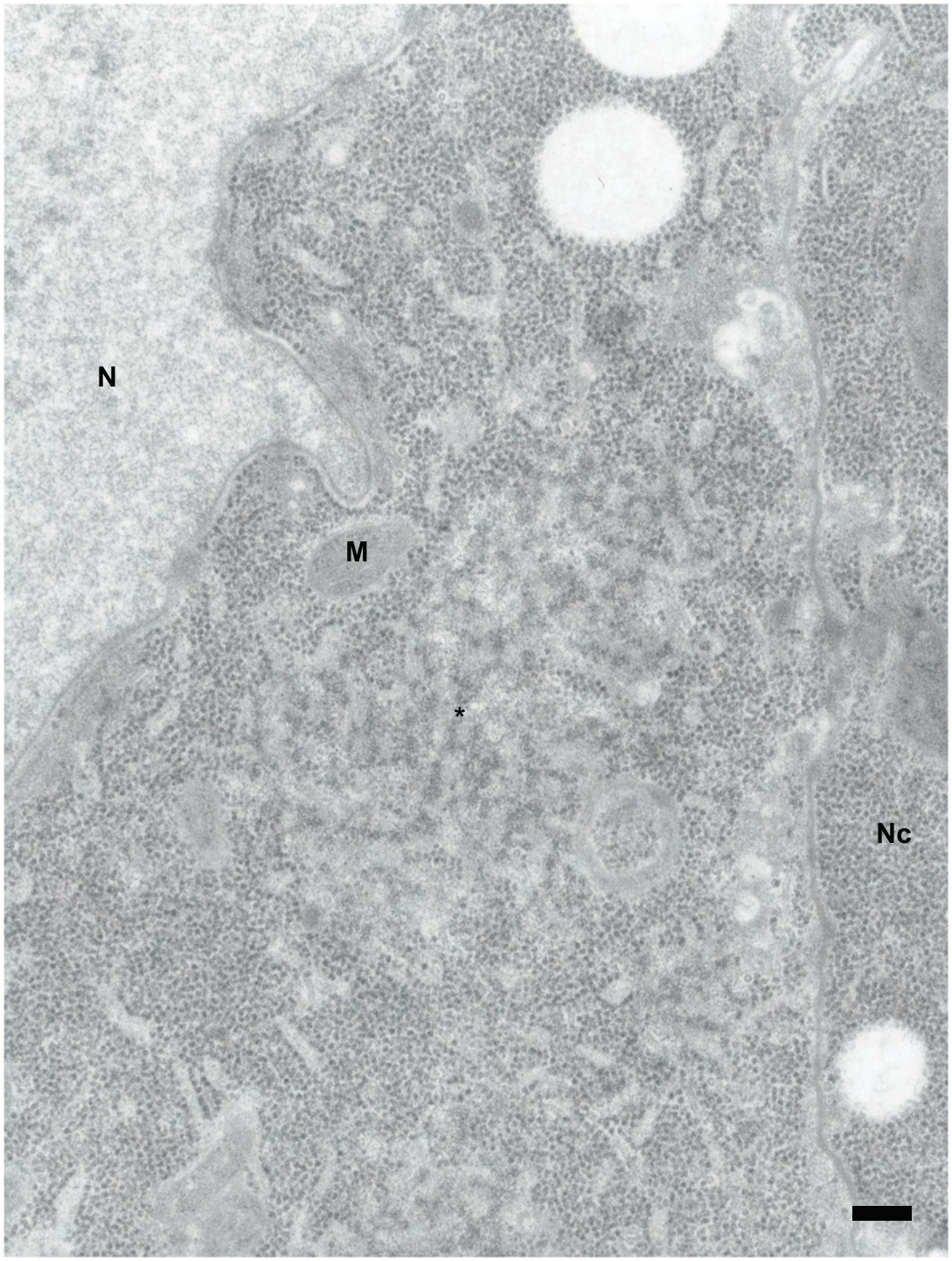

Figure 33 Sponge Body structure at a stage 7 egg chamber

Sponge Bodies in a stage 7 egg chamber oocyte.
SB (*), Mitochondria (M), Nucleus (N), Nurse cell (Nc). Scale bar 200nm

6.4. Conclusions

Although there are reports of translational studies on injected RNA in mouse (Ebert et al., 1984) and *Xenopus* oocytes (Harland and Weintraub, 1985; Harland et al., 1983) this is to my knowledge, the first time that an RNA was deliberately injected into a *Drosophila* oocyte to study translation *in vivo*. I showed here that in the case of *grk* RNA it is possible to obtain *de novo* synthesized protein by injecting in *grk* null mutant oocytes. This assay however did not allow me to study the proposed hypothesis on the role of SBs in translational regulation as the translational repressor SqdA is not recruited to keep the injected *grk* RNA repressed during transport (Caceres and Nilson, 2009). The fact that Grk protein is only found on the Golgi in stage 6 oocytes indicates that also in these early stages, the SBs are not the sites of *grk* translation. It is not clear whether *grk* mRNA is anchored at stage 6 oocytes and whether SBs are involved in this anchoring. However, the SBs seem to fulfill a very important role in early oogenesis as the oocyte cytoplasm consists mainly of SB material. The morphology of the SBs in the early stages studied, stage 6 and 7, differs clearly from those in stage 9. It is tempting to speculate a maturation of SBs during oogenesis reflecting the recruitment of protein complexes involving translational regulation. Whether the SBs become denser as a consequence of releasing the RNA for translation or because they need to release them is not clear.

7

Anchoring of *I* factor RNA

7.1. Introduction

I factor is a member of the non-long-terminal-repeat retrotransposon (non LTR) family and is similar to the LINE1 element in humans. Its transposition involves an RNA intermediate that has to be reverse transcribed to be inserted in the genome. *I* factor is bicistronic and encodes for 2 proteins. ORF1p has RNA binding properties and ORF2 encodes for a protein predicted to have endonuclease, reverse transcriptase and RNaseH activities (Fawcett et al., 1986). Transposition is taking place in the germline of the female offspring of a cross between a male that has functional copies of *I* factor known as an inducer (I) male and a female that does not contain functional copies of the *I* factor, also known as a reactive (R) female. The F1 females known as "sterilité femelle" (SF) females have a highly reduced fertility. The reciprocal cross does not result in major transposition events in the F1 generation. This phenomenon is also known as I-R hybrid dysgenesis. *I* factor and *grk* mRNA both follow the same localization pattern and the predicted structure of their localization signals are very similar (Seleme et al., 2005; Van De Bor et al., 2005). As for *grk* mRNA, the second step in transport of *I* factor is dependent on Sqd (Van De Bor et al., 2005). The mechanism of transposition of *I* factor is believed to follow the mechanism of target primed reverse transcription like other non LTR retrotransposons (Cost et al., 2002; Luan et al., 1993; Pritchard et al., 1988). Recent publications suggest that the polarity defects in the SF female germline is due to the double strand breaks (DSB) caused by transposition. These DSB lead to an activation of a meiotic DSB repair pathway including the Chk2 and ATR kinases. Chk2 and the ATR homologue Mei41 are responsible for a MT reorganization and Vasa phosphorylation. It is probably a combination of these two that lead to the patterning defects (Klattenhoff et al., 2007). Hybrid dysgenesis is likely a consequence of maternally inherited piRNA mediated silencing of the *I* factor mRNA (Klattenhoff et al., 2007, Brennecke, 2008 #4476). *grk* mRNA and *I* factor are believed to compete for components of the same localization machinery (Van De Bor et al., 2005). *I* factor transcripts and ORF1p appear as early as in the germarium of SF females and ORF1p is required for transport from the nurse cells to the oocyte (Seleme et al., 2005). The anchoring of *I* factor RNA has not been studied. It is not known how translational regulation is tied in with transposition. Studying the anchoring of *I* factor mRNA might give an insight in how translational regulation regulates transposition.

7.2. Aims of this chapter

In this chapter I study localized injected *I* factor RNA at ultrastructural level. I test whether injected *I* factor RNA localizes to anchoring structures that relate to the SBs where *grk* mRNA is anchored in.

7.3. Results

7.3.1. *I* factor RNA localizes in Sponge Bodies

As I did not succeed in performing *in situ* hybridizations on EM sections of dysgenic oocytes, I studied the anchoring of *I* factor RNA on injected RNA. For this experiment I injected biotinylated RNA into wild type oocytes and after letting the RNA localize for 45 minutes, the samples were fixed and embedded in gelatin. After sectioning, biotin was labeled with 15 nm gold. The *I* factor RNA localizes clearly in large SB like structures (Figure 34). The morphology of these SBs is identical to the ones in which *grk* RNA is anchored. Some other sections were labeled for Biotin and for Me31B, a marker for SBs. *I* factor RNA clearly localizes in Me31B positive SBs (Figure 35A). As a control I took images of Me31B positive SBs at the anterior side of the oocyte nucleus that is negative for Biotin (Figure 35B). This shows that the localization of *I* factor RNA is spatially restricted to the DA corner just like *grk* mRNA as well as the specificity of the anti biotin antibody.

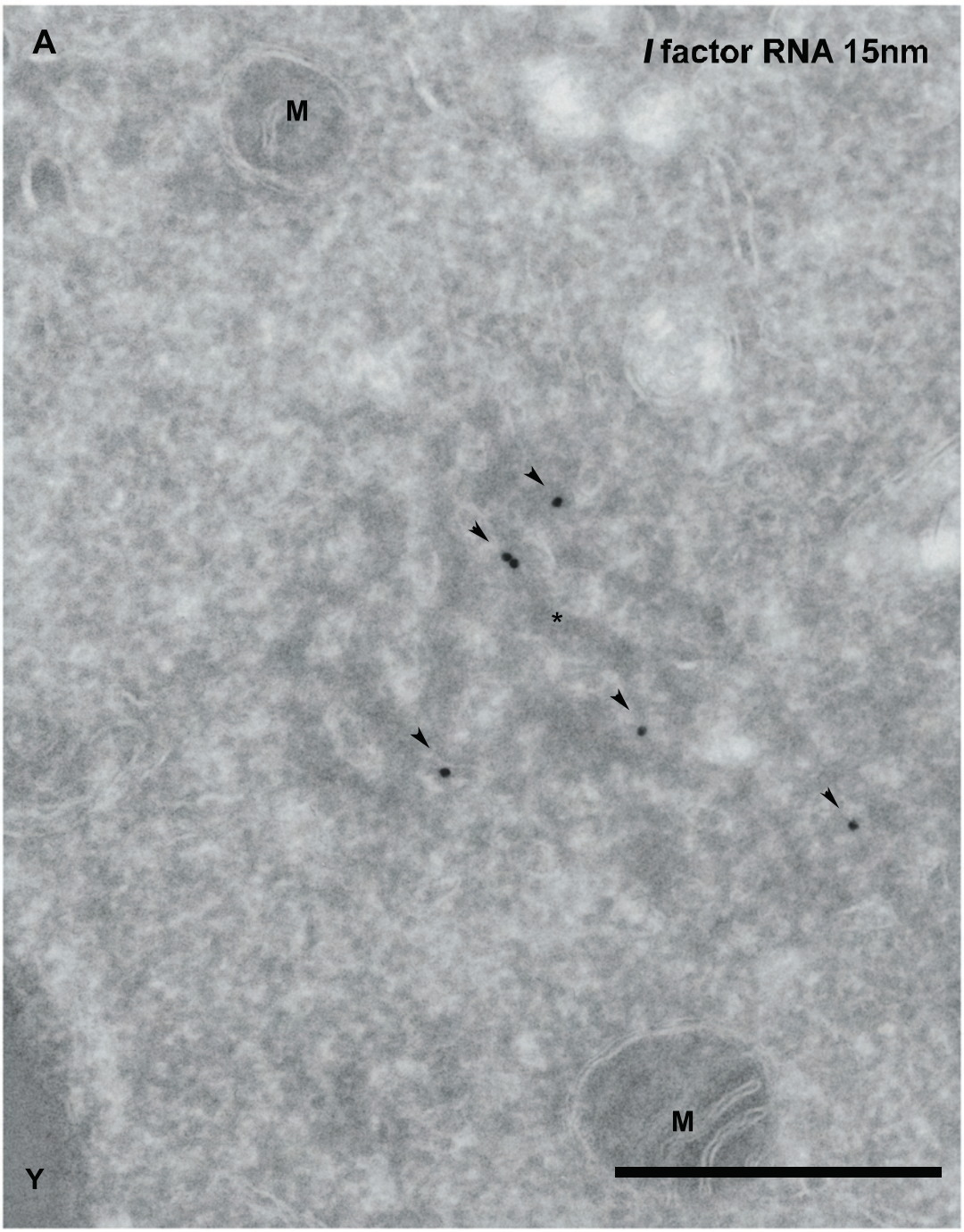

Figure 34 *I* factor RNA localizes to Sponge Bodies

(A) Cryosection of wild type oocyte injected with Dig labeled *I* factor RNA (15 nm arrowhead) localized for 45min at the DA corner.
SB (*), Nucleus (N), Yolk (Y), Mitochondria (M) Scale bar 500nm

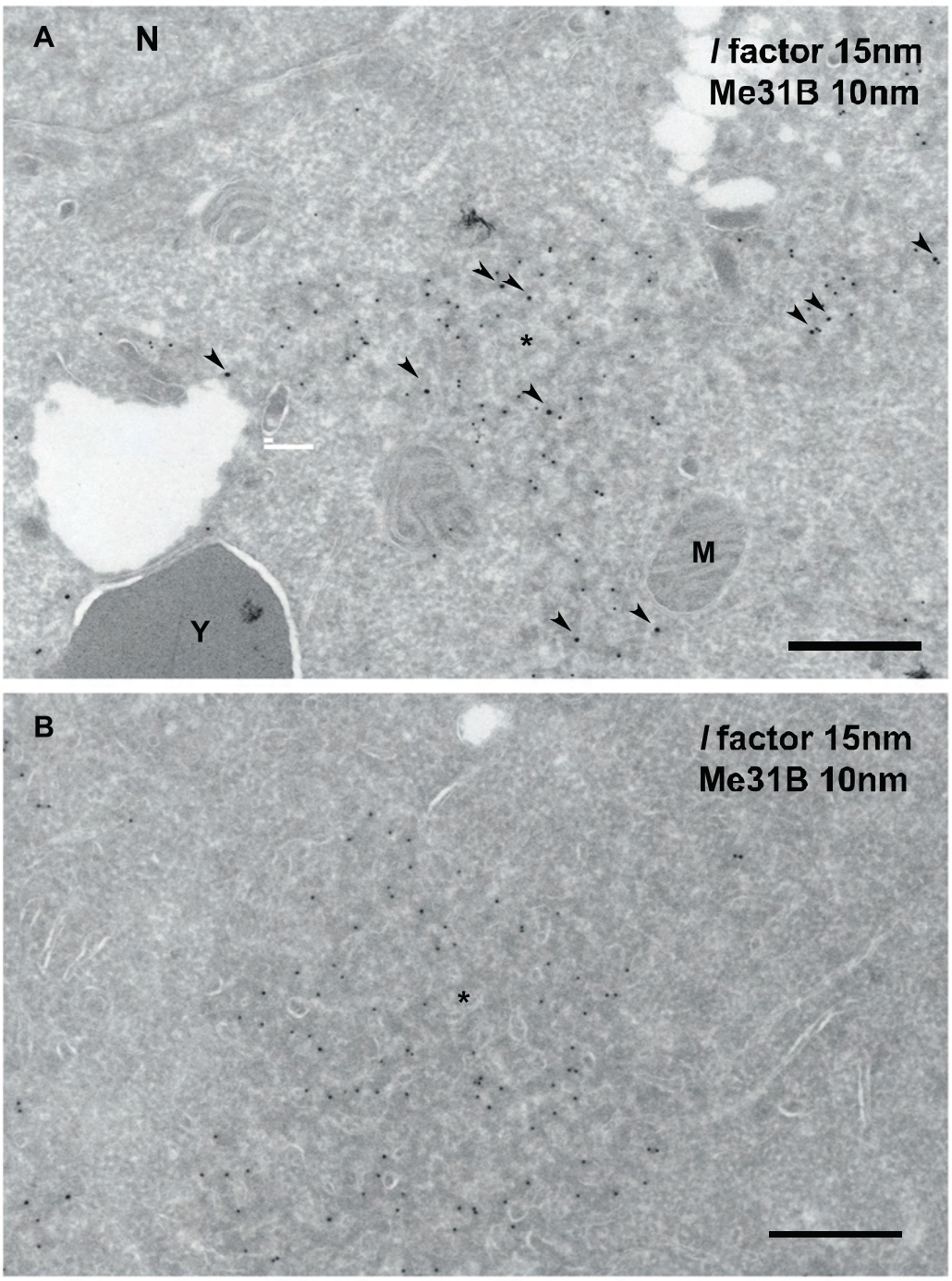

Figure 35 *I* factor RNA localizes to Sponge Bodies

(A) Cryosection of wild type oocyte injected with Dig labeled *I* factor RNA (15nm, arrowheads) and Me31B (10nm) at the DA corner. Scale bar 500nm

(B) Cryosection of wild type oocyte injected with Dig labeled *I* factor RNA (15nm) and Me31B (10nm) at the centre of the oocyte. SB (*), Nucleus (N), Yolk (Y), Mitochondria (M) Scale bar 200nm

7.3.2. Injected *I* factor and *grk* RNA localize to the same Sponge Bodies

grk and *I* factor RNA both localize to the DA corner in SBs. To test whether they are the same subset of SBs, I coinjected biotinylated *grk* RNA and DIG labeled *I* factor RNA at a 1:1 ratio in wild type oocytes. The RNA was allowed to localize for 45 minutes after which they were fixed for 3 hours. Ultra-thin sections of these oocytes were labeled for biotin and DIG. Although the morphology of these sections is of a poor quality, biotinylated *grk* RNA and DIG labeled *I* factor RNA localize to the same SBs (Figure 36).

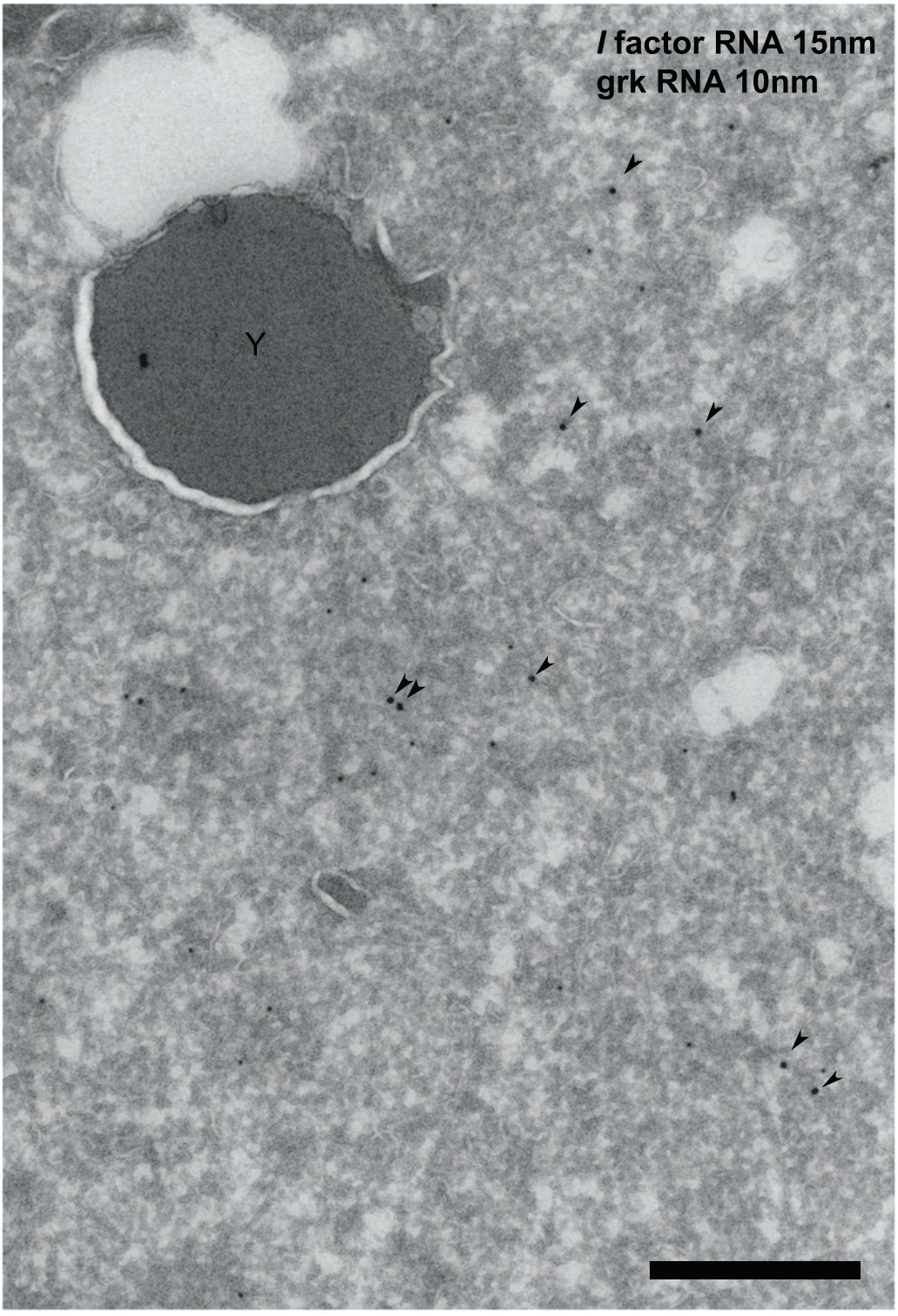

Figure 36 *I* factor and *gurken* RNA localize to the same Sponge Bodies

Cryosection of wild type oocyte injected with Dig labeled *I* factor RNA (15nm arrowhead) and biotinylated *grk* RNA at the DA corner. Yolk (Y), Scale bar 500 nm

7.4. Conclusions

I factor mRNA is just like *grk* mRNA localizing to SBs at the DA corner. Both RNAs localize to the same SBs, suggesting a similar way of translational regulation. Intriguingly, *grk* is an excreted protein whereas *I* factor mRNA and presumably ORF2p has to end up in the nucleus for transposition. The fact that two proteins with completely different destinations and function are both targeted to the same foci of translational regulation is remarkable. It is believed that *I* factor has biologically evolved to hijack the *grk* transport machinery for localization (Van De Bor et al., 2005). It seems that it also uses the anchoring structures of *grk* mRNA. I have not tested whether *I* factor mRNA is statically anchored but the similarity with *grk* mRNA localization and anchoring makes this a very likely scenario. It is unlikely that *I* factor is translated in the SBs as they are devoid of ribosomes. Because of the bicistronic nature of *I* factor it would be interesting to study it in more depth. ORF2p can detected in a crescent around the oocyte nucleus from stage 8 oocytes onwards (Eve Hartswood, unpublished data) whereas ORF1 is translated from the germarium onwards in the nurse cells until stage 10b (Seleme et al., 2005). Therefore ORF1 translation must be regulated in a different way than ORF2. How the translation of the two different proteins of the same bicistronic RNA is regulated to be translated in different locations is an interesting outstanding question. EM studies could reveal whether *I* factor transcripts are anchored in SBs before the appearance of ORF2p or after. This might then in turn shed light on Grk translational regulation. It would be interesting to study the role of Sqd in the translational regulation of the proteins encoded by *I* factor mRNA and whether *I* factor mRNA needs to recruit Sqd in the nurse cells to keep ORF2 translationally repressed during transport. This will prove to be a challenge as, except for a few isolated laboratory strains, all *Drosophila* stocks are of the inducer type, making genetic studies of *I* factor related processes difficult.

8

Conclusions and discussion

Once delivered at its final destination, many copies of *grk* mRNA are anchored in large RNP structures called Sponge Bodies (Delanoue et al., 2007). The localization and anchoring of *grk* mRNA in the SBs at the DA corner is a multi-step process (MacDougall et al., 2003). *grk* mRNA is transcribed in the nurse cells and transported in TPs along the MT into the oocyte (Delanoue et al., 2007). It is then transported by the Dynein motor in TPs along the MT in 2 steps towards the DA corner. The first step towards the anterior of the oocyte does require a functional motor containing Dhc, Egl and Bic-D but not Sqd, the second step also requires Sqd (MacDougall et al., 2003; Norvell et al., 2005). The work presented in this thesis shows that that Sqd is also required for anchoring of injected and endogenous *grk* RNA at the DA corner. By targeting the GFP fraction of a fusion protein that replaces the endogenous Sqd I was able to disrupt its anchoring function downstream of its function in transport. When Sqd function is disrupted, SBs fall apart in TPs that are presumably in continuous transport at the anterior of the oocyte like injected *grk* RNA at the anterior in a *sqd* null background. *grk* RNA moves to the anterior after disruption of Sqd, either by passive diffusion or active transport. This illustrates that Sqd has a function both in anchoring and in directed transport towards the DA corner in the second step of *grk* mRNA transport. In the alternative hypothesis that Sqd is only responsible for anchoring at the DA corner and not directing transport towards the nucleus, one would expect the TPs to accumulate at the DA corner in a non-anchored state. In a *sqd* null background, *grk* mRNA is found at the anterior instead. Intriguingly, in sqd^{1} mutants, SBs are present at the DA corner (Delanoue et al., 2007) but the majority disassembles into TPs when *grk* RNA is injected (Delanoue et al., 2007). When taken together with my data, we can deduct from this that SBs are unstable in a *sqd* null background and when an excess of *grk* RNA is introduced, this labile structures are disassembled. It shows that Sqd is required to form stable anchoring structures in the presence *grk* transcripts. We propose that Sqd is required to render transport particles anchoring competent allowing them to be incorporated into the SBs at the DA corner. With this new injection assay we were able to determine a function in anchoring for an hnRNP. Grk protein and its role in axis specification is unique for *Drosophilidae* but Sqd and the roles of hnRNPs in mRNA transport in general is highly conserved throughout the animal kingdom (Smith, 2004). The human orthologue of Sqd is hnRNP A/B. An hnRNP A/B like protein was shown to be cotransported with *mpb* RNA in cultured oligodendrocytes (Raju et al., 2008) and hnRNP A/B is able to stimulate the apical localization of *ftz*

RNA in blastoderm embryos (Lall et al., 1999). It is therefore likely that other hnRNPs are involved in anchoring of mRNAs in different model organisms. A good candidate is *mbp* mRNA in oligodendrocytes where hnRNPA2 and A3 mediate transport (Smith, 2004; Dreyfuss, 2002). The technique where transgenes carrying high affinity binding sites for the phage coat MS2 reporter protein (Bertrand et al., 1998) is becoming widespread and gene trap screens incorporating these binding loops in the genome are being set up to identify new localizing RNAs (M. Leptins lab). These transgenes will allow us to follow the RNA transport and anchoring *in vivo* together with fluorescently labeled SB markers. This could improve our understanding of how the incorporation of the TP in the anchoring structures happens. We are now relying on the artificial situation of injecting RNA and this can lead to misinterpretation of the results because the RNA has not undergone the same history as the endogenous RNA. A perfect example is the translation experiment of *grk* RNA in this thesis were *grk* RNA was translated during transport because Sqd was recruited in the oocyte instead of in the nurse cells. In the case of *mpb* RNA it would even be possible to electroporate the construct with the MS2 binding loops into a single cell to drive expression in a similar way as has been done in mouse for other constructs (Kitamura et al., 2008). The assay in which we target GFP by antibody injection rather than a functional domain opens new possibilities to disrupt the function of other essential proteins than Sqd.

Furthermore we have shown that the anchoring of injected *grk* RNA is mediated by Dhc independent from its cofactors Bic-D and Egl, required for the Dynein motor function. Taken together with the data from Delanoue et al., 2007, we propose that many Dynein motors transport multiple *grk* RNA molecules in TPs to the DA corner where Dynein converts into a static anchor in the SBs independent from its motor function. When Dynein is disrupted by antibody injection, the SBs diffuse and in a *dhc* null background, SBs are as good as absent. This is in sharp contrast with Sqd disruption where the SBs disassemble in TPs, pointing to a fundamentally different role in the SBs. Sqd is required for incorporating TPs in the SBs whereas Dynein has an integral role in the structure of the SBs.

We showed that SBs depend on RNA for their existence and that SBs are enriched in all the PB markers tested. It has been shown before that also PBs depend on mRNA for their formation (Eulalio et al., 2007b; Teixeira et al., 2005). We found proteins

involved in translational repression, translational regulation, RNA degradation and in the short RNA mediated silencing pathway. All this evidence suggests that SBs are the PBs of the oocyte. In fact, SBs are often referred to as PBs (Lin et al., 2008; Liu and Gall, 2007). Dynein has been shown to be a vital structural component of SBs and required for anchoring of *grk* mRNA. I showed by siRNA interference in S2 cells and in macrophages of mutant flies that Dynein is not a structural component of PBs in *Drosophila*. This might reflect the nature of PBs in macrophages where transport of RNAs is probably of less importance than in the oocyte or that SBs are less related to PBs than thought before. In fact, it has been reported recently that Dynein Light Chain 2A (DLC2A) is required for Stress Granule (SG) formation in rat primary neurons under arsenite induced stress. It was shown that DLC2A slightly enhances the stability of the TIA-1 complex, a sub-SG complex and that in siRNA treated cells against DLC2A SGs do not form. On the other hand they showed that the motor activity is required for assembly and disassembly of SGs by inhibiting the ATPase activity of the motor (Tsai et al., 2009). The similarities between the function of DLC2A in neuronal SGs and Dhc in SBs are striking. The structure of both SGs in primary neurons and SBs in the germline depends on a motor component. This might mean that SBs are an intermediate granule between PBs and SGs but it also implicates that motor dependent anchoring is not an isolated mechanism for *grk* mRNA in the oocyte and might therefore be more common. Future research will tell what the relation is between all the different RNA granules and whether there is a common denominator for their functions and composition. It seems to me that a lot of the granules described are in fact RNA molecules that have recruited regulating proteins involved in the process at hand. For instance the SGs have been described to form by the stepwise recruitment of chaperone proteins and proteins involved in translational regulation of the RNA (Anderson and Kedersha, 2008). These SGs have also been shown to ‘dock’ onto PBs presumably to exchange proteins and/or RNA (Anderson and Kedersha, 2008). Another explanation might be that at the periphery of the granule the RNA can be released for translation or degradation and that it recruits proteins involved in this processes upon exit of the granule. From what has been described in the literature it seems that RNA granules are an amalgam mix of interacting proteins that decorate the RNA. Disrupting the granule structure does not seem to impair the processes that normally take place in the granule (Eulalio et al., 2007). This suggests that RNA granules consist of subunits that contain all the necessary components for regulation

and that these micro units are 'glued' together in a sort of mini factory to optimize the processes. We do not know how dynamic SBs or other granules are and how transport inside a granule would occur. Ultra high-resolution microscopy and fast acquisition might shed light on how these processes are regulated. *In vitro* assembly of RNA granules could provide a useful model to study SB structure by microscopy.

Why *grk* is anchored in SBs is not clear. There is no obvious reason why a transcript has to be immobilized at its final destination. In fact, in the case of *bcd* mRNA, it has been shown that it is not anchored at the anterior in late oogenesis (Weil et al., 2006) and only at the end oogenesis it gets anchored in an actin dependent way (Weil et al., 2008). This is completely different from *grk* RNA anchoring, which is not actin dependent (Delanoue et al., 2007). One explanation for grk mRNA anchoring could be *grk* mRNA provides a Grk signal to the follicle cells while they are migrating from the nurse cells to the oocyte and the Grk signal is being transmitted to the follicle cells while they pass over the DA corner. Bram Herpers has shown that SBs do not contain functional ribosomes as they are negative for ribosomal P protein. It is therefore unlikely that *grk* mRNA is translated in the SBs. Taken together with the components of the translational regulation pathways we found in SBs, we propose that *grk* is kept translationally silent in the SBs. Previous EM studies on *grk* translation has shown that in stage 9 oocytes Grk protein can be found on a subset of Golgi at the DA corner (Herpers and Rabouille, 2004). I was able to detect Grk protein as early as late stage 6 on Golgi but never in SBs. It is therefore likely that even in early stages, *grk* is not translated in SBs. I tried to show whether *grk* RNA is anchored in SBs before or after it is translated by injecting *in vitro* transcribed RNA into a *grk* null background in order to determine the timing of translation. Although the *in vitro* transcribed RNA can be translated *in vivo*, we could not study translational regulation because the transcript needs to recruit Sqd in the nurse cells in order to remain translationally silent during transport. The experiment could be improved by injecting *grk* RNA into the nurse cells but that would prove challenging and it is not clear whether Sqd has to be recruited in the nurse cell nucleus or in the cytoplasm. Another way of approaching this problem would be to express a Grk-GFP fusion protein in an otherwise grk null background in combination with a grk-ms2 reporter construct to follow the RNA transport and translation *in vivo*. The time for GFP to fold into a fluorescent molecule might make it difficult to draw conclusions from the experiment. It is however novel to show

translation *in vivo* of an injected RNA in the oocyte. An important observation made is that the SB structure in early oogenesis is different than that of stage 9 oocytes suggesting that the composition of sponge bodies change during development. SBs in the nurse cells have a different morphology than in the oocyte in stage 6 egg chambers. The morphology of SBs in the nurse cells at stage 6 is closer to the structure of SBs at stage 9 oocytes. It might be that the SBs at stage 9 are different because there is more translation in the oocyte at that stage than in early stages. I speculate that SBs change morphology in order to be able to release the RNA for translation on the ER.

I factor mRNA also localizes to the DA corner and even competes with *grk* mRNA for the transport machinery (Van De Bor et al., 2005). I show that injected *I* factor RNA also localizes to SBs and when co-injected, they localize to the same SBs as *grk* mRNA. Sqd will most likely also play a role in the anchoring of *I* factor as injected ILS, a short localizing fragment of *I* factor, also remains at the anterior in a *sqd* null background (Van De Bor et al., 2005) like *grk* RNA. We lack unfortunately the tools to study the roles of Sqd in the anchoring of *I* factor mRNA as it is not possible to cross in SqdGFP without losing the reactivity of the strain. Studying how *I* factor regulates the translation of ORF2 at the DA corner might shed light upon how *grk* translational regulation works.

We conclude that Sponge Bodies are a very dynamic structure. Transport particles are incorporated 'feeding' it with new RNA, motor components and proteins involved in translational regulation. They probably recruit and exchange proteins from the cytoplasm and it seems that they change in structure in order to release the RNA for translation. It will have to be studied in greater depth to understand what is really happening in SBs and RNA granules in general. SBs, like PBs and probably other granules too, are a way to make the regulating processes more efficient by concentrating the proteins in a granule. Future research will have to reveal whether the novel function of RNA anchoring in a granule is a common mechanism for other RNAs in different organisms. As most localized RNAs are transported by molecular motors, it is a possibility that motor dependent anchoring in RNA granules is a common tethering mechanism. The field of RNA granule study is very immature and many different granules have been described in the literature with slightly different composition and functions. More research will have to tell how dynamic all these RNA

granules are and how they interact. As described for SGs and PBs, the other granules might also exchange proteins and RNA. How this interaction and "communication" between granules works is still a mystery. We still do not know how the proteins and RNA are spatially organized in granules and whether that affects its function. The study of *grk* mRNA translational regulation in SBs and the mechanism by which *grk* mRNA localizes to the specific subset of SBs at the DA corner might be a start to answer some of these questions.

In general, I propose a model in which *grk* mRNA is transported in TPs along the MT. These TPs consist of multiple *grk* RNA molecules together with Dynein motors and Sqd. Sqd mediates the transport from the anterior towards the DA corner and renders these TPs anchoring competent. The TPs containing multiple *grk* mRNA, Sqd and Dynein motor molecules are then incorporated in the SBs upon which Dynein converts into a static anchor and Sqd mediates the incorporation of the TPs in the SBs. The SBs then function as a storage place for the RNA where it is kept under translationally silent state until the RNA is released for translation on the ER or degraded by the machinery in the SBs.

9

Bibliography

Allison, R., Czaplinski, K., Git, A., Adegbenro, E., Stennard, F., Houliston, E., and Standart, N. (2004). Two distinct Staufen isoforms in Xenopus are vegetally localized during oogenesis. RNA *10*, 1751-1763.

Altman, D., Sweeney, H.L., and Spudich, J.A. (2004). The mechanism of myosin VI translocation and its load-induced anchoring. Cell *116*, 737-749.

Amon, A. (1996). Mother and daughter are doing fine: asymmetric cell division in yeast. Cell *84*, 651-654.

Anderson, P., and Kedersha, N. (2002). Stressful initiations. Journal of Cell Science *115*, 3227-3234.

Anderson, P., and Kedersha, N. (2006). RNA granules. The Journal of Cell Biology *172*, 803-808.

Anderson, P., and Kedersha, N. (2008). Stress granules: the Tao of RNA triage. Trends in Biochemical Sciences *33*, 141-150.

Aravin, A.A., Naumova, N.M., Tulin, A.V., Vagin, V.V., Rozovsky, Y.M., and Gvozdev, V.A. (2001). Double-stranded RNA-mediated silencing of genomic tandem repeats and transposable elements in the D. melanogaster germline. Current Biology *11*, 1017-1027.

Aronov, S., Aranda, G., Behar, L., and Ginzburg, I. (2001). Axonal tau mRNA localization coincides with tau protein in living neuronal cells and depends on axonal targeting signal. The Journal of Neuroscience *21*, 6577-6587.

Bashkirov, V.I., Scherthan, H., Solinger, J.A., Buerstedde, J.M., and Heyer, W.D. (1997). A mouse cytoplasmic exoribonuclease (mXRN1p) with preference for G4 tetraplex substrates. The Journal of Cell Biology *136*, 761-773.

Berleth, T., Burri, M., Thoma, G., Bopp, D., Richstein, S., Frigerio, G., Noll, M., and Nusslein-Volhard, C. (1988a). The role of localization of bicoid RNA in organizing the anterior pattern of the Drosophila embryo. The EMBO Journal *7*, 1749-1756.

Berleth, T., Burri, M., Thoma, G., Bopp, D., Richstein, S., Frigerio, G., Noll, M., and Nüsslein-Volhard, C. (1988b). The role of localization of bicoid RNA in organizing the anterior pattern of the *Drosophila* embryo. The EMBO Journal *7*, 1749-1756.

Bernstein, E., Caudy, A.A., Hammond, S.M., and Hannon, G.J. (2001). Role for a bidentate ribonuclease in the initiation step of RNA interference. Nature *409*, 363-366.

Bertrand, E., Chartrand, P., Schaefer, M., Shenoy, S.M., Singer, R.H., and Long, R.M. (1998). Localization of ASH1 mRNA particles in living yeast. Molecular Cell *2*, 437-445.

Bohl, F., Kruse, C., Frank, A., Ferring, D., and Jansen, R.P. (2000). She2p, a novel RNA-binding protein tethers ASH1 mRNA to the Myo4p myosin motor via She3p. The EMBO Journal *19*, 5514-5524.

Brendza, R., Serbus, L., Saxton, W., and Duffy, J. (2002). Posterior localization of Dynein and dorsal-ventral axis formation depend on Kinesin in Drosophila oocytes. Current Biology *12*, 1541.

Brendza, R.P., Serbus, L.R., Duffy, J.B., and Saxton, W.M. (2000). A function for kinesin I in the posterior transport of *oskar* mRNA and Staufen protein. Science *289*, 2120-2122.

Brengues, M., Teixeira, D., and Parker, R. (2005). Movement of eukaryotic mRNAs between polysomes and cytoplasmic processing bodies. Science *310*, 486-489.

Brennecke, J., Malone, C.D., Aravin, A.A., Sachidanandam, R., Stark, A., and Hannon, G.J. (2008). An epigenetic role for maternally inherited piRNAs in transposon silencing. Science *322*, 1387-1392.

Bullock, S.L., and Ish-Horowicz, D. (2001). Conserved signals and machinery for RNA transport in *Drosophila* oogenesis and embryogenesis. Nature *414*, 611-616.

Burkhardt, J.K., Echeverri, C.J., Nilsson, T., and Vallee, R.B. (1997). Overexpression of the dynamitin (p50) subunit of the dynactin complex disrupts dynein-dependent maintenance of membrane organelle distribution. The Journal of Cell Biology *139*, 469-484.

Caceres, L., and Nilson, L.A. (2009). Translational repression of gurken mRNA in the Drosophila oocyte requires the hnRNP Squid in the nurse cells. Developmental Biology *326*, 327-334.

Carpenter, A.T. (1994). Egalitarian and the choice of cell fates in Drosophila melanogaster oogenesis. Ciba Foundation Symposium *182*, 223-246; discussion 246-254.

Carson, J.H., Worboys, K., Ainger, K., and Barbarese, E. (1997). Translocation of myelin basic protein mRNA in oligodendrocytes requires microtubules and kinesin. Cell Motility and the Cytoskeleton *38*, 318-328.

Cha, B., Koppetsch, B.S., and Theurkauf, W.E. (2001). *In vivo* Analysis of Drosophila bicoid mRNA Localization Reveals a Novel Microtubule-Dependent Axis Specification Pathway. Cell *106*, 35-46.

Chang, W.L., Liou, W., Pen, H.C., Chou, H.Y., Chang, Y.W., Li, W.H., Chiang, W., and Pai, L.M. (2008). The gradient of Gurken, a long-range morphogen, is directly regulated by Cbl-mediated endocytosis. Development *135*, 1923-1933.

Chen, Y., Pane, A., and Schupbach, T. (2007). Cutoff and aubergine mutations result in retrotransposon upregulation and checkpoint activation in Drosophila. Current Biology *17*, 637-642.

Chu, C.Y., and Rana, T.M. (2006). Translation repression in human cells by microRNA-induced gene silencing requires RCK/p54. PLoS Biology *4*, e210.

Clark, A., Meignin, C., and Davis, I. (2007). A Dynein-dependent shortcut rapidly delivers axis determination transcripts into the Drosophila oocyte. Development *134*, 1955-1965.

Clouse, K.N., Ferguson, S.B., and Schupbach, T. (2008). Squid, Cup, and PABP55B function together to regulate gurken translation in Drosophila. Developmental Biology *313*, 713-724.

Cohen, R.S. (2005). The role of membranes and membrane trafficking in RNA localization. Biology of the Cell / under the auspices of the European Cell Biology Organization *97*, 5-18.

Coller, J., and Parker, R. (2005). General translational repression by activators of mRNA decapping. Cell *122*, 875-886.

Cost, G.J., Feng, Q., Jacquier, A., and Boeke, J.D. (2002). Human L1 element target-primed reverse transcription *in vitro*. The EMBO Journal *21*, 5899-5910.

Cougot, N., Babajko, S., and Seraphin, B. (2004). Cytoplasmic foci are sites of mRNA decay in human cells. The Journal of Cell Biology *165*, 31-40.

Dahm, R., and Macchi, P. (2007). Human pathologies associated with defective RNA transport and localization in the nervous system. Biology of the cell / under the auspices of the European Cell Biology Organization *99*, 649-661.

Darnell, J.E., Lodish, H., and Baltimore, D. (1990). Molecular Cell biology, 2nd edn (New York: Scientific American Books).

Davis, I. (2000). Visualising fluorescence in *Drosophila* - optimal detection in thick specimens. In Protein Localisation by Fluorescence Microscopy: A Practical Approach, V.J. Allan, ed. (Oxford: OUP), pp. 131-162.

Davis, I., Girdham, C.H., and O Farrell, P.H. (1995). A nuclear GFP that marks nuclei in living *Drosophila* embryos - maternal supply overcomes a delay in the appearance of zygotic fluorescence. Developmental Biology *170*, 726-729.

de Cuevas, M., Lilly, M.A., and Spradling, A.C. (1997). Germline cyst formation in Drosophila. Annual Review of Genetics *31*, 405-428.

Dej, K.J., and Spradling, A.C. (1999). The endocycle controls nurse cell polytene chromosome structure during Drosophila oogenesis. Development *126*, 293-303.

Delanoue, R., and Davis, I. (2005). Dynein anchors its mRNA cargo after apical transport in the Drosophila blastoderm embryo. Cell *122*, 97-106.

Delanoue, R., Herpers, B., Soetaert, J., Davis, I., and Rabouille, C. (2007). Drosophila Squid/hnRNP helps Dynein switch from a gurken mRNA transport motor to an ultrastructural static anchor in sponge bodies. Developmental Cell *13*, 523-538.

Deshler, J.O., Highett, M.I., and Schnapp, B.J. (1997). Localization of Xenopus Vg1 mRNA by Vera protein and the endoplasmic reticulum. Science *276*, 1128-1131.

Dreyfuss, G., Kim, V.N., and Kataoka, N. (2002). Messenger RNA binding proteins and the messages they carry. Nat Rev Mol Cell Biol *3*, 195-205.

Driever, W., and Nüsslein-Volhard, C. (1988). A gradient of bicoid protein in *Drosophila* embryos. Cell *54*, 83-93.

Duchek, P., and Rorth, P. (2001). Guidance of cell migration by EGF receptor signaling during Drosophila oogenesis. Science *291*, 131-133.

Dunand-Sauthier, I., Walker, C., Wilkinson, C., Gordon, C., Crane, R., Norbury, C., and Humphrey, T. (2002). Sum1, a component of the fission yeast eIF3 translation initiation complex, is rapidly relocalized during environmental stress and interacts with components of the 26S proteasome. Molecular Biology of the Cell *13*, 1626-1640.

Duncan, J.E., and Warrior, R. (2002). The cytoplasmic Dynein and Kinesin motors have interdependent roles in patterning the Drosophila oocyte. Current Biology *12*, 1982-1991.

Ebert, K.M., Paynton, B.V., McKnight, G.S., and Brinster, R.L. (1984). Translation and stability of ovalbumin messenger RNA injected into growing oocytes and fertilized ova of mice. Journal of Embryology and Experimental Morphology *84*, 91-103.

Emmons, S., Phan, H., Calley, J., Chen, W., James, B., and Manseau, L. (1995). Cappuccino, a Drosophila maternal effect gene required for polarity of the egg and embryo, is related to the vertebrate limb deformity locus. Genes & Development *9*, 2482-2494.

Ephrussi, A., Dickinson, L.K., and Lehmann, R. (1991). Oskar organizes the germ plasm and directs localization of the posterior determinant nanos. Cell *66*, 37-50.

Erdelyi, M., Michon, A.M., Guichet, A., Glotzer, J.B., and Ephrussi, A. (1995). Requirement for Drosophila cytoplasmic tropomyosin in oskar mRNA localization. Nature *377*, 524-527.

Eulalio, A., Behm-Ansmant, I., and Izaurralde, E. (2007a). P bodies: at the crossroads of post-transcriptional pathways. Nat Rev Mol Cell Biol *8*, 9-22.

Eulalio, A., Behm-Ansmant, I., Schweizer, D., and Izaurralde, E. (2007b). P-body formation is a consequence, not the cause, of RNA-mediated gene silencing. Molecular and Cellular Biology *27*, 3970-3981.

Eystathioy, T., Chan, E.K., Tenenbaum, S.A., Keene, J.D., Griffith, K., and Fritzler, M.J. (2002). A phosphorylated cytoplasmic autoantigen, GW182, associates with a unique population of human mRNAs within novel cytoplasmic speckles. Molecular Biology of the Cell *13*, 1338-1351.

Fawcett, D.H., Lister, C.K., Kellett, E., and Finnegan, D.J. (1986). Transposable Elements Controlling I-R Hybrid Dysgenesis in D. melanogaster Are Similar to Mammalian LINEs. Cell *47*, 1007-1015.

Ferrandon, D., Elphick, L., Nüsslein-Volhard, C., and St Johnston, D. (1994). Staufen protein associates with the 3'UTR of bicoid mRNA to form particles that move in a microtubule-dependent manner. Cell *79*, 1221-1232.

Filardo, P., and Ephrussi, A. (2003). Bruno regulates gurken during Drosophila oogenesis. Mechanisms of Development *120*, 289-297.

Findley, S.D., Tamanaha, M., Clegg, N.J., and Ruohola-Baker, H. (2003). Maelstrom, a Drosophila spindle-class gene, encodes a protein that colocalizes with Vasa and RDE1/AGO1 homolog, Aubergine, in nuage. Development 130, 859-871.

Gavis, E.R., and Lehmann, R. (1992). Localization Of *nanos* RNA Controls Embryonic Polarity. Cell *71*, 301-313.

Ghabrial, A., and Schupbach, T. (1999). Activation of a meiotic checkpoint regulates translation of Gurken during Drosophila oogenesis. Nature Cell Biology *1*, 354-357.

Ghiglione, C., Bach, E.A., Paraiso, Y., Carraway, K.L., 3rd, Noselli, S., and Perrimon, N. (2002). Mechanism of activation of the Drosophila EGF Receptor by the TGFalpha ligand Gurken during oogenesis. Development *129*, 175-186.

Ghirardello, A., Doria, A., Zampieri, S., Gerli, R., Rapizzi, E., and Gambari, P.F. (2000). Anti-ribosomal P protein antibodies detected by immunoblotting in patients with connective tissue diseases: their specificity for SLE and association with IgG anticardiolipin antibodies. Annals of the Rheumatic Diseases *59*, 975-981

Gilligan, P.C., and Sampath, K. (2008). Reining in RNA. Workshop on intracellular RNA localization and localized translation. EMBO Reports *9*, 22-26.

Gonzalez-Reyes, A., Elliott, H., and St Johnston, D. (1995). Polarization of both major body axes in *Drosophila* by Gurken-Torpedo signaling. Nature *375*, 654-658.

Gonzalez-Reyes, A., and St Johnston, D. (1998). The Drosophila AP axis is polarised by the cadherin-mediated positioning of the oocyte. Development *125*, 3635-3644.

Goodrich, J.S., Clouse, K.N., and Schupbach, T. (2004). Hrb27C, Sqd and Otu cooperatively regulate gurken RNA localization and mediate nurse cell chromosome dispersion in Drosophila oogenesis. Development *131*, 1949-1958.

Grieder, N.C., de Cuevas, M., and Spradling, A.C. (2000). The fusome organizes the microtubule network during oocyte differentiation in Drosophila. Development *127*, 4253-4264.

Gross, S.P., Welte, M.A., Block, S.M., and Wieschaus, E.F. (2000). Dynein-mediated cargo transport *in vivo*. A switch controls travel distance. The Journal of Cell Biology *148*, 945-956.

Guichet, A., Wucherpfennig, T., Dudu, V., Etter, S., Wilsch-Brauniger, M., Hellwig, A., Gonzalez-Gaitan, M., Huttner, W.B., and Schmidt, A.A. (2002). Essential role of endophilin A in synaptic vesicle budding at the Drosophila neuromuscular junction. The EMBO Journal *21*, 1661-1672.

Hachet, O., and Ephrussi, A. (2001). Drosophila Y14 shuttles to the posterior of the oocyte and is required for oskar mRNA transport. Current Biology *11*, 1666-1674.

Hachet, O., and Ephrussi, A. (2004). Splicing of oskar RNA in the nucleus is coupled to its cytoplasmic localization. Nature *428*, 959-963.

Hamilton, R.S., Hartswood, E., Vendra, G., Jones, C., Van De Bor, V., Finnegan, D., and Davis, I. (2009). A bioinformatics search pipeline, RNA2DSearch, identifies RNA localization elements in Drosophila retrotransposons. RNA *15*, 200-207.

Harding, H.P., Novoa, I., Zhang, Y., Zeng, H., Wek, R., Schapira, M., and Ron, D. (2000a). Regulated translation initiation controls stress-induced gene expression in mammalian cells. Molecular Cell *6*, 1099-1108.

Harding, H.P., Zhang, Y., Bertolotti, A., Zeng, H., and Ron, D. (2000b). Perk is essential for translational regulation and cell survival during the unfolded protein response. Molecular Cell *5*, 897-904.

Harland, R., and Weintraub, H. (1985). Translation of mRNA injected into Xenopus oocytes is specifically inhibited by antisense RNA. The Journal of Cell Biology *101*, 1094-1099.

Harland, R.M., Weintraub, H., and McKnight, S.L. (1983). Transcription of DNA injected into Xenopus oocytes is influenced by template topology. Nature *302*, 38-43.

Hawkins, N.C., Van Buskirk, C., Grossniklaus, U., and Schupbach, T. (1997). Post-transcriptional regulation of gurken by encore is required for axis determination in Drosophila. Development *124*, 4801-4810.

Herpers, B., and Rabouille, C. (2004). mRNA localization and ER-based protein sorting mechanisms dictate the use of transitional endoplasmic reticulum-golgi units involved in gurken transport in Drosophila oocytes. Molecular Biology of the Cell *15*, 5306-5317.

Hirokawa, N. (1993). Axonal transport and the cytoskeleton. Current Opinion in Neurobioly *3*, 724-731.

Hirokawa, N., and Takemura, R. (2005). Molecular motors and mechanisms of directional transport in neurons. Nature Reviews *6*, 201-214.

Hoogenraad, C.C., Akhmanova, A., Howell, S.A., Dortland, B.R., De Zeeuw, C.I., Willemsen, R., Visser, P., Grosveld, F., and Galjart, N. (2001). Mammalian Golgi-associated Bicaudal-D2 functions in the dynein-dynactin pathway by interacting with these complexes. The EMBO Journal *20*, 4041-4054.

Hoogenraad, C.C., Wulf, P., Schiefermeier, N., Stepanova, T., Galjart, N., Small, J.V., Grosveld, F., de Zeeuw, C.I., and Akhmanova, A. (2003). Bicaudal D induces selective dynein-mediated microtubule minus end-directed transport. The EMBO Journal *22*, 6004-6015.

Huttelmaier, S., Zenklusen, D., Lederer, M., Dictenberg, J., Lorenz, M., Meng, X., Bassell, G.J., Condeelis, J., and Singer, R.H. (2005). Spatial regulation of beta-actin translation by Src-dependent phosphorylation of ZBP1. Nature *438*, 512-515.

Huynh, J.R., and St Johnston, D. (2000). The role of Bic-D, Egl, Orb and the microtubules in the restriction of meiosis to the Drosophila oocyte. Development *127*, 2785-2794.

Huynh, J.R., and St Johnston, D. (2004). The origin of asymmetry: early polarisation of the Drosophila germline cyst and oocyte. Current Biology *14*, R438-449.

Ingelfinger, D., Arndt-Jovin, D.J., Luhrmann, R., and Achsel, T. (2002). The human LSm1-7 proteins colocalize with the mRNA-degrading enzymes Dcp1/2 and Xrnl in distinct cytoplasmic foci. RNA *8*, 1489-1501.

Jansen, R.P. (2001). mRNA localization: message on the move. Nat Rev Mol Cell Biol *2*, 247-256.

Januschke, J., Gervais, L., Dass, S., Kaltschmidt, J.A., Lopez-Schier, H., Johnston, D.S., Brand, A.H., Roth, S., and Guichet, A. (2002). Polar transport in the Drosophila oocyte requires Dynein and Kinesin I cooperation. Current Biology *12*, 1971-1981.

Johnstone, O., and Lasko, P. (2001). Translational regulation and RNA localization in Drosophila oocytes and embryos. Annual Review of Genetics *35*, 365-406.

Johnstone, O., and Lasko, P. (2004). Interaction with eIF5B is essential for Vasa function during development. Development *131*, 4167-4178.

Kalmykova, A.I., Kwon, D.A., Rozovsky, Y.M., Hueber, N., Capy, P., Maisonhaute, C., and Gvozdev, V.A. (2004). Selective expansion of the newly evolved genomic variants of retrotransposon 1731 in the Drosophila genomes. Molecular Biology and Evolution *21*, 2281-2289.

Kanai, Y., Dohmae, N., and Hirokawa, N. (2004). Kinesin Transports RNA; Isolation and Characterization of an RNA-Transporting Granule. Neuron *43*, 513-525.

Kawai, T., Fan, J., Mazan-Mamczarz, K., and Gorospe, M. (2004). Global mRNA stabilization preferentially linked to translational repression during the endoplasmic reticulum stress response. Molecular and Cellular Biology *24*, 6773-6787.

Kedersha, N., Cho, M.R., Li, W., Yacono, P.W., Chen, S., Gilks, N., Golan, D.E., and Anderson, P. (2000). Dynamic shuttling of TIA-1 accompanies the recruitment of mRNA to mammalian stress granules. The Journal of Cell Biology *151*, 1257-1268.

Kedersha, N., Stoecklin, G., Ayodele, M., Yacono, P., Lykke-Andersen, J., Fritzler, M.J., Scheuner, D., Kaufman, R.J., Golan, D.E., and Anderson, P. (2005). Stress granules and processing bodies are dynamically linked sites of mRNP remodeling. The Journal of Cell Biology *169*, 871-884.

Kedersha, N.L., Gupta, M., Li, W., Miller, I., and Anderson, P. (1999). RNA-binding proteins TIA-1 and TIAR link the phosphorylation of eIF-2 alpha to the assembly of mammalian stress granules. The Journal of Cell Biology *147*, 1431-1442.

Kelley, R.L. (1993). Initial organization of the Drosophila dorsoventral axis depends on an RNA-binding protein encoded by the squid gene. Genes Dev. *7*, 948--960.

Kim-Ha, J., Kerr, K., and Macdonald, P.M. (1995). Translational regulation of oskar mRNA by bruno, an ovarian RNA-binding protein, is essential. Cell *81*, 403-412.

Kim-Ha, J., Smith, J.L., and MacDonald, P.M. (1991). oskar mRNA is localized to the posterior pole of the *Drosophila* oocyte. Cell *66*, 23-35.

King, M.L., Messitt, T.J., and Mowry, K.L. (2005). Putting RNAs in the right place at the right time: RNA localization in the frog oocyte. Biology of the cell / under the auspices of the European Cell Biology Organization *97*, 19-33.

King, R.C. (1970). Ovarian Development in Drosophila melanogaster. (New York: Academic Press).

King, R.C., and Burnett, R.G. (1959). Autoradiographic study of uptake of tritiated glycine, thymidine, and uridine by fruit fly ovaries. Science *129*, 1674-1675.

King, S.M. (2000). AAA domains and organization of the dynein motor unit. Journal of Cell Science *113*, 2521-2526.

Kislauskis, E.H., Zhu, X.C., and Singer, R.H. (1994). Sequences Responsible For Intracellular-Localization Of Beta-Actin Messenger-Rna Also Affect Cell Phenotype. Journal Of Cell Biology *127*, 441-451.

Klattenhoff, C., Bratu, D.P., McGinnis-Schultz, N., Koppetsch, B.S., Cook, H.A., and Theurkauf, W.E. (2007). Drosophila rasiRNA pathway mutations disrupt embryonic axis specification through activation of an ATR/Chk2 DNA damage response. Developmental Cell *12*, 45-55.

Koch, E.A., and Spitzer, R.H. (1983). Multiple effects of colchicine on oogenesis in Drosophila: induced sterility and switch of potential oocyte to nurse-cell developmental pathway. Cell Tissue Res. *228*, 21-32.

Krichevsky, A.M., and Kosik, K.S. (2001). Neuronal RNA granules: a link between RNA localization and stimulation-dependent translation. Neuron *32*, 683-696.

Kruse, C., Jaedicke, A., Beaudouin, J., Bohl, F., Ferring, D., Guttler, T., Ellenberg, J., and Jansen, R.P. (2002). Ribonucleoprotein-dependent localization of the yeast class V myosin Myo4p. The Journal of Cell Biology *159*, 971-982.

Lane, M.E., and Kalderon, D. (1994). RNA localization along the anteroposterior axis of the *Drosophila* oocyte requires PKA-mediated signal transduction to direct normal microtubule organization. Genes & Development *8*, 2986-2995.

Larsen, K.S., Xu, J., Cermelli, S., Shu, Z., and Gross, S.P. (2008). BicaudalD actively regulates microtubule motor activity in lipid droplet transport. PLoS ONE *3*, e3763.

Lasko, P. (1999). RNA sorting in Drosophila oocytes and embryos. Faseb Journal *13*, 421-433.

Latham, V.M., Yu, E.H., Tullio, A.N., Adelstein, R.S., and Singer, R.H. (2001). A Rho-dependent signaling pathway operating through myosin localizes beta-actin mRNA in fibroblasts. Current Biology *11*, 1010-1016.

Lavoie, B., Basyuk, E., Bordonne, R., and Bertrand, E. (2004). Cell polarity and actin mRNA localization. Med Sci *20*, 539-543.

Lecuyer, E., Yoshida, H., Parthasarathy, N., Alm, C., Babak, T., Cerovina, T., Hughes, T.R., Tomancak, P., and Krause, H.M. (2007). Global analysis of mRNA localization reveals a prominent role in organizing cellular architecture and function. Cell *131*, 174-187.

Levy, J.R., Sumner, C.J., Caviston, J.P., Tokito, M.K., Ranganathan, S., Ligon, L.A., Wallace, K.E., LaMonte, B.H., Harmison, G.G., Puls, I.*, et al.* (2006). A motor neuron disease-associated mutation in p150Glued perturbs dynactin function and induces protein aggregation. The Journal of Cell Biology *172*, 733-745.

Li, P., Yang, X.H., Wasser, M., Cai, Y., and Chia, W. (1997). Inscuteable and staufen mediate asymmetric localization and segregation of prospero RNA during Drosophila neuroblast cell divisions. Cell *90*, 437-447.

Lieberfarb, M.E., Chu, T.Y., Wreden, C., Theurkauf, W., Gergen, J.P., and Strickland, S. (1996). Mutations that perturb poly(A)-dependent maternal mRNA activation block the initiation of development. Development *122*, 579-588.

Lin, M.D., Jiao, X., Grima, D., Newbury, S.F., Kiledjian, M., and Chou, T.B. (2008). Drosophila processing bodies in oogenesis. Developmental Biology *322*, 276-288.

Liu, J., Rivas, F.V., Wohlschlegel, J., Yates, J.R., 3rd, Parker, R., and Hannon, G.J. (2005a). A role for the P-body component GW182 in microRNA function. Nature Cell Biology *7*, 1261-1266.

Liu, J., Valencia-Sanchez, M.A., Hannon, G.J., and Parker, R. (2005b). MicroRNA-dependent localization of targeted mRNAs to mammalian P-bodies. Nature Cell Biology *7*, 719-723.

Liu, J.L., and Gall, J.G. (2007). U bodies are cytoplasmic structures that contain uridine-rich small nuclear ribonucleoproteins and associate with P bodies. Proceedings of the National Academy of Sciences of the United States of America *104*, 11655-11659.

Long, R.M., Gu, W., Lorimer, E., Singer, R.H., and Chartrand, P. (2000). She2p is a novel RNA-binding protein that recruits the Myo4p-She3p complex to ASH1 mRNA. The EMBO Journal *19*, 6592-6601.

Lopez de Heredia, M., and Jansen, R.P. (2004). mRNA localization and the cytoskeleton. Current Opinion in Cell Biology *16*, 80-85.

Luan, D.D., Korman, M.H., Jakubczak, J.L., and Eickbush, T.H. (1993). Reverse transcription of R2Bm RNA is primed by a nick at the chromosomal target site: a mechanism for non-LTR retrotransposition. Cell *72*, 595-605.

Lukavsky, P.J., Kim, I., Otto, G.A., and Puglisi, J.D. (2003). Structure of HCV IRES domain II determined by NMR. Nature Structural Biology *10*, 1033-1038.

Macdonald, P.M., and Kerr, K. (1998). Mutational analysis of an RNA recognition element that mediates localization of bicoid mRNA. Molecular and Cellular Biology *18*, 3788-3795.

Macdonald, P.M., Kerr, K., Smith, J.L., and Leask, A. (1993). RNA regulatory element BLE1 directs the early steps of bicoid mRNA localization. Development *118*, 1233-1243.

Macdonald, P.M., and Struhl, G. (1988). *cis*-acting sequences responsible for anterior localization of bicoid mRNA in Drosophila embryos. Nature *336*, 595-598.

MacDougall, N., Clark, A., MacDougall, E., and Davis, I. (2003). Drosophila gurken (TGFalpha) mRNA Localizes as Particles that Move within the Oocyte in Two Dynein-Dependent Steps. Developmental Cell *4*, 307-319.

Maddox, P.S., Stemple, J.K., Satterwhite, L., Salmon, E.D., and Bloom, K. (2003). The minus end-directed motor Kar3 is required for coupling dynamic microtubule plus-ends to the cortical shmoo tip in budding yeast. Current Biology *13*, 1423-1428.

Mallik, R., Carter, B.C., Lex, S.A., King, S.J., and Gross, S.P. (2004). Cytoplasmic dynein functions as a gear in response to load. Nature *427*, 649-652.

Mallik, R., and Gross, S.P. (2004). Molecular motors: strategies to get along. Current Biology *14*, 971-982.

Mallik, R., Petrov, D., Lex, S.A., King, S.J., and Gross, S.P. (2005). Building complexity: an *in vitro* study of cytoplasmic dynein with *in vivo* implications. Current Biology *15*, 2075-2085.

Manseau, L., Calley, J., and Phan, H. (1996). Profilin is required for posterior patterning of the Drosophila oocyte. Development *122*, 2109-2116.

Manseau, L.J., and Schüpbach, T. (1989). cappuccino and spire: two unique maternal-effect loci required for both the anteroposterior and dorsoventral patterns of the Drosophila embryo. Genes & Development *3*, 1437-1452.

Markussen, F.H., Michon, A.M., Breitwieser, W., and Ephrussi, A. (1995). Translational control of oskar generates short OSK, the isoform that induces pole plasma assembly. Development *121*, 3723-3732.

Martin, K.C., and Ephrussi, A. (2009). mRNA localization: gene expression in the spatial dimension. Cell *136*, 719-730.

Mehta, A.D., Rock, R.S., Rief, M., Spudich, J.A., Mooseker, M.S., and Cheney, R.E. (1999). Myosin-V is a processive actin-based motor. Nature *400*, 590-593.

Meignin, C., Alvarez-Garcia, I., Davis, I., and Palacios, I.M. (2007). The salvador-warts-hippo pathway is required for epithelial proliferation and axis specification in Drosophila. Current Biology *17*, 1871-1878.

Mesngon, M.T., Tarricone, C., Hebbar, S., Guillotte, A.M., Schmitt, E.W., Lanier, L., Musacchio, A., King, S.J., and Smith, D.S. (2006). Regulation of cytoplasmic dynein ATPase by Lis1. The Journal of Neuroscience *26*, 2132-2139.

Metschnikoff, E. (1865). Veber die Entwicklung der Cecidomyienlarven aus dem Pseudovum. Arch. furr Naturg. *Bd 1.*

Micklem, D.R., Adams, J., Grunert, S., and St Johnston, D. (2000). Distinct roles of two conserved Staufen domains in oskar mRNA localization and translation. The EMBO Journal *19*, 1366-1377.

Miller, K.G. (2004). Converting a motor to an anchor. Cell *116*, 635-636.

Mische, S., Li, M., Serr, M., and Hays, T.S. (2007). Direct observation of regulated ribonucleoprotein transport across the nurse cell/oocyte boundary. Molecular Biology of the Cell *18*, 2254-2263.

Mizuno, N., Toba, S., Edamatsu, M., Watai-Nishii, J., Hirokawa, N., Toyoshima, Y.Y., and Kikkawa, M. (2004). Dynein and kinesin share an overlapping microtubule-binding site. The EMBO Journal *23*, 2459-2467.

Mohler, J., and Wieschaus, E.F. (1986). Dominant maternal-effect mutations of Drosophila melanogaster causing the production of double-abdomen embryos. Genetics *112*, 803-822.

Mohr, S.E., Dillon, S.T., and Boswell, R.E. (2001). The RNA-binding protein Tsunagi interacts with Mago Nashi to establish polarity and localize oskar mRNA during Drosophila oogenesis. Genes & Development *15*, 2886-2899.

Montell, D.J. (2003). Border-cell migration: the race is on. Nat Rev Mol Cell Biol *4*, 13-24.

Montell, D.J., Rorth, P., and Spradling, A.C. (1992). slow border cells, a locus required for a developmentally regulated cell migration during oogenesis, encodes Drosophila C/EBP. Cell *71*, 51-62.

Morin, X., Daneman, R., Zavortink, M., and Chia, W. (2001). A protein trap strategy to detect GFP-tagged proteins expressed from their endogenous loci in Drosophila. Proceedings of the National Academy of Sciences of the United States of America *98*, 15050-15055.

Moritz, M., and Agard, D.A. (2001). Gamma-tubulin complexes and microtubule nucleation. Current Opinion in Structural Biology *11*, 174-181.

Morris, N.R. (2003). Nuclear positioning: the means is at the ends. Current Opinion in Cell Biology *15*, 54-59.

Nakamura, A., Amikura, R., Hanyu, K., and Kobayashi, S. (2001). Me31B silences translation of oocyte-localizing RNAs through the formation of cytoplasmic RNP complex during Drosophila oogenesis. Development *128*, 3233-3242.

Nakamura, A., Sato, K., and Hanyu-Nakamura, K. (2004). Drosophila cup is an eIF4E binding protein that associates with Bruno and regulates oskar mRNA translation in oogenesis. Developmental Cell *6*, 69-78.

Navarro, C., Puthalakath, H., Adams, J.M., Strasser, A., and Lehmann, R. (2004). Egalitarian binds dynein light chain to establish oocyte polarity and maintain oocyte fate. Nature Cell Biology *6*, 427-435.

Navarro, R.E., and Blackwell, T.K. (2005). Requirement for P granules and meiosis for accumulation of the germline RNA helicase CGH-1. Genesis *42*, 172-180.

Neuman-Silberberg, F.S., and Schüpbach, T. (1993). The *Drosophila* dorsoventral patterning gene *gurken* produces a dorsally localized RNA and encodes a TGF alpha-like protein. Cell *75*, 165-174.

Neuman-Silberberg, F.S., and Schüpbach, T. (1996). The Drosophila TGF-alpha-like protein Gurken: expression and cellular localization during *Drosophila* oogenesis. Mechanisms of Development *59*, 105-113.

Neuwald, A.F., Aravind, L., Spouge, J.L., and Koonin, E.V. (1999). AAA+: A class of chaperone-like ATPases associated with the assembly, operation, and disassembly of protein complexes. Genome Research *9*, 27-43.

Newmark, P.A., and Boswell, R.E. (1994). The mago nashi locus encodes an essential product required for germ plasm assembly in Drosophila. Development *120*, 1303-1313.

Norvell, A., Debec, A., Finch, D., Gibson, L., and Thoma, B. (2005). Squid is required for efficient posterior localization of oskar mRNA during Drosophila oogenesis. Development Genes and Evolution *215*, 340-349.

Norvell, A., Kelley, R.L., Wehr, K., and Schüpbach, T. (1999). Specific isoforms of Squid, a *Drosophila* hnRNP, perform distinct roles in *gurken* localization during oogenesis. Genes & Development *13*, 864-876.

Nusslein-Volhard, C., Frohnhofer, H.G., and Lehmann, R. (1987). Determination of anteroposterior polarity in Drosophila. Science *238*, 1675-1681.

Okamura, K., Ishizuka, A., Siomi, H., and Siomi, M.C. (2004). Distinct roles for Argonaute proteins in small RNA-directed RNA cleavage pathways. Genes & Development *18*, 1655-1666.

Palacios, I.M. (2002). RNA processing: splicing and the cytoplasmic localisation of mRNA. Current Biology *12*, R50-52.

Palacios, I.M., and Johnston, D.S. (2002). Kinesin light chain-independent function of the Kinesin heavy chain in cytoplasmic streaming and posterior localisation in the Drosophila oocyte. Development *129*, 5473-5485.

Pane, A., Wehr, K., and Schupbach, T. (2007). zucchini and squash encode two putative nucleases required for rasiRNA production in the Drosophila germline. Developmental Cell *12*, 851-862.

Paquin, N., and Chartrand, P. (2008). Local regulation of mRNA translation: new insights from the bud. Trends in Cell Biology *18*, 105-111.

Pelegri, F., and Lehmann, R. (1994). A Role Of Polycomb Group Genes In the Regulation Of Gap Gene- Expression In Drosophila. Genetics *136*, 1341-1353.

Peri, F., and Roth, S. (2000). Combined activities of Gurken and decapentaplegic specify dorsal chorion structures of the Drosophila egg. Development *127*, 841-850.

Piccioni, F., Zappavigna, V., and Verrotti, A.C. (2005). Translational regulation during oogenesis and early development: the cap-poly(A) tail relationship. Comptes Rendus Biologies *328*, 863-881.

Pillai, R.S., Bhattacharyya, S.N., Artus, C.G., Zoller, T., Cougot, N., Basyuk, E., Bertrand, E., and Filipowicz, W. (2005). Inhibition of translational initiation by Let-7 MicroRNA in human cells. Science *309*, 1573-1576.

Pokrywka, N.J., and Stephenson, E.C. (1991). Microtubules mediate the localization of *bicoid* RNA during *Drosophila* oogenesis. Development *113*, 55-66.

Pokrywka, N.J., and Stephenson, E.C. (1995). Microtubules are a general component of mRNA localization systems in *Drosophila* oocytes. Developmental Biology *167*, 363-370.

Pritchard, M.A., Dura, J.M., Pelisson, A., Bucheton, A., and Finnegan, D.J. (1988). A cloned I-factor is fully functional in Drosophila melanogaster. Mol Gen Genet *214*, 533-540.

Queenan, A.M., Barcelo, G., Van Buskirk, C., and Schupbach, T. (1999). The transmembrane region of gurken is not required for biological activity, but is necessary for transport to the oocyte membrane in drosophila. Mechanisms of Development *89*, 35-42.

Ramos, A., Grunert, S., Adams, J., Micklem, D.R., Proctor, M.R., Freund, S., Bycroft, M., St Johnston, D., and Varani, G. (2000). RNA recognition by a Staufen double-stranded RNA-binding domain. The EMBO Journal *19*, 997-1009.

Ran, B., Bopp, R., and Suter, B. (1994). Null alleles reveal novel requirements for Bic-D during Drosophila oogenesis and zygotic development. Development *120*, 1233-1242.

Reck-Peterson, S.L., Provance, D.W., Jr., Mooseker, M.S., and Mercer, J.A. (2000). Class V myosins. Biochimica et Biophysica Acta *1496*, 36-51.

Reich, J., Snee, M.J., and Macdonald, P.M. (2009). miRNA-dependent translational repression in the Drosophila ovary. PLoS ONE *4*, e4669.

Riechmann, V., and Ephrussi, A. (2004). Par-1 regulates bicoid mRNA localisation by phosphorylating Exuperantia. Development *131*, 5897-5907.

Rief, M., Rock, R.S., Mehta, A.D., Mooseker, M.S., Cheney, R.E., and Spudich, J.A. (2000). Myosin-V stepping kinetics: a molecular model for processivity. Proceedings of the National Academy of Sciences of the United States of America *97*, 9482-9486.

Rivas, E., and Eddy, S.R. (2000). Secondary structure alone is generally not statistically significant for the detection of noncoding RNAs. Bioinformatics *16*, 583-605.

Rivas, E., Klein, R.J., Jones, T.A., and Eddy, S.R. (2001). Computational identification of noncoding RNAs in E. coli by comparative genomics. Current Biology *11*, 1369-1373.

Robert, F., Kapp, L.D., Khan, S.N., Acker, M.G., Kolitz, S., Kazemi, S., Kaufman, R.J., Merrick, W.C., Koromilas, A.E., Lorsch, J.R., and Pelletier, J. (2006). Initiation of protein synthesis by hepatitis C virus is refractory to reduced eIF2.GTP.Met-tRNA(i)(Met) ternary complex availability. Molecular Biology of the Cell *17*, 4632-4644.

Rongo, C., Gavis, E.R., and Lehmann, R. (1995). Localization of oskar RNA regulates oskar translation and requires Oskar protein. Development *121*, 2737-2746.

Ross, J.L., Wallace, K., Shuman, H., Goldman, Y.E., and Holzbaur, E.L. (2006). Processive bidirectional motion of dynein-dynactin complexes *in vitro*. Nature Cell Biology *8*, 562-570.

Roth, S., Neuman-Silberberg, F.S., and Schüpbach, T. (1995). Dorsoventral signaling in *Drosophila* oogenesis. Journal of Cellular Biochemistry *19A*, 326.

Ryder, E., Spriggs, H., Drummond, E., St Johnston, D., and Russell, S. (2009). The Flannotator: a gene and protein expression annotation tool for Drosophila melanogaster. Bioinformatics *25*, 548-549.

Sakato, M., and King, S.M. (2004). Design and regulation of the AAA+ microtubule motor dynein. Journal of Structural Biology *146*, 58-71.

Sambrook, J., Fritsch, E.F., and Maniatis, T. (1989). Molecular Cloning : A Laboratory Manual, 2 edn (New York: Cold Spring Harbour Laboratory Press).

Sarot, E., Payen-Groschene, G., Bucheton, A., and Pelisson, A. (2004). Evidence for a piwi-dependent RNA silencing of the gypsy endogenous retrovirus by the Drosophila melanogaster flamenco gene. Genetics *166*, 1313-1321.

Saunders, C., and Cohen, R.S. (1999). The role of oocyte transcription, the 5'UTR, and translation repression and derepression in *Drosophila gurken* mRNA and protein localization. Molecular Cell *3*, 43-54.

Schmid, M., Jaedicke, A., Du, T.G., and Jansen, R.P. (2006). Coordination of endoplasmic reticulum and mRNA localization to the yeast bud. Current Biology *16*, 1538-1543.

Schneider, I. (1972). Cell lines derived from late embryonic stages of Drosophila melanogaster. Journal of Embryology and Experimental Morphology *27*, 353-365.

Schnorrer, F., Bohmann, K., and Nusslein-Volhard, C. (2000). The molecular motor dynein is involved in targeting swallow and bicoid RNA to the anterior pole of Drosophila oocytes. Nature Cell Biology *2*, 185-190.

Schroer, T.A. (2004). Dynactin. Annual Review of Cell and Developmental Biology *20*, 759-779

Schupbach, T., and Wieschaus, E. (1991). Female sterile mutations on the second chromosome of Drosophila melanogaster. II. Mutations blocking oogenesis or altering egg morphology. Genetics *129*, 1119-1136.

Seeger, M.A., and Kaufman, T.C. (1990). Molecular analysis of the bicoid gene from Drosophila pseudoobscura: identification of conserved domains within coding and noncoding regions of the bicoid mRNA. The EMBO Journal 9, 2977-2987.

Seleme, M.C., Disson, O., Robin, S., Brun, C., Teninges, D., and Bucheton, A. (2005). *In vivo* RNA localization of *I* factor, a non-LTR retrotransposon, requires a *cis*-acting signal in ORF2 and ORF1 protein. Nucleic Acids Research *33*, 776-785.

Sen, G.L., and Blau, H.M. (2005). Argonaute 2/RISC resides in sites of mammalian mRNA decay known as cytoplasmic bodies. Nature Cell Biology *7*, 633-636.

Sen, J., Goltz, J.S., Stevens, L., and Stein, D. (1998). Spatially restricted expression of pipe in the Drosophila egg chamber defines embryonic dorsal-ventral polarity. Cell *95*, 471-481.

Serano, T.L., Karlin-McGinness, M., and Cohen, R.S. (1995). The role of fs(1)K10 in the localization of the mRNA of the TGF alpha homolog gurken within the Drosophila oocyte. Mechanisms of Development *51*, 183-192.

Sharp, D.J., Brown, H.M., Kwon, M., Rogers, G.C., Holland, G., and Scholey, J.M. (2000). Functional coordination of three mitotic motors in *Drosophila* embryos. Molecular Biology of the Cell *11*, 241-253.

Shepard, K.A., Gerber, A.P., Jambhekar, A., Takizawa, P.A., Brown, P.O., Herschlag, D., DeRisi, J.L., and Vale, R.D. (2003). Widespread cytoplasmic mRNA transport in yeast: identification of 22 bud-localized transcripts using DNA microarray analysis. Proceedings of the National Academy of Sciences of the United States of America *100*, 11429-11434.

Shubeita, G.T., Tran, S.L., Xu, J., Vershinin, M., Cermelli, S., Cotton, S.L., Welte, M.A., and Gross, S.P. (2008). Consequences of motor copy number on the intracellular transport of kinesin-1-driven lipid droplets. Cell *135*, 1098-1107.

Shyu, A.B., and Wilkinson, M.F. (2000). The double lives of shuttling mRNA binding proteins. Cell *102*, 135-138.

Slot, J.W., Geuze, H.J., Gigengack, S., Lienhard, G.E., and James, D.E. (1991). Immuno-localization of the insulin regulatable glucose transporter in brown adipose tissue of the rat. The Journal of Cell Biology *113*, 123-135.

Smith, R. (2004). Moving molecules: mRNA trafficking in Mammalian oligodendrocytes and neurons. Neuroscientist *10*, 495-500.

Spradling, A.C. (1993). Developmental genetics of oogenesis. In The development of *Drosophila melanogaster*, M. Bate, and A.M. Martinez Arias, eds. (New York: Cold Spring Harbour Laboratory Press), pp. 1-70.

Srivastava, S.P., Kumar, K.U., and Kaufman, R.J. (1998). Phosphorylation of eukaryotic translation initiation factor 2 mediates apoptosis in response to activation of the double-stranded RNA-dependent protein kinase. The Journal of Biological Chemistry *273*, 2416-2423.

St Johnston, D. (2005). Moving messages: the intracellular localization of mRNAs. Nat Rev Mol Cell Biol *6*, 363-375.

St Johnston, D., Beuchle, D., and Nüsslein-Volhard, C. (1991). Staufen, a Gene Required to Localize Maternal Rnas In the Drosophila Egg. Cell *66*, 51-63.

St Johnston, D., Driever, W., Berleth, T., Richstein, S., and Nüsslein-Volhard, C. (1989). Multiple steps in the localization of bicoid RNA to the anterior pole of the *Drosophila* oocyte. Development *107*, 13-19.

Stebbins-Boaz, B., Fortner, K., Frazier, J., Piluso, S., Pullen, S., Rasar, M., Reid, W., Sinclair, K., and Winger, E. (2004). Oocyte maturation in Xenopus laevis is blocked by the hormonal herbicide, 2,4-dichlorophenoxy acetic acid. Molecular Reproduction and Development *67*, 233-242.

Stein, D., Roth, S., Vogelsang, E., and Nüsslein-Volhard, C. (1991). The polarity of the dorsoventral axis in the Drosophila embryo is defined by an extracellular signal. Cell *66*, 725-735.

Steinhauer, J., and Kalderon, D. (2005). The RNA-binding protein Squid is required for the establishment of anteroposterior polarity in the Drosophila oocyte. Development *132*, 5515-5525.

Steinhauer, J., and Kalderon, D. (2006). Microtubule polarity and axis formation in the Drosophila oocyte. Developmental Dynamics *235*, 1455-1468.

Styhler, S., Nakamura, A., Swan, A., Suter, B., and Lasko, P. (1998). vasa is required for GURKEN accumulation in the oocyte, and is involved in oocyte differentiation and germline cyst development. Development *125*, 1569-1578.

Susalka, S.J., and Pfister, K.K. (2000). Cytoplasmic dynein subunit heterogeneity: implications for axonal transport. Journal of Neurocytology *29*, 819-829.

Suter, B., and Steward, R. (1991). Requirement for phosphorylation and localization of the Bicaudal-D protein in Drosophila oocyte differentiation. Cell *67*, 917-926.

Swan, A., Nguyen, T., and Suter, B. (1999). Drosophila Lissencephaly-1 functions with Bic-D and dynein in oocyte determination and nuclear positioning. Nature Cell Biology *1*, 444-449.

Swan, A., and Suter, B. (1996). Role of Bicaudal-D in patterning the Drosophila egg chamber in mid- oogenesis. Development *122*, 3577-3586.

Swanson, M.S., and Dreyfuss, G. (1999). Preparation of heterogeneous nuclear ribonucleoprotein complexes. Methods Mol Biol *118*, 299-308.

Tautz, D., and Pfeifle, C. (1989). A non-radioactive in situ hybridization method for the localization of specific RNAs in Drosophila embryos reveals translational control of the segmentation gene hunchback. Chromosoma *98*, 81-85.

Teixeira, D., Sheth, U., Valencia-Sanchez, M.A., Brengues, M., and Parker, R. (2005). Processing bodies require RNA for assembly and contain nontranslating mRNAs. RNA *11*, 371-382.

Tekotte, H., and Davis, I. (2002). Intracellular mRNA localization: motors move messages. Trends Genet *18*, 636-642.

Theurkauf, W.E. (1992). Behavior Of Structurally Divergent Alpha-Tubulin Isotypes During Drosophila Embryogenesis - Evidence For Posttranslational Regulation Of Isotype Abundance. Developmental Biology *154*, 205-217.

Theurkauf, W.E. (1994). Premature Microtubule-Dependent Cytoplasmic Streaming In Cappuccino and Spire Mutant Oocytes. Science *265*, 2093-2096.

Theurkauf, W.E., Alberts, B.M., Jan, Y.N., and Jongens, T.A. (1993). A central role for microtubules in the differentiation of *Drosophila* oocytes. Development *118*, 1169-1180.

Theurkauf, W.E., Smiley, S., Wong, M.L., and Alberts, B.M. (1992). Reorganization of the cytoskeleton during *Drosophila* oogenesis - implications for axis specification and intercellular transport. Development *115*, 923-936.

Thio, G.L., Ray, R.P., Barcelo, G., and Schüpbach, T. (2000). Localization of gurken RNA in Drosophila oogenesis requires elements in the 5' and 3' regions of the transcript. Developmental Biology *221*, 435-446.

Thomson, T., and Lasko, P. (2004). Drosophila tudor is essential for polar granule assembly and pole cell specification, but not for posterior patterning. Genesis *40*, 164-170.

Tinker, R., Silver, D., and Montell, D.J. (1998). Requirement for the vasa RNA helicase in gurken mRNA localization. Developmental Biology *199*, 1-10.

Tokuyasu, K., and Okamura, S. (1959). A new method for making glass knives for thin sectioning. The Journal of Biophysical and Biochemical Cytology *6*, 305-308.

Tomancak, P., Guichet, A., Zavorszky, P., and Ephrussi, A. (1998). Oocyte polarity depends on regulation of gurken by Vasa. Development *125*, 1723-1732.

Tsai, N.P., Tsui, Y.C., and Wei, L.N. (2009). Dynein motor contributes to stress granule dynamics in primary neurons. Neuroscience 159, 647-656.

Unterholzner, L., and Izaurralde, E. (2004). SMG7 acts as a molecular link between mRNA surveillance and mRNA decay. Molecular Cell *16*, 587-596.

Urban, S., Lee, J.R., and Freeman, M. (2002). A family of Rhomboid intramembrane proteases activates all Drosophila membrane-tethered EGF ligands. The EMBO Journal *21*, 4277-4286.

Vagin, V.V., Sigova, A., Li, C., Seitz, H., Gvozdev, V., and Zamore, P.D. (2006). A distinct small RNA pathway silences selfish genetic elements in the germline. Science *313*, 320-324.

Vaisberg, E.A., Koonce, M.P., and McIntosh, J.R. (1993). Cytoplasmic dynein plays a role in mammalian mitotic spindle formation. The Journal of Cell Biology *123*, 849-858.

Vale, R.D. (2003). The molecular motor toolbox for intracellular transport. Cell *112*, 467-480.

Vale, R.D., and Milligan, R.A. (2000). The way things move: looking under the hood of molecular motor proteins. Science *288*, 88-95.

Van Buskirk, C., Hawkins, N.C., and Schupbach, T. (2000). Encore is a member of a novel family of proteins and affects multiple processes in Drosophila oogenesis. Development *127*, 4753-4762.

Van Buskirk, C., and Schupbach, T. (2002). Half pint regulates alternative splice site selection in Drosophila. Developmental Cell *2*, 343-353.

Van De Bor, V., Hartswood, E., Jones, C., Finnegan, D., and Davis, I. (2005). gurken and the *I* factor retrotransposon RNAs share common localization signals and machinery. Developmental Cell *9*, 51-62.

Vendra, G., Hamilton, R.S., and Davis, I. (2007). Dynactin suppresses the retrograde movement of apically localized mRNA in Drosophila blastoderm embryos. RNA *13*, 1860-1867.

Vershinin, M., Carter, B.C., Razafsky, D.S., King, S.J., and Gross, S.P. (2007). Multiple-motor based transport and its regulation by Tau. Proceedings of the National Academy of Sciences of the United States of America *104*, 87-92.

Visscher, K., Schnitzer, M.J., and Block, S.M. (1999). Single kinesin molecules studied with a molecular force clamp. Nature *400*, 184-189.

Webster, P.J., Liang, L., Berg, C.A., Lasko, P., and Macdonald, P.M. (1997). Translational repressor bruno plays multiple roles in development and is widely conserved. Genes & Development *11*, 2510-2521.

Weil, T.T., Forrest, K.M., and Gavis, E.R. (2006). Localization of bicoid mRNA in Late Oocytes Is Maintained by Continual Active Transport. Developmental Cell *11*, 251-262.

Weil, T.T., Parton, R., Davis, I., and Gavis, E.R. (2008). Changes in bicoid mRNA anchoring highlight conserved mechanisms during the oocyte-to-embryo transition. Current Biology *18*, 1055-1061.

Wek, S.A., Zhu, S., and Wek, R.C. (1995). The histidyl-tRNA synthetase-related sequence in the eIF-2 alpha protein kinase GCN2 interacts with tRNA and is required for activation in response to starvation for different amino acids. Molecular and Cellular Biology *15*, 4497-4506.

Welte, M.A., Gross, S.P., Postner, M., Block, S.M., and Wieschaus, E.F. (1998). Developmental regulation of vesicle transport in *Drosophila* embryos: Forces and kinetics. Cell *92*, 547-557.

Weston, A., and Sommerville, J. (2006). Xp54 and related (DDX6-like) RNA helicases: roles in messenger RNP assembly, translation regulation and RNA degradation. Nucleic Acids Research *34*, 3082-3094.

Wieschaus, E., Marsh, J.L., and Gehring, W.J. (1978). fs(1)K10, a germline-dependent female sterile mutation causing abnormal chorion morphology in Drosophila melanogaster. Developmental Biology *184*, 75--82.

Wilkie, G.S., and Davis, I. (2001). *Drosophila wingless* and pair-rule transcripts localize apically by dynein-mediated transport of RNA particles. Cell *105*, 209-219.

Wilkie, G.S., Shermoen, A.W., O'Farrell, P.H., and Davis, I. (1999). Transcribed genes are localized according to chromosomal position within polarized *Drosophila* embryonic nuclei. Current Biology *9*, 1263-1266.

Williamson, A., and Lehmann, R. (1996). Germ cell development in Drosophila. Annual Review of Cell and Developmental Biology *12*, 365-391.

Wilsch-Brauninger, M., Schwarz, H., and Nusslein-Volhard, C. (1997). A sponge-like structure involved in the association and transport of maternal products during Drosophila oogenesis. The Journal of Cell Biology *139*, 817-829.

White, R.A., and Lehmann, R. (1986). A gap gene, hunchback, regulates the spatial expression of Ultrabithorax. Cell 47, 311-321.

Wu, X., Tanwar, P.S., and Raftery, L.A. (2008). Drosophila follicle cells: morphogenesis in an eggshell. Seminars in Cell & Developmental Biology *19*, 271-282.

Xi, R., McGregor, J.R., and Harrison, D.A. (2003). A gradient of JAK pathway activity patterns the anterior-posterior axis of the follicular epithelium. Developmental Cell *4*, 167-177.

Yan, N., and Macdonald, P.M. (2004). Genetic interactions of Drosophila melanogaster arrest reveal roles for translational repressor Bruno in accumulation of Gurken and activity of Delta. Genetics *168*, 1433-1442.

Yang, F., Peng, Y., Murray, E.L., Otsuka, Y., Kedersha, N., and Schoenberg, D.R. (2006). Polysome-bound endonuclease PMR1 is targeted to stress granules via stress-specific binding to TIA-1. Molecular and Cellular Biology *26*, 8803-8813.

Yang, Z., Jakymiw, A., Wood, M.R., Eystathioy, T., Rubin, R.L., Fritzler, M.J., and Chan, E.K. (2004). GW182 is critical for the stability of GW bodies expressed during the cell cycle and cell proliferation. Journal of Cell Science *117*, 5567-5578.

Yu, C., York, B., Wang, S., Feng, Q., Xu, J., and O'Malley, B.W. (2007). An essential function of the SRC-3 coactivator in suppression of cytokine mRNA translation and inflammatory response. Molecular Cell *25*, 765-778.

Zimyanin, V.L., Belaya, K., Pecreaux, J., Gilchrist, M.J., Clark, A., Davis, I., and St Johnston, D. (2008). *In vivo* imaging of oskar mRNA transport reveals the mechanism of posterior localization. Cell *134*, 843-853.

Zuker, M. (2003). Mfold web server for nucleic acid folding and hybridization prediction. Nucleic Acids Research *31*, 3406-3415.

10

Appendix

Developmental Cell
Article

Drosophila Squid/hnRNP Helps Dynein Switch from a *gurken* mRNA Transport Motor to an Ultrastructural Static Anchor in Sponge Bodies

Renald Delanoue,[1,3,5] Bram Herpers,[2,3] Jan Soetaert,[1,6] Ilan Davis,[1,4,6,*] and Catherine Rabouille[2,4,*]
[1]Wellcome Trust Centre for Cell Biology, Michael Swann Building, University of Edinburgh, Mayfield Road, Edinburgh EH9 3JR, United Kingdom
[2]The Cell Microscopy Centre, Department of Cell Biology, Institute of Biomembranes, University Medical Centre Utrecht, Heidelberglaan 100, 3584 CX Utrecht, The Netherlands
[3]These authors contributed equally to this work and are listed in alphabetical order.
[4]These authors contributed equally to this work and are joint corresponding authors listed in alphabetical order.
[5]Present address: Centre de Biochimie, UMR CNRS 6543, Parc Valrose, Faculté des Sciences, 06108 Nice Cedex 2, France.
[6]Present address: Department of Biochemistry, Oxford University, South Parks Road, Oxford OX1 3QU, United Kingdom.
*Correspondence: ilan.davis@bioch.ox.ac.uk (I.D.), c.rabouille@umcutrecht.nl (C.R.)
DOI 10.1016/j.devcel.2007.08.022

SUMMARY

In *Drosophila* oocytes, dorso-anterior transport of *gurken* mRNA requires both the Dynein motor and the heterogeneous nuclear ribonucleoprotein (hnRNP) Squid. We show that *gurken* transcripts are transported directly on microtubules by Dynein in nonmembranous electron-dense transport particles that also contain Squid and the transport cofactors Egalitarian and Bicaudal-D. At its destination, *gurken* mRNA is statically anchored by Dynein within large electron-dense cytoplasmic structures known as sponge bodies. Egalitarian and Bicaudal-D contribute only to active transport, whereas Dynein and Squid are also required for *gurken* mRNA anchoring and the integrity of sponge bodies. Disrupting Dynein function disperses *gurken* mRNA homogeneously throughout the cytoplasm, whereas the loss of Squid function converts the sponge bodies into active transport particles. We propose that Dynein acts as a static structural component for the assembly of *gurken* mRNA transport and anchoring complexes, and that Squid is required for the dynamic conversion of transport particles to sponge bodies.

INTRODUCTION

mRNA localization directs the biosynthesis of proteins to specific subcellular compartments in all major model systems, including yeast, *Drosophila*, and a number of vertebrate models (St Johnston, 2005). mRNA localization occurs by several distinct mechanisms, including selective degradation (Bashirullah et al., 1999), diffusion followed by anchoring (Forrest and Gavis, 2003; Glotzer et al., 1997), and continual active transport (Weil et al., 2006), among other forms of delivery by molecular motors (Tekotte and Davis, 2002). The best-characterized case of a motor that transports RNA is Myosin V, which transports *Ash1* mRNA along actin microfilaments in yeast (Bertrand et al., 1998).

In the developing *Drosophila* oocyte, *gurken* (*grk*) mRNA encodes a secreted TGF-α signal and is localized at two different times in oogenesis, first posteriorly, then dorso-anteriorly. The Grk signal is targeted to the same locations, thus initiating the antero-posterior and dorso-ventral axes of the oocyte and future embryo (Neuman-Silberberg and Schüpbach, 1993; Gonzalez-Reyes et al., 1995; Pearson and Gonzalez-Reyes, 2004).

grk RNA is first transported from the nurse cells into the oocyte by the *Drosophila* Dynein motor (Clark et al., 2007; Caceres and Nilson, 2005), which is also required for transport to the oocyte dorso-anterior (MacDougall et al., 2003). The Dynein motor is a very large complex of many components, including the force-generating ATPase Dynein heavy chain and the Dynein intermediate and light chains (Pfister et al., 2006). The additional cofactors Bicaudal-D (BicD) and Egalitarian (Egl) are required in vivo for efficient Dynein-based mRNA transport, and are required in some way for the cargo to recruit the Dynein motor (Bullock and Ish-Horowicz, 2001; Bullock et al., 2006; Clark et al., 2007).

Although the evidence is good that Dynein is involved in the transport of various mRNAs in *Drosophila*, it is not known whether transport occurs by direct association of the mRNA cargo with Dynein or indirectly, by hitchhiking on a transport vesicle or along a membrane-bound compartment such as the endoplasmic reticulum (ER), as previously postulated for *Xenopus Vg1* (Deshler et al., 1997) and shown for *ASH1* (Schmid et al., 2006).

Once at its final destination, mRNA must be kept localized, a process that could occur by a number of possible mechanisms (Delanoue and Davis, 2005), including anchoring and continuous active transport. Actin-dependent tethering has been favored as a means of anchoring mRNA. However, F-actin is not required for anchoring of the apically localized *pair-rule* transcripts in blastoderm embryos. Instead, apical transcripts are tethered in a

microtubule- (MT) and Dynein-dependent manner, independently of the ATPase activity of the motor, BicD, and Egl, which are required for RNA transport (Delanoue and Davis, 2005). It is not currently known how *grk* mRNA is maintained at its final site of localization, nor whether any specialized structure or membrane-bound organelles are involved.

Some factors have been identified that are involved in *grk* mRNA localization (Roth and Schüpbach, 1994; Goodrich et al., 2004; Van Buskirk and Schüpbach, 2002), of which the best studied is Squid (Sqd), a *Drosophila* heterogeneous nuclear ribonucleoprotein (hnRNP) (Norvell et al., 1999). Like other hnRNPs, Squid probably binds to many RNAs in addition to *grk* in the oocyte and has many basic cellular functions. For instance, recently it was shown that Sqd is in a complex with Hrp48 and the *Drosophila* Imp protein, a complex required for *grk* and *osk* mRNA translation (Geng and MacDonald, 2006). However, the *Drosophila squid* null phenotype has a specific defect in the second step of *grk* mRNA transport rather than a more severe defect expected from an essential cellular factor (MacDougall et al., 2003; Norvell et al., 1999). It remains unclear whether Sqd is also required for RNA anchoring.

Here we address these questions by imaging and perturbing the movement and anchoring of *grk* RNA in living cells, in combination with immunoelectron microscopy (IEM) techniques we have developed to covisualize *grk* mRNA together with the components of the Dynein motor complex and its associated cofactors. We found that *grk* transcripts are transported to their final destination in nonmembrane-bound, nonmembrane transport particles directly associated with microtubules. At the dorso-anterior corner, *grk* transcripts are statically anchored in large cytoplasmic structures previously described as sponge bodies (Wilsch-Brauninger et al., 1997). We show that, as in the embryo, mRNA anchoring requires Dynein but not Egl and BicD (Delanoue and Davis, 2005), and that Dynein is required for the structural integrity of the anchoring complexes. We show that Squid is also necessary for *grk* RNA anchoring and for the efficient formation and maintenance of the sponge bodies. Our observations lead us to propose a model in which Sqd, Egl, BicD, and Dhc are all present in transport particles and sponge bodies but play distinct roles in the two steps of transport and subsequent anchoring. We further propose that Dynein is converted from an active motor acting on transport particles to a static component required for the structure of the sponge bodies and therefore for *grk* mRNA anchoring. In this model, Sqd is required in some way for the conversion of transport particles into sponge bodies and may therefore be involved in the conversion of Dynein from an active motor to a static anchor.

RESULTS

grk RNA Is Transported along MTs in Transport Particles Containing Dynein

The transport of *grk* RNA by Dynein could either be achieved by association with Dynein on MTs or indirectly by hitchhiking on another Dynein-dependent transport process, such as vesicular transport. To distinguish definitively between these possibilities, we used IEM methods on cryosections to codetect *grk* mRNA with MTs and Dynein motor components. We first studied the transport intermediates of injected biotinylated *grk* RNA in the center of early stage 9 oocytes. Twenty minutes after the injection, we fixed, recovered, and processed the egg chambers for IEM using methods we established for good membrane preservation of this tissue (Herpers and Rabouille, 2004). We found that injected *grk* RNA particles coassemble and concentrate in nonmembrane-bound electron-dense particles (Figures 1A–1C) that vary in size from 70 to 600 nm (Figures 1E and 1E′). In contrast, control injections of biotinylated *grk* RNA lacking the localization signal (*grkΔGLS*) do not assemble into transport particles and are diffusely localized in the cytoplasm (see Figure S1 in the Supplemental Data available with this article online). Although *grk* RNA transport particles are not consistently or specifically in close proximity to membrane-bound organelles, such as ER or vesicles, 67% of the observed particles are on, or within 100 nm from, the nearest MT. In comparison, only 33% of computer-generated randomly positioned particles of the same size are within the same distance from the nearest MT when placed on the same field of MTs. The difference in MT colocalization between *grk* RNA particles and randomly generated particles is statistically significant (Figures 1F and 1G).

We found that injected *grk* RNA colocalizes with the Dynein motor complex components Dhc and the motor cofactors Egl and BicD (Figures 1B, 1C, and 1I) in the transport particles. We estimate that there are likely to be many Dynein motors as well as RNA molecules in each electron-dense particle (quantified in Figures 1H and 1I). We conclude that injected *grk* RNA is transported directly on MTs by the Dynein motor in electron-dense RNP particles containing many *grk* RNA molecules and Dynein motor complexes, which we refer to as *grk* RNA "transport particles."

To investigate whether endogenous *grk* mRNA, like injected RNA, can be detected in transport particles, we developed methods of in situ hybridization on ultrathin cryosections followed by immunoelectron microscopy (ISH-IEM), allowing detection of the relatively low-abundance *grk* transcript (see Experimental Procedures). We identified endogenous transport particles as electron-dense small structures at the dorso-anterior corner that are labeled with usually one to three and sometimes more gold particles corresponding to *grk* mRNA (Figures 1D and 1H). These are smaller than the transport particles that assemble from injected *grk* RNA, although very similar in appearance and also closely associated with MTs (Figures 1F and 1G).

grk RNA Anchoring Is Static and Requires Intact MTs and Dynein, but Not Egl or BicD

To investigate whether the cytoskeleton plays a role in the retention of *grk* mRNA after transport to its final destination, we first covisualized the RNA with F-actin and MTs at the

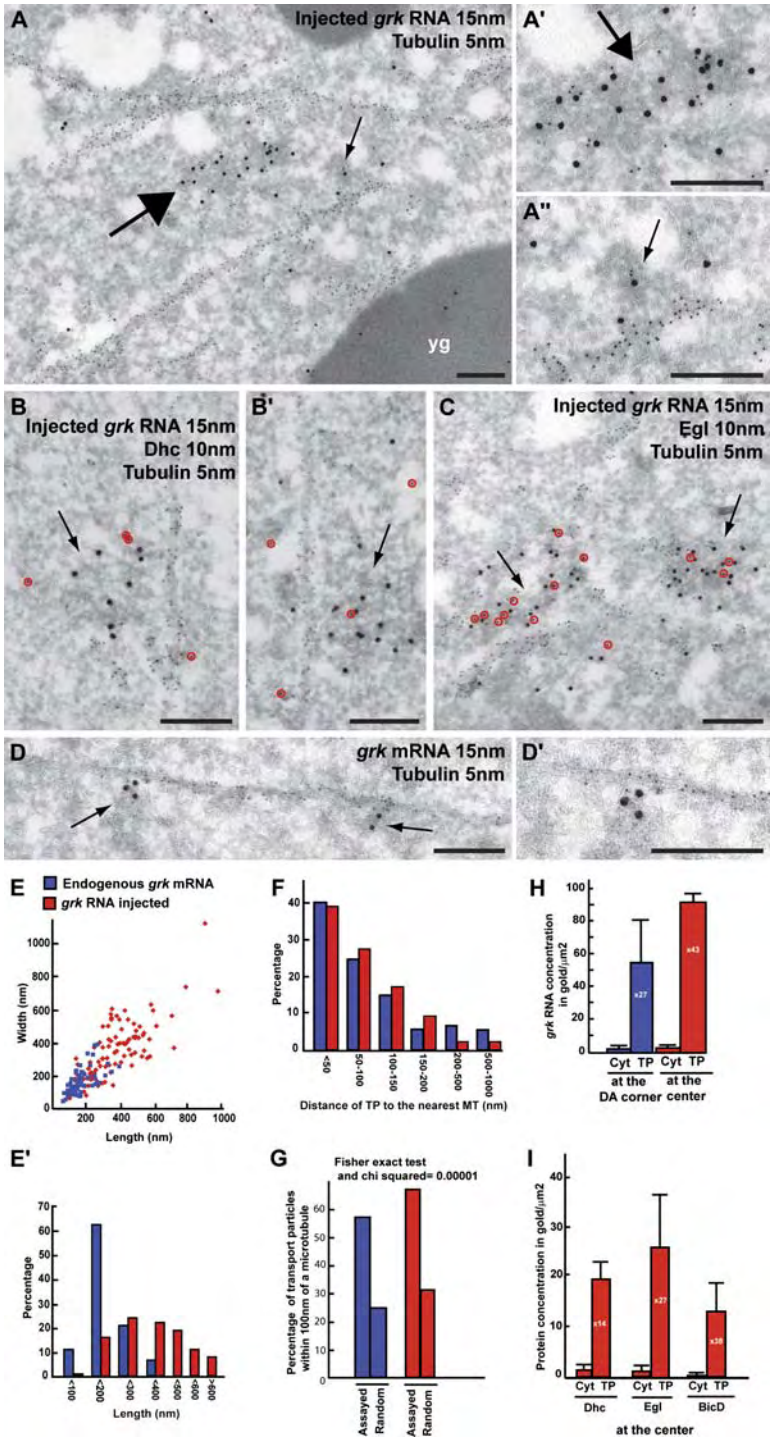

Figure 1. *grk* RNA Is Transported on MTs in Electron-Dense Nonmembrane-Bound Particles Containing Dynein

(A–A″) Wild-type oocyte injected with biotinylated *grk* RNA and fixed after 20 min. *grk* RNA (15 nm) is found in electron-dense transport particles ranging from 70 to 600 nm that are either on MTs (thin arrows) or near them (thick arrows). MTs are marked by α-tubulin (5 nm). yg, yolk granules.

(B and C) Transport particles labeled for *grk* RNA (15 nm), Dynein heavy chain (10 nm; red circles; [B and B′]), and Egl (10 nm, red circles; [C]) on MTs (5 nm).

(D and D′) Endogenous *grk* mRNA in stage 9 wild-type oocytes (15 nm) detected in transport particles associated with MTs (5 nm). In this and all subsequent figures, "*grk* mRNA" refers to the endogenous transcript and "*grk* RNA" to the injected RNA.

The scale bars represent 200 nm.

(E) Plot of the length versus width of transport particles.

(E′) Length distribution of the transport particle (nm).

(F) Distribution of the distance (nm) between a transport particle (TP) and the nearest MT.

(G) Quantification of the percentage of transport particles specifically associated with MTs (see the Supplemental Experimental Procedures).

(H) Density (in gold/μm^2) of endogenous (blue) and injected (red) *grk* RNA in transport particles (TP) compared to their surrounding cytoplasm (Cyt) (see the Supplemental Experimental Procedures). DA, dorso-anterior.

(I) Density (in gold/μm^2) of the Dynein complex components in transport particles formed upon injection of *grk* RNA (TP; red) compared to the surrounding cytoplasm (Cyt).

Error bars represent standard deviations.

site of localization by immunofluorescence. We found that *grk* RNA colocalizes with MTs (Figures 2A, 2C, and 2D) but not with F-actin (Figure S2A). We then inhibited F-actin polymerization with Latrunculin A and found that it had no effect on the localization of either endogenous or injected *grk* RNA (Figures S2B, S2C, S2E, and S2F). In contrast, depolymerizing MTs with Colcemid disrupts the localization of injected *grk* RNA (Figure 2D) and partly disrupts the localization of endogenous *grk* mRNA (Figure 2B). We conclude that MTs, but not F-actin, are required for the anchoring of *grk* mRNA at the dorso-anterior.

To test whether Dynein itself is required for this localization, we injected an inhibitory Dhc antibody into stage 9 oocytes 60 min after injection of *grk* RNA. We found that *grk* RNA anchoring is lost 3–5 min after injection of anti-Dhc antibody (Figure 2E). Similar results were obtained

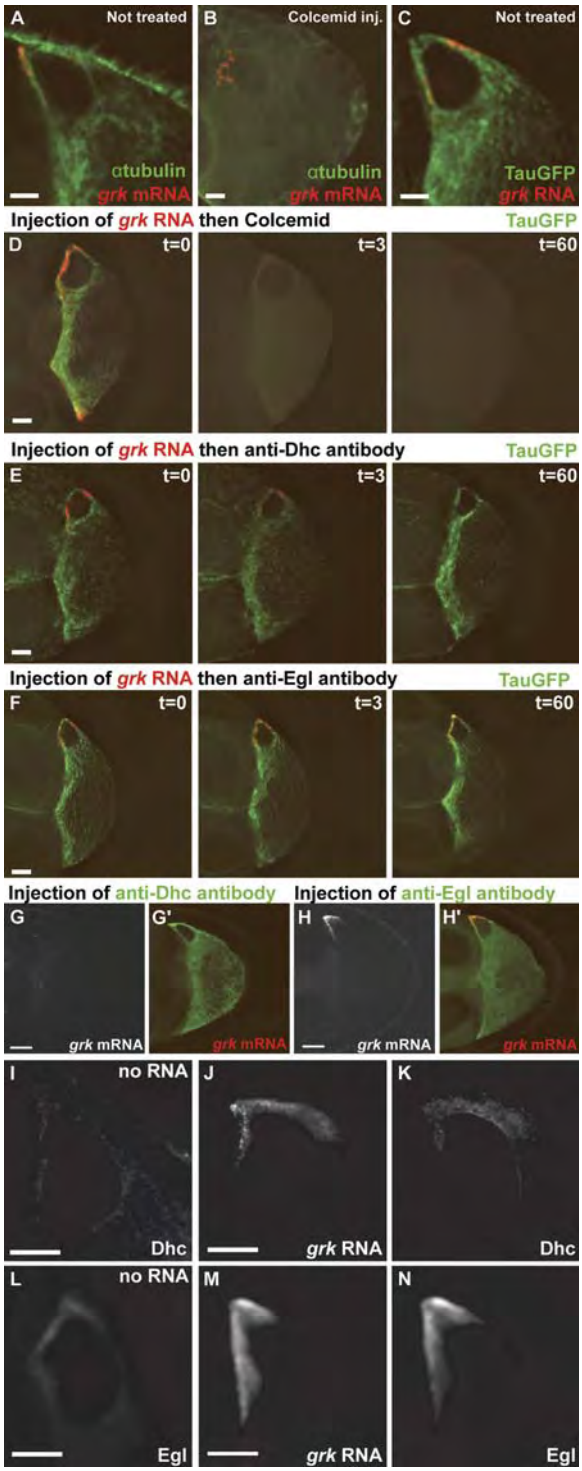

Figure 2. *grk* RNA Anchoring Depends on Intact MT and Dynein but Not Egl

(A) Endogenous *grk* mRNA in a stage 9 oocyte detected by FISH (red) colocalized with MTs (green).

(B) A stage 9 egg chamber treated for 45–60 min with Colcemid causing a severe, but incomplete, delocalization of endogenous *grk* mRNA detected by FISH (red). MTs (green) are depolymerized.

(C and D) Alexa Fluor 546-labeled *grk* RNA (red) 45 min after injection into a stage 9 oocyte expressing TauGFP (marking the MT network; green) colocalizes with MTs (C). It loses its localization upon Colcemid injection at t = 0. The anchoring of injected *grk* RNA at the cap is altered after a few minutes (t = 3 min), and at t = 60 min is no longer detected at the dorso-anterior corner (D).

(E) Alexa Fluor 546-labeled *grk* RNA (red) localized at the dorso-anterior corner in a stage 9 oocyte loses its localization upon anti-Dhc antibody injection at t = 0. At t = 60 min, no injected RNA is detected at the dorso-anterior corner.

(F) Alexa Fluor 546-labeled *grk* RNA (red) localized at the dorso-anterior corner in a stage 9 oocyte is unaffected upon anti-Egl antibody injection at t = 0. *grk* RNA anchoring at the cap remains at t = 60 min.

(G) Anchoring of endogenous *grk* mRNA (red) is disrupted by injection of anti-Dhc antibody, detected with anti-mouse Alexa Fluor 488 (green) (G′), 45–60 min after injection.

(H) Anchoring of endogenous *grk* mRNA (red) is not disrupted by injection of anti-Egl antibody, detected with anti-rabbit Alexa Fluor 488 (green) (H′), 45–60 min after injection.

(I–N) Dhc (I) and Egl (L) are slightly enriched at the dorso-anterior corner in an uninjected oocyte. Injection of Alexa Fluor 546-labeled *grk* RNA in a stage 9 oocyte leads to a large increase in detectable Dhc (K) and Egl (N), colocalized with *grk* RNA at the dorso-anterior corner (J and M).

The scale bars represent 10 μm.

with endogenous *grk* RNA (Figures 2G and 2G′). Control experiments showed that MTs are intact after the injection (Figure 2E), and injection of rabbit serum or IgG did not affect *grk* RNA anchoring (Figures S3D and S3E). In contrast, injection of anti-Egl antibodies did not lead to a loss of anchoring of either injected or endogenous *grk* RNA (Figures 2F and 2H), despite Egl being required for active Dynein motility and transport of *grk* RNA (Figures S3A and S3B). We conclude that the motor activity of Dynein is required for transport but not anchoring of *grk* mRNA.

The Dynein-dependent localization of *grk* mRNA at the dorso-anterior corner could represent a static anchoring by the Dynein motor by a similar mechanism as *pair-rule* transcripts in the blastoderm embryo (Delanoue and Davis, 2005). Alternatively, *grk* RNA could be continuously transported to the dorso-anterior by the Dynein motor, a model that predicts a continuous flow of RNA particles moving in and out the dorso-anterior area.

To distinguish between *grk* RNA static anchoring and continuous transport, we carried out fluorescence recovery after photobleaching (FRAP) experiments on fully localized injected *grk* RNA in wild-type egg chambers (i.e., 60 min after injection). We found that photobleached *grk* RNA that has completed only the first stage of transport and is temporarily localized at the anterior of the oocyte partially recovers (Figures 3A, 3C, and 3C′). The partial recovery followed by a slight drop in fluorescence is likely to be due to the fact that new unbleached RNA arriving in the anterior continues moving to the dorso-anterior. In contrast, photobleached localized *grk* RNA fails to recover at the dorso-anterior corner (Figures 3B, 3C, and 3C′). We conclude that *grk* RNA is not anchored at the anterior after completion of the first step of its localization, but is statically anchored once it arrives at the dorso-anterior corner.

An anchoring role for Dynein at the dorso-anterior corner predicts that the motor complex is recruited together with *grk* RNA to the site of anchoring. We tested this

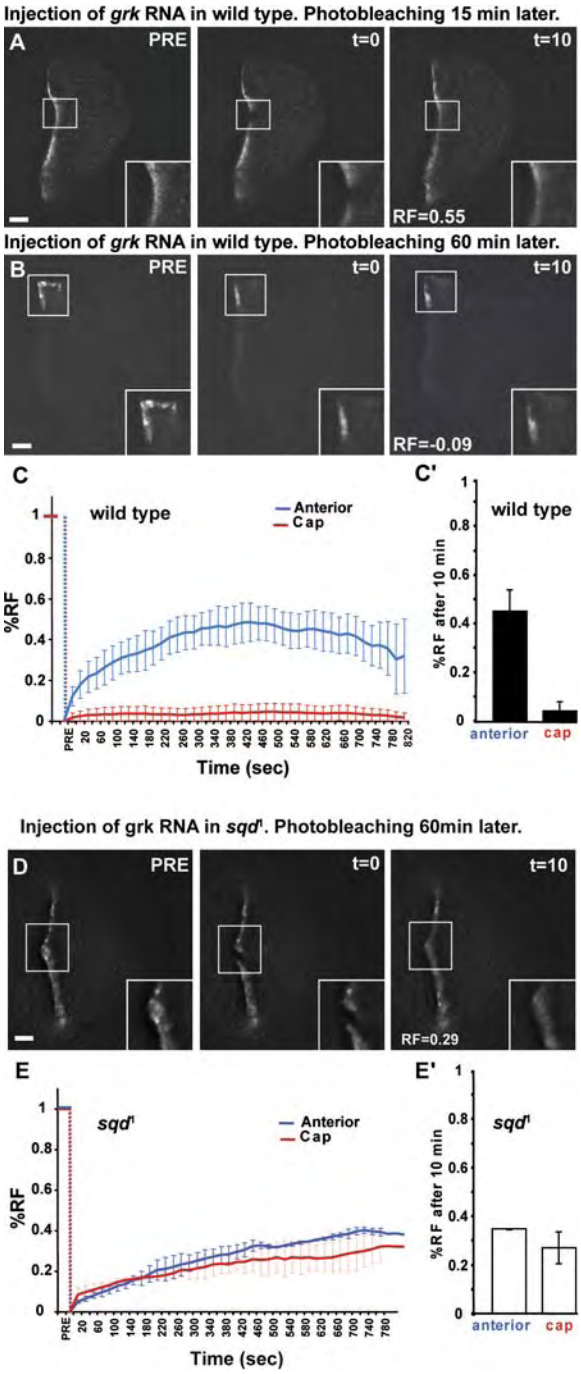

Figure 3. Injected *grk* RNA Is Statically Anchored at the Dorso-Anterior Corner in Wild-Type Oocyte but Not in *sqd*[1]

(A) A representative FRAP experiment in a living oocyte with Alexa Fluor 488-labeled *grk* RNA in midtransport (15 min after injection). At t = 0, a region of the anteriorly localized *grk* RNA is bleached (within the white square). A partial recovery of the signal is observed (recovery fraction, RF = 0.55) 10 min after bleaching (t = 10 min).

(B) A representative FRAP experiment of living oocyte showing Alexa Fluor 488-labeled *grk* RNA fully localized at the dorso-anterior corner (60 min after injection). At t = 0, a region of *grk* RNA is bleached (within the white square) and does not recover (RF = −0.09) 10 min later (t = 10 min).

(C) FRAP experiments in a wild-type living oocyte injected with Alexa Fluor 488-labeled *grk* RNA. The blue curve shows the recovery fraction (RF) at the anterior pole and the red curve shows the RF at the dorso-anterior corner. Averages and SD are made for each time point in at least three independent injected oocytes.

(C′) Percentage recovery of fluorescence 10 min after photobleaching in a wild-type oocyte. Bars represent the SD from at least three independent FRAP experiments.

(D) A representative FRAP experiment in a living *sqd*[1] mutant oocyte showing anterior localization of Alexa Fluor 488-labeled *grk* RNA (60 min after injection) immediately before photobleaching (PRE). Insets show higher magnifications of the bleached areas. The signal partly recovered 10 min after the bleaching (RF = 0.29).

(E) FRAP experiments in an *sqd*[1] living oocyte injected with Alexa Fluor 488-labeled *grk* RNA. The blue curve shows the recovery fraction (RF) at the anterior pole and the red curve shows the RF at the dorso-anterior corner. Averages and SD are made for each time point in at least three independent injected oocytes.

(E′) Percentage recovery of fluorescence 10 min after photobleaching in an *sqd*[1] oocyte. Bars represent the SD from at least three independent FRAP experiments.

Insets show higher magnifications of the bleached areas. The scale bars represent 10 μm.

prediction by visualizing components of the Dynein motor complex after injection of *grk* RNA and found that Dhc (Figures 2I–2K) and Egl (Figures 2L–2N) are both significantly enriched at the site of localization of the injected *grk* RNA, compared with uninjected controls (Figures 2I and 2L). Control injections of nonlocalizing *hunchback* (*hb*) RNA did not lead to any enrichment of Dynein motor components (Figures S3F–S3H). We conclude that Dynein is required for the static anchoring of *grk* mRNA at the dorso-anterior corner.

grk RNA Is Anchored at the Dorso-Anterior Corner in Sponge Bodies

pair-rule and *wingless* transcripts were previously shown to be statically anchored by Dynein in syncytial blastoderm embryos (Delanoue and Davis, 2005). It was hypothesized that apical mRNA anchoring occurs by the Dynein motor remaining attached to the cargo and MTs at the final destination. To test whether this hypothesis could apply to the static anchoring of *grk* mRNA in the oocyte, we used the ISH-IEM technique we developed (see above) to covisualize endogenous *grk* mRNA and the Dynein motor in stage 9 egg chambers. We found that at the dorso-anterior corner, endogenous *grk* mRNA is anchored together with the Dynein motor within large cytoplasmic structures whose ultrastructure is different in appearance from transport particles (Figures 4B–4D and 4G; see Figure S4 for an unadulterated version). Sectioning plastic-embedded wild-type oocytes revealed structures that are similar in appearance to previously described sponge bodies (Figure 4A; Wilsch-Brauninger et al., 1997) that were known to contain the protein Exuperantia (Exu) and to be found in nurse-cell cytoplasm. Although sponge bodies are present throughout the oocyte cytoplasm, the majority of *grk* mRNA is concentrated only in sponge bodies found at the dorso-anterior corner (Figures 4B–4D′). The minority of *grk* mRNA that is not in sponge bodies is found in the small transport particles we described (above) near or at the dorso-anterior corner and in the surrounding cytoplasm

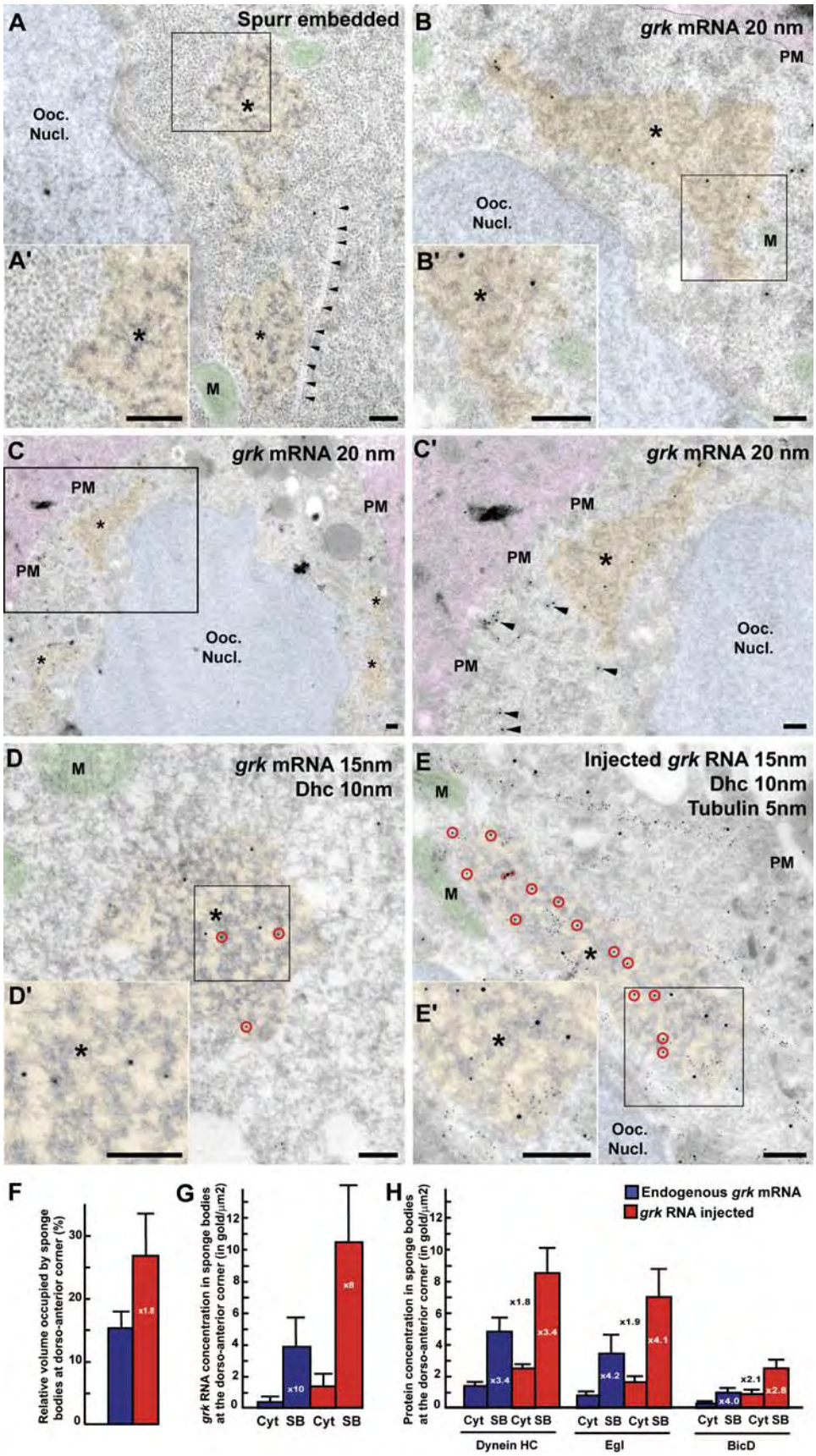
A
Spurr embedded
Ooc.
Nucl.
A'
M
B
grk mRNA 20 nm
PM
Ooc.
Nucl.
M
B'
C
grk mRNA 20 nm
PM
PM
PM
Ooc.
Nucl.
C'
grk mRNA 20 nm
PM
PM
PM
Ooc.
Nucl.
D
M
grk mRNA 15nm
Dhc 10nm
D'
E
Injected grk RNA 15nm
Dhc 10nm
Tubulin 5nm
M
M
PM
E'
Ooc.
Nucl.
F
Relative volume occupied by sponge bodies at dorso-anterior corner (%)
x1.8
G
grk RNA concentration in sponge bodies at the dorso-anterior corner (in gold/µm2)
x10
x8
Cyt SB Cyt SB
H
Endogenous grk mRNA
grk RNA injected
Protein concentration in sponge bodies at the dorso-anterior corner (in gold/µm2)
x1.8
x3.4
x1.9
x4.2
x4.1
x2.1
x4.0
x2.8
Cyt SB Cyt SB
Dynein HC
Cyt SB Cyt SB
Egl
Cyt SB Cyt SB
BicD

(Figures 1 and 4C′). Sponge bodies are not membrane bound and can be as large as 2.5 μm. They consist of ''sponge-like'' electron-dense material, forming interconnected 60–90 nm wide strands that are interdigitated with cytoplasm and ER tubules. They are often flanked by MTs (Figure 4A) and, like transport particles, are enriched in Dhc, BicD, and Egl (Figures 4D and 4H; Figures S4F–S4H). Injected *grk* RNA is also enriched in sponge bodies at the dorso-anterior corner (Figures 4E and 4G) together with Dhc (Figures 4E and 4H), BicD, Egl (Figures S4G and S4H), and Hrp48 (data not shown). Remarkably, sponge body size and number are increased at the dorso-anterior corner by injecting *grk* RNA (Figure 4F). We conclude that Dynein-rich *grk* RNA transport particles are delivered to the dorso-anterior corner where the RNA is anchored in sponge bodies together with the Dynein motor complex and its cofactors.

Dhc Is Required for the Structural Integrity of Sponge Bodies

To investigate the function of Dynein in the anchoring of *grk* RNA in the sponge bodies, we studied the effect of inactivating Dynein function after anchoring of the RNA. We injected an inhibitory anti-Dhc antibody into stage 9 oocytes 60 min after injection of biotinylated *grk* RNA, as described in Figure 2E for the light microscopy assay, except that we then processed the samples for ultrastructural analysis. We found that disrupting Dhc function leads to a rapid redistribution of *grk* RNA into the cytoplasm (Figures 5A and 5B, arrows), in agreement with the results we obtained with fluorescence microscopy (Figure 2E). Surprisingly, we also found that the sponge bodies disappeared completely, and SqdGFP, which we used as a sponge body marker (see below), was also released into the cytoplasm (Figure 5B). In contrast, the inactivation of Egl, a cofactor for Dynein-dependent RNA motility, had no effect on sponge body integrity, as assessed by morphology and by the enrichment of SqdGFP in these structures (Figure 5C).

As Dynein has previously been suggested to play a role in MT organization (Vorobjev et al., 2001; Malikov et al., 2004), we tested whether the inactivation of Dynein causes an impairment of sponge body structure by affecting the MT cytoskeleton at the dorso-anterior corner, where it is most abundant. We found that MTs that normally flank the sponge bodies were unaffected by the injection of anti-Dhc antibodies (Figure 2E; Figures 5A and 5B, row of small arrowheads). We also found that depolymerization of MTs by Colcemid treatment did not affect sponge body integrity or the distribution of SqdGFP (Figure 5D).

To test this further, we used a hypomorphic combination of *dhc* alleles ($dhc^{6\text{-}6}/dhc^{6\text{-}12}$) that allows the study of developing oocytes. We found that sponge bodies are almost completely absent in *dhc* mutants (Figure 5F), compared with wild-type oocytes, where the sponge bodies are clearly visible (Figure 5E). We detected some small electron-dense structures, which we interpret either as remnants of sponge bodies or newly assembled transport particles (Figure 5F, arrowheads). In contrast to the *dhc* mutant, we found that sponge bodies are unaffected in *egl* and *BicD* mutant oocytes (Figures 5H–5J), despite most *grk* RNA transport being disrupted (Figure 5G). Some small amount of *grk* RNA does reach the dorso-anterior sponge bodies and is anchored in *egl* and *BicD*, and this increases when the RNA is injected near the dorso-anterior corner (Figures 5H–5J).

Considering all our results together, we conclude that Dynein is required for the structural integrity of the sponge

Figure 4. *grk* RNA Is Localized with Dynein in Dorso-Anterior Sponge Bodies

See Figure S4 for an unadulterated high-resolution version.

(A and A′) Sections of Spurr-embedded wild-type stage 9 oocytes showing large electron-dense sponge bodies (*) often flanked by MTs (row of small arrowheads) at the dorso-anterior corner. The square indicates the area shown at high magnification showing the difference in morphology between sponge bodies and the surrounding cytoplasm (A′).

(B) Endogenous *grk* mRNA is detected specifically at the dorso-anterior corner (20 nm) in sponge bodies (*). The squared area is shown at high magnification (B′) illustrating the similarity to the plastic section (A′) and showing the gold-labeled RNA. The thin line marks the oocyte plasma membrane (PM).

(C) Low-magnification view of the dorso-anterior corner of a stage 9 oocyte showing the endogenous *grk* mRNA both in sponge bodies (*) and in transport particles (arrowheads). The squared area is shown at high magnification (C′).

(D) Sponge bodies (*), where the endogenous *grk* mRNA (15 nm) is found, are also positive for Dhc (10 nm; red circles). The square indicates the area shown at high magnification (D′).

(E) Injected biotinylated *grk* RNA (15 nm) and Dhc (10 nm; red circles) also colocalize in sponge bodies (*) in a wild-type stage 9 oocyte, 60 min after injection. MTs are marked by α-tubulin (5 nm). The square indicates the area shown at high magnification (E′). For clarity, the oocyte nucleus (Ooc. Nucl.) is shaded in blue, the mitochondria (M) are in green, and the sponge bodies are in orange and marked by asterisks. Cells adjacent to the oocyte are colored in pink.

The scale bars represent 200 nm.

(F) Relative volume occupied by the sponge bodies at the dorso-anterior corner before and after *grk* RNA injection (see the Supplemental Experimental Procedures).

(G) Density (in gold/μm^2) of endogenous (blue) and injected *grk* RNA (red) in sponge bodies (SB) compared to their surrounding cytoplasm (Cyt) (see the Supplemental Experimental Procedures).

(H) Density (in gold/μm^2) of Dynein complex components in sponge bodies (SB) before (blue) and after (red) injection of *grk* RNA, compared with the surrounding cytoplasm (Cyt). Note that all the components are enriched about 3-fold in the sponge bodies (white numbers within bars), and that upon *grk* RNA injection, their concentration increases further (about 2-fold; black numbers next to bars). Taking into account that the volume of the sponge bodies is also increased by 1.8-fold, the concentration of these components increases about 4-fold at the dorso-anterior corner upon *grk* RNA injection.

Error bars represent standard deviations.

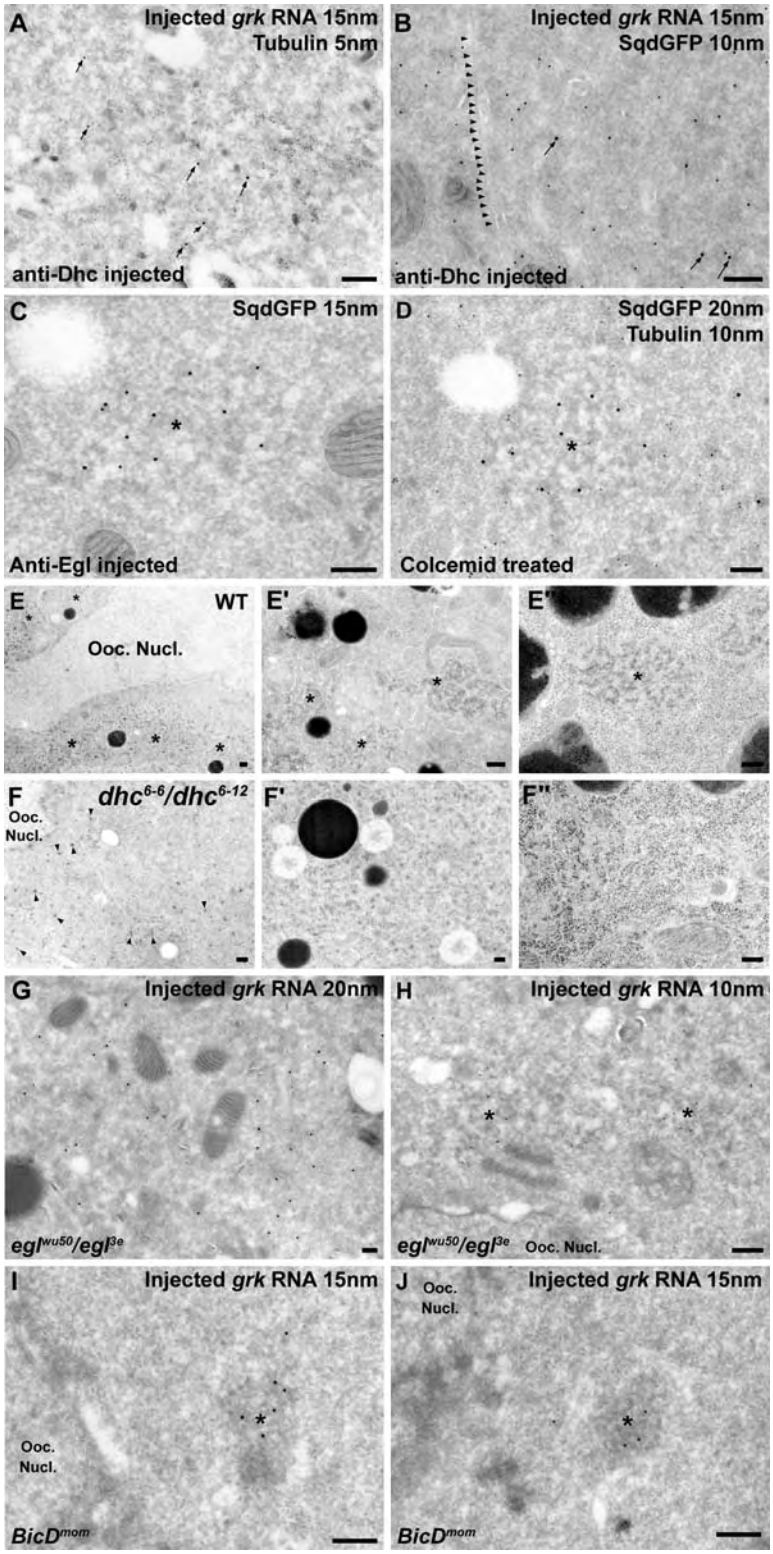

Figure 5. Dhc, but Not BicD and Egl, Is Required for the Structural Integrity of the Sponge Bodies

(A and B) Injected *grk* RNA (15 nm; arrows) and SqdGFP (10 nm; [B]) were found redistributed in the cytoplasm when SqdGFP-expressing ovaries with fully localized *grk* RNA were injected with anti-Dhc antibodies (as in Figure 2E) for 3, 5, or 10 min before fixation. Note that the sponge bodies containing *grk* RNA are no longer visible (compare to Figure 4E). Microtubules are marked with α-tubulin (5 nm; [A]) or by a row of small arrowheads (B).

(C) The inactivation of Egl by injection of anti-Egl antibody in SqdGFP oocytes does not affect sponge body structure, where SqdGFP (15 nm) remains concentrated.

(D) Colcemid treatment of SqdGFP oocytes leads to depolymerization of the microtubules (dispersed tubulin is detected with the anti-α-tubulin antibody; 10 nm) but does not affect the ultrastructure of the sponge bodies marked by SqdGFP (20 nm).

(E–E″) Three magnified images of Spurr-embedded wild-type oocytes showing that sponge bodies (*) are clearly visible around the oocyte nucleus (E) with their very characteristic structure (E′ and E″).

(F–F″) Three magnified images of Spurr-embedded *dynein* mutant oocytes showing that sponge bodies are no longer visible, and that the typical structure of electron-dense regions interdigitated with electron-light material is no longer observed. In (F), some small electron-dense structures (arrowheads) are present that could correspond to remnants of sponge bodies (*).

(G) Biotinylated *grk* RNA injected in the center of a stage 9 *egl* mutant oocyte fails to be transported to the dorso-anterior corner, does not form transport particles, and is not associated with the sponge bodies that are present.

(H) When *grk* RNA is injected at the dorso-anterior corner, it associates with the sponge bodies (*) at this location, showing that Egl is required for the transport but not the anchoring of *grk* RNA in sponge bodies.

(I and J) Biotinylated *grk* RNA injected at the dorso-anterior corner of a stage 9 $BicD^{mon}$ mutant oocyte, anchored in sponge bodies (*) at this location.

The scale bars represent 200 nm.

bodies in which it is concentrated. This function of Dynein does not require its RNA cargo transport activity, as it can occur in the absence of BicD and Egl, cofactors required for Dynein-based RNA motility in the embryo and oocyte.

Squid Is Also Enriched at the Dorso-Anterior Corner upon *grk* RNA Transport

The movement of *grk* mRNA to its site of anchoring has been previously shown to require two steps, the second

being Sqd dependent. To determine whether Sqd is present with *grk* RNA during and after completion of transport, we covisualized *grk* RNA and Sqd by IEM in SqdGFP-expressing egg chambers (Norvell et al., 2005). We found that SqdGFP colocalizes with injected *grk* RNA in the transport particles (Figures 6A and 6B). At the dorso-anterior corner SqdGFP is enriched in sponge bodies (Figures 6B and 6C), together with Dhc, BicD, and Egl (Figures 6E–6G). This raises the possibility that the enrichment of SqdGFP to the sponge bodies results from its association with the transported *grk* RNA. We tested this idea by injecting *grk* RNA and investigating whether this causes a further enrichment of SqdGFP at the same site. We found that injection of *grk* RNA into transgenic flies expressing SqdGFP leads to a strong enrichment of SqdGFP at the dorso-anterior corner (Figure 6H). We conclude that Sqd is at least partly recruited to the dorso-anterior corner through its association with *grk* mRNA.

In the Absence of Sqd, *grk* RNA Is Continuously Transported Rather Than Statically Anchored

To study in more detail the role of Sqd in *grk* mRNA localization, we studied *grk* RNA localization in *sqd* null mutant egg chambers. By injecting Colcemid or Latrunculin as in wild-type oocytes (Figure 2; Figure S2), we found that intact MTs, but not F-actin, are required for the anterior localization of injected and endogenous *grk* RNA in this mutant (Figures S5A–S5D). We then tested whether Dhc is required for the anterior localization of *grk* RNA in *sqd* mutant oocytes. The results show that the anterior localization of injected and endogenous *grk* RNA is disrupted by injection of anti-Dhc (Figures S5E and S5F) and anti-Egl (Figures S5G and S5H) but not by injection of control rabbit antiserum (Figures S5I and S5J). We conclude that in the absence of Sqd, *grk* mRNA localization at the anterior requires Dynein.

In a *sqd* mutant, Dynein could either be required for the static anchoring of the RNA at the anterior on MTs or to transport the RNA continuously at the anterior on MTs. To distinguish between these two possibilities, we carried out FRAP experiments. The results show that injected fluorescent *grk* RNA that accumulates at the anterior pole of *sqd* mutants recovers after photobleaching. The recovery was the same for the small pool of photobleached *grk* RNA localized at the dorso-anterior cap, albeit at a slightly slower rate. We conclude that in the absence of Sqd, *grk* RNA is in continuous flux at the anterior (Figures 3D, 3E, and 3E′).

Transport Particles Are Not Converted into Sponge Bodies in *sqd* Mutant Oocytes

Our results suggest that the localization at the anterior had different properties than the anchoring in sponge bodies at the dorso-anterior corner of wild-type oocytes. We used IEM to determine in which structures injected *grk* RNA is found in *sqd* mutant oocytes. We found that, despite the fact that uninjected *sqd* mutants have similar sponge bodies in shape and number to those in wild-type oocytes (Figures 7E and 7G), the vast majority of injected *grk* RNA was found in transport particles in *sqd* mutants (Figure 7A), even at the dorso-anterior corner. These transport particles also contain Dhc, BicD, and Egl (Figures 7B–7D), so in all aspects identical to wild-type transport particles. A very small proportion of *grk* RNA was also found in dorso-anterior corner sponge bodies (Figure 7F).

Taken together, our data demonstrate conclusively that *grk* transcripts are maintained at the anterior of *sqd* null mutant oocytes by continuous active transport using Dynein, rather than being statically anchored there. Therefore, Sqd is required for the movement of transport particles from the anterior to the dorso-anterior corner, raising the interesting possibility that Sqd could also be required for anchoring.

Sqd Is Required for Anchoring *grk* RNA at the Dorso-Anterior Corner

To test whether Sqd is required for the anchoring of *grk* RNA, we inactivated Sqd after *grk* RNA was fully anchored at the dorso-anterior corner. We first tried to inhibit Sqd function with two distinct anti-Sqd monoclonal antibodies, but these showed effect neither on the transport nor the anchoring of *grk* RNA. We interpret these results as indicating that these monoclonal antibodies, like many other cases, are not functionally inhibitory, as the antibody does not phenocopy the mutant phenotype. As an alternative approach, we used an Sqd protein trap line containing an intronic GFP insertion that produces an SqdGFP fusion protein acting as a fully functional replacement of the *sqd* gene (Norvell et al., 2005). We used western blots to demonstrate that the transgenic line only expressed SqdGFP fusion protein, and did not express any GFP or Sqd splice variants (Figure 8A).

We then injected an anti-GFP antibody to inactivate SqdGFP function in order to recapitulate an *sqd* mutant phenotype similar to the null allele. We found that injection of the anti-GFP antibody followed by injection of *grk* RNA leads to an accumulation of RNA at the anterior because of the disruption of the second step of *grk* RNA transport (Figure 8B). We conclude that the anti-GFP antibody disrupts SqdGFP function, thus leading to a phenotype indistinguishable from the *sqd* null allele.

To test the role of Sqd in anchoring, we allowed *grk* RNA to become fully localized for 60 min after its injection into the oocyte, at which time we injected the inactivating anti-GFP antibody. We found that within 20 min, injected *grk* RNA became detached from its site of anchoring in the dorso-anterior corner (Figure 8C) and was found completely delocalized after 50 min. To test whether Sqd is also required for the anchoring of endogenous *grk* mRNA, we injected anti-GFP antibody into SqdGFP egg chambers, and then processed them for in situ hybridization 15 min after the injection. The results show that the anchoring of endogenous *grk* mRNA is disrupted rapidly after inhibiting SqdGFP function (Figures 8D and 8D′). Control injections of anti-GFP antibody into wild-type oocytes, in which *grk* RNA was prelocalized, showed no effect on *grk* RNA anchoring (Figure 8E). Endogenous

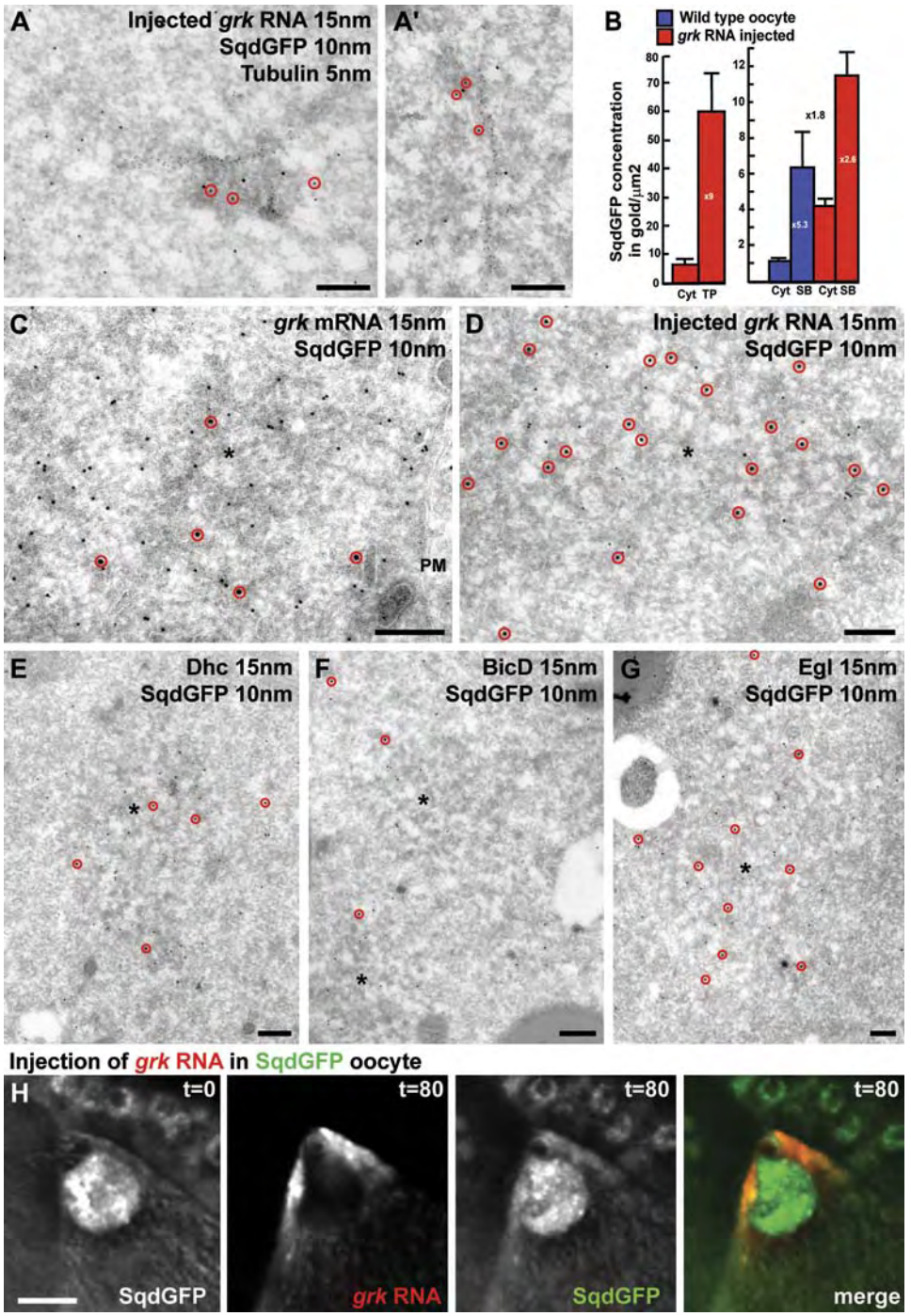

Figure 6. SqdGFP Colocalizes with *grk* RNA and the Components of the Dynein Motor Complex in Transport Particles and Sponge Bodies

(A and A′) Biotinylated *grk* RNA (15 nm) injected into a SqdGFP oocyte is found in transport particles on MTs (5 nm) together with SqdGFP (10 nm; red circles).

(B) Quantification of the concentration of SqdGFP in transport particles and sponge bodies when compared to the surrounding cytoplasm. Error bars represent standard deviations.

(C and D) SqdGFP (10 nm) colocalizes with endogenous *grk* mRNA (15 nm; red circles; [C]) and injected *grk* RNA (15 nm; red circles; [D]) in sponge bodies (*) at the dorso-anterior corner.

(E–G) SqdGFP (10 nm) colocalizes with Dhc (15 nm; red circles; [E]), BicD (15 nm; red circles; [F]), and Egl (15 nm; red circles; [G]) in sponge bodies (*).

(H) SqdGFP becomes enriched at the dorso-anterior corner upon injection of Alexa Fluor 546-labeled *grk* RNA in a stage 9 oocyte. At t = 0, SqdGFP is mostly in the nucleus. At t = 80 min, SqdGFP is enriched at the dorso-anterior corner with *grk* RNA (merge).

The scale bars represent 200 nm, except in (H), where the scale bar represents 10 μm.

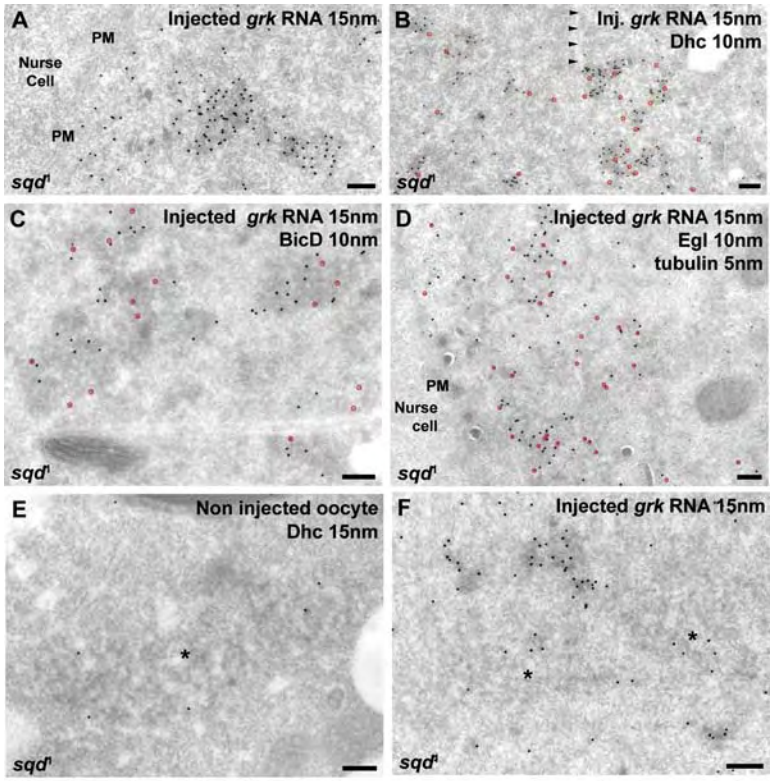

G	% of injected *grk* RNA in SB at the DA corner	volume of cytoplasm occupied by SB at the DA corner		% of injected *grk* RNA in TP along the anterior	density of injected *grk* RNA in TP (gold/μm2)
		before injection	after injection		
Wild type	75±5	15±3	27±6	0	
sqd[1]	1.5±0.2	11±2	0.5±0.5	76.6±6.4	120±35

Figure 7. Injected *grk* RNA Is Found in Transport Particles in *sqd*[1]

(A and B) In the *sqd*[1] mutant, biotinylated injected *grk* RNA (15 nm) is found at the anterior side (within 5 μm of the anterior plasma membrane) in transport particles along MTs (row of small arrowheads) that contain Dhc (10 nm; [B]). Red circles in (B) indicate Dhc that is present in transport particles.

(C and D) The transport particles described in (A) also contain BicD ([C]; 10 nm; red circles) and Egl ([D]; 10 nm; red circles) along MTs (5 nm).

(E) In a uninjected *sqd*[1] mutant oocyte, sponge bodies are also present and contain Dhc (15 nm).

(F) *sqd*[1] mutant oocyte injected with biotinylated *grk* RNA. The RNA is mostly found in transport particles but a very small amount is also found in one of the rare sponge bodies (*) that are still present after injection (see [G]). The scale bars represent 200 nm.

(G) Quantification of the conversion of sponge bodies into transport particles upon *grk* RNA injection in *sqd*[1]. Note that the sponge bodies that are present before injection (see Figure 7E) are almost absent 20 min after injection of *grk* RNA, which is found in transport particles along the anterior at a density similar to the transport particles found in the middle of wild-type injected oocytes (see Figure 1A). ± represents standard deviations.

grk mRNA in wild-type oocytes was also completely unaffected by the injection of anti-GFP antibody (Figure 8F). Finally, control injections of anti-GFP antibody into ubiquitously expressing nlsGFP or GFP transgenic lines did not have any effect on the localization of injected *grk* RNA (data not shown). We conclude that Sqd is required for anchoring both injected and endogenous *grk* mRNA at the dorso-anterior corner.

Inhibition of Dynein after anchoring of mRNA leads to the disappearance of the sponge bodies and transport particles, and to *grk* RNA being distributed throughout the cytoplasm (Figure 5). To determine whether the role of Sqd in anchoring is through being required for the structural integrity of sponge bodies, we analyzed where *grk* RNA is found after inactivation of SqdGFP. Ultrastructural analysis revealed that, when SqdGFP function is inhibited, injected *grk* RNA is found in transport particles rather than in sponge bodies (Figure 8G). These transport particles are indistinguishable from anterior *grk* RNA transport particles in *sqd* null mutants (Figure 7), suggesting that disrupting Sqd function converts sponge bodies into transport particles. Endogenous *grk* mRNA was also found in particles resembling endogenous transport particles near MTs (Figure 8H) that also contain Dynein (Figure 8I). We conclude that whereas Sqd is not required for transport particle integrity, it is essential for anchoring *grk* RNA at the dorso-anterior corner by maintaining the transcript in sponge bodies rather than in transport particles. Therefore, the role of Sqd in anchoring is distinct from that of Dhc. We propose that Sqd is required for the conversion of transport particles into sponge bodies, rather than the ability of transport particles to move. In contrast, Dhc is required for both the motility of the transport particles and for *grk* mRNA anchoring through a role in the integrity of the sponge bodies.

DISCUSSION

We have analyzed the molecular mechanism of *grk* mRNA transport and anchoring in the *Drosophila* oocyte using a number of novel methods, combining live cell imaging of oocytes with immunoelectron microscopy to covisualize *grk* RNA and transacting factors. We show that *grk* mRNA is transported in particles containing many individual RNA molecules assembled with numerous molecules of Dynein motor components and Squid. Approximately

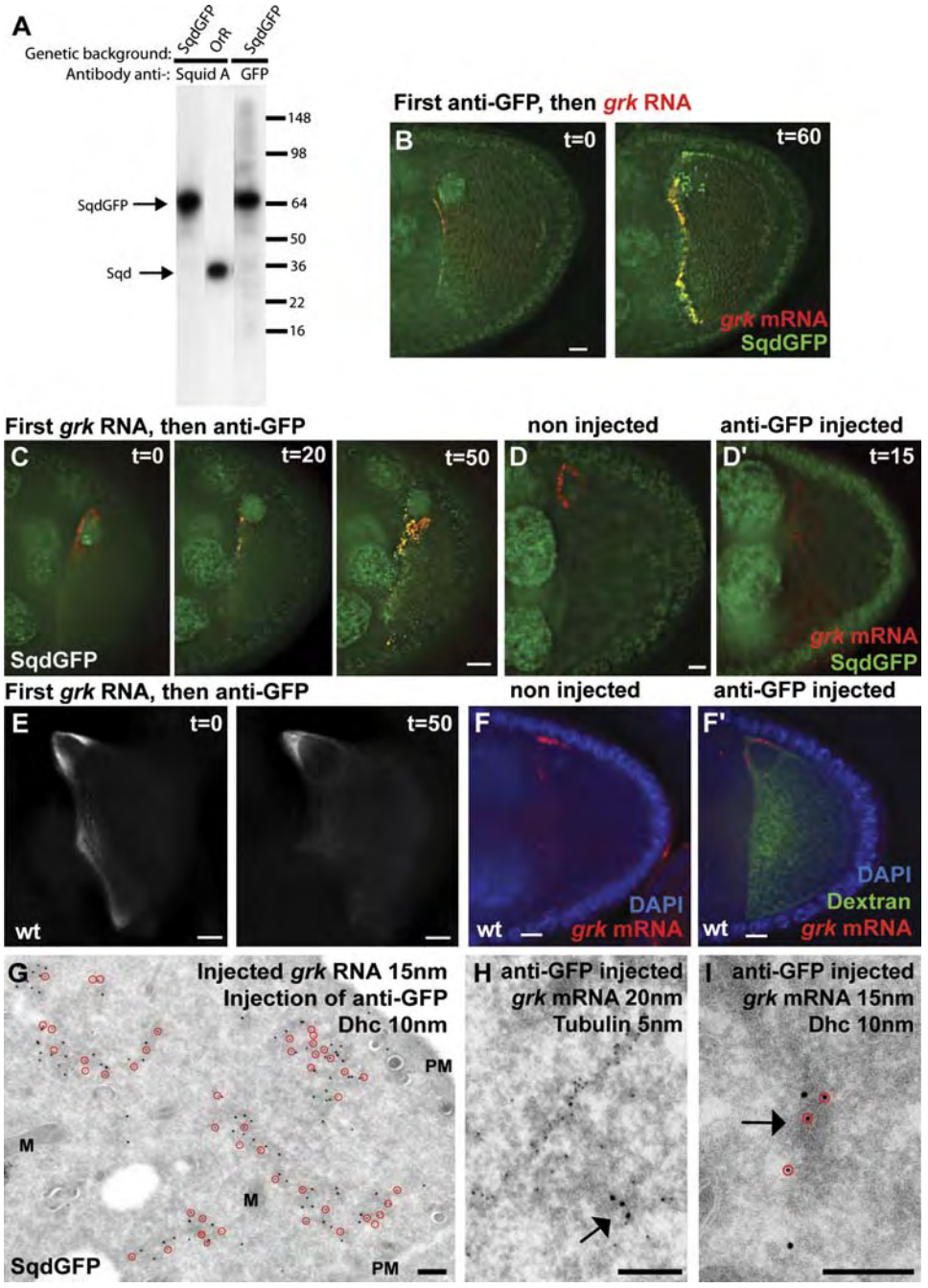

Figure 8. Sqd Is Involved in *grk* RNA Anchoring at the Dorso-Anterior Corner

(A) Western blot visualizing SqdA and SqdGFP in wild-type and SqdGFP oocytes, showing that neither GFP nor Sqd is expressed as a splice variant in SqdGFP.

(B) SqdGFP oocyte injected first with anti-GFP antibody followed by Alexa Fluor 546-labeled *grk* RNA at t = 0. *grk* RNA fails to reach the dorso-anterior corner and localizes at the anterior after 60 min (similar to *sqd*[1] mutant).

(C) SqdGFP oocyte injected with Alexa Fluor 546-labeled *grk* RNA, which became fully anchored after 60 min. anti-GFP antibody was then injected (t = 0), leading to the loss of *grk* RNA anchoring after 20 min.

(D and D′) Anchoring of endogenous *grk* mRNA (red) is disrupted by injection of anti-GFP antibody in an SqdGFP oocyte, 15 min after injection (D′). *grk* mRNA anchoring at the dorso-anterior corner is lost and the RNA is found along the anterior side.

(E) Wild-type oocyte injected with Alexa Fluor 546-labeled *grk* RNA, which became anchored. Injection of the anti-GFP antibody at t = 0 has no effect on the dorso-anterior corner localization of *grk* RNA.

(F) Anchoring of endogenous *grk* mRNA (red; detected by FISH) is not disrupted by injection of the anti-GFP antibody mixed with lysine-fluorescein-dextran (green; [F′]) in a wild-type oocyte.

two thirds of transport particles are in close association with MTs and are not consistently associated with membranes, such as ER or vesicles. This supports the idea that *grk* RNA particles are transported directly by motors on MTs. This notion is strengthened by the fact that the directed movement of the transport particles is disrupted very rapidly when MTs are depolymerized and Dhc, BicD, or Egl function is inhibited (MacDougall et al., 2003). Furthermore, the particles we observe moving along MTs in live cell imaging experiments correspond well to the similar-sized *grk* RNA-rich particles that we visualize by EM. The direct movement of *grk* RNA particles along MTs is in stark contrast to the transport of yeast *ASH1* RNA, which is thought to be cotransported with ER membrane (Schmid et al., 2006).

Once delivered to its final destination at the oocyte dorso-anterior corner, many copies of both injected *grk* RNA and endogenous *grk* mRNA are anchored in large electron-dense structures previously described as sponge bodies, together with the same components present in the transport particles, including Dynein and Squid. Sponge bodies are distinct in appearance from transport particles and have been previously described in nurse cells (Wilsch-Brauninger et al., 1997) and hypothesized to be RNA transport intermediates from the nurse cells to the oocyte. Although we have found Exu-GFP in *grk* anchoring structures (data not shown), we have identified them in the oocyte as functioning in anchoring, rather than transport, and containing components of the Dynein complex Dhc, Egl, and BicD. These data show that the endoplasmic reticulum is not involved in the transport and anchoring of *grk* mRNA, contrary to a previous proposal (Saunders and Cohen, 1999).

Transport particles and sponge bodies are related to RNA particles (also termed germinal granules, P bodies, and neuronal granules; St Johnston, 2005; Anderson and Kedersha, 2006) that display a large spectrum of sizes, composition, and morphology, reflecting several functions in RNA transport, storage, translational control, and processing. Nevertheless, it seems likely that the transport particles we have identified are related to *bcd* and *osk* mRNA granules (Chekulaeva et al., 2006; Tekotte and Davis, 2006) as well as to neuronal RNA granules (St Johnston, 2005). Our data demonstrate that sponge bodies play key roles in RNA anchoring, but it is not known whether they are also involved in translational control, degradation, and storage of mRNA.

Dynein is not only present in the sponge bodies but is also required for the static anchoring of *grk* RNA in the sponge bodies. However, anchoring does not require Egl or BicD, the motor cofactors that are required for RNA transport in the embryo and oocyte (this work; Bullock and Ish-Horowicz, 2001; Delanoue and Davis, 2005; Bullock et al., 2006; Navarro et al., 2004; Clark et al., 2007). While it is not certain whether Egl and BicD are required for cargo loading, transport initiation, or motor activity itself, our evidence shows that none of these functions are required for anchoring. *grk* RNA is therefore anchored by a similar mechanism to *pair-rule* and *wingless* transcripts in the syncytial blastoderm embryo. In both the embryo and oocyte, we propose that when the Dynein motor complex reaches its final destination, the motor becomes a static anchor that no longer depends on the transport activity of the motor.

Dynein (but not Egl and BicD) is not only a static anchor but is also required for the structural integrity of the *grk* RNA anchoring structures in the oocyte, the sponge bodies. Their rapid speed of disassembly upon Dynein inhibition (3–5 min) argues that Dynein has a direct role in anchoring and is required to form and maintain the large RNP complexes that constitute the sponge bodies. This evidence rules out that Dynein could indirectly be required for the delivery of anchoring components that are then used in anchoring *grk* when it is delivered to the sponge bodies. Dynein could also tether the cargo complex directly on the MTs when the transport particles reach their final destination, but our results show that MTs only flank the sponge bodies and are not, as predicted by this model, consistently interdigitated with most of the cargo and motor molecules we detect in the sponge bodies. This is also consistent with the fact that disassembling MTs does not lead to a change in sponge body structure and only leads to a partial loss of endogenous *grk* mRNA anchoring.

In addition to its previously documented role in the second step of *grk* mRNA transport, we have identified here a novel function for hnRNP Squid that plays an essential role in the anchoring of *grk* RNA at the dorso-anterior corner. Like Dynein, Sqd is also enriched at the site of anchoring upon injection of excess *grk* RNA. Inactivation of Sqd before transport begins leads to *grk* transport particles being present at the anterior of the oocyte in permanent anterior flux without anchoring, even for the particles that reach the dorso-anterior corner. Conversely, inactivation of Sqd after *grk* RNA arrives at the dorso-anterior corner leads to a breakdown of anchoring and the conversion of sponge bodies into anterior transport particles containing *grk* RNA. This suggests an active role for Sqd in keeping anchoring structures intact, and most likely a role for Sqd in promoting the conversion of transport particles into anchoring structures by facilitating their reorganization into anchoring complexes.

We propose that sponge bodies are assembled at the dorso-anterior corner by delivery of *grk* mRNA, Dynein

(G) Same experiment as described in (C) but with biotinylated *grk* RNA. After processing this sample for IEM, *grk* RNA (15 nm) was found along the anterior side in particles positive for Dhc (10 nm; red circles) and with the exact same features as the transport particles.
(H and I) SqdGFP oocytes injected with anti-GFP antibody (as in [D′]) were processed for ISH-IEM to detect endogenous *grk* mRNA (15 nm) that was found along the anterior side and partly in particles (arrows) positive for Dhc (10 nm; red circles; [I]) and next to microtubules (H). M, mitochondria; P, plasma membrane.
The scale bars represent 10 μm for (B)–(F) and 200 nm for (G)–(I).

motor component and Squid present together in transport particles. First, the same components are present in the transport particles and in the sponge bodies. Second, some transport particles containing endogenous *grk* mRNA are detected on dorso-anterior MTs. Third, injection of a large excess of *grk* RNA leads to an increase in the size and number of sponge bodies.

At the dorso-anterior corner, sponge bodies are maintained by both Dynein and Squid. When the Dynein motor complex reaches its final destination, the motor becomes a static anchor that no longer depends on the transport activity of the motor. Given the size of Dhc and the presence of many putative domains whose function remains elusive but that could play a central role in the switch from motor to anchor, we propose that it can associate with many other cellular factors to form a large and immobile anchoring complex. Sqd is known to be involved in translational regulation (Norvell et al., 2005), and we propose that association with this class of factors could help create a large and immobile anchoring complex. A strong link between molecular motors and hnRNPs has already been shown to control the localization of their associated mRNAs. For instance, She2 hnRNP acts as a linker between the Myosin motor complex and its mRNA cargo (Kruse et al., 2002). Kinesin and hnRNP are present together in RNA-transporting granules in neurons (Kanai et al., 2004). We propose that transport and anchoring of mRNA by molecular motors involve assembly into transport particles followed by reconfiguration of the same components into large electron-dense anchoring complexes at the final destination. Future work will establish how widely this model can be applied. It will also be interesting to determine whether the specificity of transport and anchoring of other RNA cargos in the *Drosophila* oocyte and embryo is also established by distinct combinations of RNA-binding proteins that influence the function of molecular motors. Time will tell what proportion of mRNA is anchored like *pair-rule* and *grk* transcripts by static functions of molecular motors, as opposed to other possible mechanisms of anchoring.

EXPERIMENTAL PROCEDURES

Fly Strains

Stocks were raised on standard cornmeal-agar medium at 25°C or 21°C. Wild-type was Oregon R (OrR); or SqdGFP (A. Debec); nuclear marker: four copies of the *nlsGFP* transgene (*yw; nlsGFPM; nlsGFPN*) (Davis et al., 1995); MT marker: TauGFP (D. St Johnston). Egl^{wu50}/Egl^{3e} (R. Lehmann) and $BicD^{mom}$ (B. Suter) flies were *w; Df(2L)TW119/* $BicD^{r8}$*; P [w+hsBic-D]-94/+* (Swan and Suter, 1996). *sqd* mutant alleles used were sqd^{1} (T. Schüpbach).

Injection of RNA and Inhibitors

RNA was transcribed in vitro using T7, T3, or SP6 polymerase with UTP-Alexa Fluor 546, UTP-Alexa Fluor 488, or UTP-biotin (Wilkie and Davis, 2001). We used the full-length *grk* cDNA, as smaller fragments are difficult to detect in EM. Ovaries were dissected and separated into individual ovarioles directly onto coverslips in series 95 halocarbon oil (KMZ Chemicals) and injected with labeled *grk* RNA using Femtotip needles (Eppendorf). RNA was injected at a concentration of 250–500 ng/μl, Colcemid (Sigma) at 1 mg/ml, and Latrunculin A (Sigma) at 20 mM. Anti-Dhc (D. Sharp), anti-Egl (R. Lehmann), anti-GFP (ascites from Sigma G6539, containing 25 mg/ml total protein, 5.8 mg/ml IgG), anti-Sqd (T. Schüpbach), and IgG and rabbit serum were injected at the same concentration (20 mg/ml). Each experiment was repeated with at least two different batches of RNA in a total of at least 12 and on average 25 egg chambers (Table S1). Egg chambers injected with anti-GFP antibody and 70 kDa lysine-fluorescein-dextran (Molecular Probes; injected at 0.125 mg/ml) were fixed and processed for endogenous *grk* mRNA in situ hybridization, with the uninjected controls in the same tube.

Antibodies

To detect the biotinylated RNA, we used Alexa Fluor 546-coupled avidin (Molecular Probes) or a polyclonal rabbit anti-biotin (Rockland) at 1:10,000 for IEM. We used anti-α-tubulin-FITC (Sigma; 1:1,000), monoclonal anti-α-tubulin B512 (Sigma) at 1:5,000 for IEM; rabbit polyclonal anti-Dhc, PEP1 (T. Hays) at 1:100 and 1:300 for IEM; rabbit polyclonal anti-Egl (R. Lehmann) at 1:4,000 and 1:300 for IEM; monoclonal anti-BicD 1B11 (B. Suter) at 1:20; and clones 2G10 and 4C2 at 1:20 for IEM; rabbit polyclonal anti-GFP A6455 (Molecular Probes) at 1:300 and FITC-phalloidin to label F-actin. For IEM, rabbit polyconal antibodies were detected directly with protein A gold conjugates (Department of Cell Biology, Institute of Biomembranes, Utrecht, The Netherlands). Mouse monoclonals were detected with rabbit anti-mouse (Dako; 1:250) followed by protein A gold conjugates. Anti-SqdA 2G9 (T. Schüpbach) was used at 1:1,000 for western blots.

Immunofluorescence and RNA Fluorescence In Situ Hybridization

Injected oocytes were fixed for 20 min or 1 hr in 4% paraformaldehyde (PFA; Polysciences) added directly on top of the egg chambers in halocarbon oil. Fixed oocytes were then recovered with glass pipettes into glass multiwell plates, and fixative and oil were washed away with PBS. Postfixation was performed with 4% PFA for 20 min, followed by several washes with PBT (PBS + 0.1% Tween). After fixation, ovaries were immunolabeled and processed for fluorescence in situ hybridization (FISH) as described previously (Wilkie et al., 1999) using fluorescent tyramide detection (NEN Life Sciences) and mounted in Vectashield (Vector). The digoxigenin-labeled antisense probes were prepared from a full-length *grk* cDNA (T. Schüpbach).

Four-Dimensional Imaging and Deconvolution

Imaging was performed on a wide-field DeltaVision microscope (Applied Precision, Olympus IX70 and with a Roper Coolsnap HQ, based on an original design by D.A. Agard and J.W. Sedat) with 20×/0.75 NA or 100×/1.4 NA objectives and then deconvolved using SoftWorks (Applied Precision) based on Sedat/Agard algorithms (Parton and Davis, 2006). Up to 25 egg chambers were imaged in parallel (Parton and Davis, 2005). Photobleaching experiments used a 488 nm laser with one iteration at the maximum intensity and measurement of the recovery of the fluorescence initiated 1 s later. Images were analyzed using SoftWorks (Applied Precision).

Sample Preparation for EM Analysis

Oocytes were embedded in Spurr as previously described (Herpers and Rabouille, 2004). Images were captured on a Jeol EX1200 electron microscope.

Detection of Injected *grk* RNA by Immunoelectron Microscopy

Egg chambers were injected in series 95 halocarbon oil and left for either 20 min for transport studies or 45–60 min for anchoring studies. Fixation was performed for a minimum of 3 hr using 2% electron-grade PFA and 0.2% glutaraldehyde (GA; Sigma) in 0.1 M phosphate buffer (pH 7.4), before being transferred and stored in 1% PFA in the same buffer at 4°C. Single stage 9 oocytes were embedded in blocks of 12% gelatin that were infused in 2.3 M sucrose and frozen in liquid

nitrogen. Sixty nanometer ultrathin sections were cut and collected on carbon-coated formvar copper grids as previously described (Herpers and Rabouille, 2004). The injected RNA was detected using polyclonal rabbit anti-biotin antibodies followed by protein A gold conjugates.

grk mRNA ISH-IEM

Egg chambers were fixed overnight in 4% PFA or 3 hr in 2% PFA, 0.2% GA in 0.1 M phosphate buffer (pH 7.4). Sixty nanometer sections were retrieved on carbon-coated formvar nickel grids on a drop of sucrose/methylcellulose mixture that was washed off by floating the grids three times for 5 min on drops of PBS at 37°C. The sections were postfixed in 1% GA in PBS and washed another three times in PBS. Prehybridization was performed at 37°C in 50% formamide (Sigma), 2× SSC in diethylpyrocarbonate-treated H_2O for 15 min. Biotinylated *grk* RNA probes were made according to the manufacturer's specifications (Roche) and were denatured by 10 min of boiling in hybridization buffer, and then cooled on ice. The hybridization buffer is the prehybridization buffer supplemented with 100 mg/ml dextran sulfate (Sigma), 100 μg/ml tRNA, 50 μg/ml heparin. Hybridization was performed in a humid chamber with 50% formamide at 55°C by floating the grids on the denatured probe at 0.5–1 μg/ml for 16 hr. The unbound probe was washed off by three washes of prehybridization buffer followed by the IEM labeling protocol described above. The grids were incubated with anti-biotin antibodies followed by protein A gold conjugates. In controls lacking probe, no labeling was visible in the cytoplasm except for some background labeling of sticky yolk granules and mitochondria.

Supplemental Data

Supplemental Data include six figures, one table, and Supplemental Experimental Procedures and are available at http://www.developmentalcell.com/cgi/content/full/13/4/523/DC1/.

ACKNOWLEDGMENTS

We thank the Davis and Rabouille laboratories as well as David Tollervey for helpful discussions, and Robin Allshire, Edele Marston, and Veronique van de Bor for their critical comments on the manuscript. We thank Richard Parton and David Kelly for help and advice with light microscopy, Russell Hamilton and Georgia Vendra for help with statistics, and Carine Meignin for proposing to use an anti-GFP antibody to inhibit SqdGFP. This work was supported by a Wellcome Trust Senior Research fellowship (067413) to I.D., and a Marie Curie fellowship to R.D. B.H. was funded by a Nederlandse Organisatie voor Wetenschappelijk Onderzoek (NWO) Aspasia grant (015.001.129) to C.R.

Received: August 16, 2006
Revised: January 27, 2007
Accepted: August 29, 2007
Published: October 9, 2007

REFERENCES

Anderson, P., and Kedersha, N. (2006). RNA granules. J. Cell Biol. *172*, 803–808.

Bashirullah, A., Halsell, S.R., Cooperstock, R.L., Kloc, M., Karaiskakis, A., Fisher, W.W., Fu, W., Hamilton, J.K., Etkin, L.D., and Lipshitz, H.D. (1999). Joint action of two RNA degradation pathways controls the timing of maternal transcript elimination at the midblastula transition in *Drosophila melanogaster*. EMBO J. *18*, 2610–2620.

Bertrand, E., Chartrand, P., Schaefer, M., Shenoy, S.M., Singer, R.H., and Long, R.M. (1998). Localization of ASH1 mRNA particles in living yeast. Mol. Cell *2*, 437–445.

Bullock, S.L., and Ish-Horowicz, D. (2001). Conserved signals and machinery for RNA transport in *Drosophila* oogenesis and embryogenesis. Nature *414*, 611–616.

Bullock, S.L., Nicol, A., Gross, S.P., and Zicha, D. (2006). Guidance of bidirectional motor complexes by mRNA cargoes through control of dynein number and activity. Curr. Biol. *16*, 1447–1452.

Caceres, L., and Nilson, L.A. (2005). Production of *gurken* in the nurse cells is sufficient for axis determination in the *Drosophila* oocyte. Development *132*, 2345–2353.

Chekulaeva, M., Hentze, M.W., and Ephrussi, A. (2006). Bruno acts as a dual repressor of oskar translation, promoting mRNA oligomerization and formation of silencing particles. Cell *124*, 521–533.

Clark, A., Meignin, C., and Davis, I. (2007). A Dynein-dependent shortcut rapidly delivers axis determination transcripts into the *Drosophila* oocyte. Development *134*, 1955–1965.

Davis, I., Girdham, C.H., and O'Farrell, P.H. (1995). A nuclear GFP that marks nuclei in living *Drosophila* embryos; maternal supply overcomes a delay in the appearance of zygotic fluorescence. Dev. Biol. *170*, 726–729.

Delanoue, R., and Davis, I. (2005). Dynein anchors its mRNA cargo after apical transport in the *Drosophila* blastoderm embryo. Cell *122*, 97–106.

Deshler, J.O., Highett, M.I., and Schnapp, B.J. (1997). Localization of *Xenopus* Vg1 mRNA by Vera protein and the endoplasmic reticulum. Science *276*, 1128–1131.

Forrest, K.M., and Gavis, E.R. (2003). Live imaging of endogenous RNA reveals a diffusion and entrapment mechanism for nanos mRNA localization in *Drosophila*. Curr. Biol. *13*, 1159–1168.

Geng, C., and MacDonald, P.M. (2006). Imp associates with Squid and Hrp48 and contributes to localized expression of *gurken* in the oocyte. Mol. Cell. Biol. *26*, 9508–9516.

Glotzer, J.B., Saffrich, R., Glotzer, M., and Ephrussi, A. (1997). Cytoplasmic flows localize injected oskar RNA in *Drosophila* oocytes. Curr. Biol. *7*, 326–337.

Gonzalez-Reyes, A., Elliott, H., and St Johnston, D. (1995). Polarization of both major body axes in *Drosophila* by Gurken-Torpedo signaling. Nature *375*, 654–658.

Goodrich, J.S., Clouse, K.N., and Schüpbach, T. (2004). Hrb27C, Sqd and Otu cooperatively regulate gurken RNA localization and mediate nurse cell chromosome dispersion in *Drosophila* oogenesis. Development *131*, 1949–1958.

Herpers, B., and Rabouille, C. (2004). mRNA localization and ER-based protein sorting mechanisms dictate the use of transitional endoplasmic reticulum-Golgi units involved in gurken transport in *Drosophila* oocytes. Mol. Biol. Cell *15*, 5306–5317.

Kanai, Y., Dohmae, N., and Hirokawa, N. (2004). Kinesin transports RNA: isolation and characterization of an RNA-transporting granule. Neuron *43*, 513–525.

Kruse, C., Jaedicke, A., Beaudouin, J., Bohl, F., Ferring, D., Guttler, T., Ellenberg, J., and Jansen, R.P. (2002). Ribonucleoprotein-dependent localization of the yeast class V myosin Myo4p. J. Cell Biol. *159*, 971–982.

MacDougall, N., Clark, A., MacDougall, E., and Davis, I. (2003). *Drosophila* gurken (TGFα) mRNA localizes as particles that move within the oocyte in two dynein-dependent steps. Dev. Cell *4*, 307–319.

Malikov, V., Kashina, A., and Rodionov, V. (2004). Cytoplasmic dynein nucleates microtubules to organize them into radial arrays in vivo. Mol. Biol. Cell *15*, 2742–2749.

Navarro, C., Puthalakath, H., Adams, J.M., Strasser, A., and Lehmann, R. (2004). Egalitarian binds dynein light chain to establish oocyte polarity and maintain oocyte fate. Nat. Cell Biol. *6*, 427–435.

Neuman-Silberberg, F.S., and Schüpbach, T. (1993). The *Drosophila* dorsoventral patterning gene *gurken* produces a dorsally localized RNA and encodes a TGF α-like protein. Cell *75*, 165–174.

Norvell, A., Kelley, R.L., Wehr, K., and Schüpbach, T. (1999). Specific isoforms of Squid, a *Drosophila* hnRNP, perform distinct roles in *gurken* localization during oogenesis. Genes Dev. *13*, 864–876.

Norvell, A., Debec, A., Finch, D., Gibson, L., and Thoma, B. (2005). Squid is required for efficient posterior localization of *oskar* mRNA during *Drosophila* oogenesis. Dev. Genes Evol. *215*, 340–349.

Parton, I., and Davis, I. (2005). Time-lapse cinematography in living *Drosophila* tissues. In Live Cell Imaging: A Laboratory Manual, D. Spector and D. Goldman, eds. (Cold Spring Harbor, NY: Cold Spring Harbor Laboratory Press), pp. 385–407.

Parton, I., and Davis, I. (2006). Deconvolution: lifting the fog. In Cell Biology: A Laboratory Handbook, J. Celis, ed. (New York: Academic Press), pp. 187–200.

Pearson, J., and Gonzalez-Reyes, A. (2004). Egalitarian and the case of the missing link. Nat. Cell Biol. *6*, 381–383.

Pfister, K.K., Shah, P.R., Hummerich, H., Russ, A., Cotton, J., Annuar, A.A., King, S.M., and Fisher, E.M. (2006). Genetic analysis of the cytoplasmic dynein subunit families. PLoS Genet *2*, e1.

Roth, S., and Schüpbach, T. (1994). The relationship between ovarian and embryonic dorsoventral patterning in *Drosophila*. Development *120*, 2245–2257.

Saunders, C., and Cohen, R.S. (1999). The role of oocyte transcription, the 5′UTR, and translation repression and derepression in *Drosophila gurken* mRNA and protein localization. Mol. Cell *3*, 43–54.

Schmid, M., Jaedicke, A., Du, T.G., and Jansen, R.P. (2006). Coordination of endoplasmic reticulum and mRNA localization to the yeast bud. Curr. Biol. *16*, 1538–1543.

St Johnston, D. (2005). Moving messages: the intracellular localization of mRNAs. Nat. Rev. Mol. Cell Biol. *6*, 363–375.

Swan, A., and Suter, B. (1996). Role for Bicaudal-D in patterning the *Drosophila* egg chamber in mid-oogenesis. Development *122*, 3577–3586.

Tekotte, H., and Davis, I. (2002). Intracellular mRNA localization: motors move messages. Trends Genet. *18*, 636–642.

Tekotte, H., and Davis, I. (2006). Bruno: a double turn-off for Oskar. Dev. Cell *10*, 280–281.

Van Buskirk, C., and Schüpbach, T. (2002). Half pint regulates alternative splice site selection in *Drosophila*. Dev. Cell *2*, 343–353.

Vorobjev, I., Malikov, V., and Rodionov, V. (2001). Self-organization of a radial microtubule array by dynein-dependent nucleation of microtubules. Proc. Natl. Acad. Sci. USA *98*, 10160–10165.

Weil, T.T., Forrest, K.M., and Gavis, E.R. (2006). Localization of *bicoid* mRNA in late oocytes is maintained by continual active transport. Dev. Cell *11*, 251–262.

Wilkie, G.S., and Davis, I. (2001). *Drosophila wingless* and *pair-rule* transcripts localize apically by dynein-mediated transport of RNA particles. Cell *105*, 209–219.

Wilkie, G.S., Shermoen, A.W., O'Farrell, P.H., and Davis, I. (1999). Transcribed genes are localized according to chromosomal position within polarized *Drosophila* embryonic nuclei. Curr. Biol. *9*, 1263–1266.

Wilsch-Brauninger, M., Schwarz, H., and Nusslein-Volhard, C. (1997). A sponge-like structure involved in the association and transport of maternal products during *Drosophila* oogenesis. J. Cell Biol. *139*, 817–829.